Flow heterogeneities in the UK Sherwood Sandstone Group: resolving the role of tectonic vs. sedimentary structures

Giacomo Medici

Submitted in accordance with the requirements for the degree of Doctor of Philosophy

The University of Leeds
School of Earth and Environment

July, 2017

Preface

The candidate confirms that the work submitted is his own, except where work which has formed part of jointly-authored publications has been included. The contribution of the candidate and the other authors to this work has been explicitly indicated overleaf. The candidate confirms that appropriate credit has been given within the thesis where reference has been made to the work of others.

A version of Chapter 3 is published in Sedimentary Geology (v. 329, pp. 188-210) uder the title "Palaeoenvironment of braided fluvial systems in different tectonic realms of the Triassic Sherwood Sandstone Group, UK", with the following list of authors (in order): Medici, G., Boulesteix, K., Mountney, N.P., West, J.L. and Odling, N.E.

Kevin Boulesteix collected some of the sedimentological data from the St Bees area. The candidate set the scientific scope of the work, devised and developed the methodology, collected all the data from the Doncaster area, performed all data analysis, drew all illustrations and wrote the text. The co-authors provided guidance during the design of this part of project and feedback on the manuscript.

Chapter 4 is published in the Journal of Contaminant Hydrology (v. 194, pp.36-58) under the title "Characterizing flow pathways in a sandstone aquifer: Tectonic vs. sedimentary heterogeneities" with the following list of authors (in order): Medici, G., West J.L. and Mountney, N.P. European Geophysical Ltd performed optical televiewer, wire-line and fluid logs in five boreholes (Black Ling, Bridge End Trial, Ellergill Bridge, Thornhill Trial) in the St Bees area. The candidate set the scientific scope of the work, developed the methodology, collected data from outcrop, performed all data analysis, drew all illustrations and graphs, and wrote the text. The co-hauthors provided guidance during the design of this part of project and feedback on the manuscript.

A version of Chapter 5 has been submitted to Hydrogeology Journal uder the title "Multi-scale properties of aquifers hosted in a fluvial sedimentary succession", with the following list of authors (in order): Medici, G., West J.L. and Mountney, N.P. European Geophysical Ltd performed further geophysical logs in Bridge End Trial and in Rottington Trial in the St Bees area. The candidate set the scientific scope of the work, developed the methodology, collected data from outcrop, performed all data analysis, drew all illustrations and graphs, and wrote the text. The co-authors provided guidance during the design of this part of project and feedback on the manuscript.

Acknowledgements

Abstract

Fluvial and aeolian sedimentary successions represent porous media that can host both groundwater and hydrocarbon resources. Study of their heterogeneities provides a better understanding of both contaminant dispersal in aquifers and techniques for enhancing recovery in oil reservoirs. This research investigates the hydraulic properties of a fluvial succession deposited in a continental rift setting: the Triassic St Bees Sandstone Formation, which represents the basal part of the UK Sherwood Sandstone Group in the eastern Irish Sea Basin. These fluvial deposits have also been compared to the anologous fluvial deposits of the more slowly subsiding shelf-edge basin of the eastern England Shelf aiming to constrain the effect of subsidence rates on preservation of low permeability heterogeneities.

The Triassic deposits of the St Bees Sandstone Formation were investigated from the plug up to the field-scale combining a range of sedimentological, structural, petrophyisical and hydro-geophysical tecniques. The aim of this research is to characterize the impact of sedimentary and tectonic heterogeneities on flow in the continental deposits of the Sherwood Sandstone aquifer assessing the validity of the findings up to reservoir depths.

The hydraulic properties of the St Bees Sandstone Formation are compared with those of other formations of both aeolian and fluvial origin within the Sherwood Sandstone Group, and similar siliclastic formations worldwide to achieve a more general understanding of flow behaviour in siliciclastic sedimentary successions.

In the relatively shallow (< ~100-200 m BGL) saturated zone of the St Bees Sandstone aquifer, acidic meteoric waters have enlarged fractures to create karst-like features resulting in very high field-scale hydraulic conductivity (K~10-1-100 m/day). Here, contaminant dispersal likely occurs at a relatively high rate. A deeper investigation (> 150m depth) demonstrates that the aquifer has not been subjected to rapid groundwater circulation at these depths; hydraulic conductivity is substantially lower, decreasing from K~10^{-3} m/day at 150-400 m BGL, to 10^{-4} m/day down-dip at ~1 km BGL. Pore-scale permeability becomes progressively more dominant with increasing depth. Thus, this sandstone aquifer at ~ 1 km depth approximates the hydraulic properties of analogous hydrocarbon reservoirs which are dominated by intergranular flow. The succession contains a variety of fine-grained and relatively low-permeability units including mudstone beds, interbedded with highly permeable channel deposits. Where present, a higher frequency of occurrence and greater lateral extent of mudstone units impede flow, reducing the field-scale permeability. Zones characterized by higher preservation of mudstone layers also show higher field-scale permeability anisotropy (K_h/K_v) due to a significant reduction of flow perpendicular to these fine-grained heterogeneities. In contrast, normal faults represent preferential flow pathways up to ~1 km depth, due to presence of highly connective open fractures.

Continental successions in rift settings are also characterized by aeolian deposits in the NW Triassic realm, which typically possess higher matrix permeability due to a relatively paucity of integranular clay with respect to fluvial deposits. Thus, reservoir quality rises with increasing content of preserved aeolian sediments due to the dominance of intergranular flow in silicilastic successions buried at depths > ~1 km. Deposits of aeolian-dune versus fluvial origin also exhibit contrasting hydraulic behaviour where intersected by fault zones: normal faults deform aeolian deposits and are dominated by granulation seams which would partially impede flow to production wells in analogous hydrocarbon reservoirs.

Contents

List of Tables

List of Figures

Abbreviations

c.f.	To compare
e.g.	For example exempli gratia
i.e.	That is
ltd	Limited liability company
3D	Three-dimensional
ASL	Above Sea Level
BGL	Below Ground Level
UK	United Kingdom
USA	United States of America

A list of the physical properties used in this thesis together with symbols and units is given in Appendix C

Chapter 1

Introduction

1.1 Project rationale

Fluvial and aeolian deposits form thick sedimentary successions (>1.0 km) in basins for which accommodation was generated in response to, compressional, strike-slip tectonics and extensional tectonics, as well as thermal subsidence (Bosellini, 1989; Waugh, 1973). For example, continental deposits of fluvial and aeolian origin represent much of the fill of the Paradox foreland basin in Utah (Wengerd and Strickland, 1954). Fluvial sedimentary sequences characterize pull-apart basins associated with the North Anatolian and San Andreas strike-slip faults in Turkey and USA, respectively (McLaughlin and Nilsen, 1982; Hempton and Dunne, 1984). Siliciclastic deposits of fluvial and aeolian origin also represent significant components of the fills of rift valleys that developed at the beginning of the so-called Wilson Cycle during the break-up of supercontinents (Wilson, 1963). Examples of such continental syn-rift deposits are especially well preserved in Triassic successions due to the fragmentation of Pangaea, where they are well represented in South America, North America, Europe, Africa, Asia and Australia (Walker, 1967; Waugh, 1973; Ziegler, 1982). These syn-rift siliciclastic deposits of continental origin represent porous media, which can serve as important hosts for hydrocarbon and geothermal resources (Aldinucci et al., 2008; McKie and Williams, 2009); additionally, they serve as important groundwater aquifers (Tellam, 2004; Tellam and Barker, 2006). Thus, study of stratigraphically and structural heterogeneities that might act to influence fluid flow behaviour in syn-rift continental successions is important. Study of such heterogeneities and their influence on flow provides useful information for assessing both contaminant dispersal hazard in aquifers and recovery optimization in hydrocarbon and geothermal reservoirs (Tellam and Barker, 2006; Corbett et al., 2012; Gellasch et al., 2013).

The flow of water and oil tends to be more sensitive to presence of low-permeability heterogeneities compared to the flow of low-viscosity gas (Mattax and Kyte, 1962; Alexander et al., 1987). Despite this, relatively few studies have considered aquifers as potential petroleum reservoir analogues (Alexander et al., 1987; Noushabadi et al., 2011). In fact, the great majority of scientific literature on analogues of oil reservoirs focuses on seismic and outcrop studies for sedimentary and fault structure characterization (e.g., Antonellini et al., 1994; Miall, 2006; Torabi and Fossen, 2009; Banham and Mountney, 2013). Also, several studies on the hydraulic properties of sandstone aim only to characterize the centimetre-scale properties of the rock matrix, either using core plugs or mini-permeameter on outcropping rock faces (e.g., Bloomfield et al., 2006; Bouch et al., 2006; Balsamo and Storti, 2010). However, both plug and field-scale data need to be compared jointly to assess and quantify the impact of geological heterogeneities on flow. In fact, aquifer studies at the field-scale allow effective recognition of the flow impact of a large variety of tectonic and sedimentary heterogeneities (and combinations thereof), providing useful information in terms of oil recovery optimization. This research issue is addressed in this thesis.

The absence of significant effects relating to compressional tectonics in the Triassic continental successions of NW Europe favours characterization of sedimentary (fine-grained layers) and extension-related tectonic (open fractures, cataclasite, granulation seams) heterogeneities. Such heterogeneity types are considered important in assessment of oil recovery optimization (Antonellini et al., 1994; Caine et al., 1996; Corbett et al., 2012). Additionally, the Cenozoic uplift of NW Europe created stratabound fractures in layered successions, which represent further potential flow pathways (Ameen, 1995; Carminati et al., 2009; Welch et al., 2015). Notably, the UK Sherwood Sandstone Group (Figure 1.1) in NW Europe represents a continental succession present in a rift setting. This succession is particularly favourable for studies of aquifer heterogeneity since a large amount of borehole information is available (Nirex, 1992a, b; 1993a-c; 1996a, b; 2001). A variety of background hydrogeological data

(e.g., matrix porosity and permeability tests, packer and pumping tests) is available for this Triassic succession since it represents (i) the second most important UK aquifer in terms of abstraction volume, (ii) the bedrock lithology of large industrial cities such as Birmingham, Liverpool and Manchester, and (iii) a strategic analogue for the Triassic reservoirs in the on-shore areas in Dorset (e.g. Wytch Farm oil field), as well as in the off-shore areas of the North Sea and Irish Sea (Allen et al., 1997; Smedley and Edmunds, 2002; Tellam and Barker, 2006; McKie and Williams, 2009). Notably, the Sherwood Sandstone Group outcrops in several UK Triassic basins (Figure 1.1). These basins are characterized by different subsidence rates and were located at different distances from the main sediment source area, which is represented by the Armorican Massif in northern France (Tyrrel et al., 2012; Morton et al., 2013). Plug (porosity, permeability) and field-scale (transmissivity) properties may be related to different palaeoenvironmental scenarios (aeolian vs. fluvial settings) and to different allogenic factors controlling sedimentation (e.g., tectonic subsidence and sediment source distance). Thus, the determination of relationships between hydraulic properties, tectonics and palaeoenvironment provides predictive information on reservoir quality (cf. Bridge, 2006).

Previous works which have analysed the entire Sherwood Sandstone Group have focused on specific aspects. Such studies have analysed separately sedimentological (McKie and Williams, 2009), tectonic (Knott, 1994; Chadwick, 1997) and physical properties (Allen et al., 1997, 1998; Tellam and Barker, 2006). The research undertaken as part of this study and presented in this thesis seeks to relate all these aspects using a multidisciplinary approach. Hence, a variety of sedimentological, structural and hydrogeological techniques have been applied to a specific field area in Cumbria, and compared with extensive previous information on the wider Sherwood Sandstone Group, both from the open literature, from the British Geological Survey data archive, and additionally using other field-acquired data.

The selected field area is the St Bees-Sellafield outcrop of the Sherwood Sandstone Group in West Cumbria, NW England (Figure 1.1). Here, the fluvial deposits of the Sherwood Sandstone Group in the eastern Irish Sea Basin were selected for detailed study because they show (i) relatively high abundance of fine-grained heterogeneities in core logs (Nirex, 1997), and (ii) development of brittle tectonic structures represented by stratabound joints and fault-related open fractures (Knott, 1994; Ameen, 1995; Allen et al., 1998). Also, this area offers the opportunity to re-analyse unpublished hydrogeological data (matrix porosity and permeability tests, pumping tests, fluid conductivity and temperature logs), which were acquired during the 1990s up ~1 km below the ground surface. Such data sets have been integrated with hydro-geophysical (flow-logs, optical and acoustic televiewer logs) and petrophysical data (NMR, permeability tests, SEM, petrographic microscope analyses), within this study, thereby allowing comparison of plug- and field-scale properties in fluvial deposits. Then, both newly acquired data bespoke to this study have been integrated with literature-derived data to achieve an exhaustive understanding of the hydraulic properties of both fluvial and aeolian sedimentary successions more generally.
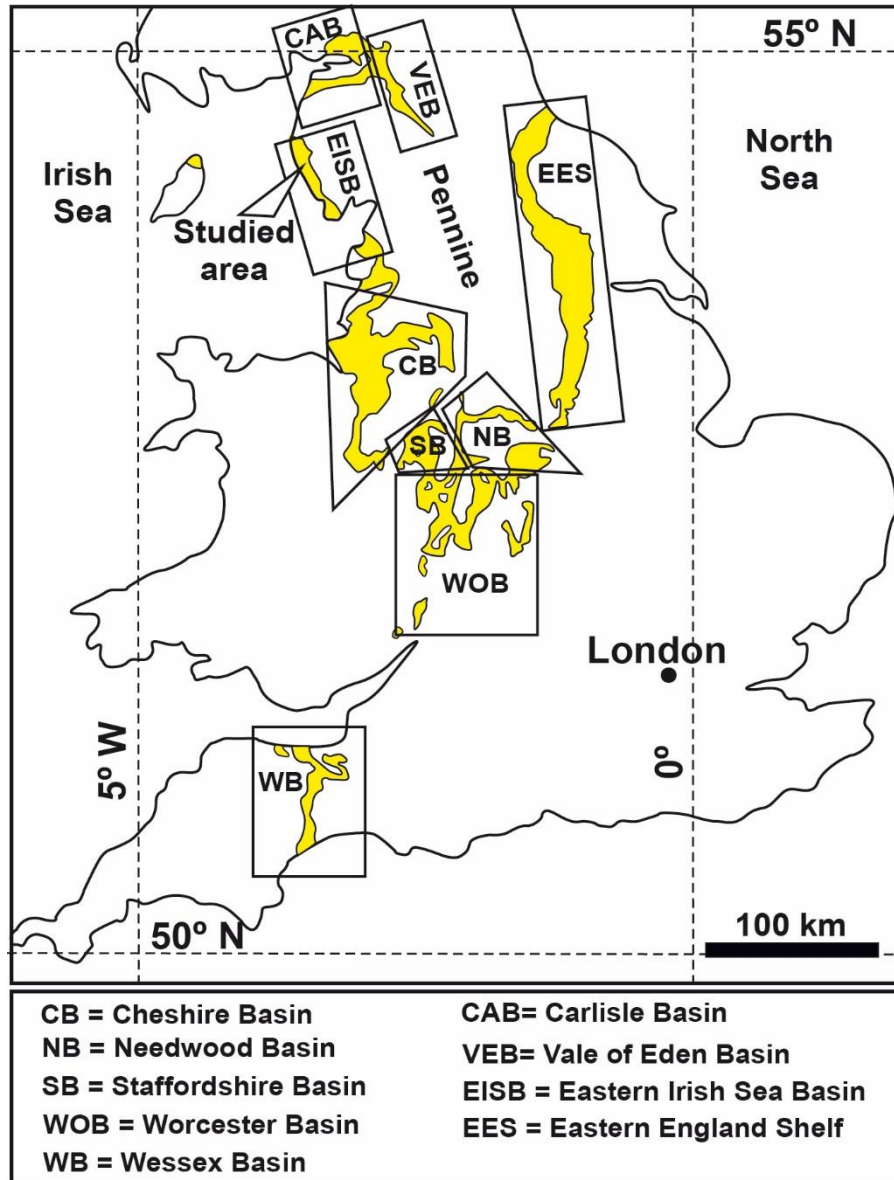
Figure 1.1: The distribution of Triassic sedimentary basins and of the Sherwood Sandstone Group (yellow) in Great Britain (modified from Wakefield et al., 2015).

1.2 Aim and objectives

The fundamental aim of this work is to establish the effective role of tectonic and sedimentary heterogeneities in a fluvial aquifer from the plug scale up to the field scale to achieve a better understanding of the upscaling properties of oil reservoirs. Establishment of the effective role of geological heterogeneities at the field scale will influence hydrocarbon exploration in

terms of drilling strategy (Clark and Pickering, 1996; Kerans et al., 1988; Zhao et al., 2008; Faulkner et al., 2009). For example, production wells may target faults if these tectonic structures represent preferential flow-pathways. Also, a range of strategies are used in hydrocarbon exploration aiming to optimize production in reservoirs which are characterized by low permeability layers interbedded with more conductive deposits (Miall, 1977; Clark and Pickering, 1996; Faulkner et al., 2010; Bense et al., 2013). Data in this thesis, in particular those acquired at shallow depths (~150 mBGL), may also serve for aquifer management purposes to constrain contaminant dispersal; notably, fracture alteration and aperture in shallow aquifers typically do not reproduce reservoir flow conditions (Worthington et al., 2016).

Ultimately, the fundamental aim of the work has been achieved by crossing a range of petrophyical and hydrogeophysical tecniques. In fact, plug-scale properties were studied including porosity, permeability and Nuclear Magnetic Resonance (NMR) T_2 distribution of the St Bees Sandstone Formation of the Sherwood Sandstone Group in Cumbria. Field-scale properties were characterized using pumping tests, logging flow, temperature and fluid conductivity. In achieving a better understanding of the upscaling properties of the fluvial St Bees Sandstone aquifer, each illustrative application represents a stand-alone piece of research (a sub-project), which each attempt to answer a series of specific research questions. These research questions are included in the following list and represent the specific objectives of this work:

- Evaluate the influence of basin type in governing the type and mechanism of preservation of a fluvial succession that accumulated and became preserved under conditions of both active extensional tectonics and passive subsidence. This part of the research provides evidence on how the relatively high subsidence of rift basins such as the eastern Irish Sea Basin of West Cumbria favours preservation of fine-grained layers in fluvial successions, which potentially represent flow barrier and baffles (cf., Alexander et al., 1987).

- Use outcrop-scale scanlines and imaging, and wireline logs to characterise potential flow heterogeneities which characterize the fluvial St Bees Sandstone aquifer. Geological heterogeneities are characterised at the field-scale using pumping tests and flow velocity logs. This allows quantification of the role of normal faults vs. un-faulted rock mass in the shallow (<~150mBGL) St Bees Sandstone aquifer (following methods of Molz et al., 1989; Day-Lewis et al., 2011). Such hydro-geophysical characterization of shallow sandstone aquifers typically provides useful information for constraining hazard from contaminant dispersal and assists aquifer management (Gellasch et al., 2013; Lo et al., 2014).

- Transmissivity values from well tests are compared with upscaled values derived from plug-test matrix hydraulic conductivities for the St Bees Sandstone aquifer, to establish the relative contribution of fracture vs. matrix flow in this fluvial aquifer at a range of depths (up to 1100 m BGL). For this purpose comparison of upscaled plug and measured field-scale permeability is discussed (using results from flow-log-analysis to obtain field-scale hydraulic conductivities), the fulfilment of this objective provides an exhaustive understanding of the flow behaviour in the shallow St Bees Sandstone aquifer.

- Document the petrophysical properties (matrix porosity and permeability, anisotropy and NMR T_2 distribution) of the sedimentary units that characterize the St Bees Sandstone aquifer in order to assess their flow barrier potential at the field scale. Permeability anisotropy (K_h/K_v) at the field scale is realised using well tests at depths > ~ 150 mBGL, i.e. where the rock matrix is expected to be a more important flowpath due to closure of discontinuities and less dissolution along fractures at such depths (Jiang et al., 2009, 2010; Worthington et al., 2016).

- Identify the respective roles of matrix, bedding plane-fractures, stratabound joints and faults on conducting flow at a range of depths (up to 1100 mBGL) under pumped conditions up to 1100 mBGL.

Pumping tests, fluid conductivity and temperature logs (pumped conditions, sampling fluid every 0.15 m) were analysed in the deep (150-1100 mBGL) St Bees Sandstone enabling acquisition of information at depths similar to those of petroleum reservoirs. Fluvial reservoirs are typically exploited at depths ranging from ~1 to ~2 km in on-shore areas in northern Europe and Africa (Rossi et al., 2002; Galeazzi et al., 2010; Worden et al., 2016).

- Place the research on the flow heterogeneities of St Bees Sandstone Formation in West Cumbria in the context of the entire UK Triassic succession and analogous successions worldwide. This provides a more complete view of the hydraulic properties of continental siliciclastic successions in rift settings for both aeolian and fluvial deposits. Properties of siciliclastic continental sequences up to ~ 4 km depth from literature are assessed. Fulfilment of this objective enables interpretation of processes of permeability variation with depth in such deposits.

1.3 Thesis outline

This work commences with a discussion of the sedimentological, structural, mechanical and hydraulic properties of the UK Sherwood Sandstone aquifer (Figure 1.2). This review (Chapter 2) highlights how the St Bees Sandstone aquifer represents a particularly mechanically resistant sandstone aquifer, which is thus heavy fractured in response to the Meso-Cenozoic tectonic events. Both newly acquired and archive data from the Environment Agency and British Geological Survey are analysed and discussed in the next three chapters (Chapters 3, 4 and 5). Necessarily, these three chapters are connected forming a coherent scenario as outlined below. Chapter 3 deals with sedimentological characterisation in core and outcrop and shows how fine-grained heterogeneities (e.g., mudstones deposited by overbank flood events and in fluvial channels) are well-preserved in the St Bees Sandstone aquifer, because of the high

subsidence rates (210 m/Myr) seen in the eastern Irish Sea Basin. Chapter 4 details how these fine-grained heterogeneities have also been detected by wire-line and optical logs, but additionally goes on to focus on field-scale hydraulic characterisation using archive pumping test and geophysical logs (both conducted in this work and archive logs from a investigation by Nirex). The respective role of matrix vs. fracture flow is discussed in first instance in the shallow (< ~ 150 mBGL) and intermediate (150-400 mBGL) St Bees Sandstone aquifer. Chapter 5 discusses the effect of matrix and fracture properties in plug- and field-scale tests more fully, and attempts to quantify the respective roles of matrix and fractures. The investigation has been extended up to ~ 1100 mBGL (Figure 1.2) using archive data from Nirex, which represents a similar depth interval to some on-shore hydrocarbon fields (Rossi et al., 2002; Galeazzi et al., 2010; Worden et al., 2016). Finally, the findings of this research on the St Bees Sandstone aquifer of the eastern Irish Sea Basin has been synthesised in Chapter 6 using literature-derived data for comparison of analogous successions worldwide, including depths up to ~4 km. Chapter 6 also includes a discussion on the hydraulic properties of the Triassic aeolian (Figure 1.2) deposits of the Sherwood Sandstone Group, the aim being to achieve a larger understanding of the hydraulic properties of continental successions generally.

Significantly, Chapter 3, 4 and 5 represent self-contained pieces of research, and were therefore conceived as stand-alone published or publishable work; as a result, the thesis lacks chapters devoted specifically to discussion of the geological background to the field area, and to explanation of methods or results, as have traditionally been presented in works of this type. Instead, the aims and objectives, details of the field area, methods and results for each sub-project are given separately in each chapter (i.e., Chapters 3, 4, and 5). Importantly, although the content of chapters is the result of work that was not carried out in the strict temporal order in which it is presented, the order of chapters does follow increasing knowledge of the studied fluvial aquifer and its wider context.

An overview of each single chapter is given in more detail in the following paragraphs, together with reference to the journal article for the chapters that have been published or have been submitted for consideration for publication (under review at the time of writing).
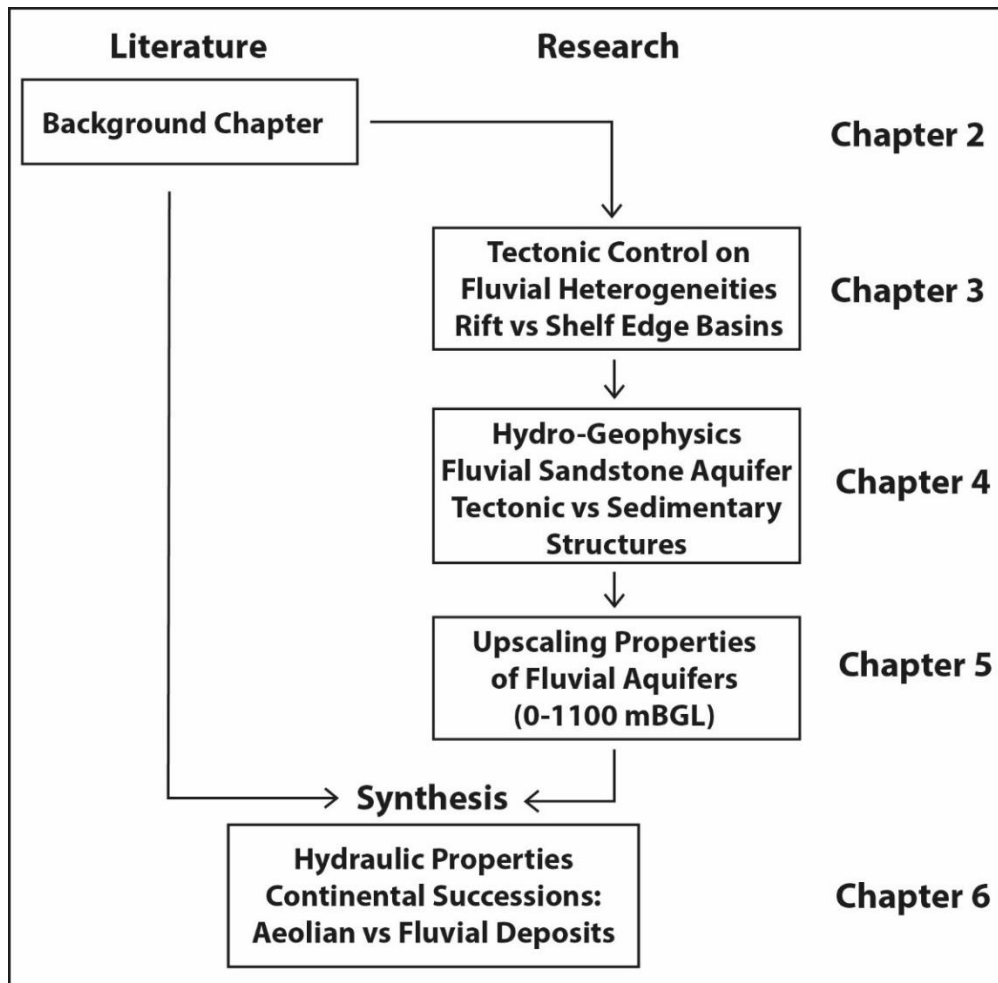
Figure 1.2: Flow chart depicting the thesis structure and relationships between background information and research undertaken.

Chapter 2: Sedimentary, tectonic and hydraulic properties of the Sherwood Sandstone aquifer

Chapter 2 discusses the current state of knowledge on the sedimentological, structural, mechanical and hydraulic features of the UK Sherwood Sandstone aquifer in the Wessex, Worcester, Needwood,

Staffordshire, eastern England Shelf, Cheshire, eastern Irish Sea, Vale of Eden and Carlisle basins (Figure 1.1). This chapter covers both the aeolian and fluvial deposits of the Sherwood Sandstone aquifer, highlighting their importance as reservoir analogues for similar continental successions in the North Sea and Irish Sea regions.

Chapter 3: Characterization of the sedimentology of the fluvial deposits of Sherwood Sandstone Group in the eastern Irish Sea Basin and eastern England Shelf

The main results of this chapter have been published as follows: Medici, G., Boulesteix, K., Mountney, N.P., West, L.J. and Odling, N.E. 2015. Palaeoenvironment of braided fluvial systems in different tectonic realms of the Triassic Sherwood Sandstone Group, UK. Sedimentary Geology, 329, pp.188-210. Doi:10.1016/j.sedgeo.2015.09.012.

Chapter 3 presents new data from outcrop and interpretation of the fluvial sedimentary architectures of the Sherwood Sandstone Group of the St Bees Sandstone Formation, eastern Irish Sea Basin (a half-graben) which is compared with similar fluvial deposits of the eastern England Shelf (a shelf-edge basin). The two studied successions represent the preserved deposits of braided fluvial systems that were influenced by common allogenic factors (climate, sediment source, delivery style); differences in preserved sedimentary style principally reflect their different tectonics settings. Thus, in this chapter, attention is given to how the different subsidence rates affected preservation of finer-grained heterogeneities, including both low-flow stage silty drape units that cap the channelized deposits and sheet-like mudstone elements that occur interbedded with channelized elements, and which represent the deposits of fluvial overbank flood events.

Chapter 4: Hydro-geophysical characterization of the St Bees Sandstone aquifer: sedimentary vs. tectonic heterogeneities

The main results of this chapter have been published as follows: Medici, G., West, L.J. and Mountney, N.P. 2016. Characterizing flow pathways in a sandstone aquifer: Tectonic vs. sedimentary heterogeneities. Journal of Contaminant Hydrology, 194, pp. 36-58. Doi: 10.1016/j.jconhyd.2016.09.008.

Chapter 4 describes in detail the sedimentary (white silty drape sandstone, mudstone occurring interbedded with fluvial channel sandstone) and tectonic (stratabound joints, normal faults) heterogeneities of the St Bees Sandstone aquifer of West Cumbria using imaging and wireline logs at relatively shallow depths (< ~ 150 mBGL). Additionally, quantitative flow logging analyses on faulted and un-faulted boreholes reveal the respective contribution to flow of (i) fault structures, (ii) principal bedding plane fractures showing development of karst-like features, and (iii) clusters of minor bedding-plane fractures. The findings of these hydro-geophysical studies have also been compared with those of an earlier investigation of the deeper St Bees Sandstone aquifer (150 to 400 m subsurface depth) and to similar sandstone deposits in the Triassic Cheshire Basin, UK. The work highlights the high efficiency of fracture flow in the St Bees Sandstone aquifer at shallow depths.

Chapter 5: Comparison of field and plug scale hydrogeological properties of the St Bees Sandstone aquifer

The main results of this chapter have been submitted for consideration for publication as follows: Medici, G., West, L.J. and Mountney, N.P. 2017. Multi-scale properties of aquifers hosted in fluvial sedimentary successions. Hydrogeology Journal, *submitted*.

Chapter 5 describes the nature of permeability from plug up to the field-scale in the Triassic St Bees Sandstone Formation, which represents a generally well-cemented fluvial sequence. Additionally, this fluvial aquifer has been studied at a range of depths from outcrop up to ~1 km depth.

Thus, both the vadose and phreatic zone of this fluvial aquifer have been studied. Also, scaling differences (permeability, flow anisotropy) have been interpreted taking into account the acquired knowledge of both the sedimentary features and fracturing pattern of the St Bees Sandstone aquifer.

Chapter 6: Discussion

Chapter 6 synthesises chapters 2, 3, 4 and 5, and discuss the new results from this research on the St Bees Sandstone aquifer with the previously published literature on the entire UK Sherwood Sandstone Group and analogous successions around the world. Additionally, the wider implications of this study are also discussed since the new findings can be used for benefit of hydrocarbon exploration to enhance oil recovery. The synthesis shows how a hydraulic study of an intermediate-to-deep (~150-1100 mBGL) fluvial aquifer can provide useful insights for hydrocarbon exploration at more elevated depths. Also, Chapter 6 presents a detailed synthesis of sedimentological, structural and hydrogeological data from the Triassic fluvial and aeolian deposits of England, showing how rift-related subsidence rates and distance from the sediment source influence the aquifer hydraulic properties, with possible application for reservoir quality prediction.

Chapter 7: Conclusions

Chapter 7 provides a concise overview of the thesis and re-considers the original questions posed in the introduction to this work. Additionally, this chapter concludes the thesis by postulating a set of additional research questions that could be used to further advance our present understanding of aquifer and reservoirs of continental origin (and indeed other siliciclastic porous media).

Chapter 2

Sedimentary, tectonic and hydraulic properties of the Sherwood Sandstone aquifer

2.1 Geological framework

The Triassic Sherwood Sandstone Group (~251-235 Myr; Induan-Ladinian) comprises a continental sedimentary succession accumulated in a series of sedimentary basins developed in the interior of the Pangean supercontinent in response to the phase of rifting that preceded the opening of the Atlantic Ocean (Coward, 1995; Glennie, 1995; Ziegler and Dèzes, 2006; Tyrrel et al 2012). The majority of the accumulated deposits of the "Sherwood Sandstone" have long been ascribed to a mixed fluvial and aeolian origin (e.g., Thompson, 1970a, b; Cowan, 1993, Thompson and Meadows, 1997; Mountney and Thompson; 2002; Holliday et al., 2008). Collectively, the assemblage of lithofacies present in the succession demonstrates accumulation under the influence of an arid to semi-arid climatic regime, which characterized the Mesozoic basins in England and SW Scotland (Figure 2.1a, b) during much of the Triassic (Warrington and Ivimey-Cooke, 1992; Glennie, 1995; Brookfield, 2004, 2008; Schmid et al., 2004, 2006).

2.1.1 Tectonics

Mesozoic extensional tectonic events created several basins and elevated areas in NW Europe during the Permo-Triassic (Figure 2.1). The morpho-structural highs served as a principal source of sediment for fluvial systems. Extensional tectonics continued after the Permo-Triassic climax and continued to affect basins in England throughout much of the Jurassic and Cretaceous (Ameen, 1995; Chadwick and Evans; 1995; Chadwick, 1997; Plant et al., 1999). Since this time, NW Europe has experienced uplift

during the Cenozoic, partly in response to vertical lithosphere rebound (Ziegler, 1987; Hillis et al., 2008; Carminati et al., 2009). The Cenozoic uplift of Great Britain has been related either to the seafloor spreading or to the transit underneath the European Plate of a lighter and buoyant asthenosphere (Brodie and White, 1994; Carminati et al., 2009). This vertical lithospheric uplift resulted in the development of vertical stratabound fractures (*sensu* Odling et al., 1999), which pervade much of the Sherwood Sandstone Group succession; this mechanism favours development of joints stopping in correspondence of the horizontal bedding discontinuities (Hitchmough et al., 2007). At the same time as vertical lithospheric movements, the Triassic basins of England were inverted with reactivation of normal faults due to the far-field effects of the Alpine orogenesis (Chadwick et al., 1994; Chadwick, 1997). The influence and record of inversion tectonics is detected principally in seismic lines from the Cheshire Basin, Needwood Basin and eastern Irish Sea Basin. Here inversion has only to slightly reduced Mesozoic downthrows (Chadwick et al., 1994). As consequence, nowadays, Triassic palaeo-horsts and basins continue to represent elevated and lowered areas, respectively (Figure 2.1a, b; Chadwick, 1997).

The Sherwood Sandstone Group outcrops as the exhumed fill of a suite of basins in England and SW Scotland (Figure 2.1b). The succession has been detected in boreholes from South of England up to the border with Scotland. The succession accumulated in a series of Permo-Triassic basins: in the West Midlands of England are the Staffordshire, Needwood and Cheshire basins; in northwest England are the eastern Irish Sea and Vale of Eden basins; and at the border between England and Scotland is located the Carlisle (or Solway) basin. All these basins represent half graben-type basins (Chadwick, 1994; Coward, 1995; Chadwick, 1997; Akhurst et al., 1998; Ambrose et al., 2014). However, in southern England, the Wessex and the Worcester basins are symmetric grabens bounded at both sides by major normal faults. To the east of the Pennine hills, the Triassic succession of the eastern England Shelf represents an exception

to this tectonic framework: this shelf-edge basin did not experience episodes of rifting activity (Bricker et al, 2012; Wakefield et al., 2015).
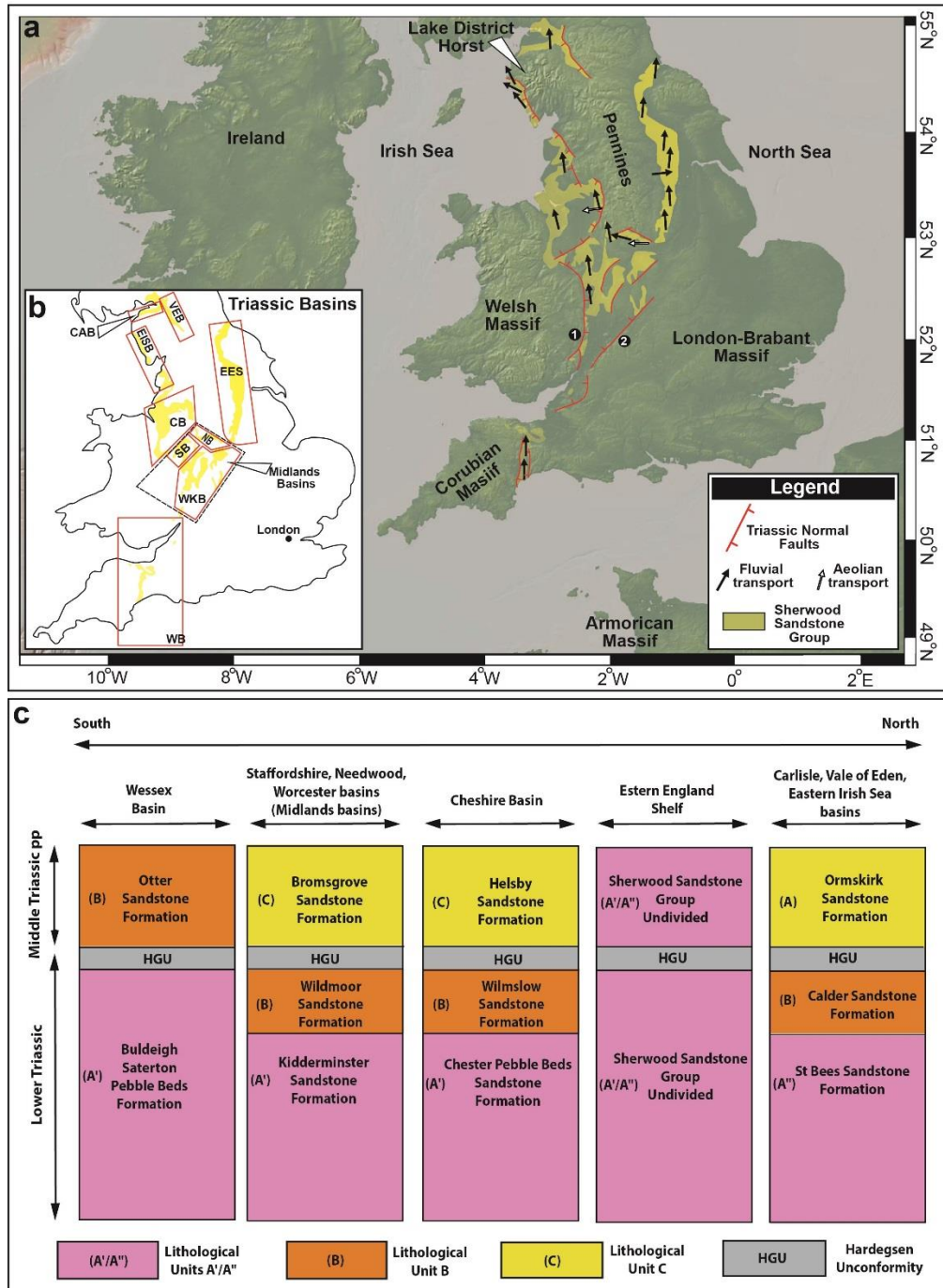
Figure 2.1: Triassic siliciclastic deposits in NW Europe. (a) Fluvial and aeolian palaeocurrents (data sources are discussed in the text), (b) Triassic basins in Great Britain (from Wakefield et al., 2015), (c) Lithostratigraphic nomenclature of the Sherwood Sandstone Group in the Triassic basins of Great Britain (modified from Ambrose et al., 2014).

The different structural styles correspond to sedimentary basins that experienced different rates of tectonic subsidence. Back stripping curves (Evans et al., 1993, Chadwick et al., 1994; Worden et al., 2016) – which were determined for the Lower Triassic using apatite fission track analysis techniques – indicate how the eastern Irish Sea Basin is characterized by relatively high rates of extensional tectonic subsidence (210 m/Myr) compared to the Cheshire (140 m/Myr) and the Wessex (10 m/Myr) basins. Furthermore, Burley (1984) determined that the maximum burial depth of the Sherwood Sandstone Group in the eastern England Shelf at the end of the Mesozoic extensional phase was limited to 1000 m, based on a study of mineralogical association of cement types. This value of maximum burial depth must be distributed over the entire Mesozoic time due to the non rifted nature of this basin which experienced slow tectonic subsidence at regular rates driven by lithostatic load and thermal lithospheric cooling (Burley, 1984; Whittaker, 1985; Green, 1989; Bray et al., 1992). Thus, the eastern England Shelf reached 1000 m of burial in ~185 Myr (Mesozoic time) providing an average subsidence of ~5 m/Myr for the eastern England Shelf (Burley, 1984, Green, 1989).

Hence, the eastern England Shelf represents the slowest subsiding Triassic basin of England, reflecting its structural framework, for which Triassic bounding faults are absent and subsidence related driving forces were dependent solely on only thermal subsidence (Mckie and Williams, 2009; Štolfová and Shannon, 2009). A paucity of diagenetic studies which might have been useful for the reconstruction of burial depths means that tectonic subsidence rates of other Triassic basins in England are poorly constrained. However, thickness of the Sherwood Sandstone succession in each Triassic sedimentary basin is well constrained by the availability of numerous seismic lines and boreholes (Allen et al., 1997; Nirex, 1997; Kattenthorn and Pollard, 2001; Edmunds and Smedley, 2002; Ambrose et al., 2014). Furthermore, the age of the Triassic Sherwood Sandstone Group succession is known from radiometric dating as well as stratigraphic relationships with adjacent units (Warrington et al., 1980; Steel and Thompson, 1983, Edwards et al., 1997, British Geological Survey, 2015).

Thus, accommodation generation rates are available for all the Triassic basins (Table 2.1) given knowledge of both thickness and time-span of accumulation. The time-averaged rate of sediment accommodation generation is obtained by dividing average thickness of the sedimentary sequence by the deposition time span of the Sherwood Sandstone Group (Table 2.1). The average thickness Sherwood Sandstone Group has been corrected using the value for the erosion due to the Hardegsen unconformity which is typically 150 m in the onshore-areas (Evans et al., 1993; Bourquin et al 2006, 2009; McKie and Williams, 2009). This unconformity has been related to a climax of extensional tectonics leading to erosion due to interplays between footwall uplift, flexural warping and isostatic rebound (Jackson and McKenzie, 1983; Evans et al., 1993; Bourquin et al., 2011). The correction has been made on calculation of sediment accommodation generation rates since this unconformity is documented across large part of the Triassic realm of NW Europe (Bourquin et al., 2006, 2011). Sediment accommodation generation rates typically reflect the rate of tectonic subsidence related to either fault-activity or thermal cooling in the UK Triassic basins (Mckie and Williams, 2009; Štolfová and Shannon, 2009). Direct relation between subsidence and tectonic activity in the tectonic realms of the Sherwood Sandstone Group can be assessed by comparing tectonic subsidence with sediment accommodation generation rates. The eastern Irish Sea Basin and the eastern England Shelf show the highest and lowest subsidence values in England, respectively (Burley, 1984; Evans et al., 1993; Chadwick et al., 1994; Worden et al, 2016). At the same time, these two Triassic basins represent two end members also with regards to sediment accommodation generation rates (Table 2.1). The Cheshire Basin is characterized both by relatively high tectonic subsidence (140 m/Myr) and accommodation generation rates which are lower only compared to those of the eastern Irish Sea Basin (Chadwick et al., 1994). However, all other Triassic basins (Wessex, Worcester, Needwood, Staffordshire, Carlisle and Vale of Eden basins) are likely to have undergone relatively slow rates of subsidence, i.e. characterized by relatively low values of sediment accommodation

generation rates, similar to the shelf-edge basin of the eastern England Shelf (Table 2.1).

Table 2.1: Age, thickness and sediment accommodation generation rates for the Sherwood Sandstone Group in the UK Triassic basins

Sedimentary basin	Time Span (Myr)	Average Thickness (m)	Accommodation Generation rate (m/Myr)
Wessex Basin	17.5 Myr (Edwards et al 1997)	200 (Allen et al 1997) (Kattenthon and Pollard, 2001)	20
Eastern England Shelf	18 Myr (Warrington et al., 1980)	10-250 (Edmunds and Smedley, 2002)	19
Cheshire Basin	6 Myr (Evans et al., 1993)	650 (Allen et al, 1997)	133
Needwood Basin	14 Myr (British Geological Survey, 2015)	350 (Wills 1970) (Ambrose et al 2014)	36
Staffordshire Basin	14 Myr (Steel and Thompson, 1983)	350 (Wills 1970) (Ambrose et al 2014)	36
Worcester Basin	14 Myr (British Geological Survey, 2015)	650 (Allen et al 1997)	57
Eastern Irish Sea Basin	12 Myr (Brookfield, 2004, 2008)	1650 (Nirex 1997)	150
Vale of Eden Basin	12 Myr (British Geological Survey, 2015)	275 (Allen et al 1997)	36
Carlisle Basin	12 Myr (Brookfield, 2004)	575 (Allen et al 1997) (Brookfield, 2004)	60

2.1.2 Sediment transport and provenance

Palaeocurrent data (Figure 2.1a) from fluvial facies are chiefly derived from cross-bedding of sand prone channel-fills (Smith and Francis, 1967; Edwards, 1967; Steel and Thompson, 1983, Smith, 1990; Gaunt et al., 1992; Powell et al., 1992; Gaunt, 1994; Jones and Ambrose, 1994; Gallois, 2004; Wackefield et al., 2015). Palaeocurrents from fluvial channels indicate a northward palaeoflow from the southern Wessex Basin via a series of linked basins to the Eastern Irish Sea, Vale of Eden and Carlisle basins in northern regions (Smith, 1990; Jones and Ambrose, 1994; Brookfield, 2004; Mckie and Williams, 2009).

Mineralogical and isotopic studies confirm how the southern Armorican Massif represents the principal sediment source for the Wessex, Worcester, Staffordshire, Needwood, Cheshire, eastern Irish Sea, Carlisle and Vale of Eden basins (Fitch et al., 1966; Manger et al., 1999; Tyrrel et al., 2012). Although detailed mineralogical and isotopic analyses are not available in the eastern England Shelf, palaeocurrents indicate a northward transport parallel to the axis of this shelf-edge basin as for the other Triassic basins (Figure 2.1, Smith and Francis, 1967; Edwards, 1967, Gaunt et al., 1992; Powell et al., 1992; Gaunt, 1994). Additionally, a northward decrease in mean grain size and maximum clast size (Smith and Francis, 1967; Allen et al., 1997; Wakefield et al., 2015) in the eastern England Shelf confirms a southern sediment source, which potentially is either represented by the Armorican or the London Brabant massifs (Figure 2.1). Several authors have identified the Armorican Massif as the primary sediment source in the eastern England Shelf (Campbell-Smith, 1963, Edwards, 1967; Warrington et al., 1980). Indeed, quarzitic breccias with clasts of similar size occur in both the southern part of the eastern England Shelf and in the Worcester Basin, Needwood and Staffordshire basins where isotopic and mineralogical analyses have confirmed the Armorican Massif as the principal sediment source (Campbell-Smith, 1963; Warrington et al.,, 1980; Fitch et al., 1966; Manger et al., 1999; Tyrrel et al., 2012).

Aeolian paleocurrent vectors derived from dune cross-bedding have been collected in the Needwood, Cheshire and eastern Irish Sea basins. Such data show bimodality, with a general pattern of north-eastward and south-westward directed aeolian dune migration (Thompson 1969, 1970a, b; Jones and Ambrose, 1994; Mountney and Thompson, 2002; McKie and Williams, 2009). Similar data on bimodality has also been recognized in other aeolian Triassic successions in NW Europe and likely reflects seasonal changes in trade winds (Mader and Yardley, 1985). Overall, south-westward dune migration is dominant in the aeolian deposits of the Sherwood Sandstone Group. This pattern might arise in response to the topography of exposed upland basement areas, which could have acted to locally divert the dominant wind direction (Jones and Ambrose, 1994; Mountney and Thompson, 2002; McKie and Williams, 2009). For example, Jones and Ambrose (1994) shows how aeolian deposits of the Calder and Ormskirk Sandstone formations are dominated by south-westward migrating dunes which are thought to have been influenced by a west-dipping topography due to the presence of the Lake District Horst (Figure 2.1).

2.2 Regional facies association

In the Triassic basins of England, facies associations (Figures 2.1b, 2.2, 2.3) show regional variations due to varying distances from the main sediment source (Armorican Massif), and tectonic and climatic variations (McKie and Williams, 2009; McKie and Shannon, 2011; Tyrrel et al., 2012). In all the Triassic basins of England, the basal part of the Sherwood Sandstone Group is exclusively characterized by fluvial deposits, which are dominated by channelized architectural elements (Ambrose et al., 2014). An overall northward decrease in mean grain-size and maximum clast size characterizes the fluvial deposits of the Sherwood Sandstone Group, reflecting the increasing distance from the sediment source (Smith, 1990; Steel and Thompson, 1983; McKie and Williams, 2009). In fact, fluvial deposits of the lower Triassic pass from conglomerates with interbedded

pebbly sandstone in the Wessex, Worcester, Staffordshire, Needwood, Cheshire and southern eastern England Shelf basins to medium-fine grained sandstone in the northern part of the eastern England Shelf, eastern Irish Sea Basin, Vale of Eden and Carlisle basins (McKie and Williams, 2009; Ambrose et al., 2014). In this work these basal fluvial deposits are differentiated as A' and A" units, which represent (i) conglomerate with pebbly sandstone and (ii) fine-medium grained sandstone, respectively (Figure 2.1b).

The Sherwood Sandstone Group passes upwards into sandy deposits which become progressively more abundant in aeolian facies (Jones and Ambrose, 1994; Mountney and Thompson, 2002; Ambrose et al., 2014). Thus, two units which are named B and C are differentiated from the basal A and A" units by presence of both aeolian and fluvial deposits. However, the lower unit B and the upper unit C are distinguished based on the relatively lower and higher occurrence of aeolian facies associations, respectively (Figure 2.1b.). Arid climatic conditions were widespread across much of NW Europe during the Lower Triassic time, although episodically wetter episodes occurred (Brookfield, 2004, 2008; McKie et al., 2009; Mckie and Shannon, 2011). Thus, the upward increasing of aeolian facies content does not reflect increasing aridity, but it is likely due to a progressive switch-off or avulsion of the southerly fluvial system (Meadows and Beach 1993a, b; Jones and Ambrose, 1994). Notably, Mckie and Williams (2009) identify a general northward increase in the proportion of aeolian facies in a comparison of the upper part of the Sherwood Sandstone Group in the Wessex Basin (8% aeolian and 92% fluvial origin Otter Sandstone Formation) and in the eastern Irish Sea Basin, Vale of Eden and Carlisle basins (99% aeolian and 1% fluvial origin Ormskirk Sandstone Formation) further north (Jones and Ambrose, 1994; Gallois, 2004; Ambrose et al., 2014). This contrast in aeolian facies content can be interpreted to have arisen in response to a gradual downstream reduction in the discharge of the braided fluvial systems with increasing distance from the sediment entering the arid-climate linked basin system (Jones and Ambrose, 1994; McKie and Williams, 2009; McKie and Shannon, 2011).

Although this is consistent with the palaeogeographic scenario for the Triassic of NW Europe, extensional tectonics may also play a role in the preferential preservation of aeolian facies favouring wind deceleration and rapid burial of sediments below the water table (Gawthorpe and Leeder, 2000; Mountney, 2012). By contrast, aeolian deposits are absent throughout the entire succession of the eastern England Shelf Basin (Smith and Francis, 1967; West and Truss, 2006; Wakefield et al., 2015). Preservation of aeolian facies in the eastern Irish Sea Basin (Calder and Ormskirk Sandstone formations) and their absence in the eastern England Shelf can also be related to the different rates of accommodation generation (Table 2.1). In fact, high rates of tectonic subsidence in the eastern Irish Sea Basin may (as in other tectonically active basins) have assisted long-term preservation of aeolian deposits by placing them beneath the local water table (cf. Howell and Mountney, 1997; Mountney, 2012; Rodríguez-López et al., 2014).
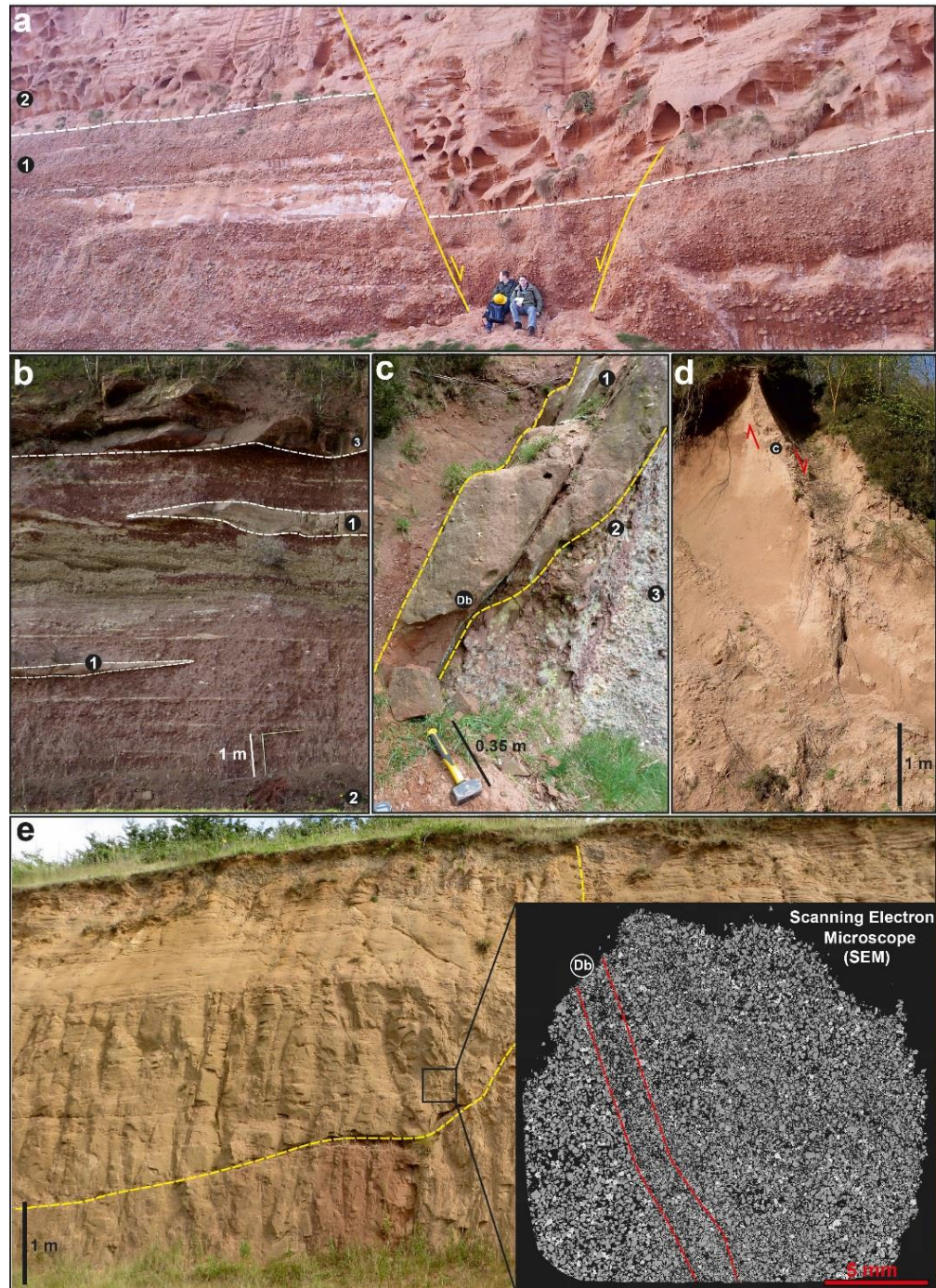
Figure 2.2: Outcropping Sherwood Sandstone Group in England (see Figure 2.1b for location of sedimentary basins). (a) Geological limit between the (1) conglomerate of the Buldeigh Saltertion Pebble Beds and the (2) aeolian Otter Sandstone formations in the Wessex Basin, (b) conglomerate and interbedded sandstone sheets in the Kidderminster Sandstone Formation of the Staffordshire Basin, (c) Fault core with granulation seams in the Kidderminster Sandstone Formation of the Staffordshire Basin, (d) Fault core in the altered Kidderminster Sandstone Formation of the Staffordshire Basin, (e) Normal fault with granulation seams in the Sherwood Sandstone Group of the eastern England Shelf.
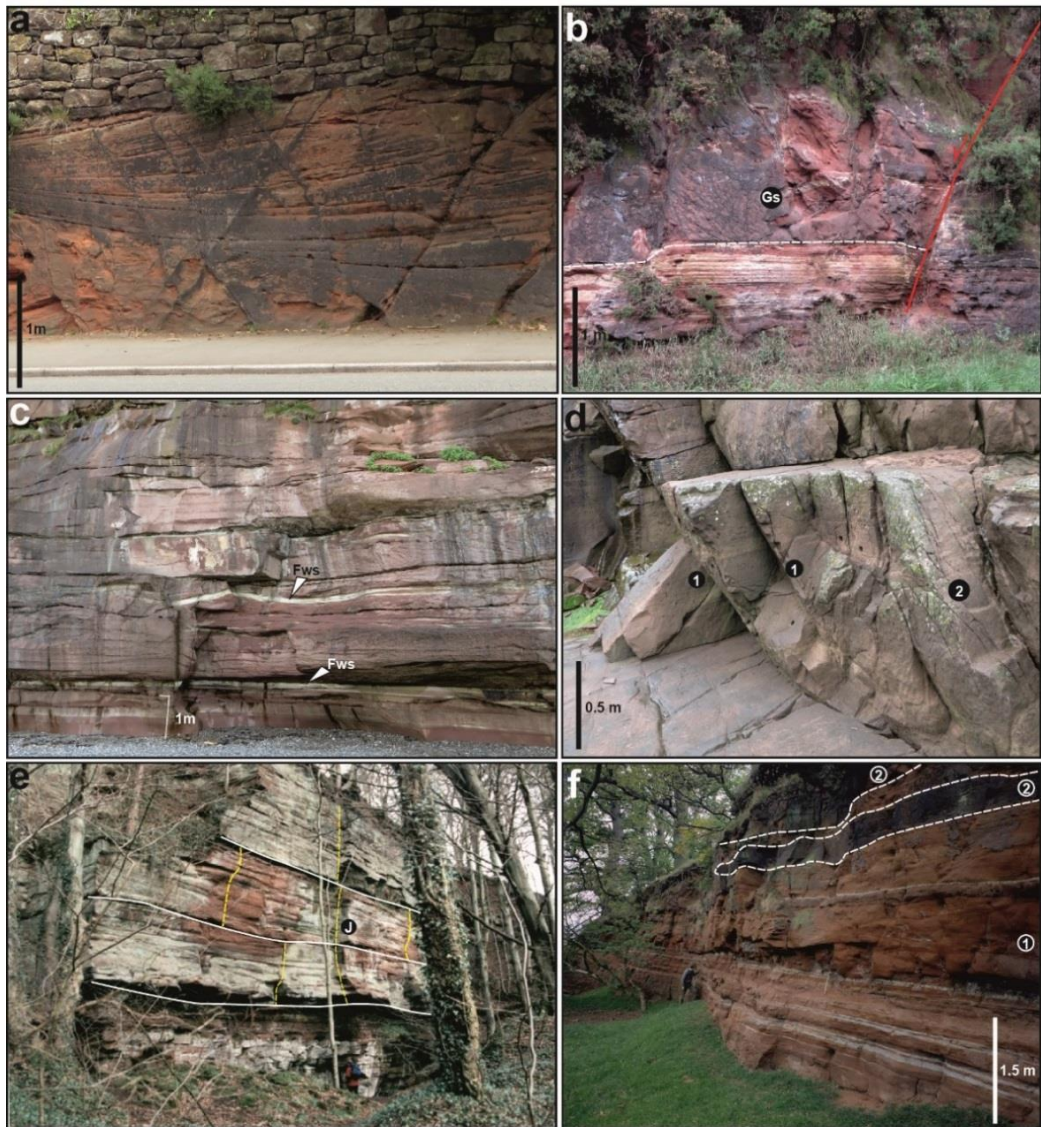
Figure 2.3: Outcropping Sherwood Sandstone Group in England (see Figure 2.1b for location of sedimentary basin). (a) Occurrence of granulation seams in conjugate sets in the aeolian dunes of the Helsby Sandstone Formation in the Cheshire Basin, (b) Swarms of granulation seams (Gs) in the in the aeolian deposits of the Helsby Sandstone Formation of the Cheshire Basin (2), (c) Amalgamated fluvial channels in the St Bees Sandstone Formation of the eastern Irish Sea Basin, (d) Normal fault in St Bees Sandstone Formation of the eastern Irish Sea Basin: (1) open fracture vs. (2) granulation seams, (e) Stratabound joints in the Ormskirk Sandstone Formation of the Cheshire Basin (Halliday et al., 2008), (f) (1) Mudstone deposited by unconfined flow and (2) fluvial channels interbedded in the basal St Bees Sandstone Formation of the Vale of Eden (from Millward et al., 2010).

2.2.1 Fluvial conglomerate and pebbly-sandstone facies association

This facies association (Figure 2.2 a-c) includes conglomerate and interfingered pebbly-sandstone (Unit A') forming successions up to hundreds of metres thick (Warrington et al., 1980; Steel and Thompson, 1983) characterizing the relatively southern Triassic grabens of the Wessex, Worcester, Staffordshire, Needwood and Cheshire basins. Also, this coarse grained facies association represents a productive hydrocarbon lithology at the Wytch Farm in Dorset and has been penetrated by wells in the western English Channel during hydrocarbon exploration (Mckie and Williams, 2009). This facies association also dominates in the southern part of the eastern England Shelf but progressively disappears northward at increasing distance from the potential sediment source represented by the Armorican and London-Brabant massifs (McKie and Williams, 2009; Wackefield et al., 2015). Notably, conglomerates interbedded with pebbly-sandstone are absent in the eastern Irish Sea Basin, Vale of Eden and Carlisle basins (Jones and Ambrose, 1994; Brookfield, 2004; Holliday et al., 2008).

These coarse-grained fluvial deposits outcropping in the Wessex, Worcester, Staffordshire, Cheshire and southern England Shelf basins typically comprise laterally extensive and amalgamated sheets of cross-bedded and parallel laminated conglomerates, together with sand-prone interbedded lenses (Figure 2.2b). The depositional environment of the conglomerate was interpreted as braided, bedload dominated and confined streams (Steel and Thompson, 1983; Smith, 1990). However, sheets of pebbly sandstone lying between the conglomerates largely represent deposition from sandwaves and dunes (Steel and Thompson, 1983).

2.2.2 Sand-prone channel and floodplain facies association

Sand-prone fluvial channels (Unit A") represent the most typical deposits in the Sherwood Sandstone Group, also forming the principal reservoir lithology for several hydrocarbon fields in the Central and Viking graben of

the North Sea and the Corrib Field in the western Irish Sea (Fisher and Mudge, 1998; Schmid et al 2004). In the subsurface as well as in outcrop, these sand-prone channels are characterized by erosively based, fining upward sandbodies up to 6 m thick, dominated by cross-bedded and parallel laminated fine to medium grained sandstone beds which are typically related to braided river systems (Jones and Ambrose, 1994; Schmid et al. 2004; Mckie and Williams, 2009; Wakefield et al., 2015; Olivarious, 2016). Sandstone-prone channel elements (Figures 2.2e, 2.3c) occur at the base of the fluvial succession in the eastern Irish Sea, Carlisle and Vale of Eden basins, where they in places occur interbedded with mudstone and sheet-like sandstone which were deposited by non-confined flood events in fluvial floodplain settings. However, the sandy channels occurring interbedded with mudstone and sheet-like sandstone represent crevasse channels (Figure 2.3f) feeding mudstone and sheet-like sandstone characterizing the floodplain (Jones and Ambrose, 1994; Brookfield, 2004; Holliday et al., 2008).

Moving upward in the fluvial successions of the basins, the sand prone-channel elements become progressively more amalgamated in the Triassic fill of the eastern Irish Sea Basin and the Carlisle and Vale of Eden basins, although mudstone elements of fluvial overbank origin remain interbedded with and, in places, occur within the channelized architectural elements (Jones and Ambrose, 1994; Nirex, 1997; Holliday et al., 2008). Sand prone-channel elements also occur in the eastern England Shelf (Figure 2.2e), where they are characterised by a progressive reduction in grain-size to the north, with increasing distance from the principal source of sediment which is represented by the Armorican Massif (Tyrrel et al., 2012). Despite this general trend, the eastern England Shelf although relatively high latitude and hence distant from the sediment source (Figure 2.1; Doncaster area) is characterized, according to core and quarry stratigraphic logs, by more abundance in pebbly-lithofacies than the eastern Irish Sea Basin. Pebbly lithofacies represent 5% and 46% in the eastern Irish Sea Basin in West Cumbria and in the eastern England Shelf in the Doncaster area, respectively (Gaunt et al., 1992; Gaunt, 1994; Nirex, 1997; Pokar et al.,

2006; West and Truss, 2006; Wakefield et al., 2015). Notably, the fluvial deposits of the eastern England Shelf are also characterized by significantly lower amount of mudstone (interlayered with sand-prone channels) compared with those of the eastern Irish Sea Basin, 2% vs. 8%, respectively (Gaunt, 1994; Nirex, 1997; Pokar et al., 2006; West and Truss, 2006; Wackfield et al., 2015). The role of tectonic subsidence as a control on fluvial lithofacies distribution in the eastern England Shelf and the eastern Irish Sea Basin represent a specific research objective of this study.

2.2.3 Aeolian facies association

Aeolian deposits (Figures. 2.2a, 2.3a, b, e) occur in the Sherwood Sandstone Group either interbedded on a metre-scale with fluvial channels or as vertically continuous intervals up to 200 m thick (Jones and Ambrose, 1994; Mountney and Thompson, 2002, McKie and Williams, 2009). Examples of the latter case are common in the eastern Irish Sea Basin since aeolian facies characterize 80% and 99% of the successions in the Calder (Unit B) and Ormskirk Sandstone (Unit C) formations, respectively (Jones and Ambrose, 1994). Aeolian deposits in the Sherwood Sandstone Group are generally dominated by cross-bedded sandy dunes, although very fine-grained sandstone of damp interdune origin also occurs (e.g., Thompson, 1970a, Mountney and Thompson, 2002). Rarely, siltstone laminae representing wet interdune deposits also characterize aeolian deposition in the Sherwood Sandstone Group (Mountney and Thompson, 2002). Notably, aeolian facies are described in all the Triassic basins in England with the exception of the eastern England Shelf (Ambrose et al., 2014). Analogous Triassic aeolian facies have been recognized in the producing hydrocarbon fields of Morecambe in the Irish Sea and Wytch Farm in Dorset (Meadows and Beach, 1993a, b; Katternhorn and Pollard, 2001). Aeolian deposits have also been intercepted in exploration wells on-shore in the North German Basin as well as off-shore in the Danish North Sea (Clemmensen, 1985; Goldsmith et al., 1995; Olivarious et al., 2015,

2016). Additionally, although the Lower Triassic in the UK and Norwegian sector of the North Sea is dominated by fluvial deposits, wind ripple laminations and small dunes have been recoded in cores (McKie et al., 2005, 2010; McKie and Williams, 2009).

2.3 Mechanical properties

The Sherwood Sandstone Group is characterized by a wide range of uniaxial compressive strength values (0-36 MPa), which describe weak up to moderately strong rocks (Hawkins et al., 1992; Yates, 1992; Charalambous et al., 2012). Uniaxial compressive strengths (UCS_{nat}) which were tested under natural saturation conditions show regional differences across Great Britain (Table 2.2). In fact, samples for the Sherwood Sandstone Group from the slow-subsiding basins of the Worcester and eastern England Shelf show UCS_{nat} <22 MPa (Thompson and Leach, 1985; Whithworth and Turner, 1989). By contrast, the Sherwood Sandstone Group in the fast subsiding basins of Cheshire and eastern Irish Sea show relatively higher UCS_{nat} values (Table 2.2). Notably, the highest values of uniaxial compressive strength (36 MPa) correspond to the basal Sherwood Sandstone of the eastern Irish Sea Basin which is the fastest subsiding Triassic basin in England (Evans et al, 1993; Chadwick et al., 1994; Worden et al., 2016). This value of uniaxial compression strength in natural conditions is higher also compared to the Triassic Sandstone of the North German Basin which show values ranging from 5 up to 11 MPa (Smoltczyk and Gartung, 1979; Yates, 1992). The hypothesis of a regional control on the mechanical properties due to different burial depths of the Sherwood Sandstone Group is also supported by the diagenetic studies undertaken on the Sherwood Sandstone Group (Burley, 1984, Worden and Burley, 2003; Worden et al. 2016). In fact, detailed studies on cement filling pores indicate how the post-uplift diagenetic events play a minor role respect to early-stage and burial diagenesis in the UK Triassic basins (Burley, 1984, Worden and Burley, 2003).

Table 2.2: Uniaxial compressional strength values under natural conditions (UCS$_{nat}$) for the Sherwood Sandstone Group across England.

Sedimentary Basin	Lithological unit	UCS$_{nat}$ (MPa)	Reference
Worcester Basin	A'/C	0-16	Whithworth and Turner (1989)
Cheshire Basin	B	31	West (1979)
Eastern England Shelf	A'	1-22	Walsby et al (1993)
Eastern Irish Sea Basin	A''	17-36	Thompson and Leach (1985)

2.4 Petrophysical properties

Petrophysical properties of the Sherwood Sandstone aquifer have been massively investigated by combining plug-scale analysis and wire-line logs due to the importance of the Sherwood Sandstone, which represents at the same time the second-most important UK aquifer and a strategic reservoir analogue for the off-shore areas in NW Europe (Tellam and Barker, 2006; McKie and Shannon, 2011; Ambrose et al., 2014; Olivarious et al., 2016). Hence, a detailed review of the available petrophysical data (Allen et al., 1997; Bloomfield et al., 2006; Bouch et al., 2006; Koukis, 1978; Nirex, 1993 a, b; Pokar et al., 2006) on the Sherwood Sandstone Group allows extraction of quantitative information on the sedimentary and tectonic heterogeneities of continental sequences.

2.4.1 Regional vs. facies control

The Sherwood Sandstone Group across Great Britain presents typical matrix porosity and hydraulic conductivity values of 15 to 30% and 0.1-8.0 m/day, respectively (e.g., Allen et al., 1997; Bloomfield et al., 2006; Pokar et al., 2006). Notably, the petrophysical properties of the Sherwood Sandstone Group shows regional differences (Table 2.3) which may be explained by the different burial history that the UK Triassic basins experienced before the Cenozoic uplift of NW Europe (Evans et al., 1993;

Carminati et al., 2009; Worden et al., 2016). Alternatively, differences in facies associations due either to the different distance from the sediment source or different proportion of aeolian versus fluvial facies may be responsible (Tellam and Barker, 2006; McKie and Williams, 2009). Subsidence and sediment accommodation generation rates (Table 2.1) are directly related in the Sherwood Sandstone. Also, the latter two factors influence the petrophysical properties of the Sherwood Sandstone aquifer (Tables 2.3). In fact, evidence of the importance of Triassic tectonics in controlling regional differences on petrophysical properties on the Sherwood Sandstone Group are evident, comparing the half graben basin of the eastern Irish Sea with the shelf-edge basin of the eastern England Shelf. The fastest subsiding basin, the eastern Irish Sea Basin and the slowest subsiding eastern England Shelf are characterized by the lowest and highest porosity and matrix permeability values, respectively (Table, 2.3).

Other Triassic basins which are characterized by intermediate subsidence or sediment accommodation generation rates show intermediate porosity and plug-scale permeability (Table 2.3). Additionally, the eastern Irish Sea and the eastern England Shelf basins also represent end members with regards to uniaxial strength (Table 2.2). Thus, subsidence rates and Triassic tectonics seem to play a key role on controlling the physical properties properties of the Sherwood Sandstone Group aquifer in England. However, facies associations play a key role on petrophysics at the scale of the single region.

The Cheshire, Midlands (i.e. Staffordshire, Needwood and Wessex basins which were grouped together by Allen et al., 1997, due to similarity in terms of facies and petrophysical properties) and eastern Irish Sea basins are characterized by occurrence of both aeolian and fluvial facies. In fact, exclusively fluvial (Kiddeminster Sandstone and Chester Pebble Beds formations) and fluvial-dominated (Wilmslow Sandstone Formation) formations are less porous (Figure 2.4a) and permeable than the aeolian-dominated formations at the scale of the single region/basin (Allen et al.,

1997). This difference is particularly large in the eastern Irish Sea Basin which is abundant in aeolian facies which are also characterized by relatively higher intergranular permeability (McKie and Williams, 2009), i.e. the Calder Sandstone Formation is characterized by 80% aeolian facies. This explains the average porosity (ϕ_{Cs}/ϕ_{Sbs}~2) and intergranular permeability (K_{Cs}/K_{Sbs}~5) increasing from the fluvial St Bees Sandstone (Sbs) to the aeolian Calder Sandstone (Cs) formations (Allen, 1997; Nirex 1993 a, b). These differences in matrix porosity (Figure 2.4a) which were measured on core plugs match the systematic increases in neutron porosity passing from fluvial to aeolian facies in wireline logs in the Triassic sandstone of NW Europe (Jones and Ambrose, 1994; Ambrose et al., 2014; Olivarious et al., 2015; 2016).

The eastern England Shelf which extends for ~200 kilometres in latitude (Figure 2.1) shows how distance from the sediment source control both lithofacies and petrophysical properties. In fact, grain size as well as relative importance of conglomerate and pebbly sandstone vs. fine to medium grained sandstone progressively decreases northwards (Edwards, 1967; Gaunt, 1994; Gaunt et al., 1992; Powell et al., 1992; Smith and Francis, 1967; Wakefield et al., 2015). Decreases in grain size at increasing distance from the southern sediment sources (Armorican and London Brabant massifs) match the decrease in porosity moving northwards (Figure 2.4b) of the eastern England Shelf (Allen et al., 1997; Koukis, 1978; Pokar et al., 2006). Additionally, plug-scale permeability also significantly reduces (~50%) northwards from the conglomerate and pebbly lithofacies of Nottinghamshire, to the fine-medium grained sandstone of the North Sea coast (Figure 2.1) in response to grain and porosity reduction (Allen et al., 1997).

Table 2.3: Porosity (ϕ) and hydraulic conductivity (m/day) of the Sherwood Sandstone Group measured both parallel (K_h) and perpendicular (K_v) respect to the bedding for the Worcester (WB), Midland (MB), eastern England Shelf, Cheshire, Eastern Irish Sea (EISB), Vale of Eden and Carlisle (CB) basins (data from Koukis et al., 1978; Nirex 1993 a, b, Allen et al., 1994; Bloomfield et al. 2006; Pokar et al. 2006).

Parameter	WB (n=114)	MB (n=410)	EES (n=1400)	CB (n=290)	EISB (n=228)	VEB (n=50)	CAB (n=16)
Maximum	ϕ= 36.0 K_h=4.3 K_v=1.2	ϕ= 36.2 K_h=15.0 K_v=12.0	ϕ= 37.4 K_h=22.5 K_v=20.5	ϕ= 34.7 K_h=4.1 K_v=3.1	ϕ= 26.3 K_h=9.4×10^{-1} K_v=2.1×10^{-1}	ϕ= 34.0 K_h=2.6×10^{-1} K_v=2.1×10^{-1}	ϕ= N/A K_h=0.5 K_v=N/A
Minimum	ϕ=3.0 K_h=2.0×10^{-6} K_v=1.9×10^{-6}	ϕ= 3.6 K_h=6.2×10^{-5} K_v=2.0×10^{-5}	ϕ= 7.8 K_h=1.0×10^{-6} K_v=1.9×10^{-6}	ϕ= 6.2 K_h=2.3×10^{-4} K_v=1.8×10^{-4}	ϕ= 1.5 K_h=2.0×10^{-6} K_v=1.9×10^{-6}	ϕ= 19.0 K_h=0.01 K_v=5.0×10^{-3}	ϕ= N/A K_h=0.2 K_v=N/A
Median	ϕ=14.8 K_h=8.9×10^{-3} K_h=2.4×10^{-3}	ϕ= 26.9 K_h=0.62 K_v=0.28	ϕ= 28.5 K_h=0.62 K_v=0.31	ϕ= 24.0 K_h=0.21 K_v=0.11	ϕ= 12.7 K_h=2.9×10^{-3} K_v= 7.0×10^{-4}	ϕ= 27.0 K_h=0.3 K_v=0.2	ϕ=N/A K_h=0.3 K_v=N/A
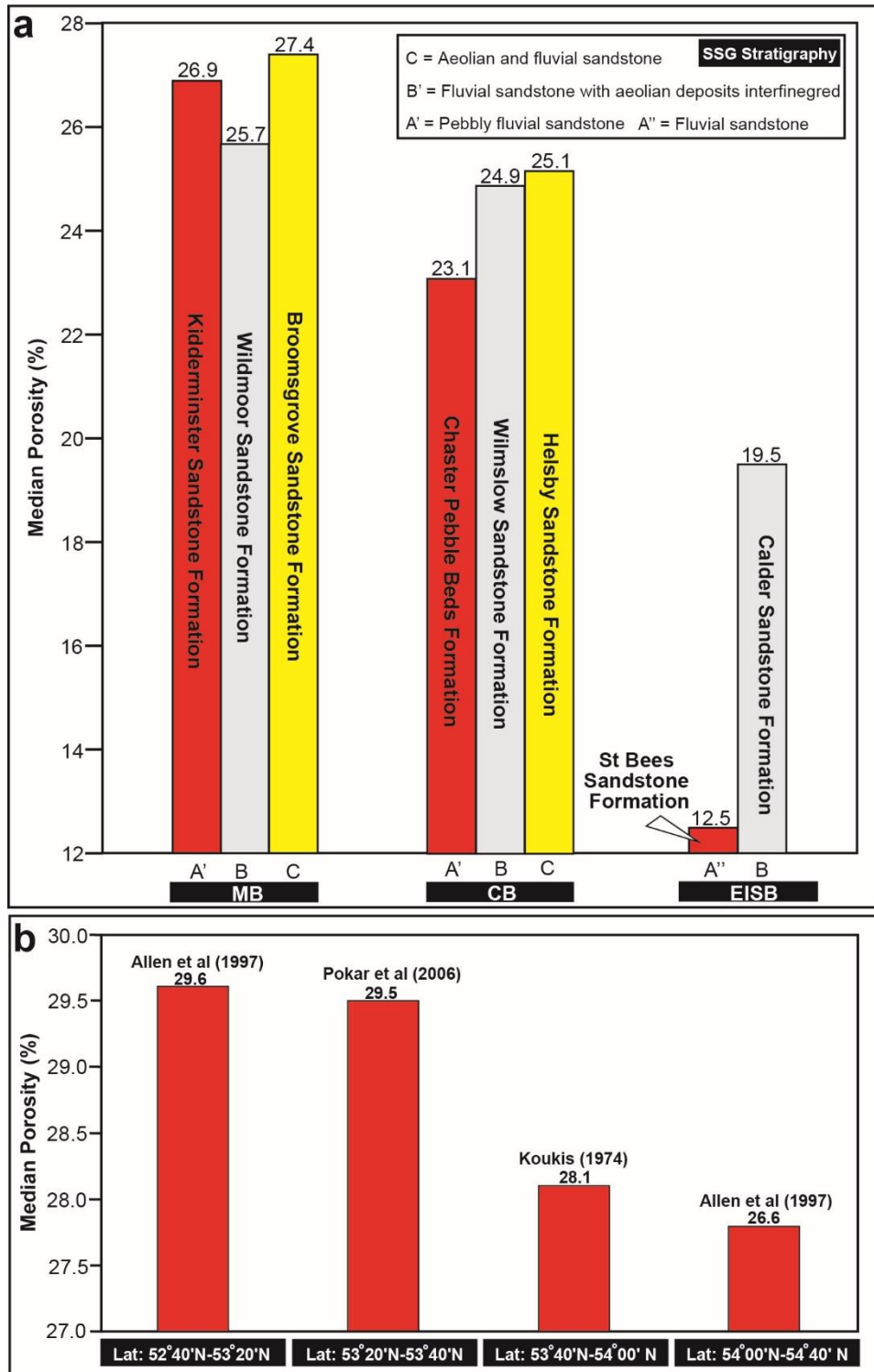
Figure 2.4: Porosity distribution at the scale of the single basin. (a) Median porosity in the Midlands, Cheshire and eastern England Shelf, (b) Median porosity vs. latitude in the eastern England Shelf

2.4.2 Low permeability layers

Low permeability layers are in first instance represented in the Sherwood Sandstone Group by mudstone deposits (Tellam and Barker, 2006). In fact, they are characterized by hydraulic conductivities ranging from 10^{-6} up to 10^{-2} m/day in the eastern Irish Sea Basin, Worcester, Needwood and Staffordshire basins significantly lower than the typical conglomeratic and sandy channel deposits of the Sherwood Sandstone Group (Figure 2.5a-g, Lovelock, 1977; Nirex 1993, b, c, Tellam and Barker, 2006). These mudstone (Figure 2.5b, c) deposits are related to non-confined fluvial events and they characterize the Triassic Sandstone also in the southern sedimentary basins (Jones and Ambrose, 1994; Smith, 1990; Ambrose et al., 2014; Wakefield et al., 2015). Plug-scale analyses realised on the fluvial St Bees Sandstone Formation also show how sheet-like sandstone due to overbank events represent low permeability layers with respect to fluvial channel deposits (Nirex, 1993 b, c).

Outcrop studies and borehole correlations show lateral continuity from a few meters up to tens of meters at increasing layer thickness (Nirex, 1997; Stanistreet and Stollhfen, 2002; Tellam and Barker, 2006). Mudstone layers also characterize aeolian palaeoenvironments representing wet interdunes.

Worcester, Staffordshire and Needwood Basins: Lithofacies vs Matrix Permeability
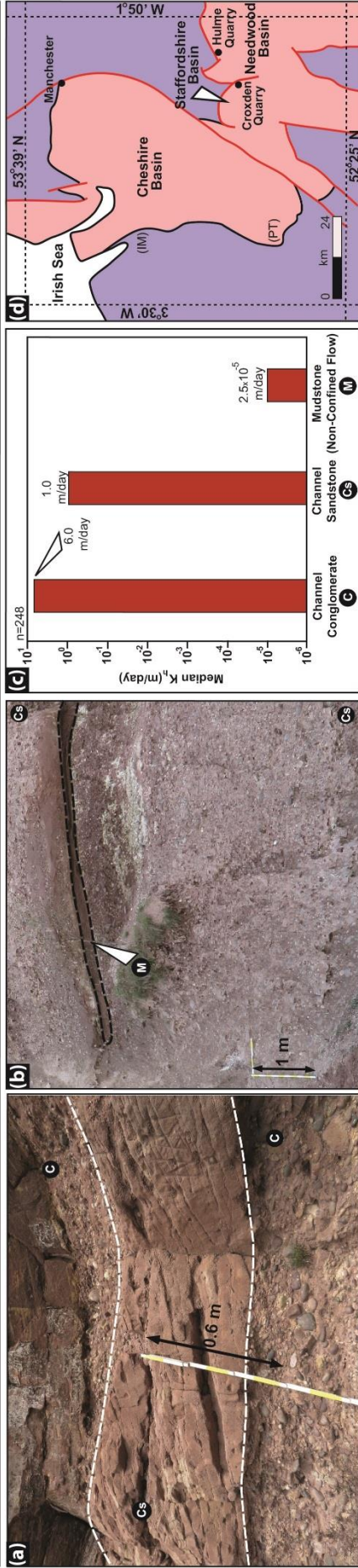
Eastren Irish Sea Basin: Lithofacies vs Matrix Permeability
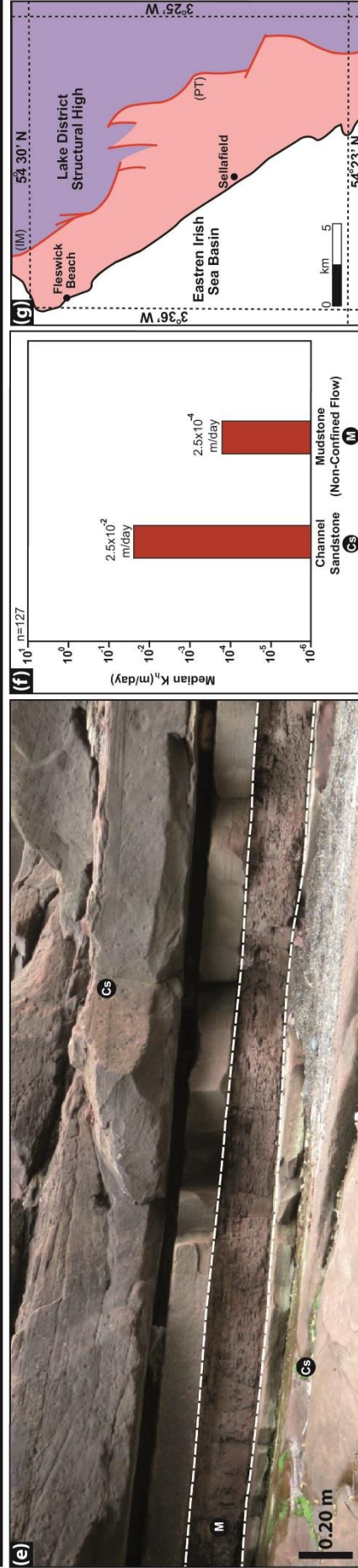
Figure 2.5: Channel sandstone and conglomerate vs. overbank mudstone in the Sherwood Sandstone aquifer. (a) Channel conglomerate and sandstone in the Kiddermister Sandstone Formation of the Staffordshire Basin (Hulme Quarry, Stoke on Trent), (b) Overbank mudstone interbedded with channel conglomerates in the Kidderminster Sandstone Formation of the Needwood Basin (Croxden Quarry, Cheadle), (c) Plug scale horizontal hydraulic conductivity for the conglomerate, sandstone and mudstone of the Kiddermister Sandstone Formation in the Worcester, Staffordshire and Needwood basins (Ramingwong, 1977; Tellam and Barker, 2006), (d) Permo-Triassic deposits (PT) and Palaeozoic Igneous Metamorphic (IM) rocks in Western England and location of the Croxden and Hulme quarries, (e) Mudstone layers (1) interbedded in fluvial channels in the St Bees Sandstone Formation of the eastern Irish Sea Basin (Fleswick Bay, St Bees), (f) Plug-scale horizontal hydraulic conductivity in the channel sandstone and overbank mudstone of the St Bees Sandstone Formation in the eastern Irish Sea Basin (Nirex, 1993 b, c), (g) Permo-Triassic deposits (PT) and Palaeozoic Igneous Metamorphic (IM) rocks in West England with location of the Fleswick Bay in West Cumbria.

2.4.3 Discontinuities

The principal discontinuities in the Sherwood Sandstone Group are characterized by fault related fractures and stratabound joints stopping in correspondence (Figure. 2.3a, b, d, e) of bedding-plane fractures (Allen et al., 1998; Tellam and Barker, 2006; Griffiths et al., 2016). Notably, the Sherwood Sandstone aquifer is entirely characterized (at least in highly mechanically resistant formations) by a stratabound joints since these discontinuities are related to the gentle flexuring of the lithosphere which affected NW Europe during the Cenozoic time (Allen et al., 1998; Hitchmough et al., 2007; Carminati et al., 2009). Deviation of stratabound fractures in correspondence of Mesozoic faults and dating of minarilzed veins indicate a Cenozoic age for such joints in the Sherwood Sandstone aquifer (Allen et al., 1998; Milodowski et al., 1998).

However, normal and strike-slip faults locally deform the Sherwood Sandstone aquifer and are characterized both by flow-conduit and barrier structures which are represented by open-fractures and granulation seams (Figure 2.3 a, b, d), respectively (Hitchmough et al., 2007; Griffiths et al.,

2016). Development of stratabound and bedding-plane fractures (Figure 2.3e) is controlled by the lithology. In fact, stratabound joints are particularly well developed in the high mechanically resistant (up to 36 MPa of UCS_{nat}) Sherwood Sandstone Group of the eastern Irish Sea and Cheshire basins where all the specific studies on bed-bound joints are concentrated (Allen et al., 1998; Ameen, 1995; Wealthall et al., 2001; Hitchmough et al., 2007). Additionally, Allen et al. (1998) recognizes how stratabound joints do not occur in pebble-bed units due to their low mechanical resistance (UCS_{nat}<22 MPa). However, at the scale of the single basin, in the Cheshire Basin, the well cemented Helsby Sandstone Formation is characterized in boreholes by a more frequent vertical occurrence of bedding plane fractures (spacing 0.1-10 m) with respect to the more friable Wildmoor Sandstone Formation (spacing 25-100 m) (Allen et al., 1997; Wealthall et al., 2001; Tellam and Barker, 2006; Hitchmough et al. 2007).

Lithology in the UK Sherwood Sandstone Group may play a key role also on controlling development of granulation seams vs. open fractures (Figure 2.3a, b, d). In fact, fault-related open fractures (Figure 2.3d) are particularly well developed in the fluvial St Bees Sandstone Formation of West Cumbria according to a number of authors (Knott, 1994; Gutmanis et al., 1998; Nirex, 1997; Allen et al., 1998). All the specific analyses realized by structural geologists on the granulation seams of the UK Triassic Sandstone focus on aeolian deposits (Figure 2.3a, b) of the Cheshire and Wessex basins (Rowe and Burley, 1997; Kattenhorn and Pollard, 2001; Griffiths et al., 2016). This contrast in structural style between fluvial (eastern Irish Sea Basin) and aeolian (Cheshire Basin) deposits has been related either to the argillaceous matrix of the St Bees Sandstone which allows brittle failure at lower stresses (Knott, 1994), or to the intense post-Triassic fault reactivation which produced open-fracturing in this highly mechanically resistant fluvial sandstone (Yates, 1992; Milodowski et al., 1998). Daw et al. (1974) has tested, using multi-stage triaxial stress experiments, plugs of the Sherwood Sandstone Group from quarries in the eastern Irish Sea Basin, Cheshire Basin, Staffordshire Basin and eastern England Shelf. Intergranular permeability is only slightly reduced (by 6-

20%) in response to an increase in lithostatic pressure of 7 MPa (Figure 2.6), representing the overburden pressure at approximately 300 m below the surface (Daw et al., 1974). By contrast, the fracture flow component is strongly reduced (by 65-80%) in experiments that apply the same amount of overburden pressure (7MPa) to plugs of the Sherwood Sandstone Group that contained single fractures (Daw et al., 1974). These plug-scale experiments highlight the potential impact that fractures such as vertical joints, bedding-plane fractures and fault-related open fractures on conducting water-flow in the UK Triassic Sandstone at shallow depths (~ < 150 mBGL).
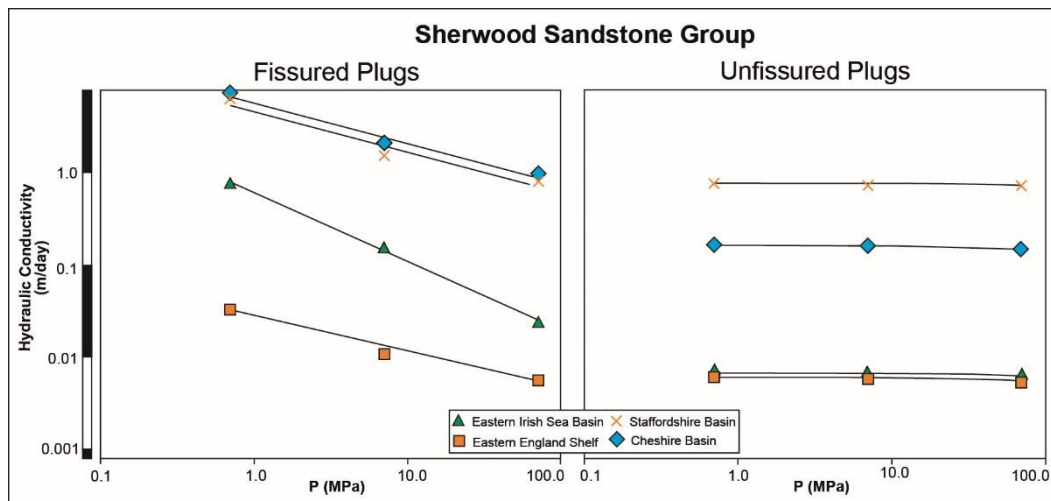
Figures 2.6: Effect of confining pressure on plug-scale permeability on the Sherwood Sandstone Group across the UK (Daw et al., 1974).

Granulation seams (Figures 2.3a, b, 2.7a, b) in the Sherwood Sandstone Group are characterized by low-porosity (4-8%) and thin cataclasites (10^{-3}-10^1 mm thick) occurring either in swarms or in conjugate sets (Rowe and Burley, 1997; Kattenhorn and Pollard, 2002; Tellam and Barker, 2006; Griffiths et al., 2016). Plug-scale permeability analyses are available with regards to the granulations seams of the Sherwood Sandstone Group (Bouch et al., 2006) showing how the low-porosity structures posses permeability from 1 up to 4 orders lower than the host rock (Figure 2.7).

Also, this contrast in permeability between granulation seams (K$_{gs}$) and host rock (K$_{hr}$) perfectly matches, and partially overlap results from the UK Penrith Sandstone and the USA Nugget Sandstone formations, respectively (Figure 2.7c).
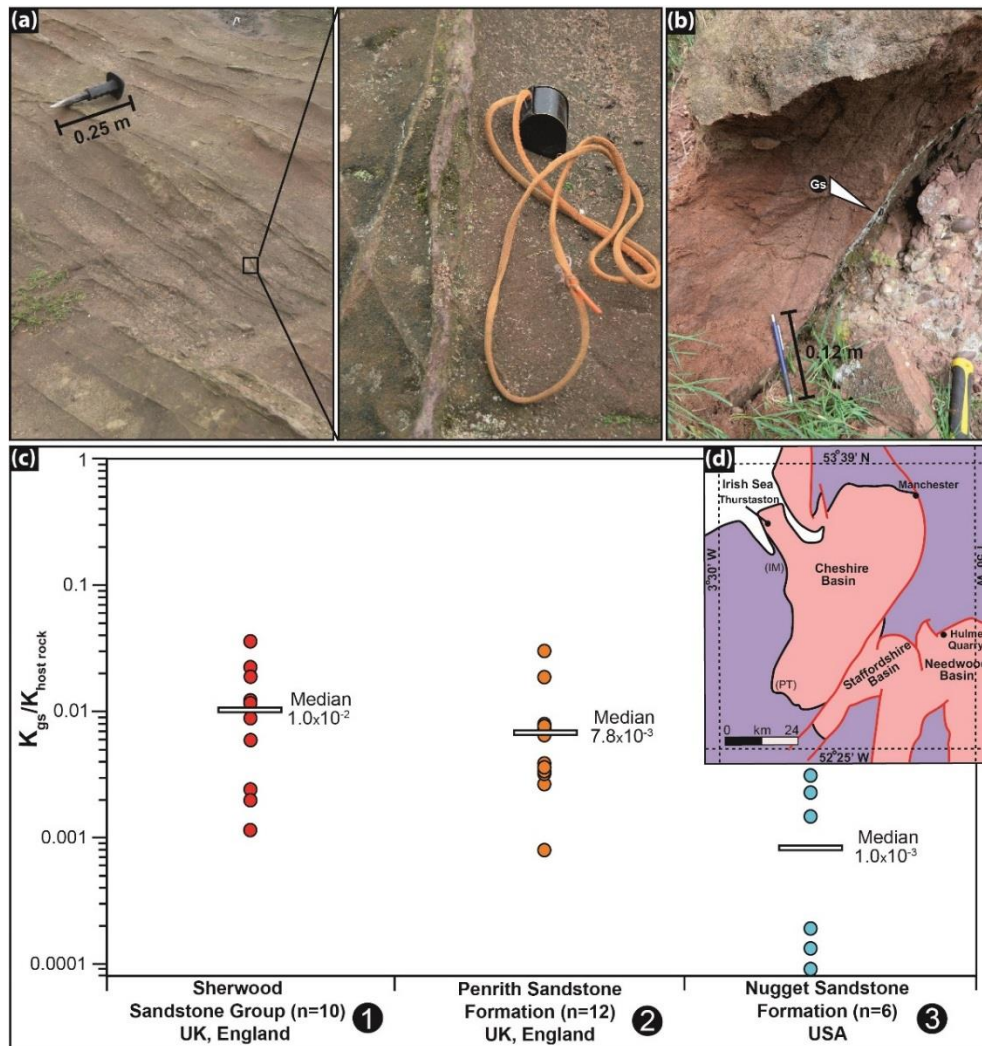
Figures 2.7: Granulations seams in fault zones. (a) Granulation seams in conjugate sets in the aeolian Helsby Sandstone Formation of the Cheshire Basin (Thurstaston, Merseyside), (b) Granulation seams in the Kidderminster Sandstone Formation in the Needwood Basin (Hulme Quarry, Stoke on Trent), (c) Granulation seam (Kgs) vs. host rock (Kgs) permeability in the Sherwood Sandstone Group (Bouch et al., 2006) in the Penrith Sandstone Formation (Tueckmantel et al., 2012) and in the Nugget Sandstone Formation (Gibson, 1998), (d) Permo-Triassic deposits (PT) and Palaeozoic Igneous Metamorphic (IM) rocks in Western England and location of the Hulme quarry and Thurstaston.

2.5 Field and regional scale Hydraulic properties

The large-scale permeability of the Sherwood Sandstone aquifer was critically reviewed aiming to find information about the effect of sedimentary and tectonic heterogeneities which may serve as a good scheme for aquifer management. This review, taking into account differences concerning lithostatic load and karst development at relatively shallow depths (<150 mBGL), also aims to provide information on the flow effects of the sedimentary heterogeneities (e.g., mudstone interlayer, pebbly lithofacies) and faults, also relevant to hydrocarbon exploration.

2.5.1 Transmissivity vs Sedimentary Basin

Permeability at the well test-scale at depths < 150 m BGL, i.e. as reflected by transmissivity from pumping tests, does not show a clear correlation with the subsidence tectonic rates and sediment accommodation rates, unlike porosity and plug-scale permeability (Tables 2.1, 2.3). Transmissivity values in the Sherwood Sandstone Group show similar values across Great Britain, i.e. median values range from 100 up to 300 m^2/day in the various Triassic basins (Figure 2.8). However, tectonic subsidence seem to play a key role on the difference between plug and field scale permeability ($K_{filed-scale}/K_{plug-scale}$). High mechanical resistance (UCS_{nat}=17-36) favours development of open fractures such as stratabound joints and bedding plane fractures, which dominate flow in the fluvial red-beds of the eastern Irish Sea Basin (Thompson and Leach, 1985). In fact, field-scale permeability is ~10^2 higher than plug-scale permeability in the eastern Irish Sea Basin of West Cumbria (Allen et al., 1997).

The ratio between plug and field ($K_{field-scale}/K_{plug-scale}$) scale is ~4 in the Sherwood Sandstone aquifer in the Cheshire Basin; this value arises from a well-developed stratabound fracturing network (pervasive due to its relatively high mechanical resentence and permeable as demonstrated by packer tests) coupled with relatively high conductivity of the matrix (Brassington and Walthall, 1985; Hitchmough et al., 2007). However, the

Triassic red-beds of Great Britain shows the lowest difference between plug and field scale ($K_{field-scale}/K_{plug-scale}$~1.5) in the slowly subsiding shelf-edge basin of the eastern England Shelf, which has the highest average values of porosity and plug-scale permeability (Allen et al., 1997). Notably, same difference between plug and field scale (~1.5) characterizes the pebble-beds of the Worcester basin and the eastern England Shelf, both characterized by relatively low values of mechanical resistance ($UCS_{nat} <$ 20 MPa) which do not favour fracture development (Ramingwong, 1974; Allen et al., 1998). A better understanding of the relative contribution to flow matrix and fracture in aquifers of aeolian and fluvial origin, comparing the Sherwood Sandstone aquifer to similar aquifers worldwide, was a specific objective of this work.
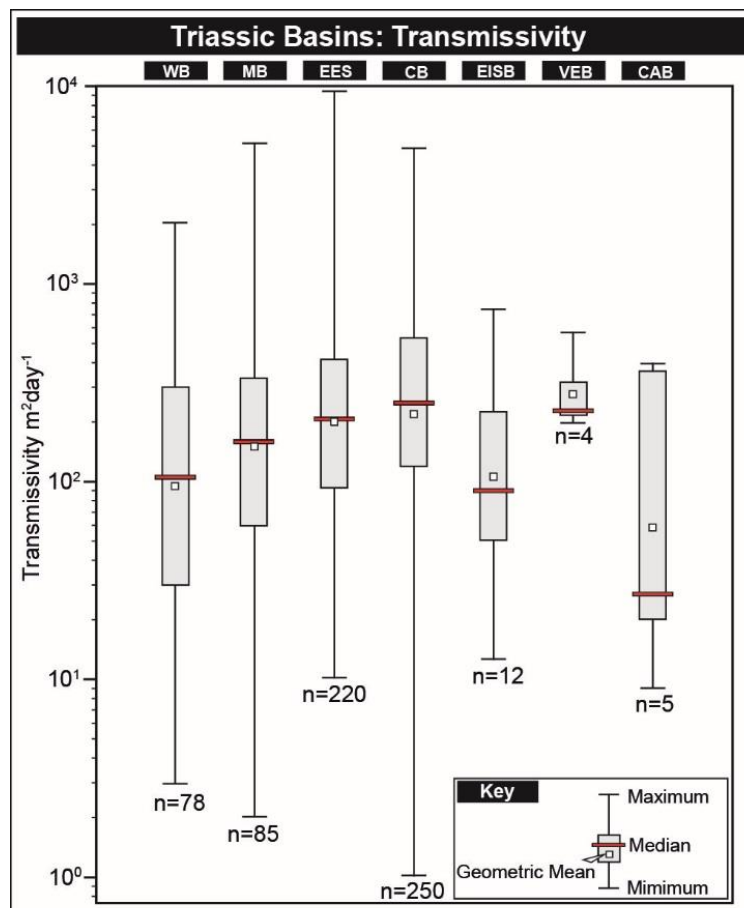
Figure 2.8: Transmissivity of the Sherwood Sandstone Group in the Triassic basins of England for the Worcester (WB), Midland (MB), eastern England Shelf (EES), Cheshire (CB), Eastern Irish Sea (EISB), Vale of Eden and Carlisle (CAB) basins (Allen et al., 1997).

2.5.2 Transmissivity vs lithofacies

The presence of conductive fractures in the UK Sherwood Sandstone aquifer at depths <150 m below the ground surface typically prevents any correlation between transmissivity and lithofacies. For example, the fluvial St Bees Sandstone (T = 20-750 m^2/day) and the aeolian Calder Sandstone (T = 100-210 m^2/day) aquifers in the eastern Irish Sea Basin which are characterized by significantly different porosity (Figure 2.4a), and plug-scale permeability values, show substantial overlap in transmissivity (Allen et al., 1997; Worthington et al., 2016). It is only matrix flow aquifers, represented by the shallow (<150 mGBL) Triassic Sandstone of the eastern England Shelf, and the deeper (> 150 mBGL) St Bees Sandstone aquifer of the Eastern Irish Sea Basin, that show correlation between transmissivity and lithofacies (Allen et al., 1997). In fact, correlation between transmissivity and lithofacies was detected in the St Bees Sandstone aquifer at depths > 150 m, i.e. where fractures are less important, allowing matrix flow (Allen et al., 1997; Streetley et al., 2000). Here, the deep St Bees Sandstone aquifer of the eastern Irish Sea Basin is characterized by lower median transmissivity in the North Head Member which has significant mudstone interlayers (about 25% of the thickness), compared to that in the South Head Member (5% mudstone) (Streetley et al. 2000), see Figure 2.9a. Also, the Sherwood Sandstone aquifer of the eastern England Shelf is characterized by a northward reduction in well test transmissivity (Figure 2.9b) fitting the contemporaneous reduction in grain size, porosity and plug-scale permeability at increasing distance from the southern sediment source (Allen et al., 1997; Koukis, 1974; McKie and Wiliiams, 2009; Pokar et al., 1997).
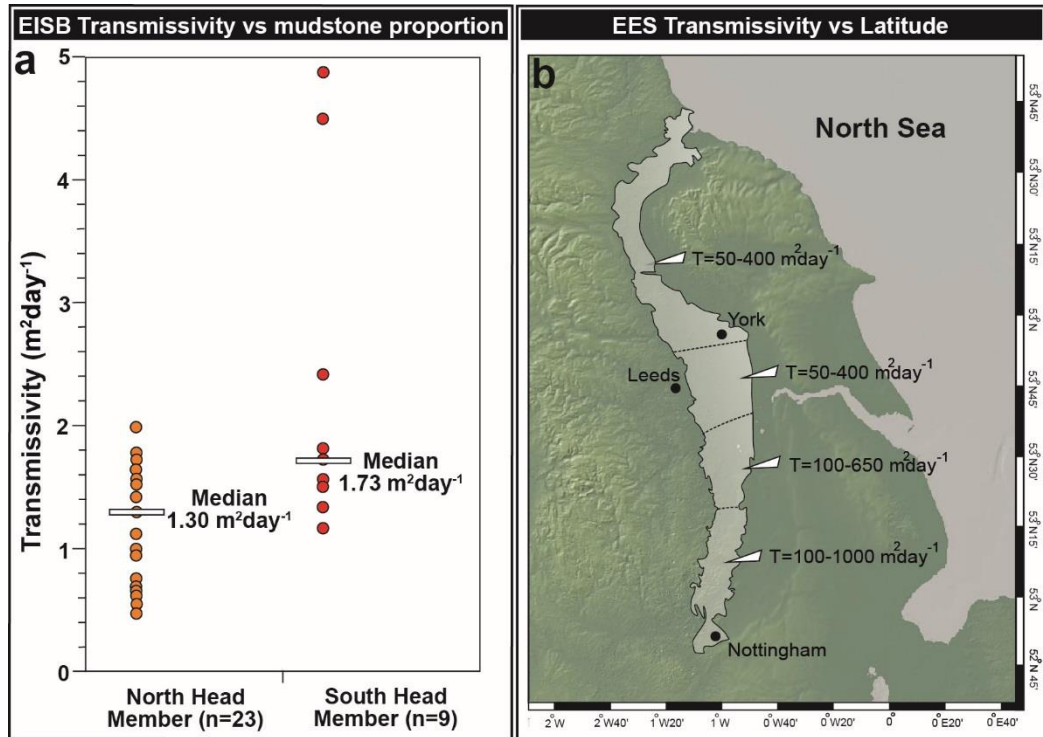
Figure 2.9: Transmissivity vs. lithofacies. (a) Transmissivity in the North Head (mudstone 25%, sandstone 75%) and the South Head (mudstone 5%, sandstone 95%) members of the St Bees Sandstone Formation in the eastern Irish Sea Basin (Streetley et al., 2000), (b) Northerly transmissivity reduction in the eastern England Shelf (Allen et al., 1997).

2.5.3 Faulting effect on permeability

Fault structures in the UK Sherwood Sandstone aquifer represent either barriers or conduits for the water flow, as typical on tectonized sandstone lithotypes worldwide (Bense et al., 2013; Mohamed and Worden, 2006; Tellam and Barker, 2006). In fact, high artesian flow to a well (470 m^3/day) has been recognized in correspondence of an extensional fault deforming the fluvial deposits of the Vale of Eden, and springs aligned in correspondence of the Pattingham Fault which dislocates the fluvial pebble beds of the Worcester Basin (Ingram, 1978; Fletcher, 1994). Hence, high artesian flow and alignment of springs in correspondence of normal faults show how water finds a preferential pathway in correspondence of the principal planes, highlighting conduit behaviour along directions parallel to the normal fault plane (Caine et al., 1996; Bense et al., 2013). Despite this,

a correlation between boreholes penetrating faults and high transmissivity in the Sherwood Sandstone aquifer reduces to a single example in the West Midlands (Allen et al., 1997). However, there is also evidence for barrier behaviour of extensional structures affecting the UK Triassic continental deposits. In fact, pumping tests with multiple observation wells indicate an elliptical cone of depression in a graben structure in the Midlands (near Birmingham) showing lack of drawdown in the footwall blocks (Fletcher, 1994). This barrier behaviour can be related to mechanical and structural characteristics of the Sherwood Sandstone Group characterizing the Needwood, Staffordshire and Worcester basins (Whithworth and Turner, 1989), i.e. low mechanical resistance (UCS_{nat}<16MPa) impedes extensive development of open-fractures. However, deformation is concentrated in correspondence of fault cores (Figure 2.2c) explaining fault compartmentalization in the Sherwood Sandstone aquifer (Chisholm, 1988; Caine et al., 1998; Faulkner et al., 2009; Tueckmantel et al., 2012; Bense et al., 2013). Further experimental evidence of the barrier hydraulic behaviour of normal faults occur in the Sherwood Sandstone in the Cheshire Basin. In fact, normal faults deforming the Wilmslow and the Helsby Sandstone formations (Cheshire Basin) were recognized as flow-barriers based on the geochemical evidence of limited water mixing between compartmentalized horsts and grabens (Mohamed and Worden, 2006). Additionally, contouring of the water table depths follow the structural trends in the Cheshire Basin (Merseyside Peninsula) providing further evidence of fault barriers in this sandstone aquifer (Mohamed and Worden, 2006; Seymour et al. 2006).

Several authors recognized a particular development of granulation seams (Figure 2.3a, b) in the aeolian deposits of the Cheshire Basin explaining the strong barrier behaviour of the extensional faults (Griffith et al., 2016; Tellam and Barker, 2006). In contrast, fault zones (Figure 2.3d) in the fluvial Triassic Sandstone (St Bees Sandstone Formation) are characterized by higher occurrence of open fractures (Knott, 1994, Nirex, 1997). This different structural style has been related to the abundant of argillaceous matrix in the Triassic fluvial deposits of the eastern Irish Sea Basin which

allows brittle failure at lower stresses, with respect to the quartz-rich aeolian dunes of the Cheshire Basin (Knott, 1994). Note that the high-mechanical resistance of the St Bees Sandstone and the intense post-Triassic fault reactivation in the eastern Irish Sea Basin have also been considered as key factors on controlling fault architecture in the West Cumbrian Triassic Sandstone (Milodowski et al., 1998). These normal faults, forming the fluvial deposits of the eastern Irish Basin, will be object of pumping and quantitative flow log analyses in this work, with the objective of constraining their hydraulic behaviour.

2.5.4 Geological and hydrogeological framework: concluding remarks

The Sherwood Sandstone Group represents a heterogeneous fluvio-aeolian succession deposited in several sedimentary basins (Wessex, Worcester, Needwood, Staffordshire, eastern England Shelf, eastern Irish Sea, Carlisle and Vale of Eden basins) which experienced different rates of subsidence and sediment accommodation generation. The key geological and petro-hydraulic properties are summarized below.

- The principal tectonic structures are characterized by stratabound joints and normal faults. Stratabound joints typically pervade the entire aquifer in the relatively mechanically resistant (UCS_{nat}>20 MPa) Sherwood Sandstone Group. However, normal faults locally characterize the aquifer. Such faults deform aeolian deposits which are dominated by granulation seams. By contrast, fluvial deposits deformed by extensional tectonics tend to be characterized by a dominance of open fractures in fault zones.

- Principal lithofacies proportions show variation at rising distance from the principal sediment source (represented by the Armorican Massif in northern France). Fluvial deposits decrease in grain-size northwards with progressive reduction in pebbly sandstones and conglomerates. However, the proportion of aeolian vs. fluvial lithofacies increase at rising distance from the Variscan uplands.

- The mechanical properties of the UK Sherwood Sandstone Group show regional differences which seem to be related to the different subsidence rates of the Triassic sedimentary basins. In fact, the highest values of mechanical resistance (UCS_{nat}=36 MPa) are registered in the eastern Irish Sea Basin which represents the fastest subsiding (210 Myr) basin in the UK Triassic realm. Additionally, the Sherwood Sandstone Group in the relatively rapidly subsiding Cheshire Basin (140 m/Myr) is also characterized by similar UCS_{nat} values (31 MPa). However, the UK Triassic sandstone shows low values of mechanical resistance (UCS_{nat}<22 MPa) in the relatively slowly subsiding Worcester and eastern England Shelf basins.

- Porosity and plug-scale permeability also show a regional distribution. In fact, porosity and plug-scale permeability show the lowest values in the rapidly subsiding basins of the eastern Irish Sea. In comparison, the eastern England Shelf which represents the most slowly subsiding basin in the UK during the Triassic is characterized by the highest values of porosity and plug-scale permeability

- The regional distribution of field-scale permeability in the Sherwood Sandstone Group is complex. Transmissivity from pumping tests show similar values across the UK ($\sim$10^1-10^2 m^2/day). However, the ratio between field to plug-scale permeability shows some correlation with tectonic subsidence rate. This ratio is very high in the eastern Irish Sea Basin ($\sim$10^2) and moderately high in the Cheshire basin ($\sim$4) which are characterized by high subsidence rates and fracture flow systems. By contrast, the ratio of plug to field scale permeability is < 2 in the slowly subsiding Worcester Basin and eastern England Shelf, where flow is dominantly through the matrix.

Chapter 3

Characterization of the sedimentology of the fluvial deposits of Sherwood Sandstone Group in the eastern Irish Sea Basin and eastern England Shelf

(Chapter published: Medici, G., Boulesteix, K., Mountney, N.P., West, L.J. and Odling, N.E. 2015. Palaeoenvironment of braided fluvial systems in different tectonic realms of the Triassic Sherwood Sandstone Group, UK. *Sedimentary Geology*. 329, pp.188-210)

3.1 Chapter overview

Fluvial successions comprising the fills of sedimentary basins occur in a variety of tectonic realms related to extensional, compressional and strike-slip settings, as well as on slowly subsiding, passive basin margins. A major rifting phase affected NW Europe during the Triassic and resulted in the generation of numerous sedimentary basins. In the UK, much of the fill of these basins is represented by fluvial and aeolian successions of the Sherwood Sandstone Group. Additionally, regions that experienced slow rates of Mesozoic subsidence unrelated to Triassic rifting also acted as sites of accumulation of the Sherwood Sandstone Group, one well-exposed example being the eastern England Shelf. The fluvial depositional architecture of deposits of the Sherwood Sandstone Group of the eastern England Shelf (a shelf-edge basin) is compared with similar fluvial deposits of the St Bees Sandstone Formation, eastern Irish Sea Basin (a half-graben). The two studied successions represent the preserved deposits of braided fluvial systems that were influenced by common allogenic factors (climate, sediment source, delivery style); differences in preserved sedimentary style principally reflect their different tectonics settings. Analysis of lithofacies and architectural elements demonstrates that both studied successions are characterised by amalgamated channel-fill elements that are recorded predominantly by downstream-accreting sandy barforms. The different tectonic settings in which the two braided-fluvial

systems accumulated exerted a dominant control on preserved sedimentary style and long-term preservation potential. On the eastern England Shelf, the vertical stacking of pebbly units and the general absence of fine-grained units reflects a slow rate of sediment accommodation generation (18-19.4 m/Myr). In this shelf-edge basin, successive fluvial cycles repeatedly reworked the uppermost parts of earlier fluvial deposits such that only the lowermost channel lags tend to be preserved. By contrast, in the eastern Irish Sea Basin of West Cumbria, the rate of sediment accommodation generation was substantially greater (119 m/Myr) such that space was available to preserve complete fluvial cycles, including silty drape units that cap the channelized deposits.

3.2. Introduction

The preserved sedimentary architecture of fluvial successions is known to vary as a function of tectonic setting, notably basin type and subsidence rate (Bridge, 2003; 2006; Weissmann et al., 2010; Colombera et al., 2013). Fluvial successions are well documented as the fill of sedimentary basins characterized by extensional tectonics in rift and intermontane settings (e.g., Leeder et al., 1996; Gawthorpe and Leeder, 2000; Cavinato et al., 2002; Ghinassi et al., 2009; Gobo et al., 2014; Santos et al., 2014), in transtensional pull-apart basins (e.g., Hempton and Dunne, 1984; Gruber and Sachsenhofer, 2001), and in compressional foreland basins (e.g., Deramond et al., 1993; Willis, 1993 a, b; Morend et al., 2002; Cain and Mountney, 2009). Additionally, fluvial successions are also present in tectonically inactive basins, including slowly subsiding shelf edges and intracratonic basins (e.g., Harris et al., 1990; Bromley, 1991; Stephens, 1994). However, the role that basin type plays in controlling the preserved sedimentary architecture in fluvial successions is not straightforward. In fact, allogenic factors (e.g., climate, base level, nature of the sediment source) act in combination to influence sedimentary processes and the resultant style of accumulation, as do autogenic processes related to the intrinsic behaviour of the type of fluvial system developing within the basin

(e.g., Ventra and Nichols, 2014). Worldwide, relatively few regions are documented where the same geological formations represent the preserved deposits of the same fluvial system in multiple sedimentary basins of different type (Bromley, 1991; Willis, 2000). Studies from such regions provide the opportunity to compare lithotype and architectural-element proportion, distribution and arrangement within the general depositional environment of fluvial systems preserved in different tectonic settings. Constraint of the role of tectonics in controlling architectural-element distribution and proportion is an important issue in fluvial sedimentology since the relative abundance of very-fine grained deposits (e.g., overbank mudstone) versus coarse grained deposits (e.g., channelized elements) is significant in the development of both hydrocarbon reservoirs and groundwater aquifers (Clark et al., 1996; Allen et al., 1997; Tellam and Barker, 2006); this is especially the case for the Triassic Sherwood Sandstone of the UK since it is host to important hydrocarbon reservoirs (Meadows and Beach, 1993a, b; McKinley et al., 2001; Schmid et al., 2004). Additionally, the unit forms the second largest groundwater aquifer in the UK (Binley et al., 2002; Smedley and Edmunds, 2002). This work investigates a Triassic fluvial succession of the Sherwood Sandstone Group in England, UK, occurring in two distinct sedimentary basins: the eastern Irish Sea Basin and the eastern England Shelf (Figure 3.1). These two Triassic depocentres record the history of accumulation of fluvial successions in two tectonically different settings, for which the style of preserved sediment fill is characterized by a range of fluvial channelized and non-channelized architectural elements. The eastern Irish Sea Basin represents a high-subsidence rift basin bounded by Permo-Triassic extensional faults (Akhurst et al., 1997, 1998; Milodowski et al., 1998; McKie and Williams, 2009). By contrast, the eastern England Shelf represents a relatively low-subsidence shelf-edge basin that never experienced episodes of fault driven sediment accommodation (McKie and Williams, 2009; Wakefield et al., 2015).

Although several studies provide useful overviews of the sedimentary structures that characterize fluvial (and aeolian and lacustrine) successions

of the Sherwood Sandstone Group in the eastern Irish Sea Basin (e.g., Macchi, 1991; Jones and Ambrose, 1994, Nirex, 1997), no detailed lithofacies and architectural-element analysis has been published previously for the parts of the succession studied here. Wakefield et al. (2015) provide a detailed description of lithofacies and architectural elements characterizing the eastern England Shelf although they do not compare the eastern England Shelf to any other tectonic realm of the Triassic in NW Europe.

The aim of this chapter is to evaluate the influence of basin type in governing the type and mechanism of preservation of fluvial successions that accumulated and became preserved under both conditions of active extensional tectonics and passive subsidence. Specific research objectives are as follows: (i) to undertake a lithofacies analysis of the fluvial successions present in the eastern England Shelf and the eastern Irish Sea Basin; (ii) to characterize and compare the form and geometry of channelized and non-channelized fluvial architectural elements; (iii) to analyse palaeoflow indicators to demonstrate both the mechanism of barform growth and migration, and to reconstruct the regional pattern of palaeodrainage; (iv) to develop a sedimentary process model to show how the preserved sedimentary architectures of the studied fluvial successions are controlled by the different tectonic settings; and (v) to present a conceptual model for braided-river systems, deposited in different tectonic settings but otherwise moderated by a common set of controlling allogenic factors. Such a model can be applied to other rift settings where basins subject to relatively high rates of subsidence coexist with slowly subsiding basins.

3.3 Geological setting

The Sherwood Sandstone Group (Wuchiapingian-Ladinian) comprises a succession of red-beds accumulated in a series of basins developed in response to the rifting phase that preceded the opening of the Atlantic

Ocean (Coward, 1995; Glennie, 1995; Ziegler and Dèzes, 2006). The "Sherwood Sandstone" has long been ascribed to a mixed fluvial and aeolian origin (e.g., Thompson, 1970a, b; Cowan, 1993, Thompson and Meadows, 1997; Mountney and Thompson; 2002; Holliday et al., 2008). Collectively, the assemblage of lithofacies present in the succession demonstrates accumulation under the influence of an arid to semi-arid climatic regime, which characterized the UK Mesozoic basins during much of the Triassic (Warrington and Ivimey-Cook, 1992; Glennie, 1995; Schmid et al., 2006; Brookfield, 2008).

Mesozoic extensional tectonic events created several basins and elevated areas in NW Europe during the Permo-Triassic. The morpho-structural highs served as a principal source of sediment for fluvial systems. The Armorican Massif (northern France) represented the main source area for sediments of the Sherwood Sandstone Group in the UK, including in offshore parts of the eastern Irish Sea Basin (Wills, 1956; Audley-Charles, 1970; McKie and Williams, 2009; McKie and Shannon, 2011). Extensional tectonics continued to affect the Permo-Triassic basins of England throughout the Jurassic and Cretaceous (Ameen, 1995; Chadwick and Evans; 1995; Chadwick, 1997; Plant et al., 1999). Latterly, during the Cenozoic, the Triassic basins were reactivated and inverted by far-field effects of the Alpine orogeny (Chadwick et al., 1994; Chadwick, 1997; Milodowski et al., 1998; Blundell, 2002; Hillis et al., 2008).

The eastern Irish Sea Basin, which extends onshore in West Cumbria (Figure 3.1), is a Triassic rift basin bounded at its eastern margin by normal faults that divide it from the Lake District morpho-structural high (Akhurst et al., 1998). Within this region, the Sherwood Sandstone Group attains a maximum preserved thickness of 1100 m (Jones and Ambrose, 1994) and is formally divided into three different formations: the St Bees, Calder and Ormskirk Sandstone formations (Barnes et al., 1994; Akhurst et al. 1997; Holliday et al., 2008). The St Bees Sandstone Formation, which is the focus of this study, is predominantly characterized by fine- to medium-grained sandstone of fluvial origin that passes upwards into the aeolian-dominated

succession of the overlying Calder Sandstone Formation (Meadows and Beach, 1993a; Jones and Ambrose, 1994; Holliday et al., 2008). The St Bees Sandstone Formation is divided into two members: the North Head Member and the overlying "St Bees Sandstone Formation above the North Head Member" (sensu Nirex, 1997). For clarity in this work, this upper member is referred to as the "South Head Member" because it is well exposed in outcrop along the South Head cliff in West Cumbria. The two members are differentiated primarily based on the abundance of fine-grained muddy sandstone and mudstone layers (Nirex, 1997). The basal 35 m of the lower North Head Member is arranged into an alternation of sheet-like sandstone elements and mudstone elements. This lower succession passes upwards into a succession dominated by sandy-channelized architectural elements (Macchi, 1991; Barnes et al., 1994; Jones and Ambrose, 1994; Nirex, 1997).

The St Bees Sandstone Formation accumulated in a rift setting in the eastern Irish Sea Basin, which underwent relatively rapid tectonic subsidence during the Upper Permian to Triassic (Chadwick et al., 1994; Brookfield, 2008; McKie and Williams, 2009). The rate of tectonic subsidence varied from 61 m/Myr to 400 m/Myr (Chadwick et al., 1994), even in marginal areas of the basin, such as West Cumbria (Akhurst et al., 1997, 1998). Based on data presented as back-stripping curves, Chadwick et al. (1994) argue that the eastern Irish Sea Basin experienced its climax of tectonic activity during the deposition of the St Bees Sandstone Formation (248-252 Myr; Brookfield, 2008). By contrast, other authors (McKie and Williams, 2009, and references therein) assign the climax of extension in the eastern Irish Sea Basin to the latest Permian to earliest Triassic, given the lack of evident growth-fault geometries in seismic lines following the earliest Triassic (see also Akhurst et al., 1997; Štolfová and Shannon, 2009). However, Meadows and Beach (1993a) interpreted growth geometries in seismic lines in the hangingwall of listric faults in the St Bees Sandstone Formation. Furthermore, Milodowski et al. (1998) demonstrated that mineralized veins in fault zones of the St Bees Sandstone and Calder formations were emplaced in the early and middle

Triassic, thereby providing additional evidence for syn-depositional activity of the rift system. Indeed, immediately after an earthquake rupture, fault zones act as pumps for fluids which tend to precipitate fracture-sealing minerals (Cox, 1987; Sibson et al., 1988; Sibson, 1996).

According to all the interpretations concerning the timing of normal fault activity in the eastern Irish Sea Basin (Meadows and Bench, 1993a; Chadwick et al., 1994; McKie and Williams, 2009; Štolfová and Shannon; 2009), the North Head Member (earliest Triassic) accumulated at the height of extensional fault activity. However, the South Head Member accumulated during the rift to post-rift transition in which accommodation was generated by continued fault activity augmented by thermal subsidence (Bond et al., 1985).

By contrast, the eastern England Shelf, which extends from the Pennines of central England, eastwards across the East Midlands and Yorkshire towards the North Sea (Whittaker, 1985; Green, 1989; Bray et al., 1992), is a shelf-edge basin that never experienced episodes of rifting activity. According to Burley (1984) the maximum burial depth of strata of the eastern England Shelf was less than 1000 m prior to Cenozoic uplift of Great Britain (Chadwick, 1997; Blundell, 2002; Hills et al., 2008). However, the burial depth in easternmost sector of the Irish Sea Basin was 3000 and 5000 m at the end of the Permo-Triassic rifting and immediately prior to Cenzoic uplift of Great Britain, respectively (Chadwick et al., 1994). Indeed, the eastern England Shelf underwent a significantly slower rate of subsidence compared to the eastern Irish Sea Basin (Burley, 1984; Chadwick et al., 1994). Accommodation in the shelf-edge basin of the eastern England Shelf was controlled largely by palaeotopography formed by the adjacent Pennine highlands to the east, such that the preserved thickness of the Sherwood Sandstone Group progressively reduces eastward as it onlaps onto a palaeo-high (Bath et al., 1987; Edmunds and Smedley, 2000; Smedley and Edmunds, 2002). Accommodation in the eastern England Shelf was generated by sediment loading and minimal

thermal subsidence, which characterized the margins of the Southern Permian Basin (Ruffel and Shelton, 1999; Wees et al., 2000).

In eastern England, the Sherwood Sandstone Group is undivided. In this region, deposits of the Sherwood Sandstone Group are exposed east of the Pennines (Figure 3.1) along the eastern England Shelf and attain a preserved thickness of up to 400 m, but thin as they onlap the Permo-Carboinferous substratum to the west (Aitkenhead, 2002; Smedley and Edmunds, 2002). The Sherwood Sandstone of the eastern England Shelf is mostly represented by fine- to medium-grained sandstone present in a range of channelized architectural elements of fluvial origin; various types of cross-bedding are common (Pokar et al., 2006; West and Truss, 2006; Wakefield et al., 2015).
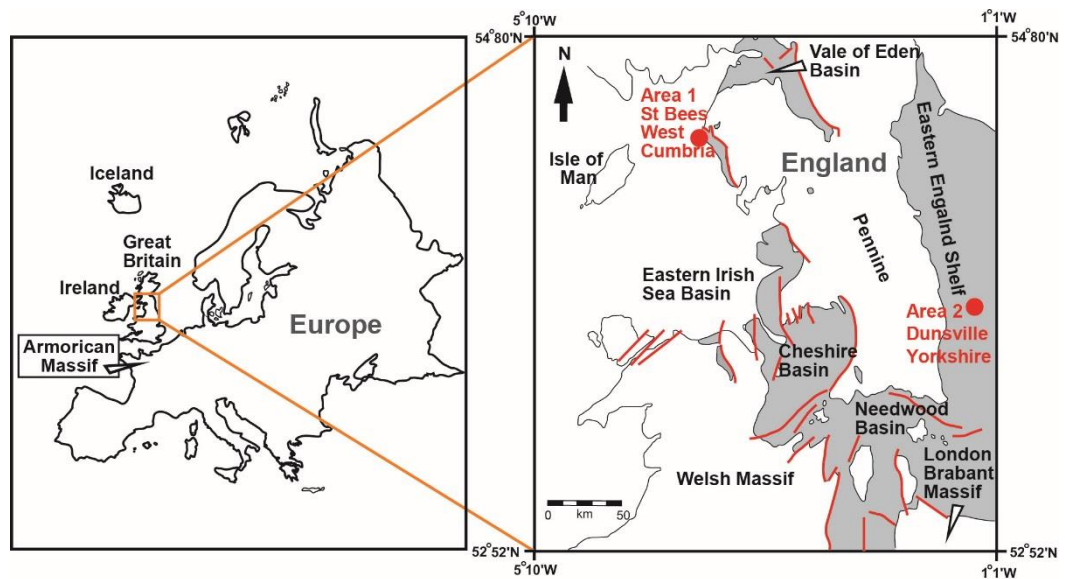
Figure 3.1: Areas of study (red), UK Permo-Mesozoic sedimentary basins (grey) and potential feeder areas (white) for the Permo-Triassic clastic deposits outcropping in England (modified from Mountney and Thompson, 2002).

3.4 Data and Methods

Twelve outcrops from natural cliffs, active and disused quarries, and with orientations both parallel and perpendicular to palaeoflow were studied: five from the eastern England Shelf and seven from the eastern Irish Sea Basin. Thirteen lithofacies are recognized on the basis of lithological characteristics recognizable in outcrop: colour, grain-size, sorting, and composition of matrix. Lithofacies have been assigned to two facies associations representative of channelized and non-confined (extra-channel) fluvial deposition. Four representative sedimentary log sections have been measured in the St Bees area (West Cumbria) and three in South Yorkshire. Additionally, a series of photomontages and architectural panels have been used to depict the distribution, style and juxtaposition of architectural elements. Erosional bounding surfaces of channelized architectural elements have been described using the most recent version of hierarchy scale described by Miall (2006). Principal erosional bounding surfaces from 5th to 6th order have been mapped on photomontages that portray 30,100 m^2 of stratigraphic succession in architectural panels. Additionally, principal erosional surfaces (from 1st to 4th order) have been mapped on 4 four highly detailed architectural-element panels that collectively portray 360 m^2 of stratigraphic succession and which record the following: (i) the distribution and association of lithofacies; (ii) the internal geometry of six types of fluvial architectural element; (iii) a hierarchy of scales of bounding surfaces that define architectural elements based on the scheme of Miall (2006); and (iv) the spatial and genetic relationships between confined and non-confined architectural elements.

Palaeocurrent analysis of data recorded primarily from dip azimuths of inclined forests of cross-bedded sets, supplemented by measurement of the axis trend of trough cross-bedded sets, has been undertaken to determine the following information: (i) regional patterns of palaeodrainage; (ii) detailed trajectories of barform growth; and (iii) potential regions of sediment provenance. Statistical analyses, including determination of vector mean and vector magnitude, were calculated using the Stereonet 9

software package (Allimendinger et al., 2012). In total, 96 and 136 palaeocurrent readings were recorded from the St Bees Sandstone Formation (West Cumbria) and the Sherwood Sandstone cropping out in Dunsville Quarry (South Yorkshire), respectively.

3.5 Architectural elements and facies

Fluvial deposits of the Sherwood Sandstone Group have been studied in the St Bees-Whitehaven area in West Cumbria and in the Doncaster area, South Yorkshire. In West Cumbria and South Yorkshire (Figures 3.2, 3.3), the fluvial deposits are composed predominantly of very fine- to medium-grained sandstone (Figures 3.4-3.6). In total, thirteen representative lithofacies of fluvial origin are recognized (Figures 3.4, 3.5 and Table 3.1) and associations of these facies comprise the internal character of six architectural elements (Figure 3.7).

In the St Bees and Whitehaven area, eleven of thirteen lithofacies are recognized and these occur in two facies associations: (i) channelized fluvial deposition, and (ii) non-confined fluvial deposition. Within these two facies associations, six architectural elements are recognized (Figures 3.8-3.12). Channelized fluvial deposition is recorded by the occurrence of interbedded channel-fill elements (F3) and laterally and vertically amalgamated channel-fill elements (F4). Non-confined fluvial deposition is characterized in the St Bees Sandstone Formation by red mudstone elements (F1), sheet-like sandstone elements (F2) and overbank elements interbedded in amalgamated channels (F5), sheet-like sandstone elements interbedded with amalgamated channels (F6).

In the Dunsville Quarry (South Yorkshire), seven lithofacies are recognized in two facies associations: (i) channelized fluvial deposition, and (ii) non-confined fluvial deposition. These two facies associations are respectively related to two architectural elements (Figures 3.13-3.15): laterally and vertically amalgamated channel-fill elements (F4) and overbank elements interbedded in amalgamated channels (F5).
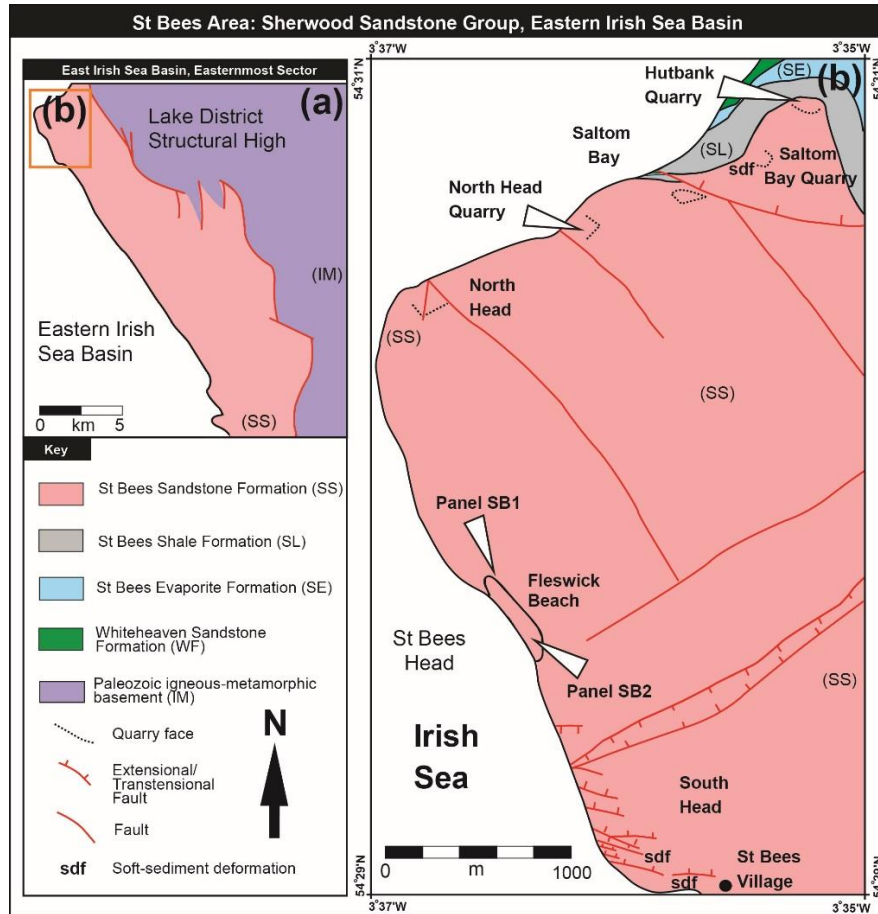
Figure 3.2: (a) Easternmost sector of the on-shore Irish Sea Basin, (b) Geological map of the St Bees area in West Cumbria (redrawn from British Geological Survey, 2000).
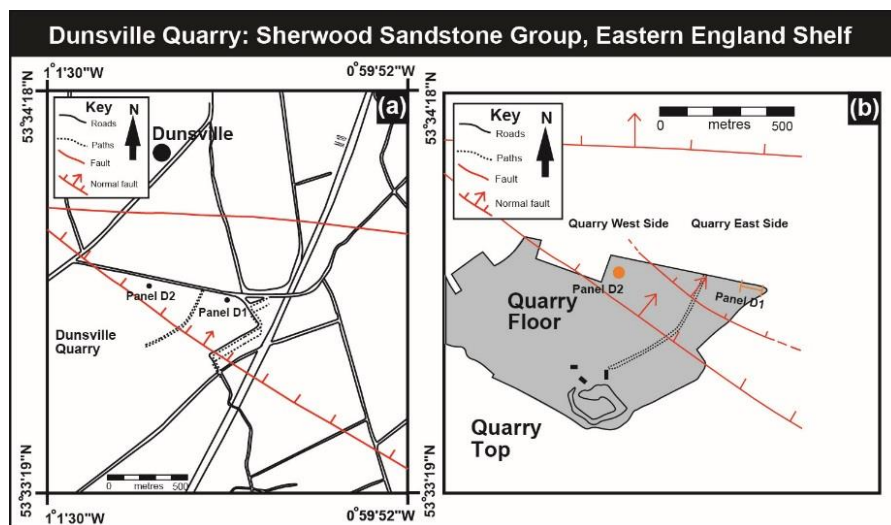
Figure 3.3: (a) Geological map of the Dunsville area in South Yorkshire, (b) Detail of the Dunsville Quarry with location of the architectural panels.

Table 3.1: Summary of lithofacies observed in the Sherwood Sandstone Group of South East Yorkshire and West Cumbria (St Bees Sandstone Formation).

Facies	Description	Interpretation
Red mudstone (Fm)	Mudstone that is red in colour and forms beds that are each 0.05-1m thick. The red mudstone is characterized by an alternation of clay- and silt-prone layers.	Thick and laterally continuous mudstone beds represent deposition from suspension during overbank events. Thin and laterally discontinuous mudstone beds record deposition from suspension in abandoned channels.
Fine grained sandstone (Fsh)	Very fine-grained sandstone that occurs in alternation with Fm to form beds that are up to 0.4 m thick. Alternatively, Fsh occurs in single layers (0.2-0.5 m thick) interbedded with medium and coarse sandstone beds. Fsh exhibits bed-parallel laminations.	Deposition during discharge events for which flow was not confined within channels. Records flow velocities that were greater than those indicated by facies Fm.
Planar cross-bedded sandstone (Fx)	Moderate- to well-sorted, fine- to medium-grained tabular sandstone arranged in beds that are 1-1.5 m thick. Fx exhibits planar cross-bedded foresets which rarely are bleached white. Cross-bedded foresets are inclined at angles of 25°-30° with respect to master bounding surfaces.	Deposition of sandy bar forms under lower flow regime conditions, including down-channel migration of sinuous-crested dunes.
Trough cross-bedded sandstone (Fxt)	Fine- to medium-grained sandstone that most commonly occurs in packages of multiple sets of trough cross-bedding. The basal surfaces of sets are erosional. This facies is arranged into beds that are each 0.5-1 m thick. Cross strata pass laterally and upward within sets into planar-tabular cross-bedded sets.	Sandy bar forms within a fluvial channel; dominantly records downstream accretion under lower flow regime conditions by the downstream migration of sinuous-crested dunes.
Horizontally laminated sandstone (Fh)	Very well-sorted, fine-grained sandstone. Fh is characterized exclusively by bed-parallel laminations in the form of primary current lineations.	Migration and deposition of sandy bar forms under upper flow regime conditions.

Facies	Description	Interpretation
Cross-bedded, pebbly sandstone (Fxpb)	Well sorted, fine to medium grained, cross-bedded pebbly sandstone. Fxpb is abundant in quartz, feldspar and rounded pebble-grade extraclasts including black concretions of heavy minerals. Pebbles range in diameter from 20-40 mm. Black clasts are typically 10-20 mm in diameter. Fxpb is also abundant in yellow (30-40 mm) and red mud clasts (5-300 mm).	Migration and deposition of pebbly bar forms under lower flow regime conditions.
Cross-bedded pebbly sandstone with sigmoidal foreset shapes (Fxps)	Well-sorted, fine- to medium-grained sandstone with pebbles. Rounded quartz and feldspar pebbles, mud clasts and black concretions are common. Pebbles range from 20-40 mm in diameter as for facies Fxpb. Mud clasts are smaller than those in facies Fxpb: their diameter ranges from 20-60 mm. Black concretionary pebbles are 10-20 mm in diameter. Cross-bedding preserves sigmoidal foreset shapes. Low-angle inclined bottom-sets are present.	Migration and deposition of sandy bar forms within a fluvial channel; downstream accretion under conditions of lower flow regime.
White, fine-grained siltstone and silty sandstone (Fwb)	Mostly fine-grained sandstone and subordinate siltstone interbedded with cross-bedded and horizontally laminated sandstone. Fwb occurs as beds that are each 0.1-0.15 m thick, with a lateral continuity of 30-50 m; typically white in colour. Abundant desiccation cracks.	Drapes that overlie bedform deposits; records deposition during relatively low-energy flow conditions.
Ripple laminated sandstone (Frc)	Moderately sorted, fine-grained sandstone. Ripple strata typically climb at angles < 10°, but can climb up to 15°. Ripple forms are sinuous crested.	Represents down-channel migration, climb and accumulation of sinuous-crested ripples.
Sandstone with deformed laminations (Fd)	Fine-grained sandstone characterized by deformed, originally horizontal laminations; deformation expressed as harmonic and disharmonic folds with antiform shapes and sand volcanoes. Disharmonic folds (flames) exhibit sharp cut of the overlying sedimentary laminations.	Deformation due to sudden water escape with increasing pressure related to rapid burial or to instantaneous seismic shaking.
Conglomerate and sandstone with extraformational clasts (Fce)	Conglomerate and sandstone with angular to sub-angular, commonly dark-coloured clasts of igneous and metamorphic origin. Most commonly these clasts occur in the lowermost 50-100 mm of sets. Clasts are 50-150 mm in diameter.	Lag deposits, representing coarsest sediment fraction transported by the flow during high-energy conditions, likely in channel thalwegs. The angular nature of the clasts reflects a limited distance of transport and a local sediment source.
Conglomerate and sandstone with intraformational clasts (Fci)	Conglomerates and sandstone; fine-to coarse grained sand matrix with reddish mudstone clasts that are 10-40 mm in diameter. Clasts are sub-rounded to sub-angular.	Intraclasts record the localised reworking of mudstone beds (Fm), with clasts derived either via erosion from the base of the channel or from bank collapse at the channel margin.

3.5.1 Red mudstone elements (F1)

Description. The basal 35 m of the North Head Member of the St Bees Sandstone Formation outcropping at Saltom Bay (Figure 3.8) is dominated by an alternation of red mudstone elements (F1) and sheet-like sandstones (F2). Red mudstone elements are characterized by mixed claystone and siltstone (Fm), and siltstone and very fine-grained sandstone with ripple forms (Frc). Claystone and siltstone beds (Fm) are 0.1 to 0.6 m thick and characterized by bed-parallel laminations (Figures 3.6, 3.9). Some parallel laminated beds rarely pass laterally into siltstone and very-fine sandstone interbeds, which preserve ripple forms.

Interpretation. Red mudstone elements (F1) and sheet-like sandstone elements (F2) likely have a co-genetic origin. During the initial flow stage, flow velocity was high and only sand was deposited. Progressively, flow velocity waned to zero and the claystone and siltstone component was deposited from suspension to form the red mudstone elements (cf., Hampton and Horton, 2007; Banham and Mountney, 2014). Ripple laminated sandstone in a floodplain environment is typically related to bedform migration by unconfined tractional flow in lower flow regime conditions (cf., Jopling and Walker, 1968; Ielpi, 2012).

3.5.2 Sheet-like sandstone elements (F2)

Description. Sheet-like sandstone elements up to 0.4 m thick are composed internally of fine-grained sandstone beds (Fsh) (Figure 3.9). The bases and tops of the sheet-sandstone bodies are generally sharp and the basal contact that divides F2 from F1 elements is erosive. There is a notable absence of upwards fining within individual beds. The lateral continuity of sheet-like sandstone and red mudstone elements exceeds the outcrop scale, which is 200 m in sections perpendicular to palaeflow as exposed at Saltom Bay Cliff (Figure 3.8a). On the basis of analysis of vertical stacking patterns, the sheet-like sandstone elements are more common and more amalgamated towards the top of the lower North Head

Member. The stratigraphic succession exposed at Saltom Bay (Figure 3.8) demonstrates how the amount of amalgamation of sheet-like sandstone elements progressively increases higher in the stratigraphic succession of the lower North Head Member. Furthermore, the amount of amalgamation of sheet-like sandstone elements also increases upwards directly below channel elements that occur interbedded in the floodplain succession (Figures 3.8b, 3.9).

Interpretation. Sheet-like sandstone elements represent repeated non-confined fluvial flood events (cf., Fisher et al. 2008). Sheet-like sandstone elements are co-genetic with red-mudstone elements and record deposition and accumulation during the initial part of a flood event. During the initial part of the flow event the energy was high and capable of erosion, as demonstrated by a sharp and erosional contact at the base of F2 elements.

The source of the sediment for accumulation of the sheet-like sandstone elements was likely crevasse-splay bodies, which introduced sand, silt and clay onto the alluvial plain during flood events (O'Brien and Wells, 1986; Smith, 1993; Bridge, 2003). In cases where sheet-like sandstone elements (F2) occur amalgamated directly below channel elements, F2 elements likely represent progradation of crevasse channels and fine-grained sandstones (Fsh) deposited in close proximity of their feeder. Thus, amalgamated sheet-like sandstone elements (F2) likely represent splay development that was proximal to the trunks of the mouth of crevasse channels (cf., Tunbridge, 1984; Ielpi, 2012).
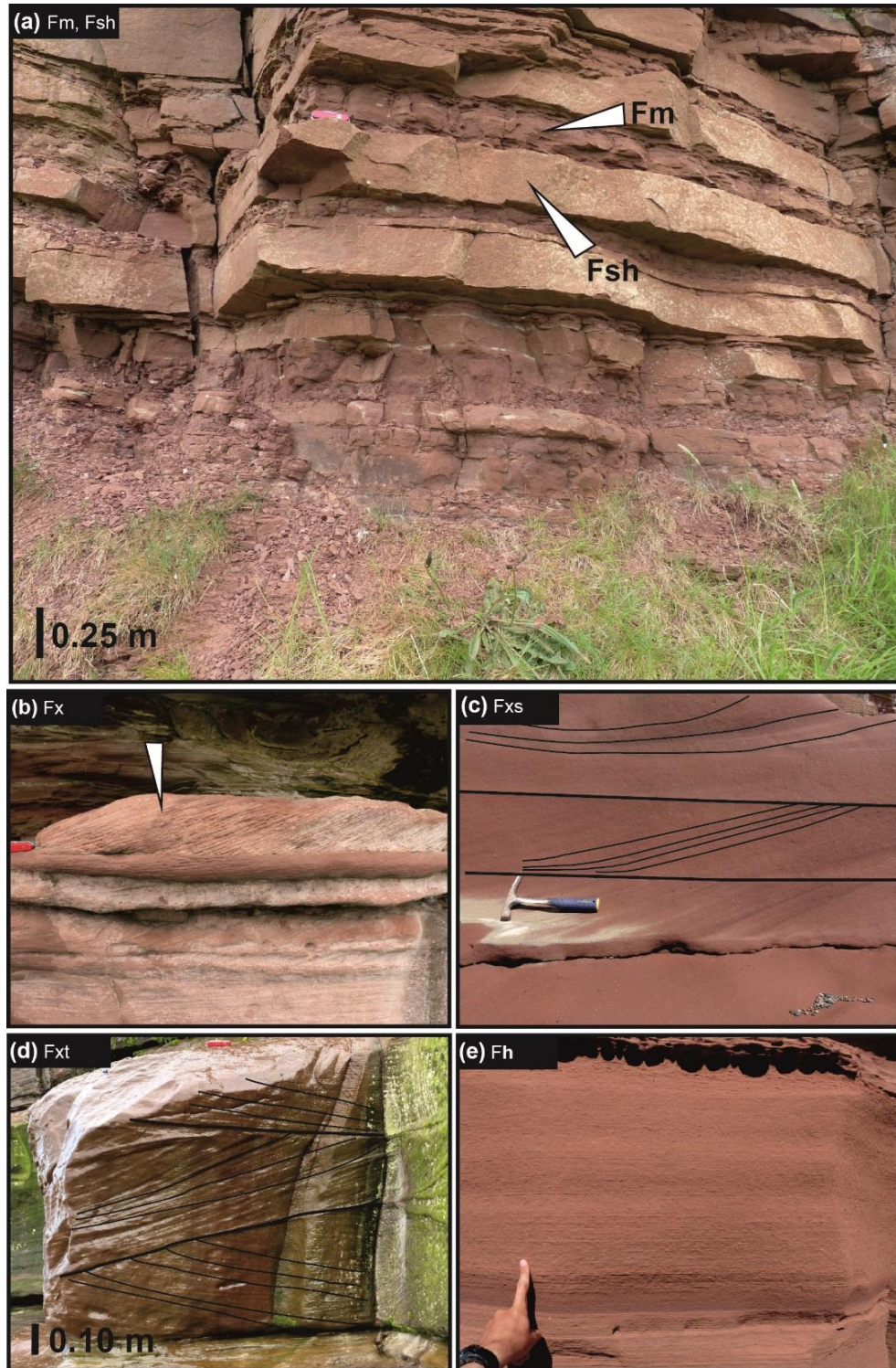
Figure 3.4: Representative lithofacies of the Sherwood Sandstone Group in South East Yorkshire and West Cumbria. (a) Alternation of red mudstone (Fm) and fine-grained sheet-sandstone (Fsh), (b) Planar cross-bedded sandstone; planar cross-beds, (c) Cross-bedded sandstone with sigmoids; sigmoidal cross-beds and mud clasts, (d) Trough cross- bedded sandstone; laminae with erosive basal contact, (e) Horizontally laminated sandstone; bed parallel laminae.
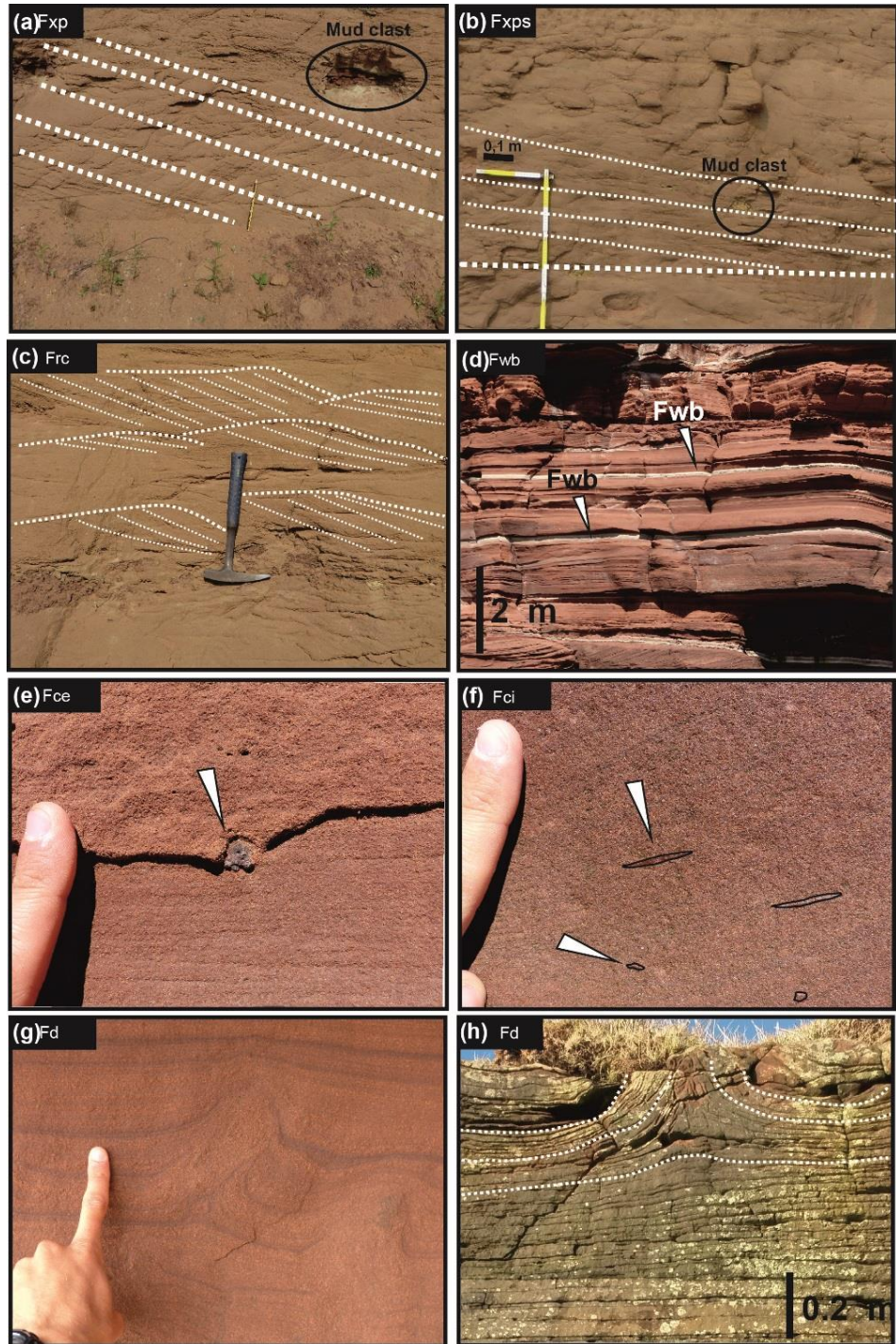
Figure 3.5: (a) Cross-bedded pebbly sandstone; planar cross-beds and mud clasts, (b) Cross-bedded pebbly sandstone with sigmoids; sigmoidal cross-beds and mud clasts, (c) Ripple cross-laminated sandstone; climbing ripples, (d) White-fine grained siltstone/silty sandstone; thin beds of fine-grained sandstone draping coarser-grained red sandstones, (e) Conglomerate/sandstone with dark extraformational clasts of igneous origin, (f) Conglomerate/sandstone with intraformational clasts, (g) Sandstone with deformed laminae; disharmonic fold (flame), (h) Sandstone with deformed laminae; sand volcano.

Figure 3.6: (a) Representative stratigraphic logs recorded in the Sherwood Sandstone Group fluvial deposits (South East Yorkshire, West Cumbria) in the locations in Figures 3.2 and 3.3, (b) Palaeocurrent data collected in the North Head Member and South Member and of the West Cumbrian St Bees Sandstone Formation and in the fluvial deposits of the Sherwood Sandstone Group in South Yorkshire.

Figure 3.7: Representative architectural elements, depicting generalized geometries and facies composition of the architectural elements characterizing the Sherwood Sandstone Group fluvial deposits (South East Yorkshire, West Cumbria).
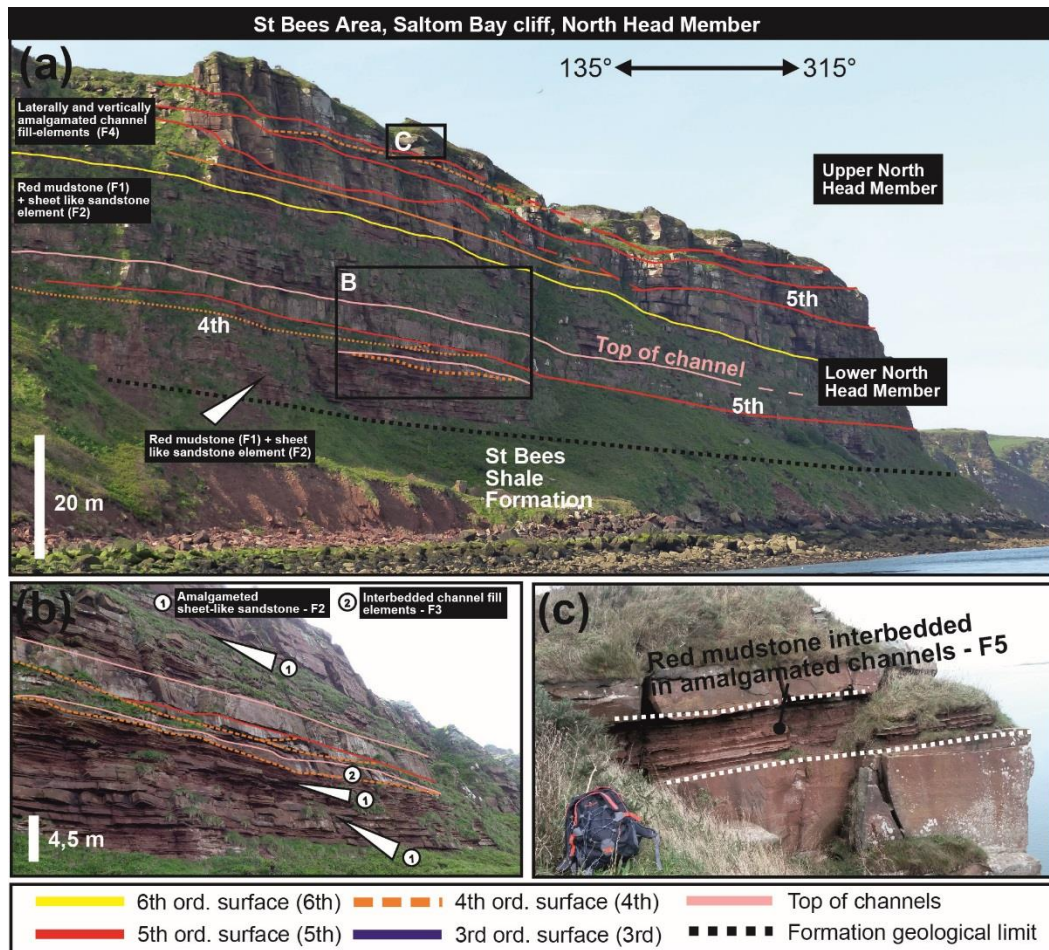
Figure 3.8: Basal part of the St Bees Sandstone Formation at Saltom Bay. (a) North Head Member outcropping at Saltom Bay (see Figure 3.2), (b) North Head Member: basal 35 m of the St Bees Sandstone Formation: '1' detail of amalgamated channel sheet-like sandstone (F2); '2' interbedded channel fill-element (F3), (c) North Head Member: detail of overbank elements interbedded in amalgamated channels (F5).

3.5.3 Interbedded channel-fill elements (F3)

Description. Channel-fill elements occur interbedded with red mudstone (F1) and sheet-like sandstone (F2) elements in the lower North Head Member at Saltom Bay (Figures 3.8, 3.9). Such interbedded channel-fill elements are delimited at their base by 4th or 5th order bounding surfaces (sensu Miall, 2006). For example, along the Saltom Bay Cliff (Figure 3.8), minor channel-fill elements are bounded by concave-upwards erosive surfaces that are typical of 4th order bounding surfaces, whereas larger

channel-fill elements interbedded with floodplain elements at Saltom Bay and North Head are bounded at their base by mostly flat, rarely concave-upwards and laterally continuous erosive surfaces, which represent 5th order bounding surfaces.

The lowermost channel body exposed at Saltom Bay is 3 m thick and extends laterally for 50 m in sections perpendicular to palaeoflow. Laterally, the same stratigraphic section is also characterized by a fluvial interbedded (F3) and amalgamated channelized body (F4), which is 5 m thick and extends for at least 200 m in section near-perpendicular to palaeoflow, exceeding the outcrop extent. The internal lithofacies composition of F3 architectural elements is well exposed in a disused quarry (Hutbank Quarry) where a multi-storey channel body is exposed (Figure 3.9). The internal facies arrangement of the channels (F3) comprises vertically stacked sets of compound cross-bedded units (Fx, Fxs, Fxt), which are each up to 1 m thick. Multiple 3rd order bounding surfaces characterize the multi-storey channel-fill and these are delineated from the basal 4th order bounding surface (Figure 3.9) in that the former downlap the basal erosive surface at angles of up to 25°. Additionally, multiple 3rd order bounding surfaces cut sets of cross-beds at low angles (usually < 15°) and are directly overlain by conglomerate lags comprising both intraclasts and dark igneous extraclasts (Fci, Fce), comprising 5% and 10% of the deposit, respectively.

Interpretation. Channel-fill architectural elements represent sediment bodies formed by stacked-fluvial bars, themselves formed from compound cross-bedded units (Fx, Fxs, Fxt). Overall, the main cliff section at Saltom Bay and Hutbank Quarry (Figures 3.6, 3.9) reveals the degree of amalgamation of sheet-like elements (Figure 3.8b) fed by crevasse splay. This degree of amalgamation of F2 architectural elements increases higher in the stratigraphic succession below the erosive contact with the channel-fill elements (F3) interbedded in floodplain deposits. The systematic passage between amalgamated sheet-like sandstone elements (F2) and channelized elements (F3) shows the transition between distal crevasse

splay deposits (sheet-like sandstone) and crevasse channels interbedded in the alluvial plain (cf., Banham and Mountney, 2014). Progradation of the fluvial system over time may explain the stacking of crevasse channels above sheet-like sandstones (Jones and Ambrose, 1994). Alternatively, channel avulsion, possibly driven by activity on basin-margin faults, may explain the systematic transition between sheet-like sandstones fed by crevasse-splays into crevasse channels (cf., Leeder and Gawthorpe, 1987; Stouthamer and Berendsen, 2001; Aslan et al., 2006). Indeed, given that normal faults of half grabens generate increased accommodation towards the bounding extensional fault, deposits related to avulsions of crevasse channels tend to become preferentially stacked in locations close to the bounding tectonic structures (Leeder and Gawthorpe, 1987). The presence of black igneous extraclasts in the fill of the crevasse-channels indicates a source from the Ordovician Borrowdale Volcanic Group (Strong et al., 1994), which has previously been interpreted to form part of the Lake District structural high (Jones and Ambrose, 1994).
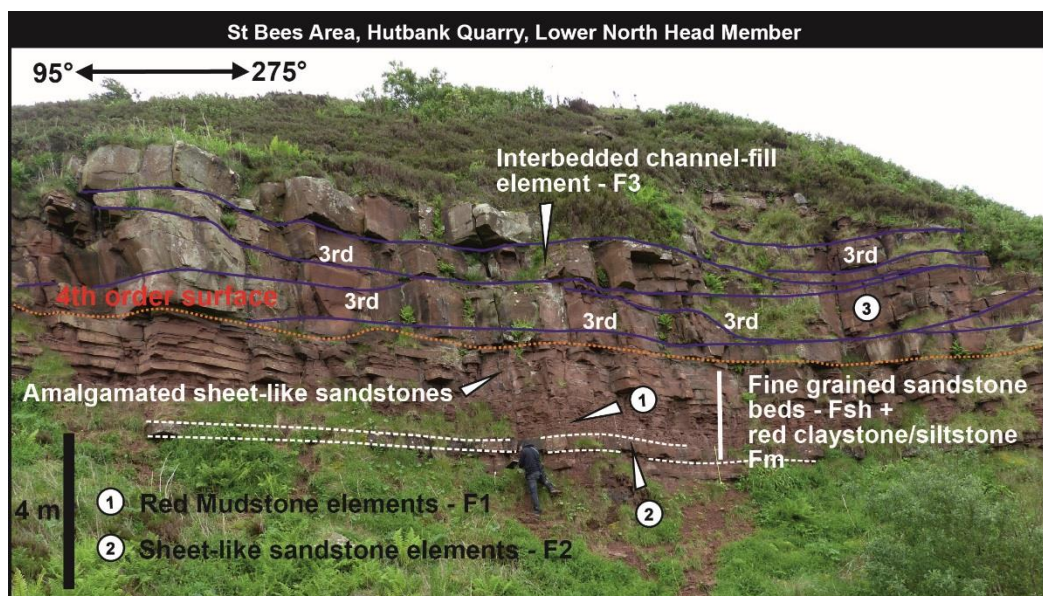
Figure 3.9: Lower North Head Member; '1' Alternation of red mudstone and '2' sheet-like sandstone elements with an interbedded channel-fill element outcropping in the upper part of the Hutbank Quarry (see Figure 3.2).

3.5.4 Laterally and vertically amalgamated channel-fill elements (F4)

Description. Amalgamated channel-fill elements form 70% of the upper part of the North Head Member (Figure 3.10). The degree of amalgamation of F4 elements increases higher in the stratigraphy, and in the South Head Member these elements represent the 95% of the stratigraphic record. In the North Head Member, channels are separated by units of mudstone (Figure 8c, F5) that are each up to 1 m thick, whereas in the South Head Member F4 elements are more amalgamated and F5 overbank elements are only rarely preserved.

Extrabasinal clasts of igneous origin comprise <2% of F4 elements in the St Bees Sandstone Formation, compared to 10% in the conglomerate lags of F3 channelized elements interbedded with floodplain deposits. Furthermore, igneous extraclasts are rare in F4 elements in the lower part of the South Head Member and are completely absent in the upper part.

Laterally and vertically amalgamated channel-fill elements (F4) are characterized in both West Cumbria and South Yorkshire by stacked barform deposits that comprise the fill of individual channel bodies (Figures 3.10-3.15). The major bar structures comprise medium- to well-sorted, compound cross-bedded sets (Fx, Fxs, Fxt, Fxpb, Fxps) and horizontally planar sandstone (Fh) characterized by current lineations. Facies successions of different types of predominantly cross-bedded sets are characterized by upwards coarsening and decreasing textural maturity (Fx, Fxpb, Fxps, Fxs, Fxt), with most successions capped by horizontally laminated beds (Fh). Barform deposits of F4 elements are asymmetrical in cross-section (Figures 3.11, 3.13a) revealing 1st, 2nd and 3rd order erosional bounding surfaces that dip towards the dominant palaeoflow direction. Additionally, 2nd and 3rd order erosional bounding surfaces are commonly overlain by sets that preserve avalanche deposits on their downstream faces. Dune-scale bedforms that are superimposed upon barform deposits differ from major bar-structures in that the former are dominated by trough cross-bedding (Fxt). Indeed, trough cross-bed sets comprise 60% of preserved dune bedform deposits but only 15% of barform deposits, which

are instead dominated by planar and sigmoidal cross-bed sets (Fx, Fxs, Fxpb, Fxpx; collectively 60%). Ripple forms (Frc) and planar and sigmoidal cross-beds (Fx, Fxs) characterize dune-scale bedforms, accounting for 10% and 20% of these bedforms, respectively. Ripple forms (Frc) are commonly preserved climbing in downstream directions (Figure 3.5). Compound cosets of dune-scale strata form sand bodies up to 1.5 m thick with troughs that are <1 m wide (Figure 3.14). Dune-scale bedforms are asymmetrical in cross-section; 1st- and 2nd order erosional bounding surfaces dip towards the palaeoflow direction (Figure 3.15). Foresets of dune-scale bedforms dip at angles up to 30°, whereas set and coset 3rd and 4th order bounding surfaces typically dip at angles up to 20° and 10°, respectively. Red silty mudstones (Fm) are commonly associated with amalgamated channel-fill elements (F4) and form thin, 0.05 to 0.1 m-thick beds that drape the surface of cross-bedded sandstone bodies and which lack evidence of an erosional contact (Figures 3.10 and 3.13b).

Major barforms are characterized by a low-spread of cross-bed foresets azimuths. Foreset azimuths from cross-bedded sandstone beds (Fx, Fxs, Fxt) measured in the North Head and South Head members show an average palaeo-bedform migration direction towards the NNW (mean vector = 333°; mean vector length = 0.90; n=96). Palaeocurrent data (Figure 3.6b) recorded from barform structures of the North Head Member indicate a vector mean of 318°, whereas cross-beds of stacked barforms of the South Head Member indicate a vector mean of 338° (Figure 3.6b). Cross-bed foreset azimuths measured from cross-bedded sandstones (Fx, Fxps) that form stacked barform deposits at Dunsville Quarry (Figure 3.6b) record an average palaeocurrent direction towards the NNE (mean vector = 024°; mean vector length = 0.94; n=136); cross-bed foreset mean azimuths are 027° (n=19) and 023° (n=117), respectively for facies Fx and Fxps (Figure 3.6b).

Despite the various common sedimentological characteristics between the studied stratigraphic successions in Cumbria and South Yorkshire, units of very fine-grained bleached sandstones and siltstones (Fwb) characterize

only the amalgamated channels of the St Bees Sandstone Formation. Horizontally-laminated medium grained sandstones (Fh) and cross-beds (Fx, Fxs, Fxt) are commonly draped by these fine-grained bleached sandstones and siltstones (Fwb). These fine grained bleached sandstones are up to 0.2 m thick and they have a lateral extent of 2 to 10 m both parallel and perpendicular with respect to the palaeoflow. Amalgamated channel-fill elements (F4) in West Cumbria are additionally characterized by soft-sediment deformation structures in horizontally laminated sandstones (Fh). Soft-sediment deformed structures consists of small-scale (10-40 cm) isolated structures forming harmonic and a variety of disharmonic folds (Fd; Figures 3.5, 3.12a-d). Additionally, soft-sediment deformed sandstone (Fd) consists of laterally extensive horizons (5-6 m) which show upwards increasing of deformation and top-truncation of the folded laminae (Figure 3.12d).

Two sedimentary facies that are only present in F4 elements at Dunsville Quarry are cross-bedded pebbly sandstone (Fxp) and cross-bedded pebbly sandstone with sigmoids (Fxps). These facies comprise well sorted, medium-grained sandstone beds that are characterized by rounded pebbles of extra-clasts (20 to 40 mm in diameter) and mud intraclasts up to 0.3 m in diameter. Cross-bedded pebbly sandstone (Fxp) and cross-bedded pebbly sandstone with sigmoids (Fxps) represent the most abundant lithofacies at Dunsville Quarry, together representing 50% of amalgamated channel-fill elements (F4).

Interpretation. Barforms of laterally and vertically amalgamated channel-fill elements (F4) record dominantly downstream accretion as demonstrated by the presence of 2nd and 3rd order erosional bounding surfaces that dip towards the palaeoflow direction, with avalanche deposits also present on the downstream facing foresets (Miall, 1977; Macchi, 1991). Barforms characterized by cross-beds (Fx, Fxpb, Fxps, Fxs, Fxt) and superimposed horizontally laminated deposits (Fh) (Figure 3.11b) might represent subaqueous bar platforms formed by cross-bedded sets that fine upwards within F4 elements into horizontally laminated supra-platform deposits that

signify episodic emergence (Steel and Thompson, 1983). This explains the upwards coarsening and decrease in textural maturity of both cross-beds (Fx, Fxpb, Fxps, Fxs, Fxt) and horizontally laminated beds (Fh) (Steel and Thompson, 1983). This superimposition of facies reflects the migration of bar heads and bar tails over the bar platform (Bluck, 1971, 1979) and demonstrates bifurcation of flow around mid-channel longitudinal bars (cf., Haszeldine, 1983; Steel and Thompson, 1983). The occurrence of downstream accreting barform deposits characterized by a low spread of foreset cross-bed dip azimuths and the bifurcation of flow around mid-channel longitudinal bars which is typical of braided-fluvial systems (Bridge 1985, 1993, 2006; Collison, 1986). The dune-scale bedforms record downstream accretion since the 1st and 2nd order erosional bounding surfaces dip towards to the palaeoflow direction and ripples that climb in a downstream direction are present. Such dunes are commonly reported from sand-dominated braided-river systems (e.g., Bristow, 1988; Reesink and Bridge, 2009; Ghinassi, 2011). Additionally, the generally coarse-grained composition of sand deposits, the paucity of mudstone and the abundance of planar cross-bedding have long been recognized as characteristics of braided fluvial systems (Coleman, 1969; Bristow, 1988).

The growth direction of the sandy barforms is directed towards the NNW and NNE in the St Bees area (Cumbria) and in the Dunsville Quarry (South Yorkshire), respectively. The internal facies arrangement of the bar elements is such that cross-bedded sets and cosets represent barforms deposited under conditions of lower flow regime (Harms and Fahnestock, 1960; Miall, 1977). Horizontally laminated, planar sandstone facies with current lineations represent barforms whose upper surfaces experienced conditions of upper flow regime (Collinson et al., 2006).

Dune-scale bedform deposits that are superimposed upon barform deposits represent trains of dunes that were at least 1.5 m high (based on preserved set thicknesses), and which had crestline sinuosities that were <1 m wide (each separated by 2nd order erosive surfaces); these dunes

moved over the fronts of the larger bars (cf., Rubin and Carter, 2006; Ashworth et al., 2011).

In both the studied localities, red mudstone (Fm) units drape upper bar-surface topography and such deposits record accumulation under conditions of very low energy that likely occurred during the latest stages of a depositional event within a fluvial channel when the finest components were deposited in ponds developed in bar-top hollows via suspension settling (Bridge, 2006). These red-silty drape deposits (Fm) are more abundant in the St Bees Sandstone Formation of West Cumbria that the deposits in South Yorkshire.

The white, very fine-grained bleached sandstones and siltstones (Fwb) that are present in F4 elements only in the St Bees Sandstone Formation apparently accumulated as drapes over bed forms during episodes of low-stage flow (Jones and Ambrose, 1994). These Fwb deposits are coarse-grained equivalents to the red-silty drape deposits (Fm) and consequently record deposition under slightly higher energy conditions.

Small-scale and isolated soft-sediment deformation structures in F4 elements of the St Bees Sandstone Formation are typically related to lateral and vertical shear stresses triggered by water escape and bedform collapse occurring during high discharge events (cf., Owen and Moretti, 2011; Owen and Santos, 2014). These small-scale bedforms, if strongly asymmetric (disharmonic folds, flames), can also be related to relatively high rates of basin subsidence and penecontemporaneous sediment accumulation whereby recently accumulated deposits subsided rapidly beneath the water table (cf., Anketell et al., 1970; Moretti et al., 2001; Owen and Moretti, 2011). However, soft-sediment deformation occurring as laterally extensive horizons is commonly ascribed to seismic activity (Owen and Santos, 2014; Ielpi and Ghinassi, 2015).

The relative abundance of cross-bedded pebbly sandstones with pebbles of both intraclast and extraclast origin in South Yorkshire may be related to: (i) a higher energy braided fluvial system; (ii) lower rates of subsidence and

accommodation generation, which facilitated the reworking of fine-grained deposits in the upper part of fluvial bars and preferential preservation of channel base (thalweg) deposits (Burley, 1984; Chadwick et al., 1994); or (iii) a closer proximity of the depocentre to the sediment source area.
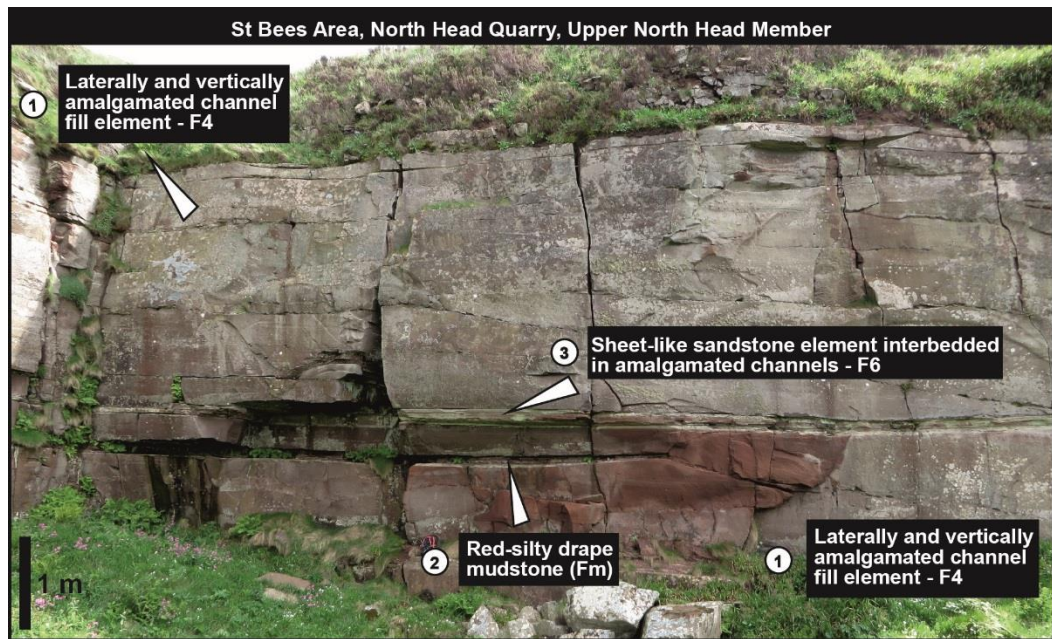
Figure 3.10: Upper part of the North Head Member outcropping in the North Head Quarry (see Figure 3.2): '1' coarse sandstone of laterally and vertically amalgamated channel-fill complexes; '2' Red-silty drape mudstone part of amalgamated channel-fill complexes; '3' Sheet-like sandstone element interbedded in amalgamated channel-fill complexes.
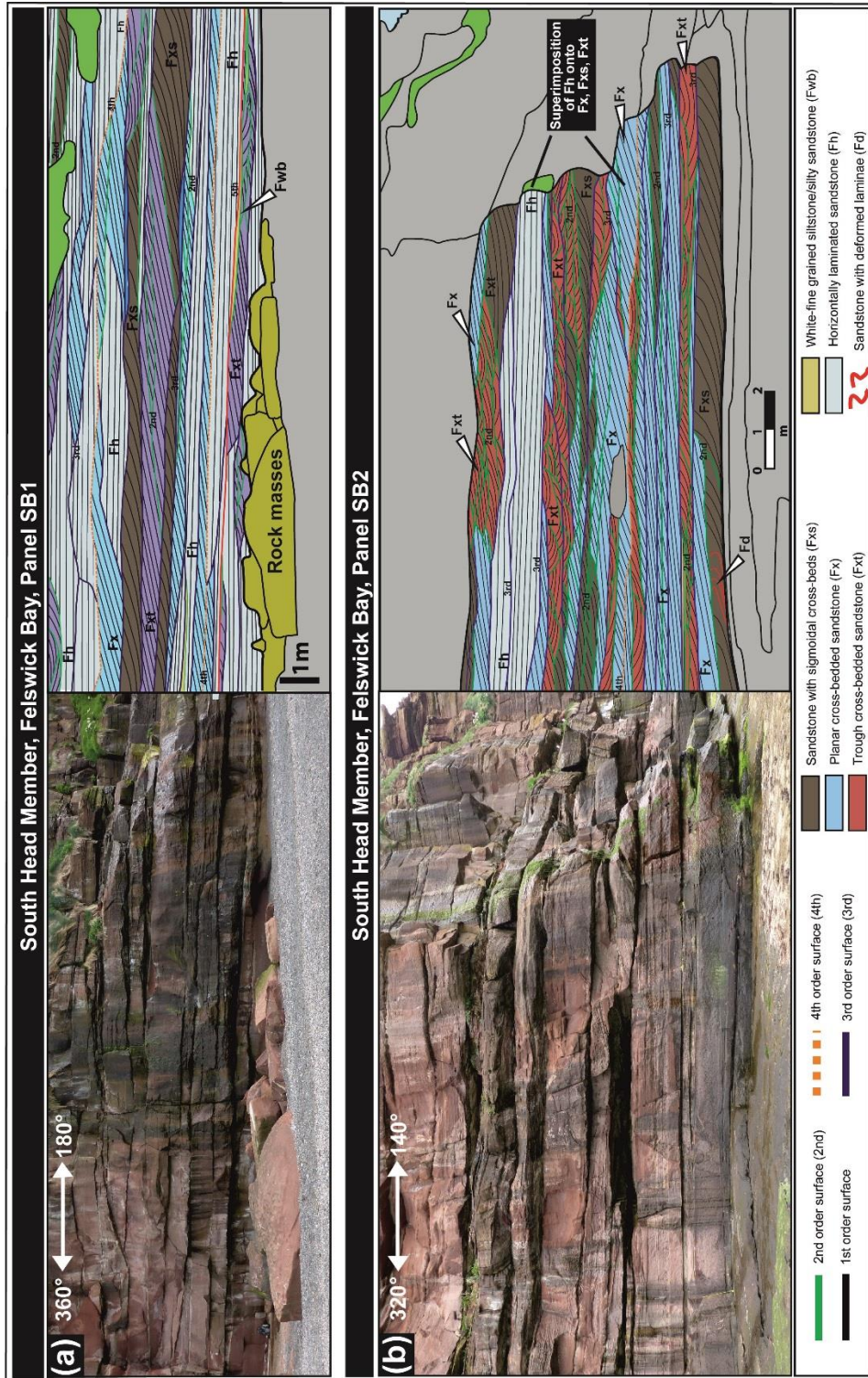
Figure 3.11: Architectural panels showing the fluvial architecture of laterally and vertically amalgamated channel-fill elements in a section perpendicular to palaeoflow direction (South Head Member) at the Fleswick Bay (see Figure 3.2). (a) Downstream dipping of 2nd and 3rd erosive bounding surfaces with occasional avalanche face, (b) Superimposition of bed-parallel beds (Fh) of bar platform onto cross-beds (Fx, Fxs) representing supra-platform deposits.
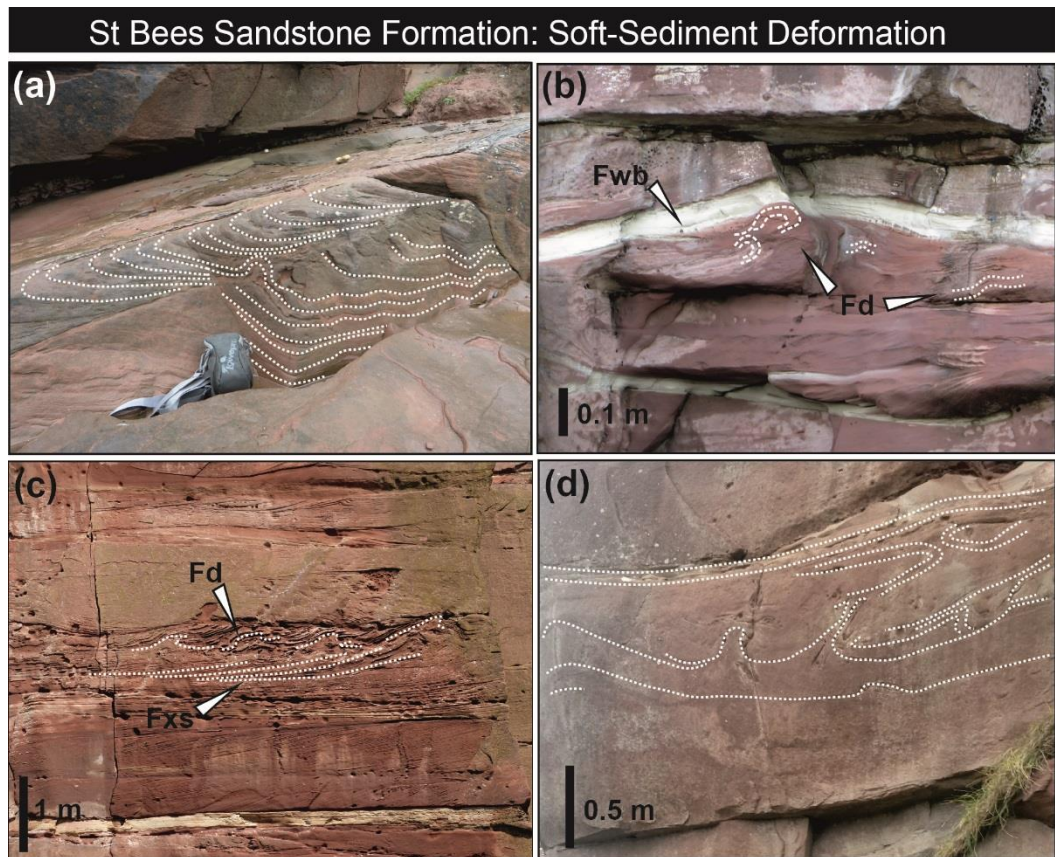
Figure 3.12: Soft-sediment deformation (Fd) in the St Bees Sandstone Formation (West Cumbria) outcropping at South Head (see Figure 3.2). (a) Small scale harmonic folds deforming though cross-bedded sandstone (Fxt), (b) Small scale harmonic and disharmonic folds top-truncated by white silty sandstone (Fwb), (c) Disharmonic folds and flames deforming cross-bedded sandstone with sigmoidal forest shapes, (d) Detail of large scale soft-deformation (harmonic folds, flames, sand volcanoes) showing an upwards increase in the intensity of deformation.

78
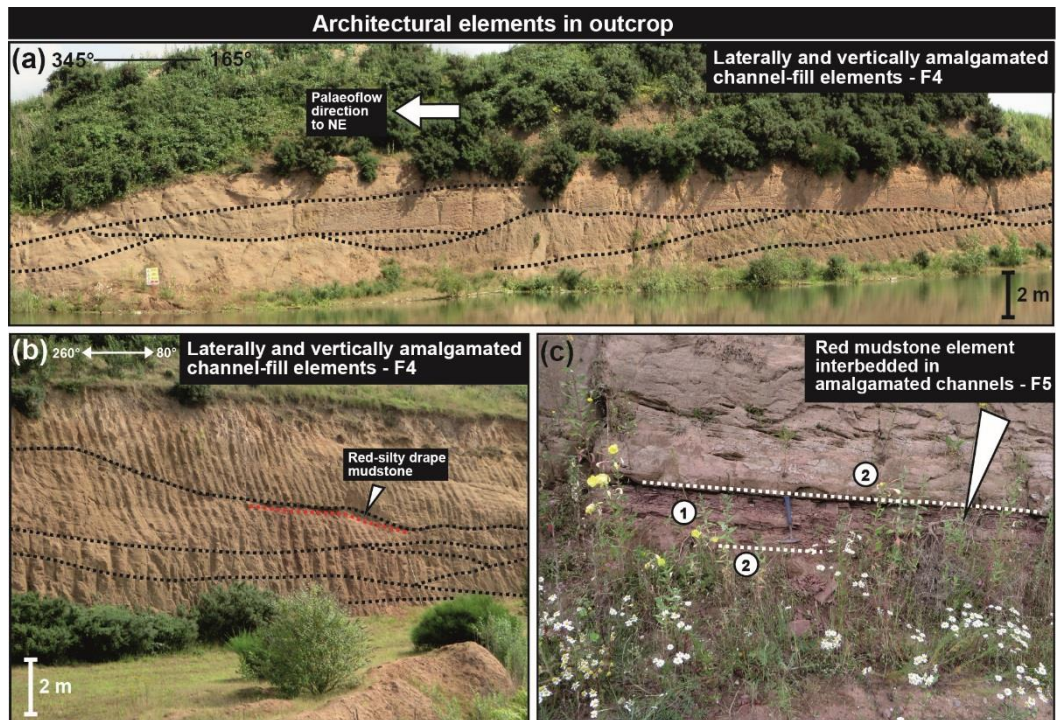
Figure 3.13: Sherwood Sandstone Group outcropping in the Dunsville Quarry (see Figure 3.3). (a) Laterally and vertically amalgamated channels elements outcropping in Dunsville Quarry: downstream accretion of sandy bed-forms, (b) Laterally and vertically amalgamated channel elements outcropping in the Dunsville Quarry in view perpendicular with respect to the palaeoflow: red-silty mudstone draping a sandy bar form, (c) Overbank element: '1' red silty mudstone related to unconfined flow; '2' channelized architectural elements at top and bottom of the overbank element.
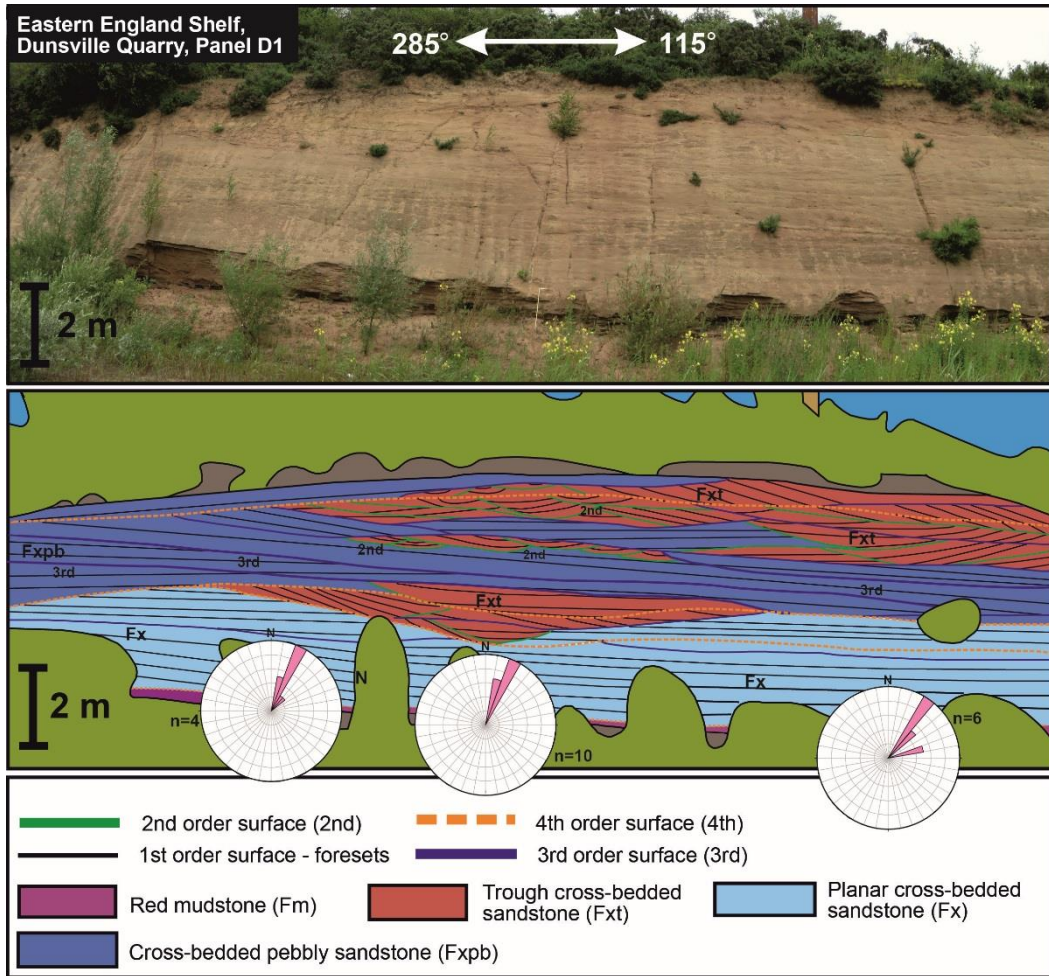
Figure 3.14: Architectural panel showing the fluvial architecture of laterally and vertically amalgamated channel fill elements of the Sherwood Sandstone Group (Dunsville Quarry, see Figure 3.3). View perpendicular to palaeoflow direction.
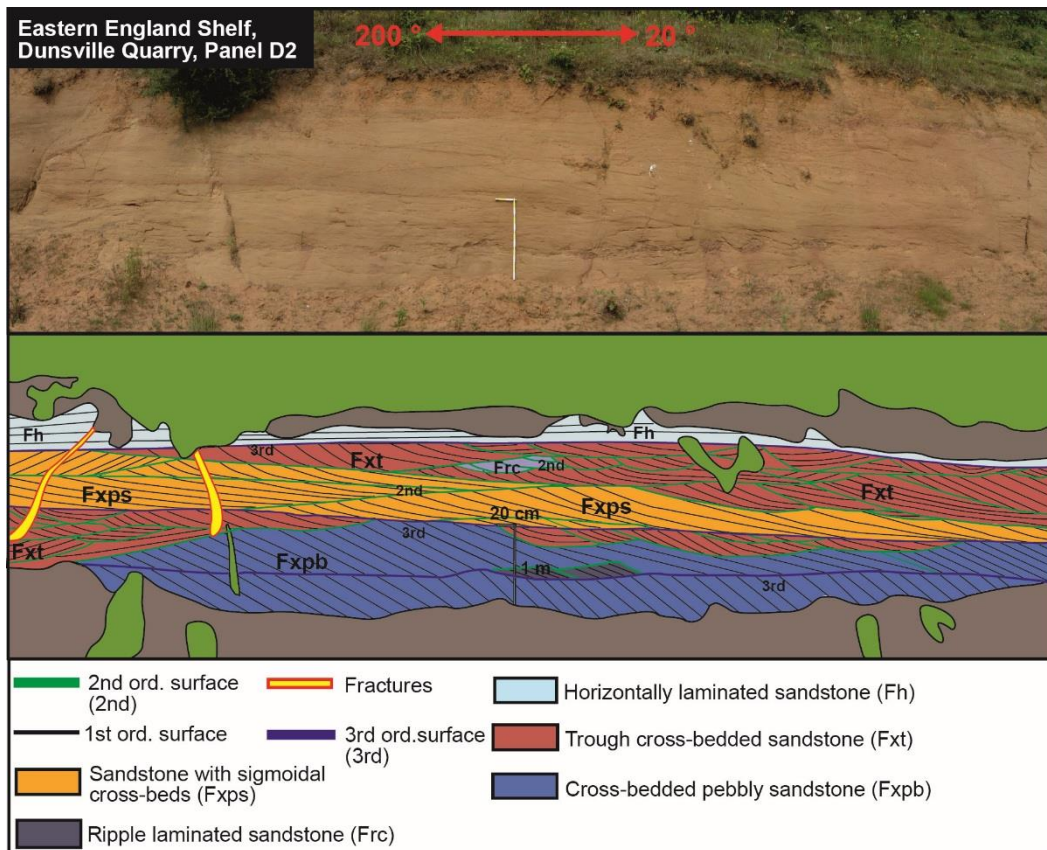
Figure 3.15: Architectural panel showing the architecture of dune scale bed-forms of laterally and vertically amalgamated channel-fill complexes of the Sherwood Sandstone Group (Dunsville Quarry, see Figure 3.3) in a section oriented parallel to inferred palaeoflow.

3.5.5 Red mudstone interbedded with amalgamated channels (F5)

Description. Red mudstone interbedded with laterally and vertically amalgamated channel fill-elements (F5) is characterized by reddish claystone and siltstone (Fm) as F1 elements. Despite this lithological common feature, F5 elements differ from F1 elements in that the former occurs preserved between laterally and vertically amalgamated channel-fill elements (F4) and are not regularly interbedded with sheet-like sandstone. In the Upper North Head and South Head members of the St Bees Sandstone Formation (Figure 3.8c), F5 elements composed of red mudstone are up to 0.6 m thick, and comprise 18% of the succession. In the South Head Member, F5 overbank elements comprise 5% of the

succession and are up to 0.3 m thick. Similar red mudstone (Fm) deposits interbedded with amalgamated channels (F5 elements) are also present in the studied successions in South Yorkshire. Here, red mudstone units are arranged into single beds up to 0.4 m thick (Figure 3.13c). In all observed instances, the lateral extent of the fine-grained overbank deposits exceeds that of outcrop scale.

Interpretation. These red mudstone F5 elements represent sediment deposits accumulated following overbank flood events (Kumar et al., 1999; Newell et al., 1999; Stanistreet and Stollhofen, 2002). Such flood events were characterized by relatively low energy and transport of very-fine grained material (Platt and Keller, 1992; Owens et al., 1999; Ghazi and Mountney, 2009, 2011). The overbank deposits record non-confined flow at times when fluvial discharge exceeded the bank full capacity of the fluvial channels (Bridge, 2003, 2006; Cain and Mountney, 2009).

3.5.6 Sheet-like sandstone elements interbedded with amalgamated channels (F6)

Description. Rare, sheet-like sandstones (F6) occur preserved between amalgamated channel fills (Figure 3.10) in the upper North Head Member and in the South Head Member. These sheet-like sandstone elements (F6) are exclusively characterized by fine-grained sandstone sheet-beds (Fsh). F6 architectural elements differ from F2 elements since the former do not occur regularly interbedded with red mudstone elements (F1).

Interpretation. Sheet-like sandstone elements interbedded with amalgamated channel-fill elements (F6), like F5 elements, represent sediment deposits accumulated following overbank flood events (Kumar et al., 1999; Newell et al., 1999; Stanistreet and Stollhofen, 2002). Sheet-like sandstone (F6) bodies occur interbedded with channel fills in cases where the velocity of the unconfined flow was higher with respect to the flow velocity that deposited red mudstone during unconfined discharge events (Hampton and Horton, 2007; Banham and Mountney, 2014).

3.6 Discussion

Lithofacies and architectural element analyses have revealed how the Sherwood Sandstone Group in the successions from both West Cumbria and South Yorkshire is dominated by fluvial bar structures. These stacked barforms appear asymmetrical in along-stream cross-sections (Figures 3.11, 3.13) with 1st and 2nd order erosive bounding surfaces dipping in the palaeoflow direction. Furthermore, 2nd and 3rd order bounding surfaces also show avalanche surfaces dipping towards the palaeoflow. Dune-scale bedforms dominated by trough cross-bedding and ripple forms occur superimposed upon barform deposits (Figure 3.15). Dunes and barforms record downstream accretion since erosive bounding surfaces dip towards the palaeocurrent direction and ripple forms climb downstream (Collinson, 1986; Bristow, 1988; Bridge, 2006; Rubin and Carter, 2006). Therefore both scales of bedform evolved predominantly by downstream accretion. The presence of downstream-accreting bedforms characterized by a low-spread of foreset cross-dip azimuths is indicative of flow bifurcation around mid-channel longitudinal bars in a braided-fluvial system (Haszeldine, 1983; Steel and Thompson, 1983; Bridge 1985, 2003, 2006; Collison, 1986). The generally coarse-grained composition, paucity of mudstone, and the abundance of planar cross-bedded sandstone have long been associated with braided-fluvial systems (Coleman, 1969; Bristow, 1988). Additionally, the two successions are characterized by: (i) barform elements that are elongated in a downstream direction and which preserve avalanche deposits on their lee slopes, (ii) a relative abundance of trough cross-bedded dune-scale deposits, and (iii) lack of a well-developed cyclicity, which typically portray so-called Platte-type braided river systems (sensu, Miall, 1977). All these sedimentological characteristics support the interpretation of a sandy braided river system for the studied fluvial successions in both the eastern Irish Sea Basin and the eastern England Shelf.

Palaeocurrent data from the St Bees Sandstone Formation in the St Bees-Whitehaven area record a palaeoflow direction towards the NNW (Figures

3.6b and 3.18), which implies a palaeodrainage parallel to the Triassic boundary faults of the eastern Irish Sea Basin (Figure 3.2b), an arrangement also interpreted more regionally from the easternmost sector of this basin (Jones and Ambrose, 1994; Nirex, 1997; McKie and Williams, 2009).

Palaeocurrent indicators from the eastern England Shelf succession record palaeodrainage towards the NNE which is consistent with the regional drainage pattern of Sherwood Sandstone Group deposits (Figure 3.16). Despite sporadic exceptions occurring in the Sheffield area, the spread of palaeocurrents for strata of the eastern England Shelf ranges from NE to NW, yielding a general sense of transport for the braided fluvial system towards the north or NNE (Edwards, 1967; Smith and Francis, 1967; Gaunt et al., 1992; Powell et al., 1992; Gaunt, 1994; Wakefield et al., 2015). Further evidence of this paleodrainage (Figures 3.16 and 3.17a) is indicated by a northward decrease in pebbly lithofacies that likely reflects increasing distance from the principal sediment source (Edwards, 1967; Smith and Francis, 1967; Gaunt et al., 1992; Powell et al., 1992; Gaunt, 1994). Regional palaeogeographic reconstructions of the Triassic rift systems of NW Europe (McKie and Williams, 2009; McKie and Shannon, 2011; Tyrrell et al., 2012), coupled with sediment provenance studies, demonstrate that the primary sediment source was the Armorican Massif (northern France) for both studied braided-fluvial systems (Wills, 1956; Audley-Charles, 1970; Mckie and Williams, 2009; Tyrrell et al., 2012; Morton et al., 2013). The Welsh Massif located 200 km south of the eastern Irish Sea Basin represents a likely secondary source of sediment for the St Bees Sandstone Formation (McKie and Williams, 2009; Tyrrell et al., 2012) and the Lake District Massif also contributed sediment from 30 km to the west (Jones and Ambrose, 1994; Strong et al., 1994). The London-Brabant Massif located 200 km south of the eastern England Shelf represents a likely secondary source of sediment for the Sherwood Sandstone Group in South Yorkshire (Figure 3.1). The regional distribution of palaeocurrent indicators and clast provenance excludes the palaeo-Pennine as a significant sediment source; the palaeoflow is directed parallel to this

Triassic palaeo-morphological high for both the studied fluvial systems (Figure 3.1).

The Armorican Massif occupied a palaeogeographic position ~550 to 600 km south of the eastern Irish Sea Basin and eastern England Shelf (McKie and Williams, 2009; McKie and Shannon, 2011). Thus, the two studied depocentres received sediment that had been carried via a major fluvial system for a similar distance from both its primary and potential secondary sources.

Although the two braided fluvial successions accumulated in two tectonically different sedimentary basins (Green, 1989; Bray et al., 1992; Jones and Ambrose, 1994; Nirex, 1997; Akhurst et al., 1998), they share many similarities: (i) they are characterized by the same general depositional environment (braided fluvial system); (ii) they both have the same primary sediment source (Wills, 1956; Audley-Charles, 1970; Mckie and Williams, 2009; Tyrrell et al., 2012; Morton et al., 2013); (iii) they both accumulated at the same time in basins that shared a common palaeolatitude; and (iv) they both accumulated under the influence of an arid climate such that vegetation cover was limited, as envisaged for other similar Triassic fluvial successions in NW Europe (Brookfield, 2004, 2008; Bourquin et al., 2009; McKie and Williams, 2009, Mckie and Shannon, 2011). Consequently, several of the principal allogenic factors that controlled the sedimentation process (climate, sediment source, bank stability and delivery style) were the same for both successions.

The braided-fluvial deposits of the tectonically active eastern Irish Sea Basin (Figure 3.18a) have an average preserved thickness of 475 m in West Cumbria, which accumulated in 4 Myr (Brookfield, 2008), yielding a time-averaged accumulation rate of 119 m/Myr. By comparison, the average preserved thickness of the Triassic braided-fluvial deposits on the eastern England Shelf is 200 m. This thickness of sediments accumulated in 18 Myr (Warrington, 1980), yielding a time-averaged accumulation rate of 11 m/Myr, this slower rate having been controlled by the slow rate of accommodation generation in this shelf-edge basin. However, this rate on

the eastern England Shelf is difficult to quantify accurately due to the presence of the Hardegsen unconformity, which occurs at the top of the succession (Bachmann et al., 2010). This Triassic region-wide unconformity typically corresponds to 150 m of erosion of stratigraphic succession in on shore regions elsewhere in NW Europe (e.g., Evans et al., 1993; Bourquin et al., 2006). Adding this potential value of erosion to the average preserved thickness (200 m) for the eastern England Shelf, the time-averaged accumulation rate might have potentially been as high as 19.4 m/Myr. However, this rate is still substantially lower than that of the eastern Irish Sea Basin.

The thickness of the braided-fluvial deposits of the eastern England Shelf and eastern Irish Sea Basin are strongly influenced by the regional tectonic background. Indeed, the preserved thickness of Triassic fluvial deposits of the eastern Irish Sea Basin varies systematically between the hangingwall and footwall of Triassic boundary faults (Jones and Ambrose, 1994; Nirex, 1997). The thickness of the Triassic fluvial deposits in the eastern England Shelf is constant along the strike of the shelf-edge basin but decreases progressively towards the palaeo-morphological structural high of the Pennines (Bath et al., 1987, Edmunds and Smedley, 2000; Aitkenhead, 2002; Smedley and Edmunds, 2002). This demonstrates that local variations of discharge conditions played a relatively minor role in determining the preserved sediment thickness with respect to tectonic background.

Although the fluvial deposits of West Cumbria and South Yorkshire are characterized by a similar degree of sand sorting, suggesting a comparable local discharge conditions, the stratigraphic succession of South Yorkshire is characterized by a relative paucity of fine to medium grained sandstone beds and a near complete absence of mudstone facies that drape barform tops (Figures 3.6a, 3.17b, c). The information collected in outcrop is supported by published well logs (Gaunt et al., 1992; Gaunt, 1994; Nirex, 1997; Pokar et al., 2006; West and Truss, 2006; Wakefield et al., 2015). Collectively, these data allow for upscaling of the outcrop information to that

of the basin. In both core and outcrop, sandy lithofacies (Fsh, Fx, Fxs, Fxt, Fh, Fwb, Fd) represent 52% and 87% of the succession, whereas pebbly lithofacies (Fxpb, Fxps, Fci, Fce) represent 46% and 5% in the eastern England Shelf and eastern Irish Sea Basin, respectively (Table 3.2). Core logs coupled with quarry face logs confirm the relative proportion of mudstone (Fm) with respect to sandy and pebbly lithofacies (Fsh, Fx, Fxs, Fxt, Fd, Fh, Fwb, Fxpb, Fxps, Fci, Fce): the Triassic fluvial deposits of the eastern England Shelf are characterized by significantly lower amount of mudstone compared to the eastern Irish Sea Basin, 2% versus 8%, respectively (Table 3.3).

Given that the two studied depocentres are characterized by a common set of controls and taking into account that they were governed by a similar local energy regime, differences related to the relative abundance of pebbly deposits versus fine-grained sandstone and mudstone deposits are most likely a function of the different tectonic backgrounds. In the eastern England Shelf succession, the vertical stacking of pebbly units and the general absence of fine-grained units reflect the slow rate of accommodation generation (cf., Colombera et al., 2015). In fact, in this shelf-edge basin successive fluvial cycles repeatedly reworked the uppermost parts of earlier fluvial deposits. Consequently, only the basal-most channel lags tend to be preserved, whereas the finer-grained uppermost parts of fluvial cycles tend to be reworked. By contrast, in the eastern Irish Sea Basin of West Cumbria, the rate of accommodation generation was substantially greater such that space was available to preserve more complete fluvial cycles (Figure 3.18b, c), including the finer-grained overbank units that cap the channelized deposits (Figure 3.6a). Preservation of aeolian facies in the eastern Irish Sea Basin (Calder and Ormskirk Sandstone formations) and their absence in the eastern England Shelf can also be related to the different rates in accommodation generation, whereby high rates of tectonic subsidence in the eastern Irish Sea Basin assisted long-term preservation of aeolian deposits by placing them beneath the local water table (Howell and Mountney, 1997; Mountney, 2012; Rodríguez-López et al., 2014).

Another important difference between the studied fluvial successions is the presence of intense soft-sediment deformation only in the West Cumbrian St Bees Sandstone Formation; no soft-sediment deformation has been observed in the succession studied at Dunsville Quarry (this work) and in the Styrrup Quarry (Wakefield et al. 2015). Indeed, the occurrence of intense soft-sediment deformation in the Triassic deposits is likely related to accumulation in tectonically active basins. Development of intense soft-sediment deformation may be related to (i) movement on basin-bounding faults that resulted in seismic activity, or to (ii) rapid rates of subsidence related to both fault activity and lithosphere cooling (Akhurst et al., 1997, 1998; Milodowski et al., 1998; McKie and Williams, 2009). Such activity allows the accumulating succession to rapidly subside beneath the local water table, thereby rendering non-lithified deposits prone to liquefaction and de-watering in response to either seismic shaking or sediment loading (Anketell et al., 1970; Mohindra and Bagati, 1996; Blanc et al., 1998; Moretti, 2000; Moretti et al., 2001; Berra and Felletti, 2011; Owen and Moretti, 2011; Owen et al., 2011; Santos et al., 2012; Üner et al., 2012; Owen and Santos, 2014; Ielpi and Ghinassi, 2015).

Table 3.2: Summary of the relative proportion of sandy and pebbly lithofacies in the eastern England Shelf and eastern Irish Sea Basin from previously published stratigraphic logs.

Reference	Sedimentary basin	Log type	Field site / borehole name	Latitude; longitude (WGS84)	Stratigraphic section logged (m)	Pebbly lithofacies logged (m)	Sandy lithofacies logged (m)	(Pebbly lithofacies)/ (Sandy lithofacies)
Wakefield et al., 2015	East England Shelf	Quarry face sections	Styrrup Quarry	53.405160; -1.091439	23	16	14	1.1
Gaunt, 1994	East England Shelf	Core	Hatfield Lane Water Borehole	53.546590; -1.049778	172	55	117	0.5
Gaunt, 1994	East England Shelf	Core	Hatfield Woodhouse 1	53.579621; -0.968079	235	235	25	9.4
Gaunt, 1994	East England Shelf	Core	Hatfield Main Colliery 1	53.593770; -1.0151773	165	165	100	1.6
Nirex, 1997	East Irish Sea Basin	Core	Sellafield Repository	54.924638; -3.561894	391	21	360	0.06

Table 3.3: Summary of the relative proportion of muddy versus sandy plus pebbly lithofacies in the eastern England Shelf and eastern Irish Sea Basin from previously published stratigraphic logs.

Reference	Sedimentary basin	Log type	Field site / borehole name	Latitude; longitude (WGS84)	Stratigraphic section logged (m)	Mudstone logged (m)	Sandy + pebbly lithofacies logged (m)	(Mudstone)/ (Sandy+Pebbly lithofacies)
Wakefield e al., 2015	East England Shelf	Quarry face sections	Styrrup Quarry	53.405160; -1.091439	23	0.1	22.4	0.004
Pokar et al., 2006	East England Shelf	Core	Dunsville 1	53.563661; -1.015575	14	0.6	13.5	0.04
Pokar et al., 2006	East England Shelf	Core	Eggborough	53.702131; -1.138074	19	0	19	0
West and Truss, 2006	East England Shelf	Core	Great Heck	53.674660; -1.070514	10	0.16	9.4	0.017
Gaunt, 1994	East England Shelf	Core	Pollington Water Borehole	53.684856; -1.111172	182	1.4	96.9	0.014
Nirex, 1997	East Irish Sea Basin	Core	Sellafield Repository	54.924638; -3.561894	425	34	391	0.09

The basal part of the St Bees Sandstone Formation registers a systematic up-succession increase in the amalgamation of sheet-like sandstone elements to a level directly beneath the interbedded channel-fills (F3). Furthermore, this also characterizes the stratigraphy beneath the base of the succession dominated by laterally and vertically amalgamated channel-fill elements (F4). This superimposition of crevasse channels (F3) and laterally and vertically amalgamated channel-fill elements (F4) onto amalgamated sheet-like sandstones (F2) may be explained through the northwards progradation of the braided-fluvial system (Jones and Ambrose, 1994). The progressive northwards advancement of channelized architectural elements (F3, F4) could have created the superimposition of these channelized bodies onto sheet-like sandstones of crevasse-splays which represent the distal expression of both interbedded (F3) and amalgamated (F4) channel-fills.

Another process that could explain this is avulsion driven by fault activity typical of half-grabens, as modelled by Leeder and Gawthorpe (1987). Given that normal faults of half-grabens, generating increased accommodation towards the bounding extensional fault, increased avulsion of crevasse channels would be expected closer to bounding tectonic structures (Bridge and Leeder, 1979; Leeder and Gawthorpe, 1987; Doglioni et al., 1998). Consequently, interbedded channels are predicted to progressively shift over time towards the bounding normal faults where they become stacked onto the lateral expression of the crevasse channels represented by amalgamated sheet-like sandstones (O'Brien and Wells, 1986; Smith, 1993; Bridge, 2003).
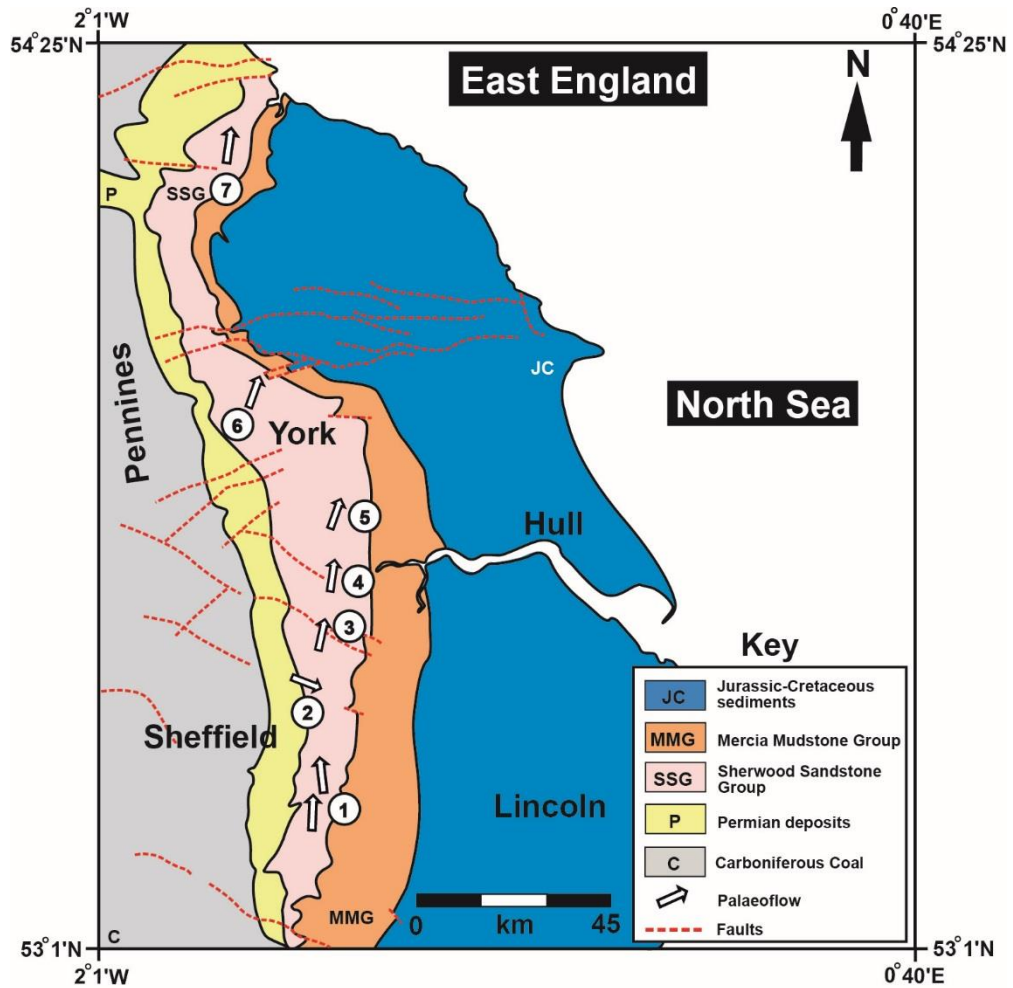
Figure 3.16: Geological map of east England (redrawn from British Geological Survey, 2000) showing the direction of palaeoflow along the eastern England Shelf: (1) Edwards, 1967; (2) Wakefield et al., 2015; (3) Fieldwork in the Dunsville Quarry (this study); (4) Gaunt, 1994; (5) Gaunt et al., 1992; (6) Powell et al., 1992; (7) Smith and Francis, 1967.
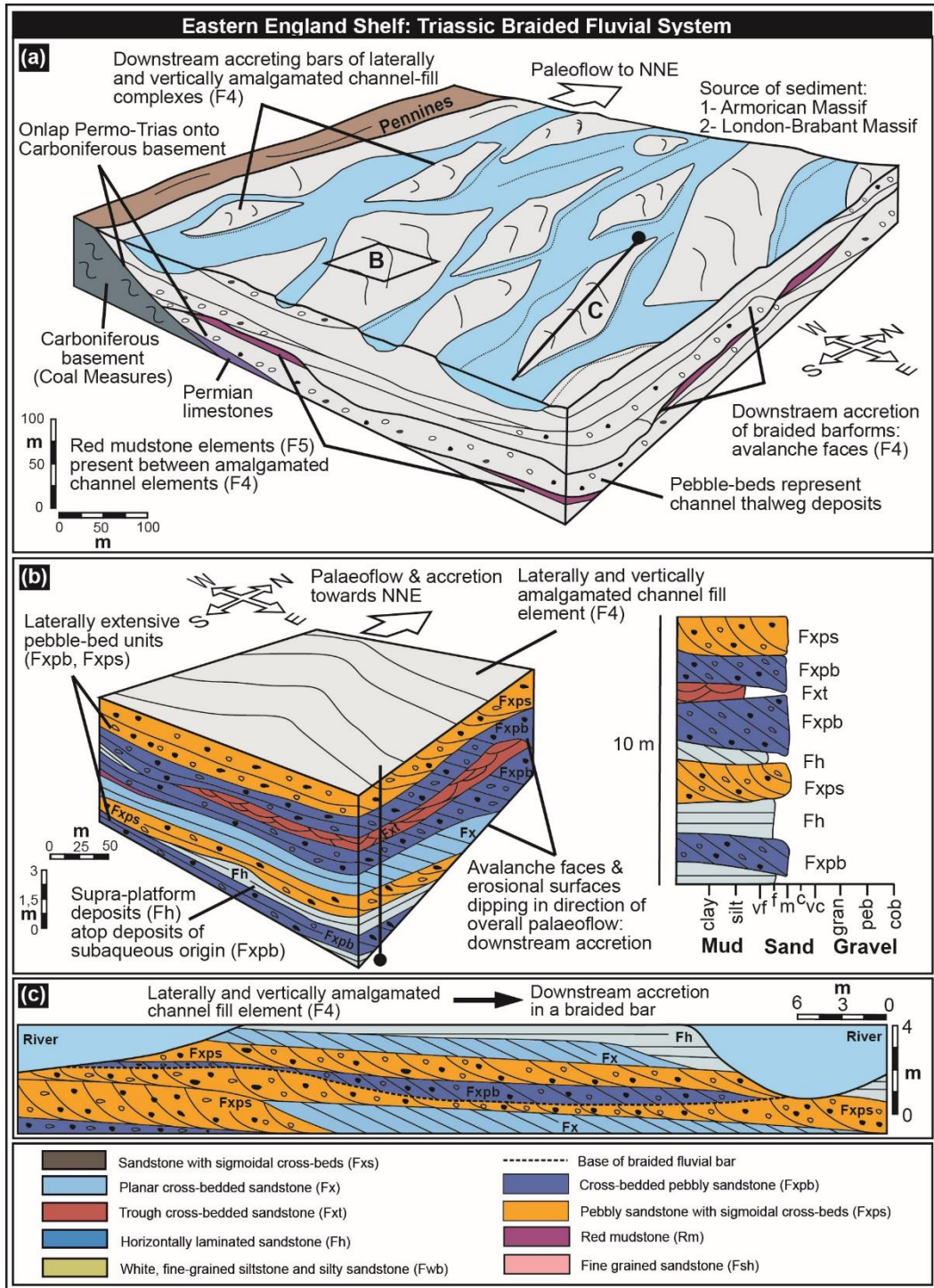
Figure 3.17: Summary model of the vertical and lateral architecture of the Sherwood Sandstone Group braided deposits of the eastern England Shelf. (a) Braided river system in shelf edge-basin (eastern England Shelf), (b) Depositional model of the Sherwood Sandstone Group of South Yorkshire, (c) Cross-section of a typical braid bar characterizing the Sherwood Sandstone Group of South Yorkshire.
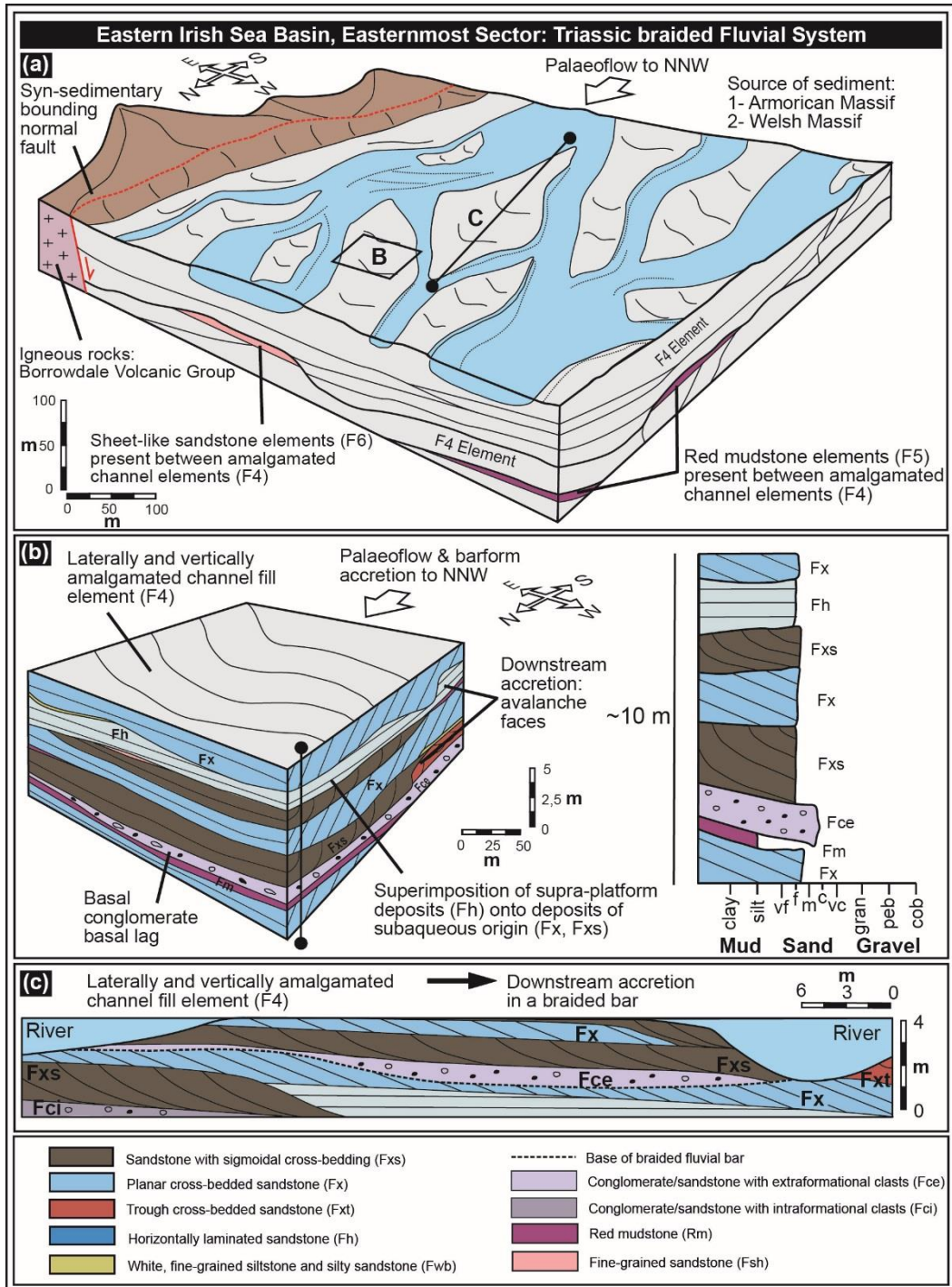
Figure 3.18: Summary model of the vertical and lateral architecture of the Sherwood Sandstone Group braided deposits in the easternmost sector of the eastern Irish Sea Basin. (a) Braided river system in the half-graben basin of the eastern Irish Sea Basin, (b) Depositional model of the St Bees Sandstone Formation of West Cumbria, (c) Cross-section of a typical braid bar characterizing the St Bees Sandstone Formation.

3.7 Conclusions

The fluvial systems of the St Bees Sandstone Formation of the eastern Irish Sea Basin and the undivided Sherwood Sandstone Group of the eastern England Shelf are both dominated by downstream-accreting sand-prone macroforms (bar deposits) that record evidence for the superimposed development of mesoforms indicative of the development of sinuous-crested dunes upon mid-channel bars. Despite the presence of many common depositional features between the two braided-river successions, three key differences relating to the style of preserved sedimentary architecture are identified: (i) differences in the thickness of the sediment preserved by erosion between a shelf-edge and a half-graben basin; (ii) the presence of thick pebble-beds characterized by compound cross-bedding only in the braided-fluvial deposits of the eastern England Shelf (shelf-edge basin); and (iii) the relative paucity in the eastern England Shelf of either fine-grained deposits stacked between pebbly units or mudstones draping bar-tops.

The studied fluvial successions were affected by a similar set of allogenic factors, including climate, sediment source and sediment delivery style. However, a principal difference was the differential rates of accommodation generation at the time of sedimentation in response to differing tectonic subsidence between the two basins. Dividing the pre-existing average thickness values by the age of the fluvial deposits of the eastern Irish Sea Basin and eastern England Shelf has allowed constraint of the preserved thickness sedimentation rate which was 119 Myr for the easternmost Irish Sea Basin. However, the preserved sedimentation rate for the eastern England Shelf ranges from 18 up to 19.4 Myr given the uncertainty associated with the Hardegsen unconformity. Basins subject to a faster rate of subsidence (e.g., eastern Irish Sea Basin) tend to be characterized by greater preserved thickness and by the preserved expression of more complete fluvial depositional cycles representative of channel cutting, filling by fine-grained sandy barforms and abandonment as represented by silty drape bar-top deposits. However, in the eastern England Shelf, the vertical

stacking of pebbly units and the general absence of fine-grained silty units reflect the slow rate of accommodation generation. In this shelf-edge basin, successive fluvial cycles repeatedly reworked the uppermost parts of earlier fluvial deposits such that it is typically only the lowermost channel deposits (lags) that are preserved, whereas the finest uppermost parts of the cycles are reworked.

Chapter 4

Hydro-geophysical characterization of the St Bees Sandstone aquifer: sedimentary vs. tectonic heterogeneities

(Chapter published: Medici, G., Mountney, N.P. and West L.J. 2015. Characterizing flow pathways in a sandstone aquifer: Tectonic vs. sedimentary heterogeneities. *Journal of Contaminant Hydrology*. 194, pp.36-58)

4.1 Chapter overview

Sandstone aquifers are commonly assumed to represent porous media characterised by a permeable matrix. However, such aquifers may be heavy fractured when rock properties and timing of deformation favour brittle failure and crack opening. In many aquifer types, fractures associated with faults, bedding planes and stratabound joints represent preferential pathways for fluids and contaminants. In this paper, well test and outcrop-scale studies reveal how strongly lithified siliciclastic rocks may be entirely dominated by fracture flow at shallow depths ($\leq$ 180 m), similar to limestone and crystalline aquifers. However, sedimentary heterogeneities can primarily control fluid flow where fracture apertures are reduced by overburden pressures or mineral infills at greater depths.

The Triassic St Bees Sandstone Formation of the East Irish Sea Basin (UK) represents an optimum example for study of the influence of both sedimentary and tectonic aquifer heterogeneities in a strongly lithified sandstone aquifer-type. This fluvial sedimentary succession accumulated in rapidly subsiding basins, which typically favours preservation of complete depositional cycles including fine grained layers (mudstone and silty sandstone) interbedded in sandstone fluvial channels. Vertical joints in the St Bees Sandstone Formation form a pervasive stratabound system whereby joints terminate at bedding discontinuities. Additionally, normal faults are present through the succession showing particular development

of open-fractures. Here, the shallow aquifer (depth ≤180 m) was characterised using hydro-geophysics. Fluid temperature, conductivity and flow-velocity logs record inflows and outflows from normal faults, as well as from pervasive bed-parallel fractures. Quantitative flow logging analyses in boreholes that cut fault planes indicate that zones of fault-related open fractures characterise ~ 50% of water flow. The remaining flow component is dominated by bed-parallel fractures. However, such sub-horizontal fractures become the principal flow conduits in wells that penetrate the exterior parts of fault damage zones, as well as in non-faulted areas.

The findings of this study have been compared with those of an earlier investigation of the deeper St Bees Sandstone aquifer (180 to 400 m subsurface depth) undertaken as part of an investigation for a proposed nuclear waste repository. The deeper aquifer is characterised by significantly lower transmissivities. High overburden pressure and the presence of mineral infillings, have reduced the relative impact of tectonic heterogeneities on transmissivity here, thereby allowing matrix flow in the deeper part of the aquifer. The St Bees Sandstone aquifer contrasts the hydraulic behaviour of less-mechanically resistant sandstone rock-types. In fact, the UK Triassic Sandstone of the Cheshire Basin has low-mechanically resistance and flow is supported both by matrix and fractures. Additionally, faults in such weak rocks are dominated by granulation seams representing flow-barriers which strongly compartmentalise the UK Triassic Sandstone in the Cheshire Basin.

4.2 Introduction

Quantitative studies for gaining an improved understanding of flow pathways represent a key issue for groundwater protection and catchment planning for all aquifer types. This chapter focuses on lithified sandstone aquifers and aims to characterise the role various types of sedimentary and tectonic heterogeneities on aquifer behaviour and contaminant transport in the phreatic zone. The rate of passage of inorganic (e.g., NAPL, nitrogen,

phosphate and chlorinated solvents) and organic (e.g., bacteria, virus) contaminants flowing through a sandstone matrix are controlled by a range of sedimentary heterogeneities (Zhu and Burden, 2001; Lawrence et al., 2006; Tellam and Barker, 2006; Rivett et al., 2011; Qin et al., 2013; Mobile et al., 2016), such as the presence of relatively low permeability mudstone layers. Alternatively, contaminants may be transported at higher flow velocities along mechanical discontinuities of tectonic origin, such as bedding parallel fractures, vertical joints or fault-related fracture corridors (Huyakorn et al., 1994; Odling and Roden, 1997; Barker et al., 1998; Steele and Lerner, 2001; Berkowitz, 2002; Rutqvist and Tsang, 2003; Hartmann et al., 2007; Faulkner et al., 2009; Bradbury et al., 2013; Cilona et al., 2015). The relative importance of matrix versus fracture flow is known to vary as a function of depth, owing to different sensitivities to geochemical alteration (e.g., diagenesis) and overburden pressure (Zoback and Byerlee, 1975; Howard, 1988; Akin, 2001). Thus, a specific study, which combines hydraulic tests (pumping tests, flow logging) at different depths, may provide an improved understanding of the relative importance of porous matrix versus fractures in controlling groundwater flow and contaminant transport in sandstone aquifers (Tellam and Barker, 2006; Gellasch et al., 2013). In other studies multi-level sampling arrays have been used to detect traces of contaminants in relation to bedding parallel fractures in sandstone aquifers (e.g., Powell et al., 2003; Gellasch et al., 2013). The hydrogeology of faults represents a further specific key issue in groundwater protection since such structural discontinuities can act as either barriers or preferential pathways for contaminants (Caine et al., 1996; Mohamed and Worden, 2006; Bottrell et al., 2008; Bense et al., 2013). Furthermore, water wells have been recognized both as preferential pathways for and sources of contaminants (Avci, 1992). Hence, pollutant plumes may be exacerbated by the interaction between groundwater and boreholes (Rivett et al., 1990; Avci, 1992; Hammond, 2016). The use of well tests in a fractured media allows us to test the interaction between all preferential pathways for contaminant transport which are represented by boreholes, tectonic open fractures and permeable sedimentary layers (Bauer et al., 2004; Odling et al., 2013).

Previous quantitative studies, involving hydraulic tests in lithified sandstone aquifers (Price et al., 1982; Brassington and Walthall, 1985; Runkel et al., 2006; Hitchmough et al., 2007; Gellasch et al., 2013; Lo et al., 2014), have focused on determining only the role of sub-horizontal discontinuities on water flow, including their connections through vertical stratabound joints. In contrast, past studies of the hydrogeology of faults in sandstone aquifers have focused on plug-scale fault rock samples and mini-permeameter outcrop experiments. Such studies have aimed to quantify the sealing potential of normal faults on hydrocarbon reservoir analogues (e.g., Antonellini et al., 1994; Torabi and Fossen, 2009; Balsamo and Storti, 2010; Tueckmantel et al., 2012). Consequently, quantitative hydraulic studies that encompass multiple aquifer heterogeneities, such as sub-horizontal stratigraphic discontinuities linked by multi-layer vertical fractures and extensional faults, are lacking.

This work investigates the sandstone aquifer of the Triassic St Bees Sandstone Formation, which represents the basal part of the Sherwood Sandstone Group – the second most important UK aquifer in terms of the amount of groundwater abstracted (Allen et al., 1997; Binley et al., 2002; Smedley and Edmunds, 2002). The Sherwood Sandstone Group has been the object of recent studies of sedimentary heterogeneities (e.g., Wakefield et al., 2015; Newell and Shariatipour, 2016). Results from these works have demonstrated how the St Bees Sandstone Formation represents an optimum analogue for the characterization of sedimentary heterogeneity in analogous subsurface hydrocarbon reservoirs of fluvial origin that accumulated in rapidly subsiding basins, such as those of the East Irish Sea Basin (Chadwick et al., 1994; Akhurst et al., 1998). Such conditions typically allow preservation of low-permeability units, including mudstone lenses that occur interbedded in otherwise sandstone-dominated successions (Miall, 1977; Colombera et al., 2013). Notably, the St Bees Sandstone aquifer is entirely characterised by a stratabound fracturing system (*sensu* Odling et al., 1999; Gillespie et al., 2001; Odonne et al., 2007; Rustichelli et al. 2013, 2016), which is particularly pervasive in this aquifer due to its layered nature coupled with high mechanical resistance

(Bell, 1992; Ameen, 1995). Fault zones in this aquifer are characterised specifically by the development of open fractures and a paucity of low-porosity deformation bands (Knott, 1994). Consequently, the St Bees Sandstone aquifer represents an optimum laboratory to test a wide range of aquifer heterogeneities of both tectonic (e.g., vertical joints, bedding parallel and extensional fractures) and sedimentary origin (e.g., mudstone layers), which are especially well represented in this aquifer (Bell, 1992; Jones and Ambrose, 1994; Knott, 1994; Ameen, 1995). Additionally, parts of the St Bees Sandstone aquifer that are buried at depths greater than 180 m, have been the object of a hydro-geophysical characterization, which commenced in the early 1990s as part of the planning of the proposed Sellafield nuclear waste repository (e.g., Appleton, 1993; Michie, 1996; Milodowski et al., 1998; Nirex, 1992 a, 1992b, 1992c, 1993a, 1993b, 1993c; Streetly et al., 2000, 2006). Thus, this study area offers the opportunity to compare hydro-geophysical studies undertaken at different depths, thereby allowing the opportunity to distinguish the depth-sensitivity of tectonic flow pathways versus matrix flow.

Specific research objectives are as follows: (i) use hydro-geophysics to constrain all the potential flow heterogeneities using imaging and wireline well-logs; (ii) quantify the role of individual structure types in terms of their contribution to flow using fluid temperature, conductivity and velocity logs; (iii) compare the hydro-geophysical characterization undertaken at shallow depths (≤180 m) as an outcome of this work, with previous studies that characterised the aquifer properties at greater depths (180 to 400 m); and (iv) compare the hydraulic characteristics of the St Bees Sandstone aquifer with those of less-mechanically resistant sandstone aquifers.

4.3 Hydrogeological background

The Sherwood Sandstone Group (Lower Triassic) is a red-bed succession that has long been ascribed to a mixed fluvial and aeolian origin (e.g., Ixer et al., 1979; Turner, 1981; Mountney and Thompson; 2002; Tellam and

Barker, 2006; Bashar and Tellam, 2011). This sandstone-dominated succession represents the UK's second most important aquifer. Contamination has arisen due to agricultural activity, and the release of industrial waste and sewage in urban areas (Rivett et al., 1990; Barrett et al., 1999; Bloomfield et al., 2001; Gooddy et al., 2002; Powell et al., 2003; Bottrell et al., 2008; Zhang and Hiscock, 2010, 2011; Rivett et al., 2012; Cassidy et al., 2014). In West Cumbria (Figure 4.1a, b), the Sherwood Sandstone Group attains a typical thickness of 1300 m (Jones and Ambrose, 1994; Nirex, 1997) and is formally divided into three different formations: the St Bees, Calder and Ormskirk Sandstone formations (Barnes et al., 1994; Holliday et al., 2008). The St Bees Sandstone aquifer, which is the focus of this study, is predominantly characterised by fine- to medium-grained sandstone of fluvial origin that passes upwards into the aeolian-dominated succession of the overlying Calder Sandstone Formation (Jones and Ambrose, 1994; Holliday et al., 2008). The Cumbrian Coastal Group, which underlies the St Bees Sandstone aquifer, is characterised by shale and gypsum, anhydrite and dolomite evaporite deposits, and represents a basal aquiclude lithology for the St Bees Sandstone aquifer (Figure 4.1; Smith, 1924; Strong et al., 1994; Holliday et al., 2008).

The field site is located in the St Bees-Egremont area in NW England (Figure 4.1a, b) where the St Bees Sandstone aquifer is confined by glacial and alluvial Quaternary deposits (McMillan et al., 2000). The St Bees Sandstone Formation is divided into two members: the North Head Member and the overlying South Head Member (see Chapter 3). The two members are differentiated primarily based on the abundance of fine-grained mudstone layers which range in grain size from clay to coarse silt (Jones and Ambrose, 1994; Nirex, 1997). The basal 35 m of the lower North Head Member is arranged into an alternation of fine-grained sandstone and mudstone beds. This basal part of the aquifer passes upwards into a succession dominated by sandstone, with mudstone layers representing only 25% and 5% of the entire succession in the upper North Head and South Head members, respectively (Barnes et al., 1994; Jones and

Ambrose, 1994; Nirex, 1997). Water boreholes in the St Bees Sandstone aquifer of West Cumbria are designed with long screens (80-149 m) to penetrate only the South and upper part of the North Head members aiming to avoid the potential low permeability unit which is represented by the mud-prone lower part of the North Head Member (Allen et al., 1997).

Tectonic heterogeneities, which characterise the UK Sherwood Sandstone aquifer, are represented by normal faults and stratabound joints (Cassidy et al., 2014; Allen et al., 1998). On a local scale, detailed studies of the tectonic structures of the St Bees Sandstone Formation have been undertaken by Knott (1994), Ameen (1995) and Gutmanis et al. (1998) as part of a series of radioactive waste disposal assessments associated with the Sellafield repository. These studies confirm the typical pattern of tectonic structures of the UK Sherwood Sandstone, for which high-angle normal faults and stratabound joints characterise the studied aquifer.

Knott (1994) highlights the relatively minor occurrence of granulation seams (*sensu* Pittman, 1981; Knott et al., 1996; Beach et al., 1999; Hitchmough et al., 2007) in the fault zones of the St Bees Sandstone Formation compared to deposits of the Sherwood Sandstone Group across the UK more widely, where such tectonic structures are more abundant (Knott, 1994; Griffiths et al., 2016). Stratabound joints, which characterise the entire aquifer, have been related in the study area to the Cenozoic uplift of NW Europe (Barnes et al., 1994; Nirex, 1997). Additionally, the fracture network which characterises the St Bees Sandstone aquifer also includes bedding and cross-bedding fractures. These sub-horizontal discontinuities are related to the opening of sedimentary discontinuities due to reduction of the vertical stress tensor in response to the Cenozoic lithospheric uplift of NW Europe (Ameen, 1995; Allen et al., 1998; Odling et al., 1999; Gillespie et al., 2001; Duperret et al., 2012). Layered aquifers of the north-western European region are typically characterised by similar fracturing patterns (e.g., Odling et al., 1999, Gillespie et al., 2001; Duperret et al., 2012). The Sherwood Sandstone Group across the UK presents typical matrix hydraulic conductivity and porosity values of 0.1-8.0 m/day and 15

to 30%, respectively (e.g., Allen et al., 1997; Bloomfield et al., 2006; Pokar et al., 2006). Shear strength is typically characterised by low values ranging from over-consolidated sand to weak rock (Hawkins and McConnell, 1992; Yates, 1992). In this hydro-mechanical framework, the St Bees Sandstone aquifer of West Cumbria represents an exception in the red-bed successions of the UK Sherwood Sandstone Group. Indeed, the interquartile range for plug-scale hydraulic conductivity ranges from 3.0×10^{-4} to 2.5×10^{-2} m/day and from 13% to 20% for porosity, these values are much lower compared to the petrophysical properties of the Sherwood Sandstone Group across other parts of the UK (Allen et al., 1997). Furthermore, the St Bees Sandstone Formation is relatively mechanically resistant; it is commonly used as a building stone in the West Cumbrian region (Bell, 1992). Additionally, intergranular permeability is only slightly reduced (by 6%) in response to an increase in lithostatic pressure of 7 MPa, representing the overburden pressure at approximately 300 m below the surface (Daw et al., 1974). However, the fracture flow component is substantially removed (by 80%) in experiments that apply the same amount of overburden pressure (7MPa) to plugs of the St Bees Sandstone Formation that contained single fractures (Daw et al., 1974).

Large-scale hydraulic tests in the Sherwood Sandstone Group of West Cumbria are summarized by Allen et al. (1997) with regards to shallow water wells. However, Streetly et al. (2000) investigated the more deeply buried parts of the St Bees Sandstone aquifer in the context of an investigation for a proposed radioactive waste repository at Sellafield. The two different groups of pumping tests data described by Allen et al. (1997) and Streetly et al. (2000) show different transmissivities. These hydraulic tests were undertaken at shallow (zero to 180 m) and greater (180 to 400 m) depths and show a decreasing transmissivity with increasing subsurface depth of two orders of magnitude (10^2). Furthermore, pumping tests undertaken by Streetly et al. (2000) on the deep St Bees Sandstone aquifer as part of the planning for the Sellafield radioactive waste repository show how the stratigraphic units of the North Head Member which are characterised by a higher occurrence of mudstone beds are also

characterised by relatively lower aquifer transmissivity (T= 0.46 - 1.99 m^2/day; median = 1.30; σ = 1.42; n=23). In contrast, the South Head Member of the St Bees Sandstone Formation (which is dominated by channel-sandstone deposits) is characterised by aquifer transmissivities ranging from 1.17 up to 4.88 m^2/day (median = 1.73; σ = 1.31; n=9). The fact that no systematic comparison of these datasets has been undertaken previously, so as explain the depth dependence of transmissivity is part of the rationale for the work reported in this paper. Additionally, the interpretation of variations in transmissivity as function of depth is coupled in this work with the quantification of the different contribution of tectonic structures (faults, bedding fractures and joints) on water flow at shallow depths (≤ 180 m).

4.4 Experimental methods

4.4.1 Wireline and optical televiewer logging

Five pre-existing monitoring wells (0.15 to 0.20 m in diameter; 90 to 152 m depth), which are located at different distances from mapped fault traces, were geophysically logged (Figure 4.1b; Table 4.1). Mechanical calliper, natural gamma, resistivity, gamma-gamma density, neutron porosity and optical televiewer (ALT QL40 mk5) logs were recorded, along with the structure picking (*sensu* Williams and Johnson, 2004) of both sedimentary and tectonic heterogeneities, to characterise the orientation of geological heterogeneities. This structure picking allowed plotting of open fractures (n = 583), thin white sandstone beds (n = 279) and thin red mudstone beds (n = 28), as well as the calculation of vector mean statistics for the orientation of each group of heterogeneities using the Stereonet 9 software package (Allimendinger et al., 2012). Fractures present in the St Bees Sandstone, and recorded in the logs, comprised bedding plane fractures, cross bedding fractures, vertical joints and fault related-open fractures. Granulation seams were not detected by the automated structure picking procedure since such tectonic structures occur in only one well (Ellergill Bridge) as

tortuous and short (0.05-0.1 m) bands that do not fully cut across the entire borehole width.
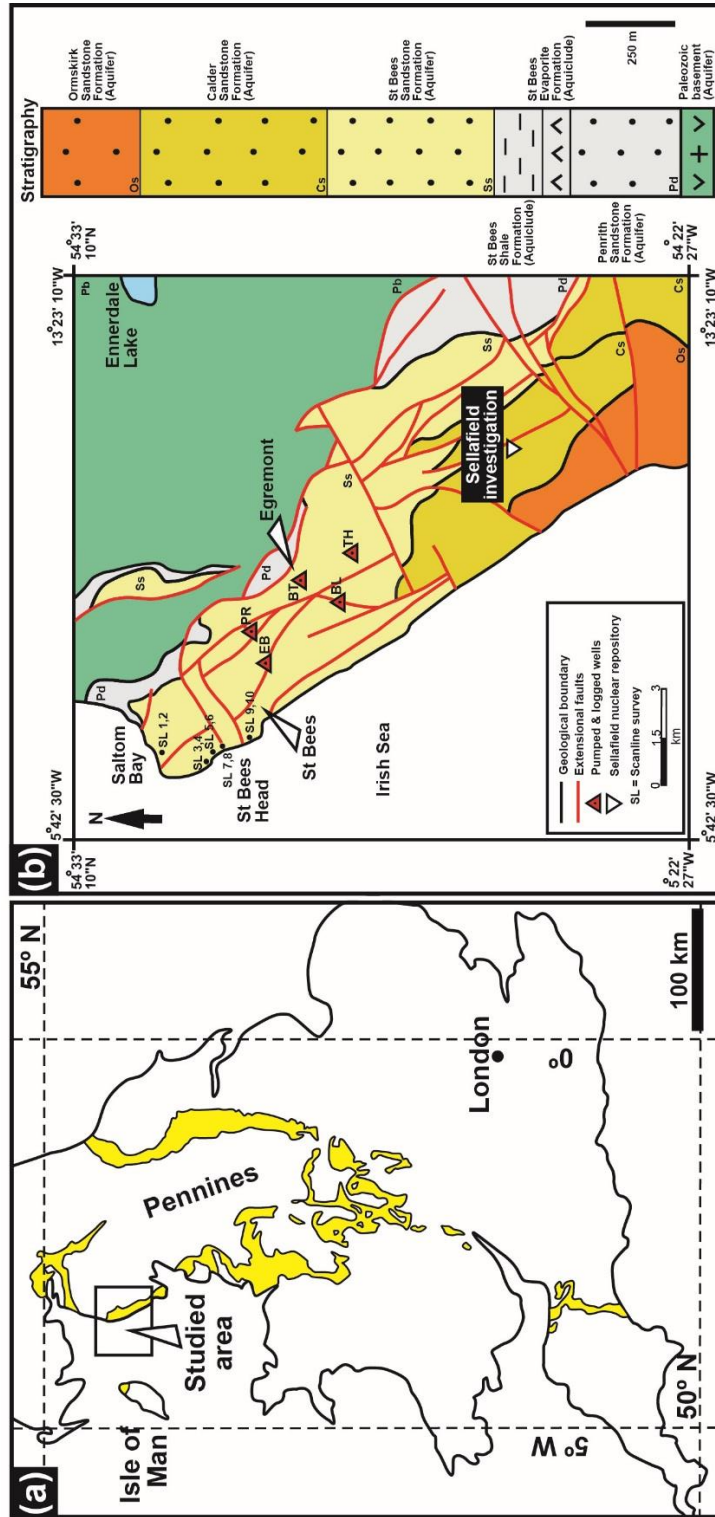
Figure 4.1: Study area. (a) Map depicting surface expression of the Sherwood Sandstone Group (yellow colour) in England, UK (Redrawn from Wakefield et al., 2015), (b) Geological map of the field site with stratigraphic column and location of the scanlines (SL 1-10) and of the 5 logged wells (Redrawn from British Geological Survey, 2015): Black Ling (BL), Bridge End Trial (BT), Ellergill Bridge (EB), Pallaflat Reservoir (PR), Thornhill Trial (TH).

Table 4.1: Construction details and distance from mapped fault traces for the five logged wells shown in Figure 4.1.

Field site/well name	Borehole diameter (m)	Casing depth (m) BGL; ASL	Screen length (m)	Distance from mapped fault trace (m)
Black Ling	0.20	26; 34	84	0
Bridge End Trial	0.20	14; 28	76	95
Ellergill Bridge	0.15	21; 72	84	10
Pallaflat Reservoir	0.20	6; 98	146	0
Thornhill Trial	0.20	10; 31	107.5	340

4.4.2 Scanlines-stratabound joints at cliff outcrops

Scan-line surveys have been performed at cliff outcrops around St Bees Head (see Figure 4.1) to characterise the stratabound fracturing system present in the St Bees Sandstone aquifer, since vertical boreholes numerically underestimate sub-vertical fractures (Terzaghi, 1965). The chosen methodology is specific for stratabound joints (Rustichelli et al., 2013) and involves the recording of 5 parameters: strike orientation, dip inclination, fracture horizontal spacing distance, percentage of infilled fractures and the thickness of the mechanical layer which contains the joints. Ten scanlines were measured along five different study sites (at each site two orthogonal horizontal scanlines lines have been realised to avoid bias). A total of 188 discontinuities which includes sub-vertical joints (n=140), cross (n=21) and bedding parallel (n=27) fractures were recorded and plotted on stereonets (cf., Allimendinger et al., 2012).

4.4.3 Pumping tests

Historical single-borehole pumping test data from the studied wells have been re-analysed using the ESI AquiferWin32 V.5 software package to obtain reliable transmissivity values to use for a quantitative flow-log analysis. Step tests have been analysed using the method of Eden and Hazel (1973) and the associated recovery using the method of Theis (1935). Data from pumping tests characterised by a constant abstraction flow are also available; for these data the recovery phase has been analysed using the Theis methodology.

Furthermore, the analysed pumping tests have been integrated with previously published pumping test data also acquired, to characterise the St Bees Sandstone aquifer more fully (Allen et al., 1997; Streetly et al., 2000). This was done to characterise transmissivity ranges from the shallow (n = 21) and the deep (n = 32) parts of the aquifer.

4.4.4 Upscaling hydraulic conductivity

Transmissivity values from well tests are compared with upscaled values derived from hydraulic conductivities that are available in literature for the St Bees Sandstone aquifer in West Cumbria, to establish the relative contribution of fracture versus matrix flow in the shallow aquifer (Nirex, 1992a, 1992c, 1993b, 1993c; Allen et al., 1997). The horizontal hydraulic conductivity from sandstone plugs was upscaled using the geometric mean for the screen length (Table 4.1) of each flow-logged well to compute the screen transmissivity. Flow in this upscaling approach is assumed perpendicular to the screen consistent with the layered nature of the aquifer and sub-horizontal dip of the beds (10°). Geometric and harmonic means are typically used for upscaling of hydraulic permeability in heterogeneous sandstone aquifer or reservoir types (Chen et al., 2003; Jackson et al., 2003). We used the geometric mean since better represents the sensitivity of horizontal flow to layer permeability variation. For example, Zheng et al. (2000) has found a better match between plug and field scale transmissivity

upscaling the K_h geometric mean rather than K_h harmonic mean in sandstone fluvial reservoirs.

4.4.5 Temperature, conductivity and flow velocity logs

Both pumped and ambient-flow velocity, fluid temperature and conductivity logs have been recorded in all five study wells using a Geovista mk2 impeller flow meter (minimum observable flow rate of 10 mm/s according to the manufacturer). Flow-log analyses aimed to determine the hydraulic conductivity (k_i) of each identified hydraulic layer i, with thickness (Δz_i) from the computed partial transmissivity (T_i) using equation (1),

$$T_i = k_i \times \Delta z_i \tag{1}$$

A quantitative approach has been used to analyse flow meter data to determine partial transmissivity (T_i) by combining overall well transmissivity values derived from the pumping test analyses with fluid velocity logs. The quantitative method adopted for the flow log analysis comprises a model to determine transmissivity value of fracture rock zones (Paillet, 1998, 2000). Day-Lewis et al. (2011) provides a computer program for the latter model, called "Flow-Log Analysis of Single Holes (FLASH)". This program is based on the multi-layer Thiem (1906) equation (2), which describes confined radial flow in both ambient and stressed flow conditions,

$$Q_i = \frac{2\pi T_i(h_w - h_i)}{\ln(r_0/r_w)} \tag{2}$$

where Q_i is the volumetric flow into or out of the well from layer i; h_w and h_i are, respectively, the hydraulic head in the well (which has radius r_w) and

in the far-field at r_0 (the radius of influence); T_i is the transmissivity of layer i. The FLASH program has an optimizing calibration method which aims to minimize difference between data and model misfit. The model misfit is generated based on the differences ($h_w - h_i$) between the water level in the borehole (h_w) under pumped and ambient conditions and the far-field heads (h_i). The automated model calibration of the FLASH program is based on a Generalized Reduced Gradient algorithm which was developed by Lasdon and Smith (1992). Four of the five wells examined did not show significant diameter variations, but in two cases (Black Ling, Pallaflat Reservoir wells) diameter variations > 30% occurred in correspondence of faults in thick intervals (2-5 m). Here, water flow (Q_i) was manually corrected for these borehole diameter changes.

Drawdowns in the wells between pumped and ambient conditions are assumed to represent aquifer drawdowns; head losses between the well and the aquifer (skin effects, wells losses) are assumed to be small. Additionally, the FLASH program requires information concerning well construction (top and bottom elevations of open section, well diameter), depth of the water table and an estimate of the radius of influence of pumping (r_0=50 - 165 m)[1] in each borehole.

The Day-Lewis et al. (2011) methodology has been applied to flow-log analyses in three of the five wells (Black Ling, Bridge End Trial, Thornhill Trial), which all showed strong flows under ambient conditions (up to 80 mm/s upflow). This is consistent with the results of Brassington (1992) who found significant ambient upflows in open wells in the study area. However, logs carried out in the two remaining wells (Ellergill Bridge, Pallaflat Reservoir) could not be successfully analysed using the Day-Lewis et al. (2011) methodology, possibly due to lower ambient flow rates (0-18 mm/s)[2]. Hydraulic effects associated with irregular borehole diameter and resulting

---

[1] Radius of influence for the entire pumped interval was found using the transient flow equation assuming a storativity value of 2×10^{-4} (Allen et al., 1997) and water that has been pumped for a period of 20 minutes. Radius of influence range from 50 to 165 m, although the FLASH program is strongly insensitive to r_0 since this parameter appears inside the logarithm of equation (2).

[2] Ambient flow in Ellergill Bridge and Pallaflat Reservoir is close to the nominal detection limit of the flow meter (10 mm/s).

changes in flow velocity which may trigger water turbulence may also have contributed (Grass, 1971, Tsang et al., 1990; Paillet, 2004). Instead, these well logs were analysed using a simpler approach that assumes quasi-steady state flow in pumped conditions, but negligible head difference between layers and vertical ambient flow in the borehole, and hence only requires data from the pumped flow-logs (Molz et al., 1989; Fienen et al., 2004; Parker et al., 2010). This methodology determines the transmissivity T_i for each layer, simply from the proportion of total inflow to the well entering from that layer under pumped conditions, and the overall well pumping test transmissivity T. The proportion of the total inflow is given by the change in vertical flow velocity between the top and bottom of layer i, divided by the maximum flow velocity i.e. that above the highest permeable zone, v_{max}, i.e,

$$\frac{T_i}{T} = \frac{\Delta v_i}{v_{max}}$$

(3)

Layer hydraulic conductivity k_i is then determined according to equation (1). This method essentially neglects ambient head difference between the layers as a source of vertical flow within the well, whereas the Day-Lewis et al. (2011) methodology accounts for this.

4.5 Results and discussion

4.5.1 Aquifer heterogeneities

The optical televiewer logs acquired from the five wells confirm that the characteristics of the St Bees Sandstone aquifer observed in outcrop are also present in the subsurface. The principal heterogeneities are represented by thin mudstone (0.01 to 0.65 m) and white silty sandstone (0.01 to 0.50 m) interbeds in red sandstone, and also by bedding plane fractures, vertical joints and brittle cataclastic faults (Figures 4.2, 4.3 a-c,

4). Vertical joints form a stratabound system in the St Bees Sandstone aquifer since they stop at bed-parallel fractures and sedimentary heterogeneities.

Bedding planes observed both at outcrop along the South Head cliff (Figures 4.2 a), and in three of the five logged wells (Black Ling, Bridge End Trial, Ellergill Bridge) dip towards the SW at 5º to 20º (mean vector dip azimuth = 228°; mean vector dip angle = 12°; vector magnitude = 0.99; n = 439). By contrast, in the two remaining wells (Thornhill, Pallaflat Reservoir) bedding planes dip towards SE at 5º to 15º (mean vector dip azimuth = 150°; mean vector dip angle = 7°; vector magnitude = 0.98; n = 192).

The Black Ling and Pallaflat Reservoir wells penetrate fault zones, as shown in the geological map (Figure 4.1b). Normal faults are well exposed along the South Head Cliff and show development of open fractures, although granulation seams are also present in the damage zones (Figure 4.2b). For these wells, the optical logs (Figure 4.3c) show zones which are characterised by a cataclasite with brittle open fractures. Such features represent the typical fault core (*sensu* Caine et al., 1996) in the study area according to Gutmanis et al. (1998) and Nirex (1997). However, although situated on a fault trace, the Ellergill Bridge well apparently cuts only the external part of the fault damage zone, as shown by sub-vertical granulation seams (Figure 4.3d). Indeed, granulation seams dominate the external parts of fault damage zones more widely in the study area (Gutmanis et al., 1998). Fault-related and principal bedding plane fractures that are imaged in optical televiewer logs are altered by groundwater flow. These fractures possess small cavities, which act to enlarge tectonic discontinuities (Figure 4.3b, c, e). Additionally, some other fractures (Figure 4.3f) are partially filled by calcite, which represents the soluble cement of the St Bees Sandstone aquifer (Strong et al., 1994; Milodowski et al., 1998). The wells that intersect faults confirm the observation of Gutmanis et al. (1998): cataclastic fault cores with open fractures and granulation seams occur in the fault damage zone.

Figure 4.2: St Bees Sandstone Formation (see Figure 4.1 for outcrop locations). (a) Photograph and panel of St Bees Sandstone Formation in a cliff section at St Bees Head. The exposure shows the layered nature of the St Bees Sandstone aquifer with beds 1-1.8 m thick commonly separated by white silty sandstone beds (transparent blue). Joints (yellow) are largely truncated by individual bed parallel discontinuities (white), (b) Extensional fault at the St Bees village: '1' principal fault plane highlighted by water seepage, '2' fault related open fractures locally occurring as conjugate sets, '3' bedding-parallel fracture cutting the fault structure, '4' detail of granulation seams.
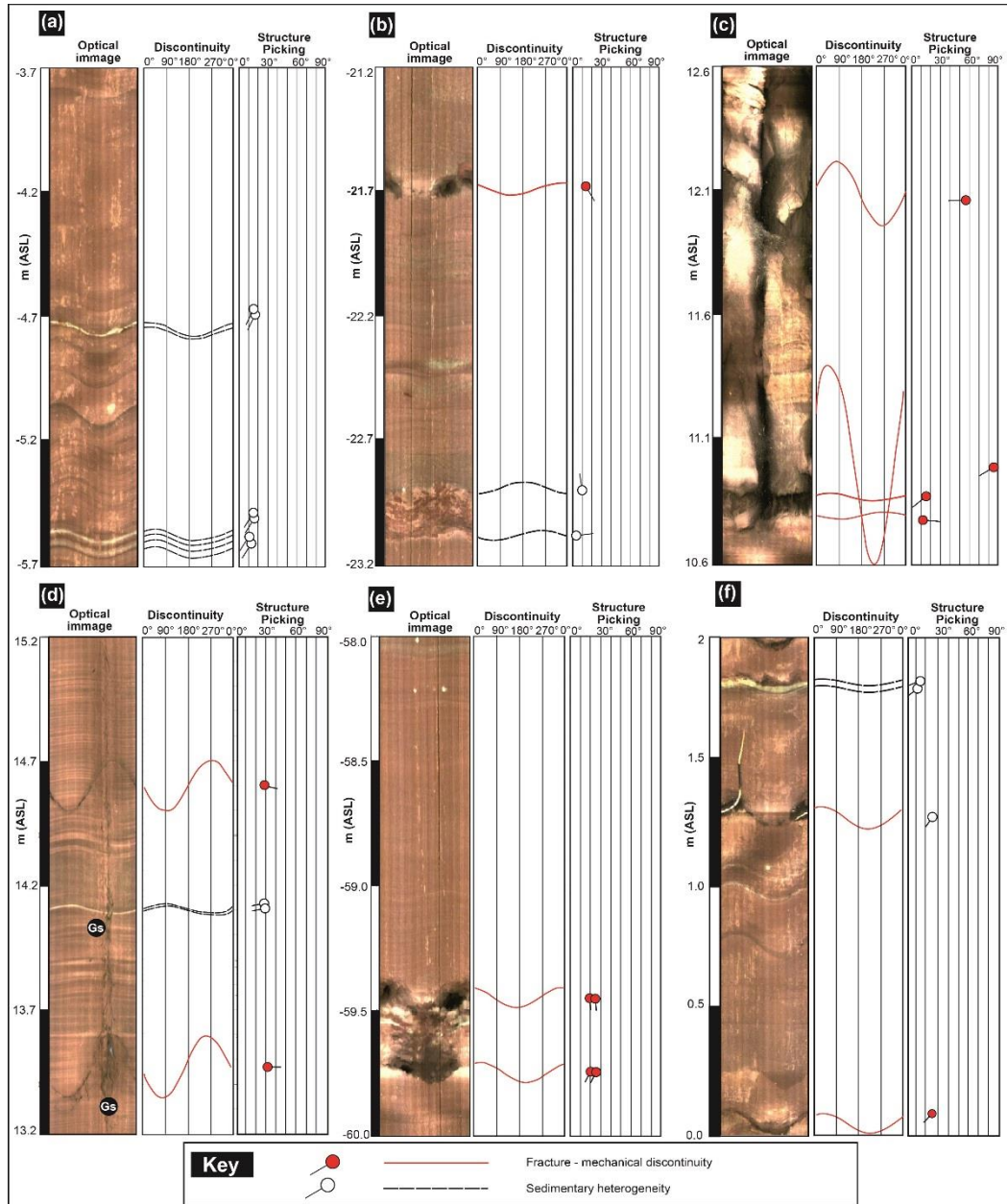
Figure 4.3: Principal heterogeneities in the St Bees Sandstone aquifer and structure picking of discontinuities; (a) white siltstones (black dashed lines), (b) mudstones (black dashed lines) and bedding plane fractures enlarged by small cavities (red solid lines), (c) fault cataclasite with open fractures (red solid lines), (d) White sandstone (black dashed line) and medium angle joints (red solid lines) cutting (Gs) granulation seams (e.g., white sandstone - black dashed lines), (e) bed-parallel fractures enlarged by small cavities, (f) bed-parallel fracture and vertical joint partially filled by calcite veins.

The sedimentary heterogeneities of the St Bees Sandstone aquifer have been recognized by integrating optical televiewer and wireline logs (Figure 4.4). The results of the geophysical characterization are summarized in stereonet plots with regards to the orientation of both sedimentary and tectonic heterogeneities (Figure 4.5). Additionally, the vertical occurrence of these structures is summarized in Table 4.2. Sedimentary heterogeneities (Figure 4.4) are represented by thin white sandstones (91%) and thin mudstones (9%), typically red in colour. The white sandstone (Figure 4.4, feature 1) is characterised by low neutron porosity (14 to 18%) and resistivity (50 to 80 $\Omega \cdot$m), and high values of gamma-gamma density (2.4 to 2.6 g/cm^3) and natural gamma (70 to 100 CPS). The mudstones (Figure 4.4, feature 2) are also characterised by low porosity (10 to 18%) and resistivity (40 to 70 $\Omega \cdot$m), and high values of gamma-gamma density (2.4 to 2.55 g/cm^3) and natural gamma (80 to 110 CPS). Despite this, mudstone beds (Hm) can be easily distinguished from the white sandstones (Hws) using the optical televiewer log data, since the former are distinctly red in colour (Figures 4.3b and 4.4). Mudstone beds (Hm) occur with a lower frequency than the white sandstone beds (Hws); average vertical spacing is 16.1 m and individual beds are 0.01 to 0.65 m thick (mean = 0.10 m; σ = 9.91 m; n = 28). In contrast, white sandstone beds are 0.01 to 0.50 m thick (mean = 0.04 m; σ = 5.88 m; n = 279); they show an average spacing in the boreholes of 2.1 m. Mudstone (Hm) and white sandstone (Hws) beds together are both characterised by finer grain size (silt, fine sand), lower porosity (10 to 18%) and high natural gamma (>70 CPS) values which represent typical petro-lithological characteristics associated with clay mineral and mica bearing units (Hurst, 2000; Rider, 2000; Bloomfield et al., 2006; Yang and Aplin, 2007). Petrological studies on the sedimentary heterogeneities of the St Bees Sandstone Formation confirm the presence of fine-grained clay and mica enriched horizons (Strong et al., 1994). Units enriched in clay minerals represent partial barriers to the fluid flow in matrix-flow aquifer types (Tellam and Barker, 2006) and typically impede movement of high-density contaminants (e.g., DNAPL) moving towards the bottom of the phreatic zone (Oostrom et al., 1999; Conrad et al., 2002; Lawrence et al., 2006). Furthermore, in the

Sherwood Sandstone Group of NE England, mudstone and fine-grained sandstone layers represent thin lower aquicludes for seasonal perched aquifers in the vadose zone (West and Truss, 2006).

Table 4.2. Vertical spacing data for fracture and sedimentary heterogeneities in the five logged wells.

Type of heterogeneity	Code	Population (n.)	Vertical spacing range (m)	Average vertical spacing (m)	Standard deviation σ (m)
Tectonic-reactivation master beds	S1	439	0.01-6.54	1.2	1.27
Tectonic-reactivation cross beds	S2	39	0.05-20.01	7.8	7.77
Tectonic-stratabound joints	S3+S4	42	0.48-30.16	8.3	7.68
Tectonic-stratabound joints	S5+S6	13	3.54-42.06	16.7	12.46
Tectonic/artificial fractures	S7	50	0.05-54.56	5.7	7.43
Sedimentary (i) mudstone	Hm	28	0.1-50.55	16.1	15.55
Sedimentary (ii) White sandstone	Hws	279	0.02-19.35	2.1	2.38
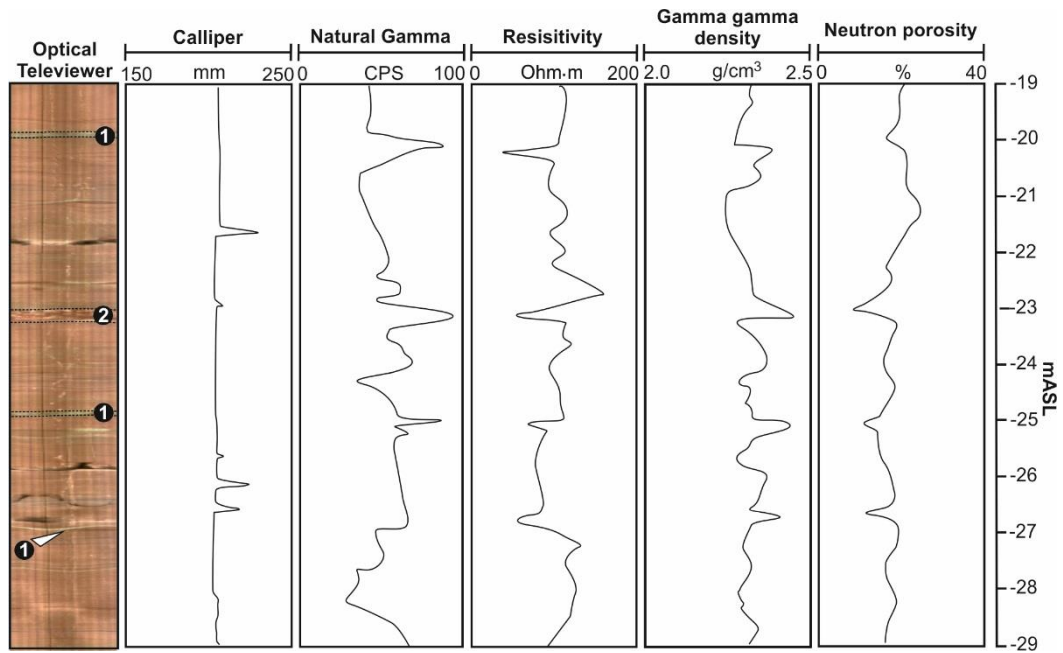
Figure 4.4: Wireline logs from Thornhill Trial well showing the geophysical response of (1) white sandstone and (2) mudstone.

Tectonic features recognized in the optical televiewer and wireline logs include vertical joints, fault related-open fractures and granulation seams. Bedding plane and cross-bedding plane fractures detected by televiewer and wireline logs are typically related to the mechanical reactivation of sedimentary structures in response to a lithospheric uplift or gentle folding of a layered stratigraphic succession (Ameen, 1995; Allen et al., 1998; Odling et al., 1999; Odonne et al., 2007). Hence, these low-angle inclined fractures must be considered tectono-sedimentary heterogeneities. Calliper logs show diameter increases of the borehole in correspondence with bedding plane fractures (S1) ranging from 1% to 20%, and up to 66% where brittle cataclastic faults are present.

All five studied wells are vertical. Eighty-two per cent of fractures possess inclinations <35°. As a consequence, moderate-angle inclination (35° to 60°) characterises only the 7% of fractures, whereas high-angle to vertical inclinations (60° to 90°) characterise 11% of the fractures. However, note that moderate and high angle inclined fractures are under-sampled in vertical boreholes. The Terzaghi (1965) Correction was applied in

contouring to remove bias due to the vertical orientation of the borehole (Figure 4.5a). Discontinuities (Figure 4.5) have been grouped into seven different sets (S1, S2, S3, S4, S5, S6, S7). Set 1 (S1) is represented by large bedding plane fractures which gently dip (1° to 20°) both towards SW and SSE. Set 2 (S2) always dips towards NNW (20° to 35°), which is the typical orientation of the cross-bedding in the study area (Jones and Ambrose, 1994) and likely represents the mechanical reutilization of such discontinuities. Sets S3, S4, S5, S6 are high-angle (65° to 90°) stratabound joints, which terminate where they intersect sub-horizontal discontinuities (Figure 4.2). Sets S3 and S4 are NW-SE striking and dip towards NE and SW, respectively; Sets S5 and S6 also represent high-angle stratabound joints and respectively dip towards NW and SW (Figure 4.5c, d). However, fractures of Set 7 (S7) are randomly oriented and show dip angles that vary from 40° to 65°. Such discontinuities (S7) are likely either fault related or caused by drilling.

Vector mean statistics (Figure 4.5 c, d) confirm that the four sets of inclined fractures (S3, S4, S5, S6) are related to the stratabound fracturing system since they are characterised by two orthogonal systematic orientations (Odling et al., 1999; Odonne et al., 2007; Rustichelli et al. 2013, 2016).

Mean vectors (Figure 4.5) of sedimentary heterogeneities consisting of mudstones and thin white sandstones (Hws, Hm) and bedding plane fractures (S1) show how such sub-horizontal structures possess similar orientations. Evident superimposition of poles to planes in stereoplots confirms how S1 structures are closely related to these sedimentary heterogeneities. Indeed, bedding-plane fractures (S1) represent the mechanical reactivation of the main erosive bounding surfaces and minor planar laminations, which have themselves been the object of previous sedimentological studies (e.g., Jones and Ambrose, 1994).

Evidence of the mechanical reutilization of erosive bounding surface in the St Bees Sandstone aquifer is related to the fact that the average vertical spacing of S1 fractures in boreholes (1.2 m) matches the average vertical

spacing of the 3rd order erosive bounding (*sensu* Miall, 2006) described in Chapter 3 and Nirex (1997) in the study area.

In contrast to the wells which intersect predominantly mainly sub-horizontal features (82%), the scanline surveys have been performed to characterise the multi-layered sub-vertical stratabound-type joints (S3, S4, S5, S6). Stratabound joints represent 75% of the recorded discontinuities; bedding parallel (S1) and cross-bedding (S2) fractures account for the 25% of the total. These low angle inclined fractures (S1, S2) represent minor fissures (length in vertical face = 0.1-1m; spacing = 0.2-8.2 m) which are confined, as the sub-vertical joints, within the major plane beds (Figure 4.2a; Table 4.2).

These structural surveys confirm that two orthogonal sets of bed-perpendicular joints are present in the studied sandstone (Figure 4.6a). The two joint sets strike NNW-SSE and ENE-WSW as in the water wells (Figure 4.5). Additionally, the horizontal spacing of the sub-vertical joints ranges from 1.1 m to 1.9 m. This spacing range matches closely with the thickness of the mechanical bedding layers (1.3 to 1.9 m) which vertically limit the joints (Table 4.3). Consequently, the two sets of stratabound orthogonal joints fracture the aquifer into blocks that approximate a cubic shape with an average length of 1.5 m for each face (Figure 4.6b).

Only 8% of fractures seen in the cliffs are filled by clay. Additionally, fracture aperture seen in the cliff exposures ranges from 1 mm to 20 mm, but is likely enhanced by the unconfined free face and these values are, hence, likely to be unrepresentative of the aquifer properties at depth (Jiang et al., 2009, 2010; Kana et al., 2013). Major vertical joints are visibly persistent in plant view up to 10 m, although exposure is limited along the cliffs at South Head. Moreover, outcrops along the intertidal zone at South Head and Saltom Bay cliffs (Figure 4.1) show how NNW-SSE striking joints (S3, S4) are horizontally more extended than the principal ENE-WSW striking joints (S5, S6). Indeed, sets S3 and S4 also occur with a higher frequency than sets S5 and S6 in boreholes (Table 4.2).

The fracture system that characterises the St Bees Sandstone aquifer away from faults shows typical characteristics of a stratabound system. This pattern of fractures is common worldwide to any layered aquifer that has experienced lithospheric uplift (e.g., Gillespie et al., 2001; Billi, 2005; Odonne et al., 2007; Korneva et al., 2014). Indeed, orthogonal sets of vertical joints, which terminate at their point of intersection with bedding planes, represent tectonic features which typically characterise the Sherwood Sandstone aquifer across the UK. These features have been related to Cenozoic uplift events (Chadwick, 1997; Allen et al., 1998; Wealthall et al., 2001; Hitchmough et al., 2007; Hillis et al., 2008; Carminati et al., 2009).

Table: 4.3. Fracture spacing and mechanical layer thickness data from scanlines of outcropping rock faces (for key see Figure 4.1b).

Station; scanline code	Scanline orientation	Scanline length (m)	Bed thickness (m)	Fracture sets	Average horizontal spacing (m)	Standard deviation σ (m)
North Head Quarry; SL1	N° 60 E	23.6	1.60	S1, S2	4.18	4.49
				S3, S4	1.95	1.42
North Head Quarry; SL.2	N° 40 W	12.1	1.45	S1, S2	2.88	2.04
				S5, S6	1.07	0.82
North Fleswick Bay; SL3	N° 85 E	14.7	1.30	S1, S2	8.00	2.60
				S3, S4	1.23	1.02
North Fleswick Bay; SL4	N° 5 W	6.9	1.40	S1, S2	3.50	3.00
				S5, S6	1.37	1.05
Fleswick Bay 1; SL5	N° 75 E	11	1.70	S1, S2	2.50	2.30
				S3, S4	1.56	1.35
Fleswick Bay 1; SL6	N° 15 W	11.9	1.70	S1, S2	1.33	0.86
				S5, S6	1.67	1.64
Fleswick Bay 2; SL7	N° 75 E	27.8	1.90	S1, S2	3.65	2.25
				S3, S4	1.73	0.96
Fleswick Bay 2; SL8	N° 15 W	24.2	1.25	S1, S2	3.88	2.14
				S5, S6	1.61	1.44
South Head Cliff; SL9	N° 2 W	13.2	1.30	S1, S2	5.00	2.80
				S5, S6	1.06	0.47
South Head Cliff; SL10	N° 88 E	21.3	1.60	S1, S2	4.50	3.54
				S5, S6	1.49	1.58
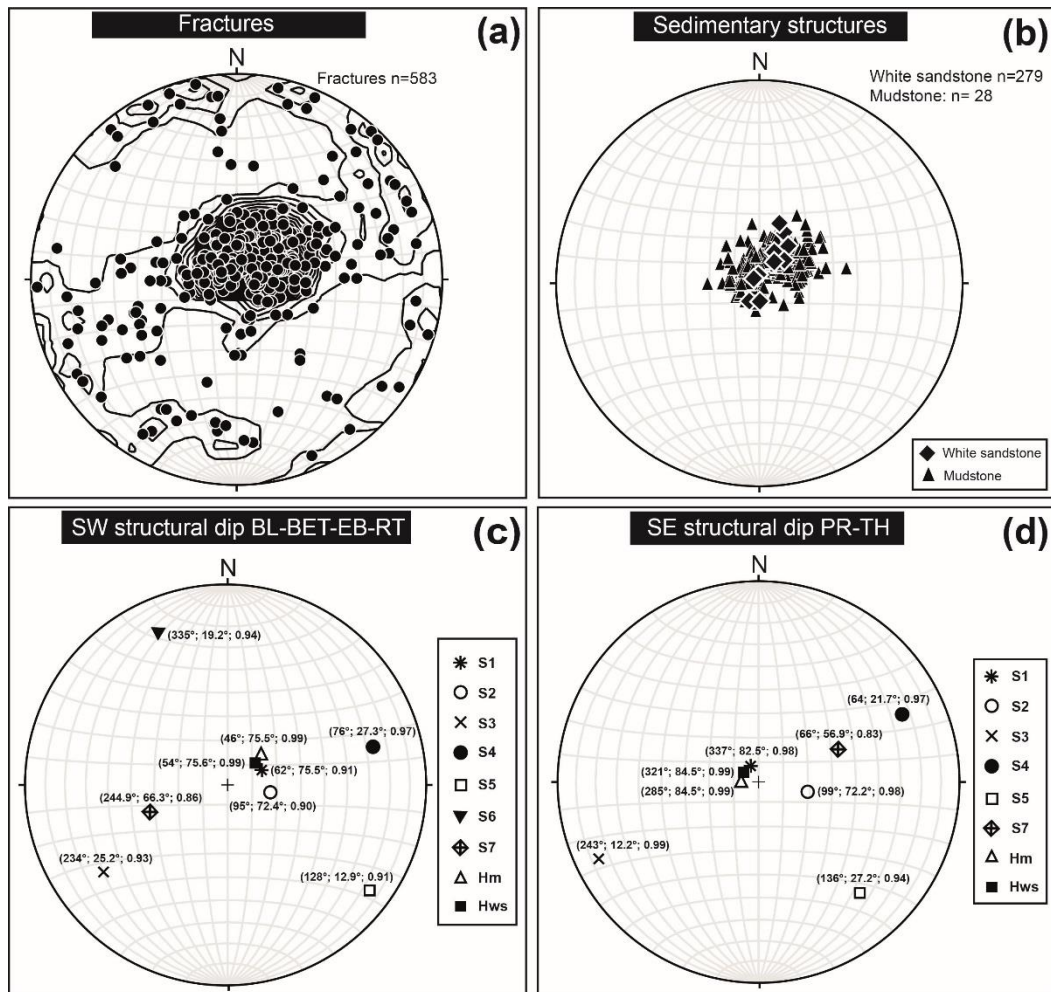
Figure 4.5: Stereoplots (upper hemisphere, equal area); (a) Pole diagrams of fractures for all wells, (b) Pole diagrams of sedimentary heterogeneities for all wells, (c) Mean vectors of fracture families and sedimentary heterogeneities in wells characterised by SW structural dip; trend, plunge and magnitude of mean vectors are reported in brackets, (d) Mean vectors of fracture families and sedimentary heterogeneities in wells characterised by SE structural dip; trend, plunge and magnitude of mean vectors are reported in brackets.
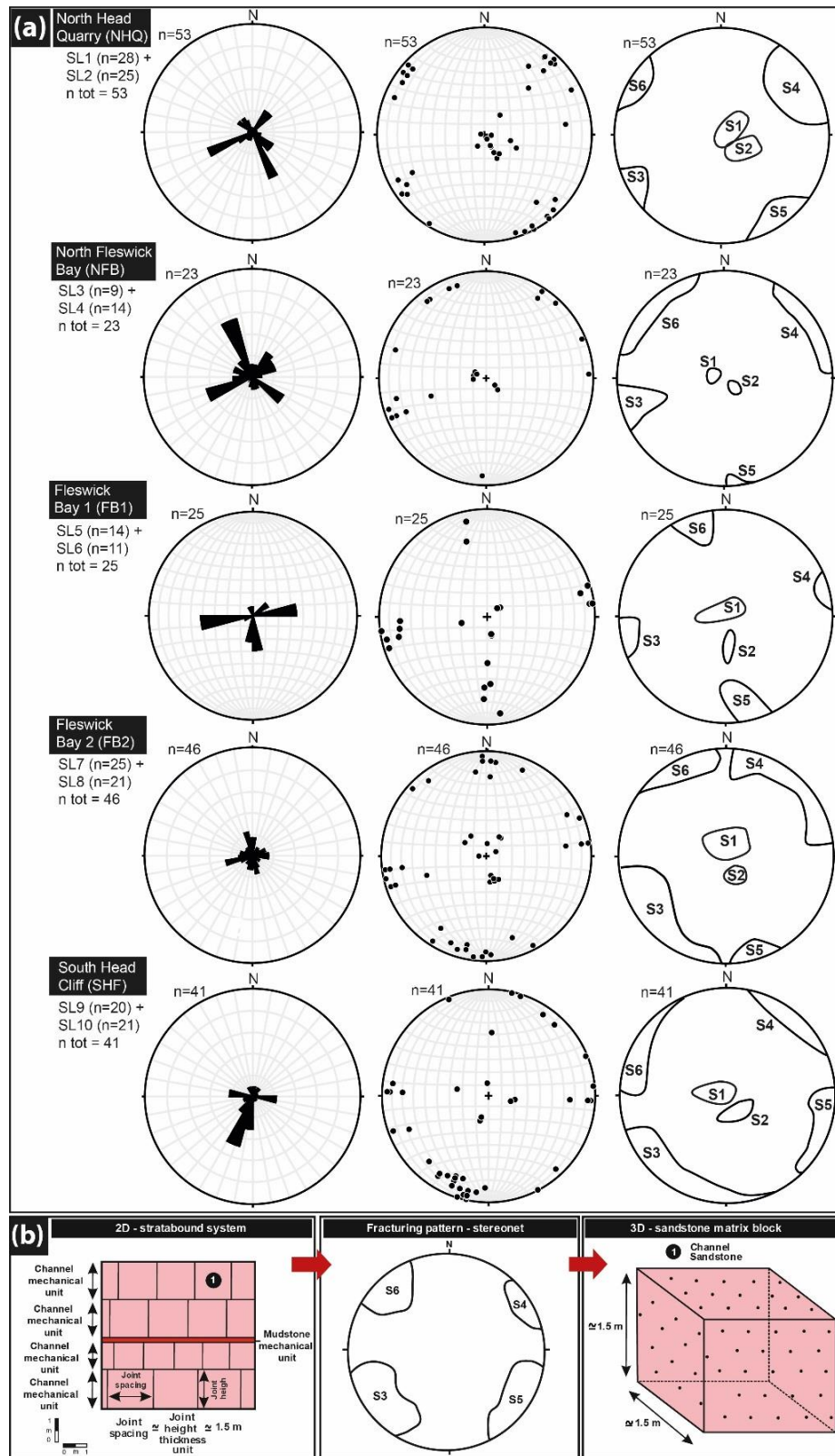
Figure 4.6: Stratabound-type fractures in the St Bees Sandstone aquifer. (a) Stereoplots (upper hemisphere, equal area) which includes rose diagrams, Kamb contours (contouring area = 1.5% of net area) and grouping of joints families from scan line surveys, (b) Conceptual model of the stratabound fracturing system.

4.5.2 Pumping test analyses

Single-borehole pumping tests conducted previously to this study (Figures 4.7a, b; 4.8) have been re-analysed for the five wells that were subject to flow velocity logging, to identify their overall transmissivity to allow quantitative flow-log analysis. Transmissivity values are summarized in Tables 4.4 and 4.5 and range from 35 to 910 m^2/day. Using Eden and Hazel and Theis solutions it is not possible to calculate the storage coefficient of aquifers from single-well tests (Butler, 1990; Sethi, 2011). Single-well step-drawdown tests should constitute at least 4 steps and data here meet these criteria (Figures 4.7a; 4.8). These well step-drawdown tests (Figures 7a, 8; Table 4.4) have been analysed using Eden and Hazel (1973) which, except for Ellergill Bridge[3], fit the validity conditions suggested by Mathias et al. (2008) and Mathias and Todman (2010) specifically in fractured aquifer-types. These authors show how step-drawdown tests are generally appropriate for the calculation of aquifer parameters where final step flow rates are greater than 350 m^3/day. Alternatively, step-drawdown tests characterised by lower flow rates (<350 m^3/day) but with a step duration of less than 60 minutes also reproduce reliable aquifer parameters. Our step-drawdown curves show optimum fits since residual mean (0.01-0.15 m^2/day) and residual standard deviation (0.16-0.80 m^2/day) are characterised by significant lower values compared to transmissivities (41-913 m^2/day).

Recovery phases of the step-tests and those of the tests of longer duration at constant flow rate (Figure 4.7 b) have also been analysed, following Theis (1935). This methodology also determines transmissivity from single borehole tests assuming non-steady state horizontal flow.

---

[3] Ellergill Bridge represents the only drawdown well test which does not meet the validity conditions demonstrated by Mathias and Todman (2010). To address this issue, the 5th step test of duration > 60 minutes has been neglected in calculating transmissivity, which itself yields reliable values close to other well tests analysed for this borehole (Table 4.4).

Table 4.4: Summary of transmissivity and parameters (step test flow rate, formation loss, turbulent well loss) used for the Eden and Hazel (1973) analysis.

Field site/borehole name	Number of Steps	Flow rates (m³/day)	Turbulent Head Loss (day²/m⁵)	Formation loss (day/m²)	Transmissivity (m²/day)
Black Ling	5	640, 870, 1140. 1320, 1440	$1.6*10^{-6}$	$1.8*10^{-3}$	99
Bridge End Trial	5	734, 834, 1040, 1370, 1520	$1.1*10^{-5}$	$4.4*10^{-3}$	51
Ellergill Bridge	5	40, 70, 110, 160, 280	$2.2*10^{-7}$	$2.6*10^{-3}$	41
Pallaflat Reservoir	4	61, 400, 690, 780	$1.5*10^{-5}$	$4.4*10^{-3}$	66
Thornhill	6	51, 1390, 1740, 2040, 2140, 2220	$4.1*10^{-7}$	$3.6*10^{-3}$	913

Table 4.5: Summary of transmissivity values from all pumping tests data available for the 6 studied wells which also includes transmissivity from the upscaling of K_h geometric mean of cored sandstone plugs.

Field site/well name	Constant Rate Tests (Recovery phase) Theis, 1926 T (m²/day)	Step Tests Drawdown phase Eden and Hazel, 1973 T (m²/day)	Step Tests (Recovery phase) Theis, 1926 T (m²/day)	Upscaled transmissivity T (m²/day)
Black Ling	135	99	80	1.09
Bridge End Trial	54	51	42	0.99
Ellergill Bridge	53	41	35	1.09
Pallaflat Reservoir	51	66	-	1.90
Thornhilll Trial	754	913	695	1.40

A comparison of the transmissivity values calculated using all the available datasets (Table 4.5) indicates that recovery phase Theis analysis of step-tests yields transmissivity values 14 to 24% lower than the Eden and Hazel (1973) analysis of the drawdown phase. This systematic difference in transmissivity between step-drawdowns and relative recovery may be related to the fact that well loss correction is neglected in the Theis recovery analysis, and this method consequently underestimates transmissivity (Clark, 1977). However, Theis recovery analysis of the longer constant rate tests produced transmissivity values both higher and lower than the Eden and Hazel analyses of step tests (Table 4.5). These differences probably arise due to the different test durations and hence volume investigated which resulted in a lack of well loss correction in some wells (Neuman and Di Federico, 2003; Le Borgne et al., 2004; Le Borgne et al., 2006a, b; Noushabadi et al., 2011). Given both the wide range in durations and investigated volumes associated with the recovery of constant rate tests, and the neglection of well loss in all the available recovery datasets,

transmissivities derived from the Eden and Hazel approach have been used here for flow-logging analysis. These drawdown step tests show how aquifer transmissivities range from 41 up to 99 m^2/day for four of the five flow-logged wells. Only Thornhill Trial shows a significantly higher transmissivity value (913 m^3/day); this well seems to be influenced by the River Ehen which represents the principal river in the Sellafield plain and is only 100 m distant (British Geological Survey, 2015; Merritt and Auton, 2000). Black Ling (66 m^2/day) and Pallaflat Reservoir (99 m^2/day) are the only wells drilled in correspondence of mapped fault traces on the geological map (Figure 4.1b, Table 4.1); these show transmissivities at the upper end and in the middle of the range 41 up to 99 m^2/day respectively top (Table 4.5).
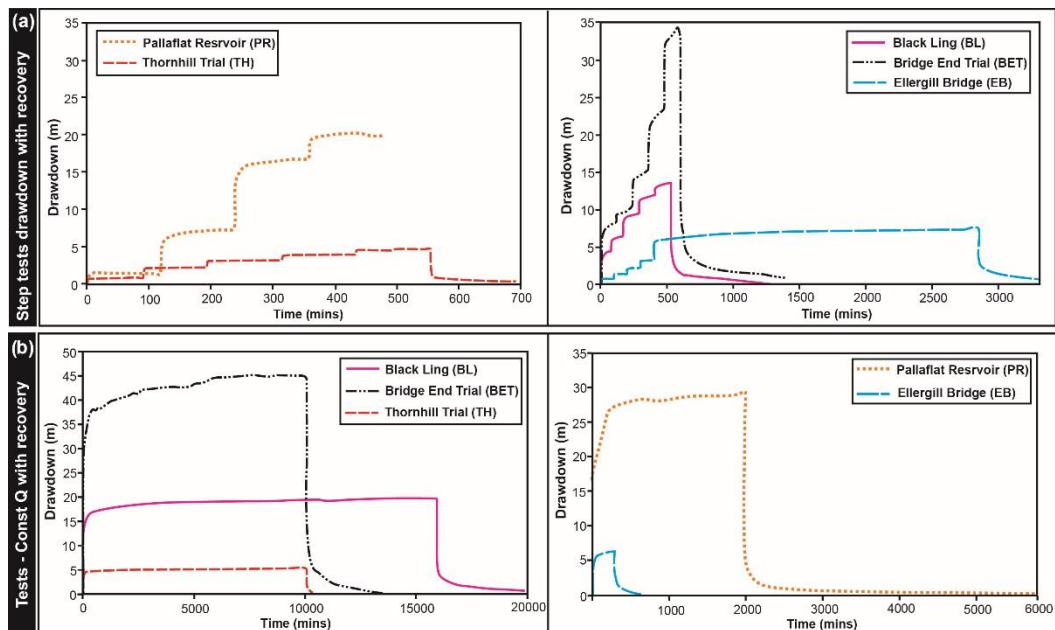
Figure 4.7: Pumping test data; (a) Drawdown and recovery vs. time curves of step tests for the five pumped wells, (b) Drawdown and recovery vs. time curves for the five studied wells when pumped at a constant flow rate.

4.5.3 Upscaling hydraulic conductivity

Available transmissivity values from pumping tests for the five studied boreholes (Table 4.5) are compared with the screen transmissivity which is obtained from the upscaling of cored hydraulic conductivity values available for the St Bees Sandstone aquifer. These plug-scale hydraulic conductivities show similar ranges across the Egremont-Sellafield area (Figure 4.1). In fact, hydraulic conductivity from cored plugs range from 8.3×10^{-6} up to 1.2 m/day and from 4.2×10^{-6} up to 0.8 m/day for the Egremont and Sellafield area, respectively (Nirex, 1992a, 1992c, 1993b, 1993c; Allen et al., 1997). Thus, these values have been grouped together in order to upscale screen transmissivity in the five studied boreholes aiming to maximise sample representability. The horizontal hydraulic conductivity (K_h) from sandstone plugs have been upscaled since it represents preferential flow direction in a layered aquifer which is characterised by sub-horizontal beds (dip angle = 5°-20°; mean vector = 10°; n = 631) and sandstone represents 95% of thickness penetrated in the five boreholes. The K_h geometric mean of sandstone plugs (n = 177) is 1.3×10^{-2} m/day. These average values has been multiplied by the screen length (see Table 1) to compute upscaled geometric transmissivities in each flow-logged borehole (Table 4.5).

The screen transmissivities which are obtained by the upscaling of K_h geometric mean show values $\sim 10^{2}$ lower than transmissivity from well tests ($T_{well\ test}/T_{screen}$ = 35-653; arithmetic mean = 153; σ = 224). Thus, well tests transmissivity values are significantly higher than those implied for the matrix by upscaling, suggesting that fractures dominate response during pumping tests.

4.5.4 Fluid logs

The FLASH program for flow log analysis (Day-Lewis et al., 2011) is suitable both for aquifers dominated by matrix and fracture flow and is commonly used in the analysis of sandstone aquifers (e.g., Gellasch et al., 2013; Lo et al., 2014). Here the program was used for analysing flow velocity profiles of shallow boreholes in "fracture mode" instead of "layer mode", since the water flow in the shallow aquifer tested here is dominated by fractures. Indeed, flow velocity profiles from this study show major changes in correspondence to tectonic discontinuities. Analysis of fluid velocity, temperature and conductivity curves was compared with optical televiewer images aiming to estimate the percentage of flowing fractures. The proportion of flowing fractures was found to be ~10%, which includes fractures that bound flow zones (n=33) in the five studied wells and a clusters of fault-related fractures in the Back Ling and Pallaflat Reservoir wells (n=23).

Velocity, temperature and conductivity logs carried out in Bridge End Trial and Thornhill Trial wells characterise the aquifer away from fault zones, according to the geological map (Figure 4.1b; Table 4.1). The background information (Nirex, 1997; British Geological Survey, 2015) also does not indicate the presence of fault-related structures near these three wells. Optical televiewer and calliper logs confirm how the fracturing network of these wells is not characterised by fault-related structures i.e. an absence of displaced horizons, cataclasites and intervals characterised by significant diameter variations. Thus, the fracturing pattern is dominated by bedding plane fractures (S1) and vertical joints (S3, S4, S5, S6); cross-bedding (S2) and drilling-induced fractures (S7) also occur. Temperature, conductivity and velocity logs were measured initially in ambient conditions and then under pumped conditions: pumping rates were 190 m^3/day in Bridge End Trial and 242 m^3/day in Thornhill Trial. Pumping was maintained at a constant rate for 20 minutes before flow logging using a tool-speed of 10 m/min (wells were logged both downwards and upwards but the downward flow logs are presented and analysed here, as these have better

data quality). Additionally, temperature and fluid conductivity were also logged under ambient and pumped conditions.

The FLASH program has been used to constrain hydraulic conductivity from fluid velocity logs; fluid conductivity, temperature and flow velocity, in both ambient and stressed conditions are reported (Figures 4.8 and 4.9). The modelled parameters which are represented by T_{factor} (ratio between single layer and well test transmissivity, T_i/T), Δh_i (difference in head between the well and the far-field for each layer) and the hydraulic conductivity for each layer (k_i), are summarized in Table 4.6. Interpretations of flow velocity log profiles (Figure 4.8) are based on the selection of marked changes of the fluid flow velocity, which divides the open well section into hydraulic layers (Figures 4.8, 4.9). Six layers (L1-6) were modelled for Bridge End Trial and Thornhill Trial. Typically layer boundaries identified in this way corresponded to bedding plane fractures (S1) seen in the optical televiewer logs. Some layer boundaries are marked by sharp changes of flow velocity, which then remains substantially constant within the zone. Such layers include L2 and L3 in Thornhill Trial (Figure 4.8 a) and L3 and L5 in Bridge End Trial (Figure 4.8b). Thus, these layers are internally impermeable and only the sub-horizontal fractures at their boundaries conduct flow into the well. Flow velocity (Figure 4.8) in other modelled layers is characterised by a basal change and then by a constant slope within the layer (e.g. L5 in Thornhill Trial). This means that other permeable structures contribute to the flow within these layers. Indeed, the optical televiewer and calliper logs indicate the presence of minor fractures characterised by further bed-plane (S1), cross-bed (S2) discontinuities, stratabound joints (S3, S4, S5, S6) and rare non-natural fractures (S7) within such layers.

Layer hydraulic conductivity values from the wells that are not close to fault traces typically range from 0.1 to 4.6 m/day (Table 4.6), although values higher than 5 m/day occur where a layer is bounded by prominent bed-parallel fractures. These S1 discontinuities are characterised, according to the calliper log, by up to 20% borehole diameter enlargement. Thornhill

Trial (Figure 4.8a) well is characterised by both inflow and outflow horizons. Inflows occur in the lower part of the Thornhill Trial borehole (Figure 4.8a) and are associated with marked changes in both water resistivity and temperature; the upper parts of these wells are characterised by outflows (seen as reducing upward ambient flow near the top of the open section). By contrast, Bridge End Trial (Figure 4.8b) is artesian and hence overflowed throughout logging; it is thus characterised only by inflows. Note that the lack of variation of fluid conductivity and temperature at the outflow horizons identified in Figure 4.8a is expected, since there is no contribution of water flowing from different compartmentalised levels. Bedding plane fractures have been found in this analysis to be important flow pathways both in ambient and stressed conditions. Alteration (detected by the optical televiewer) acts to enlarge these permeable fractures (K>5 m/day) that may transport contaminants in groundwater at high flow velocities. Barker et al. (1998) found using tracer tests in the Sherwood Sandstone Group in the Cheshire Basin flow velocities up to 140 m/day which are more typical of carbonate karst aquifers, suggesting how enlarged fractures may transport contaminants at velocities which are unexpected for a siliciclastic porous aquifer.

Table 4.6: Parameters computed from the FLASH program for Thornhill Trial, Bridge End Trial and Black Ling wells.

Layer code	Layer bottom depth (m ASL)	T factor	Layer hydraulic conductivity, K_i (m/day)	Layer far-filed hydraulic head, Δh_i (m)
THORNHILL TRIAL				
L8	14.5	0.21	20.6	-1.1
L7	-2.7	0.12	6.5	-0.5
L6	-14.2	0.05	4.0	0.6
L5	-26.2	0.23	17.5	0.3
L4	-45.9	0.10	4.6	0.4
L3	-59.8	0.10	6.6	0.3
L2	-71.6	0.19	14.7	0.7
L1	-76.5	0.00	0.0	0.3
BRIDGE END TRIAL				
L6	11.6	0.12	0.4	5.0
L5	-23.5	0.05	0.1	3.3
L4	-24.7	0.53	22.5	2.1
L3	-36.4	0.10	0.4	4.9
L2	-44.3	0.21	1.4	3.3
L1	-50.0	0.00	0.0	3.0
BLACK LING				
L4	-14.7	0.2	0.4	-0.34
L3	-22.2	0.1	1.3	0.91
L2	-40.5	0.2	1.1	0.39
L1	-50.0	0.5	5.2	0.03

Flow-logging analyses undertaken in other lithified and fractured sandstone aquifers (Runkel et al., 2006; Gellasch et al., 2013; Lo et al., 2014) away from fault zones show similar results, which are represented by significant velocity variation in correspondence of large bedding fractures which bound the modelled flow zones. Additionally, Morin et al. (1997) in the Passaic Sandstone in New Jersey and Bouch et al. (2006) in the Sherwood Sandstone aquifer of the Cheshire Basin found low proportion (<20%) of fractures with measurable flow using borehole flow-logging similarly to this work (where the proportion was approximately 10%). Hitchmough et al. (2007) also pointed out the importance of bedding-parallel fractures on conducting water flow in the Sherwood Sandstone aquifer in the Cheshire Basin at relatively shallow depths (≤ 180 m). These authors found analysing fluid-logs that 9% of fractures produced detectable flow, similar to our hydrogeophysical study.

Flowing low-angle inclined fractures (<25°), as seen in our study of the St Bees Sandstone Formation, are also common for non-faulted wells in fractured limestone, dolostone and gneiss subjected to flow logging (e.g., Paillet, 1998, 2004; Le Borgne et al., 2006a), these include fractures along sub-horizontal foliations in gneiss and bedding discontinuities in carbonate rocks.
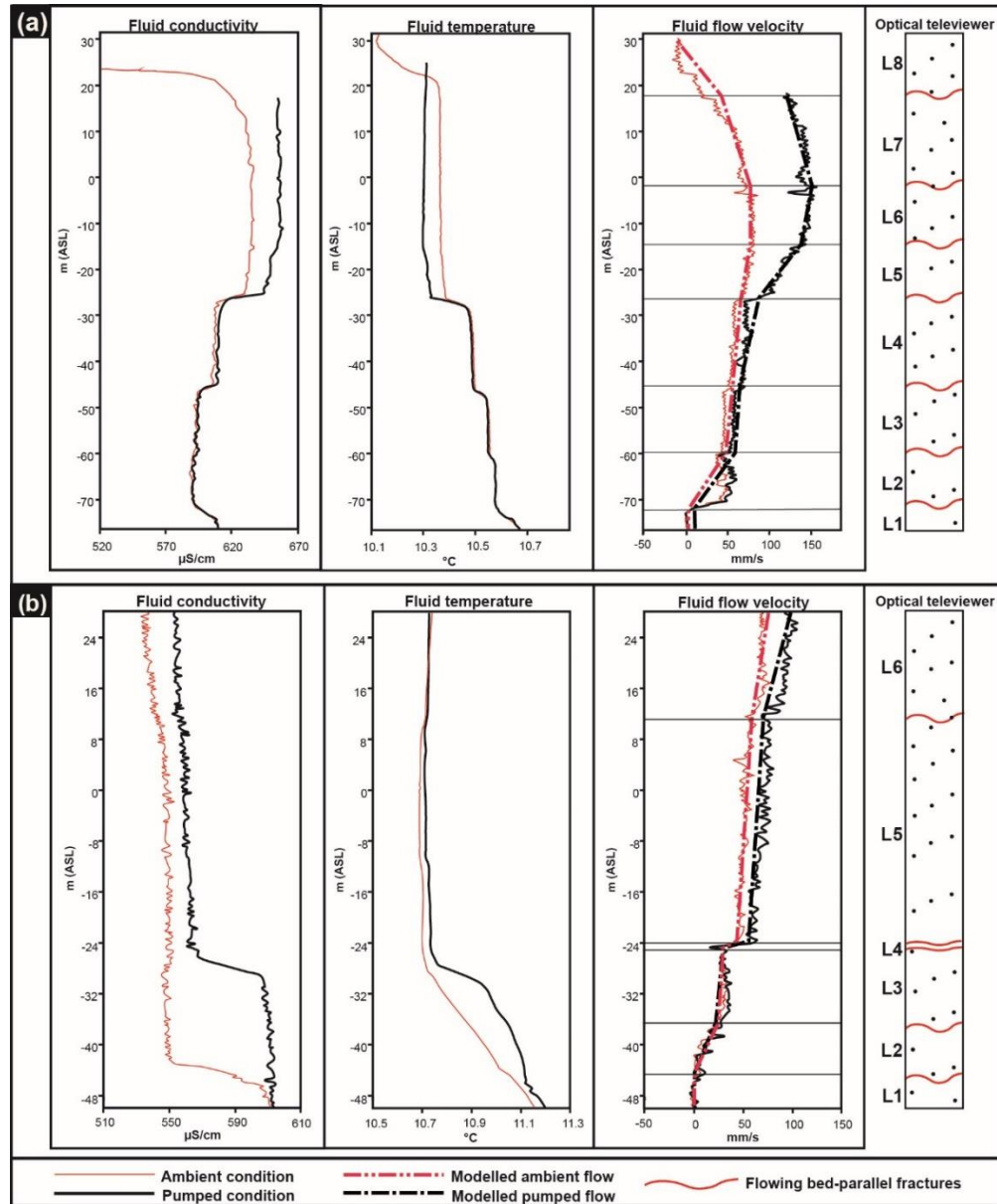
Figure 4.8: Fluid logging in wells far from mapped fault traces; fluid conductivity, temperature and velocity logs and modelled flow rate (FLASH generated) profiles for (a) Thornhill Trial and (b) Bridge End Trial wells.

Flow velocity, temperature and conductivity logs have also been carried out in three of the five wells which have been drilled close to fault traces (Figure 4.1; Table 4.1), to characterise the impact of fault zones on flow. Flow logging was performed under ambient and pumped conditions, as previously described for the non-faulted wells: pumping rates were 216

m^3/day in Black Ling, 225 m^3/day in Ellergill Bridge and 181 m^3/day in Pallaflat Reservoir (Figure 4.1b).

Background information (British Geological Survey, 2015; Nirex, 1997) indicates the presence of extensional faults in correspondence of Black Ling, Ellergill Bridge and Pallaflat Reservoir wells (Figure 4.1b; Table 4.1). Optical televiewer and calliper logs confirm how the fracturing network of these wells is affected by fault-related structures such as cataclasites, open fractures and granulation seams. Indeed, optical televiewer logs show fault cataclasites (Figures. 4.3, 4.9a, b) in Black Ling well between 16 and 22 mASL, and also at the bottom of the well which is collapsed due to the presence of a major cataclastic fault structure. Pallaflat Reservoir (Figure 4.9b) well is also affected by faulting between 10 and 14 mASL. However, Ellergill Bridge well cuts only the external part of a fault zone so it does not show cataclasites. In this well vertical granulation seams are detected by the optical televiewer log. Bedding plane fractures (S1), cross-bed fractures and vertical joints (S3, S4, S5, S6), which characterise the entire aquifer, complete the fracturing pattern in these three faulted wells.

Calliper logs indicate enlargement of the well diameter in correspondence of fault cataclasites by up to 66%, 54% and 30% in the Black Ling, Ellergill Bridge and Pallaflat Reservoir wells, respectively. By contrast, in boreholes that are not characterised by faulting, the well diameter does not increase more than 20% in correspondence to major bedding plane discontinuities.

Velocity flow logs in these three wells (Black Ling, Ellergill Bridge, Pallaflat Reservoir; Figure 4.9) have been complicated by problems related to water turbulence due to variations in borehole diameter or low ambient flow rates (0-18 mm/s) close to the nominal detection limit of the flow meter (Grass, 1971; Tsang et al., 1990; Paillet 2004; Day-Lewis et al. 2011). Consequently, fitting experimental flow profiles in Ellergill Bridge and Pallaflat Reservoir wells using the FLASH program proved problematic, although a fit was obtained for Black Ling well (Figure 4.9a). The interpretation of the Black Ling flow velocity profile uses four flow zones; the upper flow zone includes a section showing fault cataclasites near the

top of the well, which does not cause any inflow or outflow. Notably, temperature and conductivity logs also do not show any anomaly in correspondence of this feature. However, a major cataclastic fault is present at the bottom of the logged interval (Figure 4.9a) and a collapse is present directly below the end of logged interval; these zones contribute 50% of flow into the Black Ling well; analysis indicates a hydraulic conductivity of 5.2 m/day (L1, Table 4.7).

Pallaflat Reservoir well (Figure 4.9b) shows cataclasites between 10 and 14 mASL that produces 47% of the flow; analysis indicates a hydraulic conductivity of 7.4 m/day (L3, Table 4.7). Despite the different methodologies used to quantify the water flow, in both cases cataclasites characterise about the 50% of the flow in a single-well test. However, the other 50% of the flow in both Pallaflat Reservoir and Black Ling wells derives from large bedding plane fractures (S1), which represent further important flowing discontinuities.

Ellergill Bridge well (Figure 4.9c; Table 4.7) cuts the external part of a fault damage zone and does not appear to cross-cut the fault core; no cataclasites or fractures showing displacement, are observed. Consequently, flow in this borehole is dominated by bedding -plane fractures. Indeed, 42% of the transmissivity is related to the L2 zone, which represents a cluster of S1 fractures. The upper zone above this characterises the remaining 58% of the transmissivity. Ellergill Bridge well shows hydraulic behaviour similar to the non-faulted wells that have been previously described (Bridge End Trial, Thornhill Trial). All these flow-logged boreholes are characterised by major single bedding fractures, as well as clusters of minor bedding fractures, which give flow zones with hydraulic conductivity higher than 5 m/day. Consequently, bedding fractures (S1) can produce hydraulic conductivities comparable to cataclasite flow zones.

Table 4.7: Parameters computed from flow log analysis for Pallaflat Reservoir and Ellergill Bridge wells using equation (3).

Layer code	Layer bottom depth (m ASL)	Delta V/Vmax	Layer hydraulic conductivity, K_i (m/day)
PALLAFLAT RESERVOIR			
L4	14.5	0.29	0.4
L3	10.28	0.47	7.4
L2	-14.4	0.24	0.6
L1	-34.0	0.00	0.0
ELLERGILL BRIDGE			
L3	56.76	0.58	1.2
L2	55.14	0.42	10.7
L1	0	0.00	0.0

Previous application of flow logging in faulted zones in crystalline rocks (e.g., Davison and Kozak, 1988; Martin et al., 1990; Le Borgne et al., 2006a; Roques et al., 2014) show similar result to the St Bees Sandstone aquifer, in that flow is dominated both by fault-related features and also by sub-horizontal, bedding-related discontinuities, with no contribution from the rock matrix evident.
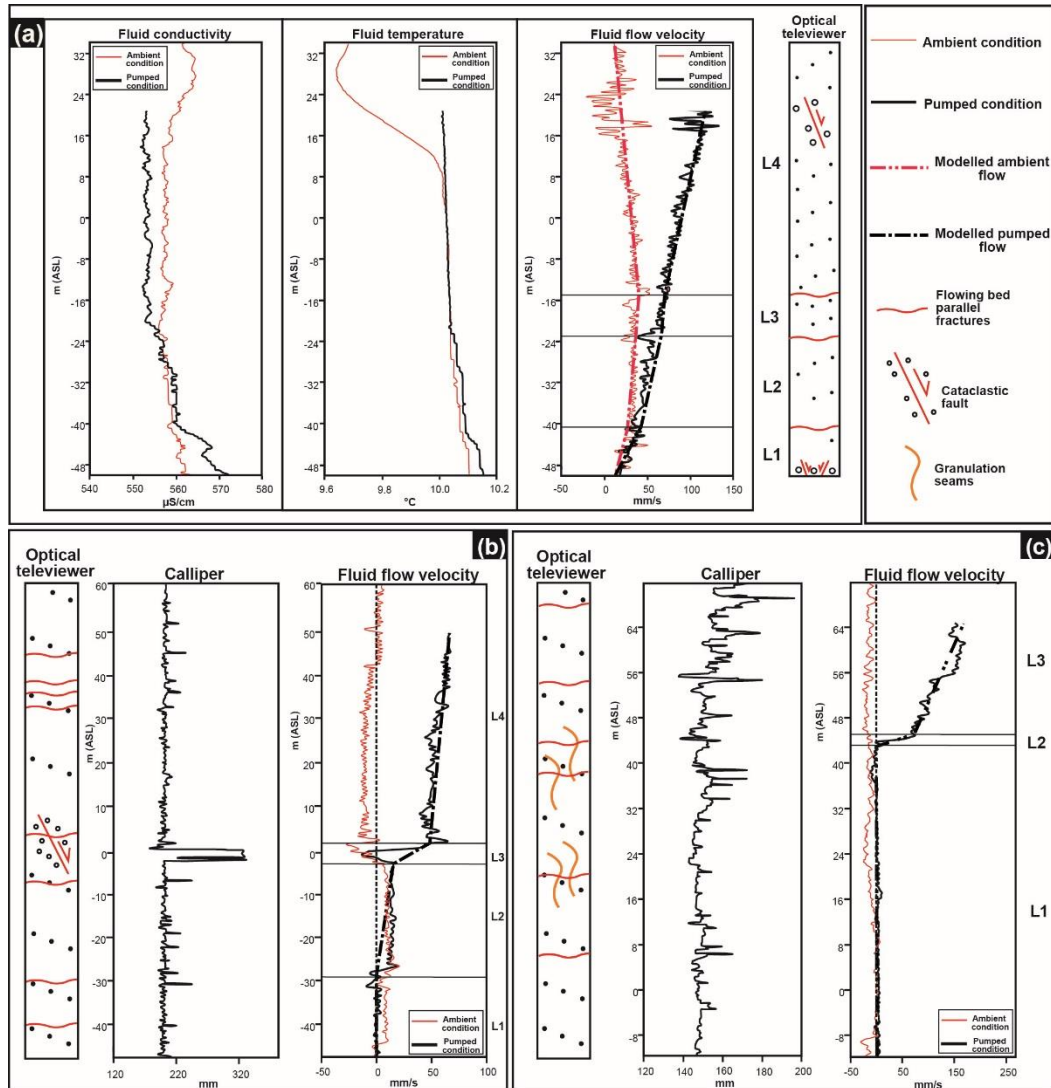
Figure 4.9: Fluid logging in wells in fault zones; logs of fluid conductivity, temperature and velocity and model flow rate (FLASH or equation. (3) generated) profiles for (a) Black Ling. Calliper and flow velocity logs for (b) Pallaflat Reservoir and (c) Ellergill Bridge

4.6 Sherwood Sandstone aquifer in other areas

The hydro-geophysical characterization of the shallow Bees Sandstone aquifer (≤180 m) of the East Irish Sea Basin is compared in this work with both (i) the deep St Bees Sandstone aquifer (180 to 400 m subsurface depth) undertaken as part of the investigation for the Sellafield nuclear waste repository; and (ii) the Sherwood Sandstone aquifer of the Cheshire Basin which was previously investigated by crossing borehole logging,

packer and intergranular permeability tests (Martin et al., 1990; Allen et al., 1997).

The comparison between the hydro-geophysical characterization undertaken in this work with that of the deeper St Bees Sandstone aquifer (Streetly et al., 2000) aims to provide an improved understanding of the mechanisms that reduce both permeability and contaminant transport velocities at increasing depths in a strongly lithified sandstone aquifer-type. Our results are also compared with those from previous studies of the Sherwood Sandstone aquifer of the northern Cheshire Basin, where analogous succession are also fractured and layered but less mechanically resistant, and characterised by higher matrix porosity and hydraulic conductivity values (Bell, 1992; Yates, 1992; Allen et al., 1997). Furthermore, normal faults in the northern Cheshire Basin have been the object of hydrogeological studies from the mid 1800s to present (Morton, 1870; Moore, 1902; Tellam, 2004; Mohamed and Worden, 2006; Seymour et al., 2006; Griffiths et al., 2016), which allows comparison of their hydraulic behaviour with those in the St Bees Sandstone aquifer (West Cumbria, East Irish Sea Basin).

4.6.1 Review of pumping tests in the St Bees Sandstone aquifer

Pumping test transmissivity (Figure 4.10) values from the five studied wells in the West Cumbrian region have been integrated with all the available hydraulic tests that have previously been realised in the St Bees Sandstone aquifer (Allen et al., 1997; Streetly et al., 2000). Additionally, all the information concerning both transmissivity values and test parameters has been summarized in Table 4.8. Transmissivity values of the shallow part of the St Bees Sandstone aquifer have been plotted in a single box plot (box plot A, Figure 4.10), which collates hydraulic test data from both the West Cumbria and Carlisle areas. These values have been grouped together because the aquifer is characterised by the same lithological features and similar intergranular permeability (Nirex, 1992a, 1992c, 1993b, 1993c;

Jones and Ambrose, 1994; Allen et al., 1997; Brookfield, 2004, 2008) across these areas. However, all the transmissivity values obtained during the hydrogeological investigation of the more deeply buried St Bees Sandstone aquifer in Sellafield (Streetly et al., 2000) have been plotted in a separate box plot (box plot B, Figure 4.10).

The two groups of hydraulic tests show a systematic difference of two orders of magnitude (10^2) between each pair of statistical parameters (maximum, minimum, 25th percentile, 75th percentile, geometric and harmonic means). The two groups of hydraulic tests are characterised by similar screen length and borehole diameter ranges (Table 4.8). Although the two groups differ in flow rates and test duration with generally lower flow rates and longer test durations for the Sellafield group, this is likely to be simply a consequence of the lower transmissivities seen here. In fact, only low extraction rates were achievable, and a longer test duration was needed to produce a measurable response. Additionally, although the two groups of pumping tests differ for flow rates and test duration; these two physical parameters show wide ranges of values which are reported in Table 4.8. Consequently, there is always partial superimposition with regards to flow rates and pumping duration comparing pumping tests in the shallow and the deep St Bees Sandstone aquifer.

Table 4.8: Transmissivity (T) ranges for the shallow (this work; Allen et al., 1997) and deep investigations (Streetly et al., 2000) of the St Bees Sandstone aquifer.

Reference	Area	n.	Depth interval (m)	T m^2/day	Flow rate, Q m^3/day	Test Duration mins	Screen length (m)	Borehole diameter (m)
This work	St Bees	6	10 - 159	51 - 754	40 - 2220	650 - 5810	84 - 152	0.15 - 0.2
Allen et al., 1997	St Bees	6	15 - 123	70 - 220	260 - 3740	441 - 87552	35 - 111	0.20 - 0.60
Allen et al., 1997	Carlisle	9	10 - 180	9 - 1268	267 - 1439	2880 - 13325	60 - 170	0.22 - 0.60
Streetly et al., 2000	Sellafield	32	180 - 400	0.46 - 7.8	22 - 65	8640 - 31680	20 - 180	0.15- 0.54

Matrix permeability values from cored plugs show similar values for the shallow and deep St Bees Sandstone aquifer. In fact, plug-scale hydraulic conductivity ranges are 8.3×10^{-6} - 1.2 m/day and 4.2×10^{-6} - 0.8 m/day for the shallow and the deep aquifer, respectively (Nirex, 1992a, 1992c, 1993b, 1993c; Allen et al., 1997). Additionally, plug scale permeability tests (Nirex, 2001) show that only low permeability units ($K < 10^{-3}$ m/day) which are represented by sheet-like sandstone and mudstone in this aquifer show sensitivity of K to salinity variation. Given all these elements, the observed differences in transmissivity are most likely to result from higher fracture permeabilities which localize inflow and outflow horizons at depths shallower than 180 m (Figure 4.11a). Hydraulic head measurements which have been realised by a Westbay monitoring system in the Sellafield plain show how the aquifer is characterised by a horizontal hydraulic gradient which is essentially constant with depth (Black and Brightman, 1996). Additionally, the St Bees Sandstone aquifer is ~ 100 times more transmissive in its shallow part than buried below 180 m (Streetly et al., 2000). Thus the shallow St Bees Sandstone aquifer must be characterised by higher groundwater flow rates which will act further to enhance alteration of fractures. The relatively high permeability of fractures in the shallow part of the aquifer (≤ 180 m) may be related either to fracture closing with

increasing depth, or to alteration of fractures as is typical in the shallow part of sandstone aquifers (Figure 4.11 a; Wray, 1997; Jiang et al., 2009, 2010). Calcite represents the soluble cement in the St Bees Sandstone aquifer (Strong et al., 1994; Milodowski et al., 1998) and evidence of elevated groundwater flow enhancing dissolution of this mineral along fractures is provided by borehole optical televiewer images showing partially mineralized fractures (Figure 4.3f). Furthermore, optical televiewer logs also indicate the occurrence of small cavities that enlarge tectonic fractures (Figure 4.3b, c, e) such as bedding plane (S1) and fault-related (S7) fractures; these may also be a result of calcite dissolution.

The highly permeable shallow aquifer shows a developed fracturing network, which is characterised by flowing open fractures (Figure 4.11a; faults, bedding fractures). These tectonic fractures are capable of conduit fluid flow at low confining pressure (<5 MPa), but their permeability reduces at higher pressures, as demonstrated by multistage permeability tests based on analysis of plugs of the St Bees Sandstone Formation (Daw et al., 1974).

The deep St Bees Sandstone aquifer, is also characterised by a reduction of transmissivities (25%) occurring in association with mudstone units (Streetly et al., 2000). This lower transmissivity in the mudstone-rich basal sedimentary sequence may be related to one or more of the following: (i) flow through the low-permeability mudstones characterizing the basal stratigraphy in a matrix-flow aquifer (Alexander et al., 1987); (ii) further reduction of fracture aperture due to the lithostatic load (Jiang et al., 2009, 2010); or (iii) less development of fracturing due to stress release on the plastic mudstone-beds (Reks and Grey, 1982). Matrix flow as principal flow driver in the deep St Bees Sandstone aquifer is supported by the first derivative of recovery tests undertaken by Streetly et al. (2000). In fact, these curves show no multiple plateaus which characterise first derivatives in double-porosity media (Zhang et al., 2000; van Tonder et al., 2001; Dewandel et al., 2011; Odling et al., 2013). Additionally, well test transmissivity values in the deep St Bees Sandstone aquifer (Streetly et al.,

2000; see bottom line of Table 4.8) better match our upscaled transmissivity values derived from plug-scale hydraulic conductivity (see Table 4.5) indicating that pores are the main flowpaths in the deeper aquifer. Thus, the transmissivity reduction (25%) in the lower sedimentary sequence must be related to flow through the low permeability mudstones which characterise the base of the sedimentary sequence. However, fracture flow may remain significant in the presence of faults, since well tests on the deep aquifer undertaken with packers in the vicinity of normal faults show relatively high transmissivity values (Figure 4.11b; Nirex, 1992b, 1993a; Streetly et al., 2000).
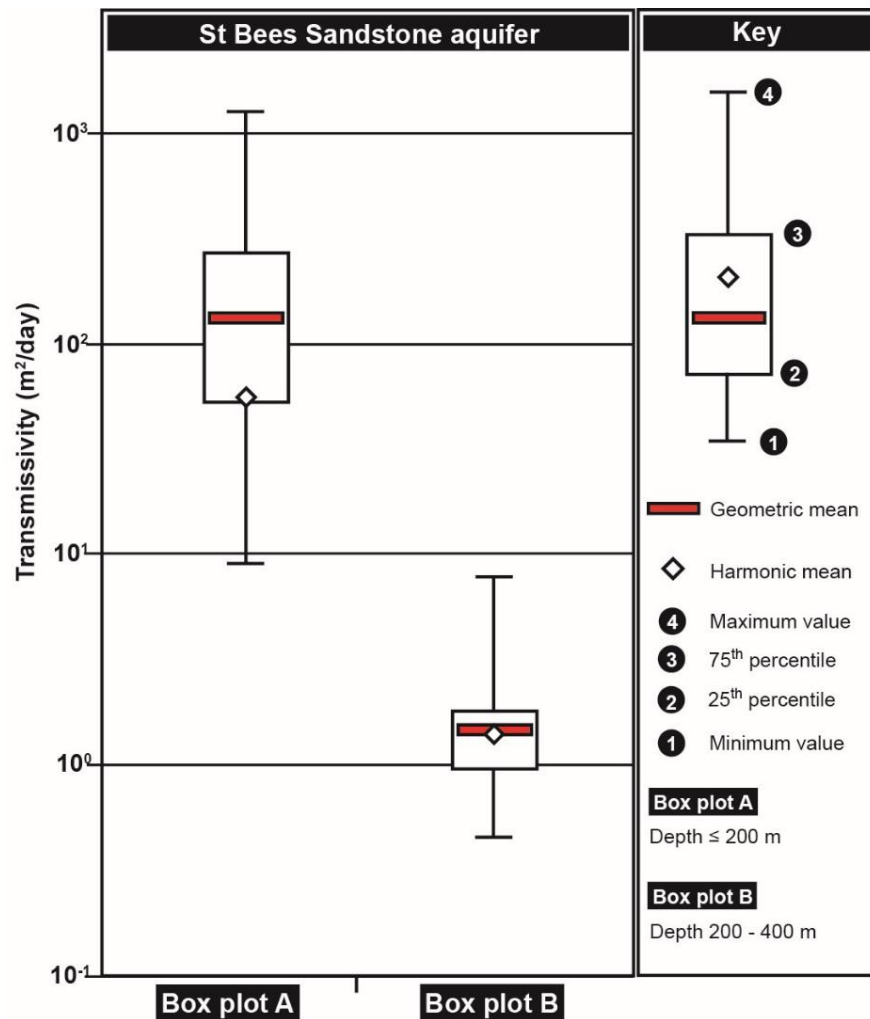
Figure 4.10: Box plots summarizing the statistics of the available pumping tests in the St Bees Sandstone aquifer: shallow ≤ 180 m (box plot A) and deep > 180 m (box plot B).

4.6.2 Comparison with Sherwood Sandstone aquifer in the Cheshire Basin

The Sherwood Sandstone Group in the northern Cheshire Basin (Figure 4.1) has been the object of several hydrogeological studies which includes packer, pumping tests, intergranular permeability and tracer tests (Allen et al., 1997; Barker et al., 1998; Brassington and Walthall, 1985).

The lowermost part of this group is represented by the Chester Pebble Beds Formation, which is dominated by a coarse to medium grained pebbly sandstone of fluvial origin. The overlying Wilmslow and Helsby Sandstone formations are characterised by a weak, fine-grained sandstone of aeolian and fluvial origin (Mountney and Thompson, 2002; Mohamed and Worden, 2006). Overall the Sherwood Sandstone Group of the Cheshire Basin is mechanically less resistant (overconsolidated sand to weak rock), and is characterised by higher porosity (interquartile range = 21.6-26.5%) and lower hydraulic conductivity (interquartile range = 0.08-1.5 m/day) values compared to the West Cumbrian St Bees Sandstone aquifer (Daw et al., 1974; Bell, 1992; Yates, 1992; Allen et al., 1997).

Brassington and Wealthall (1985) have undertaken packer and pumping tests at relatively shallow depths (≤ 130 m) in the Sherwood Sandstone aquifer of the Cheshire Basin comparing them with the upscaling of the hydraulic conductivities from cored plugs. Plugs for hydraulic conductivity measurements were from the same borehole and well logging did not show presence of fault structures.

The findings of the work undertaken by Brassington and Wealthall (1985) in the Sherwood Sandstone of the Cheshire Basin contrasts with the upscaling of the hydraulic conductivity realised for the shallow St Bees Sandstone aquifer in this work. The authors found that, as for the shallow St Bees Sandstone aquifer, the upscaled screen transmissivity remains lower than the field test transmissivity. However, the ratio between plug and field scale T was < 10 ($T_{Well\ test}/T_{Screen}$ = 1.9-6.9), which contrasts with the larger ratios seen here for the St Bees Sandstone aquifer ($\sim 10^2$).

Packer and fluid-logs tests also show how the difference between plug and field scale values resulted from a few (3-4 per each borehole) flowing bedding plane fractures. By contrast, there is a good match between T values from the two studied scales (plug and field scale) in the remaining part of the borehole. This hydraulic behaviour is common to other sandstone aquifers worldwide in non-faulted areas. In fact, flow in well tests in the Penrith (NW England) and in the Cambrian Sandstone (North America) aquifers is characterised both by intergranular porosity and large bedding-parallel fractures (Price et al., 1982; Gellasch et al., 2013). The St Bees Sandstone aquifer at relatively shallow depth (≤ 180 m) is also characterised by major flowing bedding fractures with hydraulic conductivity higher than 5 m/day. However, flow in the St Bees Sandstone aquifer not in correspondence with major bedding fractures seems to be dominated by fractures as associated with minor cross-bedding and sub-vertical (stratabound joints) fractures. The fact that the upscaling of plug-scale hydraulic conductivity showed such a large difference with respect to the well tests (~10^2) effectively excludes the matrix as significant flow contributor during pumping.

Hydraulic conductivity profiles from packer tests in deep boreholes (230 up to 400 m deep) that penetrate the Sherwood Sandstone aquifer in the Merseyside area (Cheshire Basin) show a reduction in permeability below 150 m similarly to our study in West Cumbria (Brassington and Walthall, 1985; Allen et al., 1997). Tracer tests undertaken by Barker et al. (1998) show a karst-like flow velocity (140 m/day) in the shallow Sherwood Sandstone aquifer of Merseyside. Alteration along fractures in the shallow Sherwood Sandstone aquifer (≤ 180 m) has been detected in this work by the optical televiewer which confirms how groundwater alteration plays a key role on creating a high permeability zone. Thus, the Sherwood Sandstone aquifer in West Cumbria as well as in Merseyside shows a permeable shallow part (≤ 180 m) which is characterised by potential high flow velocity with bedding fractures representing 'karstified' flow-pathways (Brassington and Walthall, 1985; Allen et al., 1997; Barker et al., 1998).

Normal fault zones in the Wilmslow and Helsby Sandstone formations of the Sherwood Sandstone Group in Merseyside appears substantially different with respect to the St Bees Sandstone Formation as they are dominated by granulation seams (Griffiths et al., 2016). By contrast, fault zones in the St Bees Sandstone Formation of the East Irish Sea Basin are characterised by a higher occurrence of open fractures (Figure 4.2b). This different structural style has been related either to the argillaceous matrix of the St Bees Sandstone which allows brittle failure at lower stresses, or to the intense post-Triassic fault reactivation which produced open-fracture in this strongly lithified sandstone (Knott, 1994; Milodowski et al., 1998). This different structural style seems to affect the fault zone hydraulic characteristics in the Sherwood Sandstone aquifer in West Cumbria and Merseyside. Bedding-parallel fractures cut granulation seams in fault damage zones and water flow seems to be dominated by these sub-horizontal fissures (Figure 4.9c, Ellergill Bridge) masking the barrier potential of granulation seams perpendicular to the fault plane. Fault slip planes and open fractures characterise 50% of flow entering boreholes penetrating fault cores (Figure 4.9 a, b).

Thus, faults in this lithified sandstone represent primary conduits for fluid flow and show low barrier potential (Figure 4.11b). By contrast, normal faults deforming the Wilmslow and the Helsby sandstone formations (Cheshire Basin) were recognized as flow-barriers based on the geochemical evidence of limited water mixing between compartmentalised horsts and grabens (Mohamed and Worden, 2006). It has been suggested that barrier behaviour led to K values at the regional scale of only 0.05 m/day perpendicular to the fault plane in the weak-rock Sherwood Sandstone of the Cheshire Basin (Seymour et al., 2006).
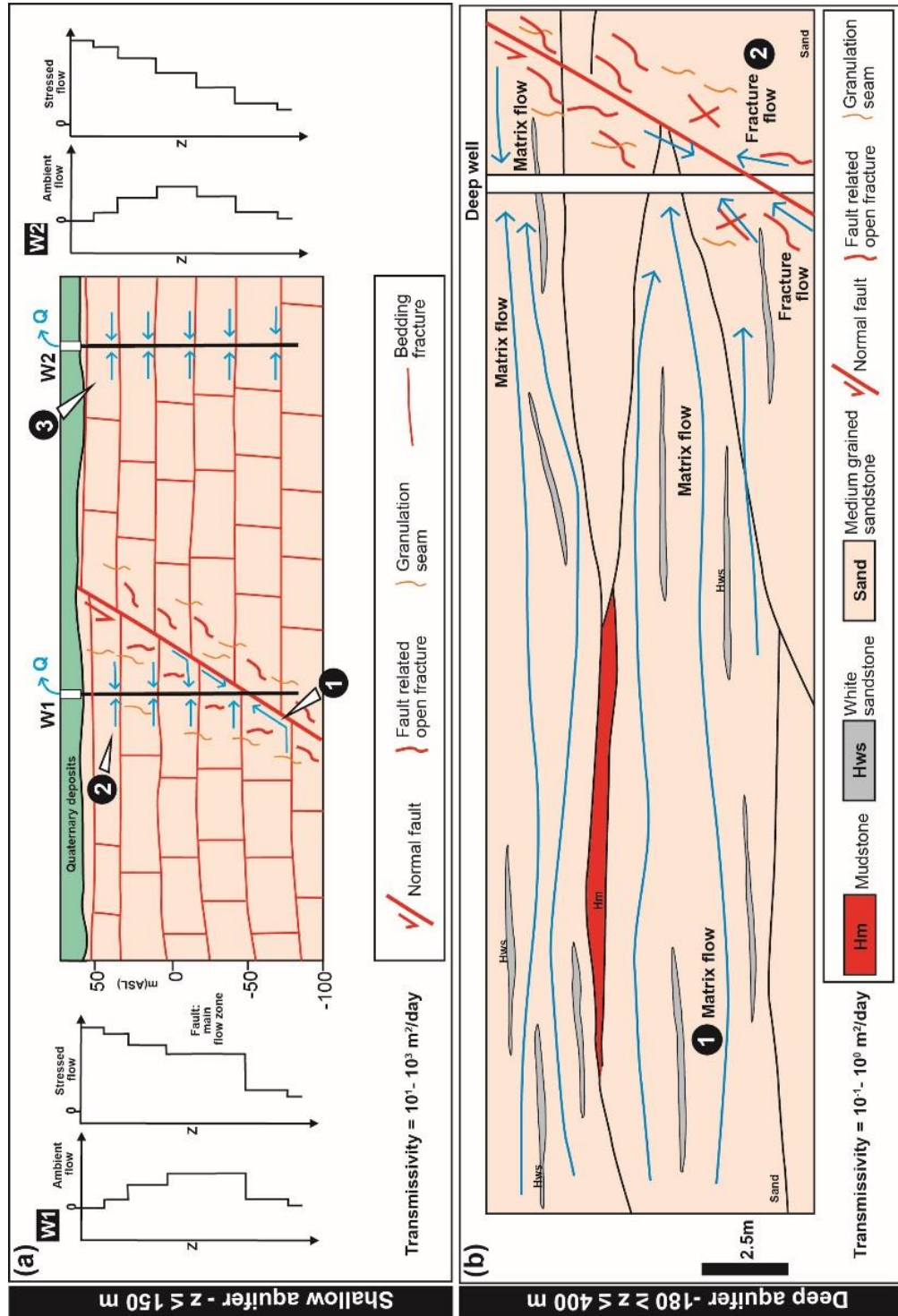
Figure 4.11: Conceptual model of the flow system in a fractured well-lithified fluvial sandstone aquifer. (a) Water flow in a shallow sandstone aquifer in: (1) fault core and internal damage zone, (2) external fault damage zone, (3) area not affected by faulting. (b) Typical sedimentary units and water flow in a deep well lithified fluvial sandstone aquifer dominated by (1) matrix flow in areas far away from fault zones, (2) both matrix and fracture flow in fault cores and damage zones.

4.7 Conclusions

The hydro-geophysical characterization of the St Bees Sandstone aquifer of West Cumbria undertaken in this work has highlighted the presence of a pervasive stratabound fracture network characterizing the sandstone aquifer. These stratabound fractures show two sets of orthogonal vertical joints that stop at their point of intersection with low-angle-inclined bedding parallel fractures. The key sedimentary heterogeneities include thin, low-porosity layers characterised by mudstone and fine-grained sandstone. Collectively, these features form matrix blocks, which may be approximated as cubes with dimensions of 1.5 m length.

Normal faults, locally, complicate the fracturing pattern, since further open fractures cutting both stratabound joints and bedding plane fractures occur in fault cores and damage zones.

In the shallow aquifer tested here (≤ 180 m depth), marked temperature, conductivity and flow velocity variations in well-bore fluid logs are localized to bedding parallel fractures and faults, which represent the main borehole inflow and outflow points. Clear indications of the importance of fractures in contributing flow to wells in the shallow aquifer include (i) sharp changes in flow-log fluid velocity in association with principal fractures, and (ii) stratigraphic intervals up to 15 m thick showing no detectable inflows, suggesting how matrix is a minor contributor to permeability in the shallow (≤180 m depth) part of the aquifer.

Quantitative analysis of well-bore flow logs from the St Bees Sandstone aquifer shows that flow zones characterised by hydraulic conductivity higher than 5 m/day typically represent up to 50% of the overall transmissivity, and are represented by the following structures: cataclasite sections where fault planes intersect the wells; single large bedding fractures; and clusters of minor bedding fractures. Specifically, fault-related fracture-corridors dominate the flow in wells which cross-cut cataclastic fault cores, because fault-related fractures establish communication between flowing bedding plane fractures. However, bedding fractures

become the principal flow conduits to wells in the external part of fault damage zones or in non-faulted areas. Fluid flow along these bedding plane fractures is likely enhanced by stratabound joints which are undersampled in vertical boreholes.

The St Bees Sandstone aquifer at depths > 180 m was the object of a hydro-geophysical characterization as part of the planning of the proposed Sellafield nuclear waste repository in the 1990s. This deep aquifer is characterised by transmissivity values which are two orders of magnitude lower than the St Bees Sandstone aquifer investigated at shallower depths (≤180 m). Since petrophysical properties and hydraulic flow regime are essentially similar to that for the shallow aquifer, the large difference in transmissivity most likely arises from higher fracture permeability at depths shallower than 180 m. Such a difference may arise because fractures are more open at relatively low vertical confining pressure (<5 MPa) in the shallower part of the aquifer. Additionally, tectonic fractures in the shallow aquifer show alteration, as indicated in optical televiewer logs. This probably arises from shallow groundwater flow leading to calcite dissolution along tectonic features. Data from the low transmissivity deep sandstone aquifer (≥180 m depth) show that those stratigraphic units characterised by a higher occurrence of mudstone beds are characterised by relatively lower transmissivity than those dominated by medium-grained channel sandstones. This, coupled with a match between upscaled plug and field-well test scale, suggests that the matrix is a significant contributor to flow at these depths (180 to 400 m). This does not seem to be the case in the shallower aquifer because of the much larger permeability of the fracture network, which dominates over flow associated with the heterogeneous sedimentary matrix.

The Triassic St Bees Sandstone aquifer in the East Irish Sea Basin represents an example of a mechanically resistant sandstone aquifer-type which is characterised by (i) fluid flow entirely dominated by fractures in its shallow part; and (ii) extensional faults representing significant flow conduits. This contrasts the Sherwood Sandstone aquifer of the Cheshire

Basin that mechanically weaker is characterised by water flow supported both by matrix and fractures, and normal faults represent significant flow-barriers.

Chapter 5

Comparison of field and plug scale hydrogeological properties of the St Bees Sandstone aquifer

(Chapter submitted: Medici, G., Mountney, N.P. and West L.J. 2017. Multi-scale properties of aquifers hosted in a fluvial sedimentary succession. *Hydrogeology Journal. Submitted*)

5.1 1 Chapter overview

Fluvial sedimentary successions represent porous media hosting groundwater, hydrocarbon and geothermal resources. Here, we describe the permeability characteristics, from plug- to field-scale, of an arenaceous fluvial succession: the Triassic St Bees Sandstone Formation (UK). Within such lithified successions, dissolution associated with the circulation of meteoric water results in increased permeability to depths of at least 150 m below ground level (BGL) in aquifer regions that are subject to rapid groundwater circulation. Here, acidic meteoric waters have dissolved pore-filling calcite in the vadose zone, and enlarged fractures to create karst-like features resulting in very high field-scale hydraulic conductivities ($K\sim10^{-1}$-10^{0} m/day) in the shallow phreatic zone. Thus, contaminant transport is likely to occur at relatively high rates. In a deeper investigation (> 150m depth), the aquifer has not been subjected to rapid groundwater circulation; field-scale hydraulic conductivity is lower, decreasing from $K\sim10^{-2}$ m/day at 150 - 400 m BGL, to 10^{-3} m/day down-dip at ~ 1km BGL, where the pore-fluid is hypersaline. Here, pore-scale permeability becomes progressively dominant with increasing depth. Plug-scale permeability tests indicate how fluvial channel elements represent the most permeable lithology. The succession is strongly heterogeneous; it contains a variety of fine-grained, anisotropic and relatively low-permeability units, including mudstone beds. Hence, at greater depths where matrix permeability dominates field-scale permeability anisotropy (K_h/K_v) is higher in zones characterized by increased preservation of low-permeability heterogeneities. Where present

a higher frequency of occurrence and greater lateral extent of mudstone units impedes vertical flow, creating a relatively high anisotropy of a type common in other fluvial successions.

5.2 Introduction

Fluvial deposits form thick sedimentary successions (>0.5 km) in basins for which accommodation was generated in response to extensional, compressional and strike slip tectonics as well as thermal subsidence (Waugh, 1973; Bosellini, 1989; Ielpi and Ghinassi, 2015: Carvalho and Vesely, 2017). Thick accumulations of fluvial sediments of Triassic age are especially widespread, being represented in South and North America, Europe, Africa, Asia and Australia; many such examples form the fill of rift valleys that developed due to the break-up of Pangaea (Walker, 1967; Waugh, 1973; Ziegler, 1982). Notably, fluvial (sandstone) and lacustrine (shale, evaporite) deposits in rift settings commonly overlie crystalline basement rocks (as in this study example). In fact, cyclical fragmentation of cratons over geological time scales places these sediments, which form rift-basin fills, upon relatively low permeability meta-igneous basement rocks. In some basins, these basement rocks are used or have been proposed to host nuclear waste repositories (Waugh, 1973; Michie, 1996; Berglund et al., 2009). Furthermore, fluvial deposits represent porous media, which can serve as important hosts for hydrocarbon and geothermal resources (Ruggieri and Giannelli, 1999; McKie and Williams, 2009); additionally, they serve as important groundwater aquifers (Tellam, 2004; Barker and Tellam, 2006).

This study presents a quantitative analysis to show how sedimentary and tectonic heterogeneities influence fluid flow in a fluvial sandstone-aquifer at a variety of scales, up to 1100 m below the ground surface. Assessment of groundwater behaviour at such depths is important in geoscience since median depth of well screens for water abstraction ranges worldwide from 25 to 68 m below the ground surface (De Simone, 2008; Toccalino et al.,

2010; Worthington et al., 2016), whereas depth intervals associated with nuclear waste repositories are typically 200 to 1100 m BGL (Voss and Andersson, 1993; Min et al., 2004; Martin and Christansson, 2009; Tsang et al., 2012). Furthermore, exploitation of high enthalpy geothermal reservoirs typically involves extraction of fluids at depths of ~1000 m from sandstone and carbonate reservoir rocks, such as reservoirs of geothermal fields along the eastern margin of the Tyrrhenian Sea (Truesdell and White, 1973; Ruggieri and Gianelli, 1999; Aldinucci et al., 2008). Fluvial sedimentary successions also represent productive hydrocarbon reservoirs in on-shore regions of North Europe, North Africa and in Middle East at depths ranging from ~1000 m and ~2000 m (Selley, 1978; Sadooni and Alsharhan, 2004; Bourquin et al 2010; Galeazzi et al., 2009; Nguyen et al., 2013). Investigation depths of > 150m BGL are sufficient to avoid 'karstic' features common at shallower depths (Worthington et al., 2016). Hence, petro-hydraulic characterization at these depths (>150 m BGL) can also provide insights for enhancing recovery in such reservoirs. Thus, the research presented here may find application in (i) safeguarding water supply from wells, (ii) influencing the design of deep geological repositories, and (iii) enhancing recovery in geothermal and hydrocarbon reservoirs (Zheng et al., 2000; Huysmans and Dassargues, 2006; Gellasch et al., 2013; Bianchi et al., 2015; Olivarious et al., 2015; Worthington et al., 2016).

Previous hydro-geophysical characterization studies of sandstone aquifers have mostly focused on the first 150 m below the ground surface, providing information on the effects of bedding parallel fractures and faults on water flow (Runkel et al., 2006; Hitchmough et al., 2008; Gellasch et al., 2013; Lo et al., 2014). Several petro-hydraulic studies conducted on sandstone lithotypes (including fluvial deposits) have been undertaken on successions at depths > ~1000 m using data from hydrocarbon fields (e.g., Zhang et al., 2000; Baas et al., 2007; Corbett et al., 2012). Thus, multi-disciplinary studies that investigate the permeability and upscaling properties of fluvial aquifers (and sandstone aquifers more generally) are lacking for successions at depths of investigation of 150 m - 1100 m BGL.

This research investigates a specific fluvial aquifer, the Triassic St Bees Sandstone Formation, Cumbria, UK (Figure 5.1a), which has been the object of several studies of sedimentary heterogeneities (e.g., Jones and Ambrose, 1994). The St Bees Sandstone Formation is well-suited to the study of aquifer heterogeneities since it accumulated in the rapidly subsiding (210 m/Myr) eastern Irish Sea Basin (Chadwick et al., 1994; Akhurst et al., 1998). High rates of subsidence allowed accumulation and preservation of fine-grained argillaceous lithotypes (e.g. mudstone) typical of deposition in fluvial overbank settings in response to non-confined flood events (see Chapter 3). Such overbank deposits tend to be preferentially preserved in basins subject to rapid rates of subsidence whereby channel emplacement by avulsion does not fully rework them (Colombera et al., 2013).

Fine-grained fluvial deposits of overbank origin represent potential low-permeability layers that are particularly well preserved in this sedimentary basin. Furthermore, the St Bees Sandstone aquifer is characterized by stratabound-type fractures (*sensu* Odling et al., 1999; Rustichelli et al. 2013, 2016), which are particularly pervasive in this aquifer due to the layered nature of sandstone beds that possess high mechanical resistance (Daw et al., 1974; Bell, 1992). Thus, the St Bees Sandstone aquifer represents an optimum laboratory to test a wide range of aquifer heterogeneities of both tectonic (e.g., vertical joints, normal faults) and sedimentary origin (e.g., mudstone and very fine grained sandstone layers) (Bell, 1992; Jones and Ambrose, 1994; Knott, 1994; Ameen, 1995). Additionally, parts of the St Bees Sandstone aquifer were drilled in the early 1990s to depths ranging from 150 to 1100 m as part of the planning for the proposed Sellafield nuclear waste repository (Appleton, 1993; Michie, 1996). Thus, this area offers the opportunity to re-analyse unpublished hydrogeological data (pumping tests and fluid conductivity and temperature logs), which were acquired during the 1990s. Such data sets can be integrated with hydro-geophysical (flow-logging, acoustic televiewer) and petrophysical data (NMR, permeability tests, SEM, petrographic microscope) aiming to compare plug and field-scale properties.

The aim of the research presented in this chapter is to quantitatively characterize the impact of geological heterogeneities in fluvial aquifer types up to 1100 m BGL. Specific research objectives are as follows: (i) to document the petrophysical properties of features that serve as sedimentary flow heterogeneities in the St Bees Sandstone aquifer; (ii) to constrain the role of burial history on the physical properties of the aquifer; and (iii) to identify the respective roles of matrix, bedding plane-fractures and other tectonic structures (stratabound joints and faults) on conducting flow at a range of scales (plug vs. well-test scale) and depths (up to 1100 m BGL) under pumped conditions; and (iv) to determine and interpret horizontal and vertical permeability anisotropy (K_h/K_v) values occurring in this fluvial aquifer type at both plug and well-test scales.

5.3 Hydrogeological setting

The Sherwood Sandstone Group (Lower Triassic) is a continental succession that has long been ascribed to a mixed fluvial and aeolian origin (e.g., Thompson, 1970; Turner, 1981; Mountney and Thompson; 2002; Tellam and Barker, 2006). This sandstone-dominated succession represents the UK's second most important aquifer in terms of abstraction volumes (Binley et al., 2002; Smedley and Edmunds, 2002; Bricker et al., 2012; Abesser and Lewis, 2015). Contamination has been detected in the aquifer due to agricultural activity, and the release of industrial waste and sewage in urban areas (Barrett et al., 1999; Bloomfield et al., 2001; Bottrell et al., 2008; Lawrence et al., 2006; Zhang and Hiscock, 2010, 2011; Rivett et al., 2012; Cassidy et al., 2014)**.** Also, the Sherwood Sandstone Group hosts important hydrocarbon resources on-shore in Dorset (~1500 m BGL), as well as in the Irish Sea and in the North Sea (McKie and Williams, 2009; McKie and Shannon, 2011).

The Sherwood Sandstone Group of West Cumbria was deposited on the edge of the eastern Irish Sea Basin, which itself represents a rift basin bounded at its margin by extensional faults that divide it from the Lake-

District palaeo-horst (Figure 5.1b). In this region, the Sherwood Sandstone Group attains a typical thickness of 1300 m (Nirex, 1993a, 1997) and is formally divided into three different formations: the St Bees, Calder and Ormskirk Sandstone formations (Barnes et al., 1994; Holliday et al., 2008). The study area is located in the St Bees-Sellafield area in NW England (Figure 5.1). Here, the St Bees Sandstone aquifer is covered by glacial Quaternary deposits, which are characterized by an interbedded succession of clays, silts, sands and gravels (McMillan et al., 2000; Merritt and Auton, 2000). Aquifer recharge mostly arises from streams (Calder and Ehin rivers) which run off the relatively impermeable rocks of the Lake District Massif to the east (McMillan et al., 2000). For this study, the shallow (<150 m BGL) hydro-geophysical characterization of the St Bees Sandstone aquifer has been undertaken in the northern sector of the study area, whereas hydro-geophysical data of the deep St Bees Sandstone aquifer (200-1100 m BGL) are from the southern Sellafield area (Figure 5.1b, c). Here, a deep geological repository was planned during the 1990s and a series of boreholes were drilled between fault-bounded blocks of the rift basin in the east, and the coastline to the west (Sutton, 1996). The combination of the westward dip of the beds (5°-20°) and down-throw associated with normal faulting places the St Bees Sandstone aquifer at greater depths, beneath increasing thicknesses of the overlying Calder and Ormskirk Sandstone formations, towards the west (Figure 5.1b).

The St Bees Sandstone aquifer is dominated by fine- to medium-grained sandstone of fluvial origin that passes upwards into the overlying aeolian-dominated succession (Jones and Ambrose, 1994; Holliday et al., 2008). The Brockram Formation, which consists of low permeability deposits of Permian age (conglomerate with a silty matrix, evaporites and shale) underlies the St Bees Sandstone aquifer forming an acquiclude unit (Allen et al., 1997; Streetly et al., 2000).

The St Bees Sandstone Formation is characterized by fluvial deposits of a braided-fluvial system (Jones and Ambrose 1994). The St Bees Sandstone Formation is divided into two members: the North Head and the overlying

South Head members (see Chapter 3). The two members are differentiated based on the abundance of fine-grained mudstone layers that range in grain size from clay to coarse silt (Jones and Ambrose, 1994; Nirex, 1997). The basal 35 m of the lower North Head Member is characterized by an alternation of fine-grained sandstone and mudstone beds. This basal aquifer passes upward into a succession dominated by sandstone, with mudstone interlayers representing only 25% and 5% of the overall succession in the upper North Head and South Head members, respectively (Barnes et al., 1994; Jones and Ambrose, 1994; Nirex, 1997). Tectonic heterogeneities, which characterize the UK Sherwood Sandstone Group both where it is of fluvial and aeolian origin, are represented by extensional faults and vertical joints in West Cumbria (Chadwick, 1997; Allen et al., 1998). Bed-bound vertical joints form a pervasive fracturing network; the joints terminate against bedding-parallel fractures. Locally, normal faults, complicate the fracturing pattern; such faults are characterized by higher occurrence of open fractures with respect to granulation seams in the fluvial deposits of the St Bees Sandstone Formation with respect to the aeolian Calder and Ormskirk Sandstone formations (Knott, 1994).

Deposits of the Sherwood Sandstone Group across the UK yield typical matrix porosity values of 15 to 30% and matrix hydraulic conductivity values of 0.1 - 8.0 m/day (e.g., Allen et al., 1997; Bloomfield et al., 2006; Pokar et al., 2006). However, the St Bees Sandstone Formation shows relatively low porosity (ϕ_{median}=15.0%) and plug-scale permeability (K_{median}=9.0×10^{-3} m/day) values compared to the entire Sherwood Sandstone Group. The St Bees Sandstone Formation in the southern part of the Egremont-Sellafield plain is overlain by the aeolian deposits of the Calder and Ormskirk Sandstone formations which are more porous (ϕ_{median}=19.5%) and permeable (K_{median}=4.0×10^{-2} m/day). Wireline logs in the Triassic reservoirs of the Irish and North Sea off-shore areas confirm that the rock matrix is more porous and permeable in these aeolian deposits than in the fluvial facies (Ambrose et al., 2014: Olivarious et al., 2015).

Historically, pumping tests undertaken at shallow (<150 m BGL) depths yield relatively high transmissivity values throughout the St Bees-Sellafield coastal plain (Figure 5.1) in both wells penetrating the fluvial (T=30-700 m^2/day) and aeolian (T=100-220 m^2/day) deposits (Allen et al., 1997). Pumping tests were also undertaken at greater depth (200 to 400 m BGL; Streetley et al., 2000) in the fluvial St Bees Sandstone aquifer. In this work hydro-geophysical data from the St Bees Sandstone fluvial aquifer at up to 1100 m BGL will also be considered, in order to achieve a better understanding of the mechanisms that control hydraulic conductivity with depth.
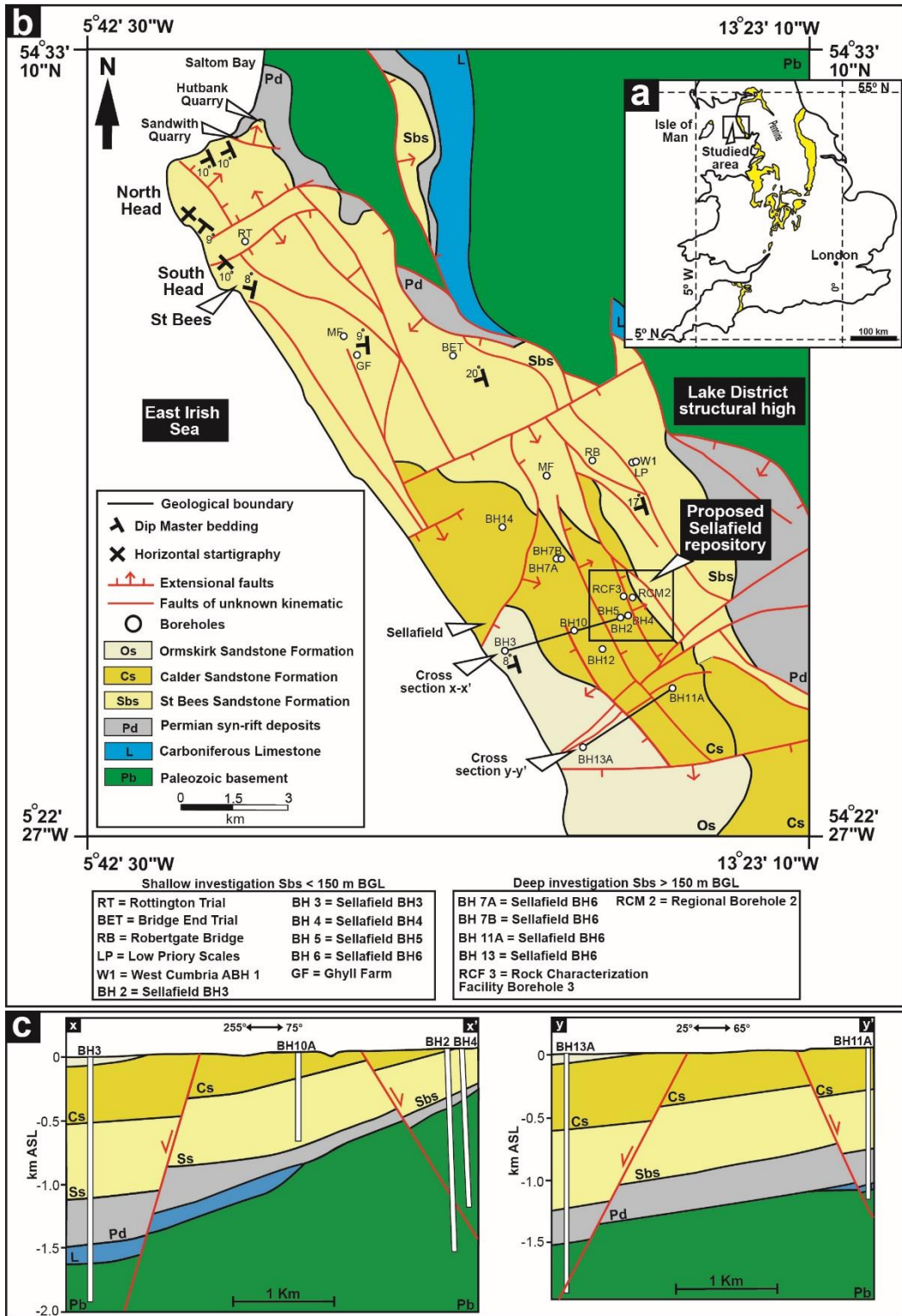
Figure 5.1: Study area. (a) Sherwood Sandstone Group in England, (b) Geological Map of West Cumbria in the St Bees-Sellafield area showing wells referred to in this study, (c) Geological cross-sections of the study area (Redrawn from British Geological Survey, 2016).

5.4 Methods

The St Bees Sandstone aquifer from outcrop (Figure 5.2) up to 1100 m BGL has been investigated in this work at both plug and field scale. Plug-scale petrophysical analysis (petrographic microscope, scanning electron microscope with EDX, NMR, porosity and permeability tests), field-scale pumping tests, televiewer, static (calliper, gamma-ray, neutron porosity) and fluid (temperature, conductivity and flow velocity) logs were analysed, the aim being to characterize the upscaling properties of this fluvial aquifer-type.

5.4.1 Plug-scale petro-hydraulic characterization

Twenty-two core plugs from the St Bees Sandstone Formation of the eastern Irish Sea Basin were obtained from outcrops at South Head cliff, Sandwith and Hutbank quarries (Figure 5.1; Table 5.1). These plugs were characterized for porosity, permeability, nuclear magnetic resonance (NMR) response, and using petrographic microscope and SEM analyses. Plugs of cylindrical shape (diameter = 18 mm; length = 60 mm) were first tested for permeability. Next, porosity was calculated using the liquid saturation method based on Archimedes' principle and then NMR analysis was realised. Water of composition representative of the Sherwood Sandstone aquifer groundwater was synthetized in laboratory (pH = 7.7; Salinity = 67 µS/m; Lewin et al., 1994) and was used to clean plugs prior to porosity and permeability measurements.

A constant flow-rate permeameter equipped with a pressure transducer was used to measure saturated hydraulic conductivity on cylindrical plugs cored in orientations both parallel and perpendicular to the bedding (Table 5.1). Differential pressures used for permeability tests ranged from 0.1 up to 30 kPa. NMR tests were realised providing both total porosity and T_2 (transverse relaxation time) distribution (Hussein et al., 2011; Megawati et al., 2012). NMR measurements were made using a Resonance Instruments MARAN 2 spectrometer at ambient pressure and 34 °C at a proton resonance frequency of 2.2 MHz. The T_2 relaxation curves were

measured by using a repetition time of 10 s, the number of echoes set to 8000, inter-echo spacing of 200 µs, the number of scans set to 100 and receiver gain set to 65. Finally, polished blocks and petrographic thin sections were prepared from core plugs which were previously tested for NMR, porosity and permeability analyses. The petrographic microscope was coupled with the X-ray energy histograms from the energy dispersive spectrometry (EDX) of the scanning electron microscope (SEM) to detect mineralogical species. Additionally, petrographic microscope and SEM images were studied to constrain plug-scale sedimentary heterogeneities. Laboratory tests undertaken in this work were also compared with plug-scale permeability measurements on St Bees Sandstone aquifer from the literature (Tables 5.2, 5.3; see references therein).

5.4.2 Field-scale hydro-geophysical characterization

Historical single-borehole pumping test data from the studied wells have been re-analysed using the ESI AquiferWin32 V.5 software package to obtain reliable transmissivity values from single-borehole pumping tests from both the shallow aquifer (<150 m BGL; Bridge End Trial, Rottington Trial, West Cumbria ABH 1; all UK Environment Agency groundwater monitoring wells) and the deep aquifer beneath the Calder and Ormskirk Sandstone formations (150-1100 m BGL, conducted in deep Sellafield boreholes BH2 and BH3). Transmissivity values were converted into mean field-scale hydraulic conductivity by dividing by well-screen length; this assumes sub-horizontal flow. This assumption is reasonable given the layered nature of the aquifer ($K_h > K_v$ at the field scale, Streetly et al. 2000). Additionally, calliper and acoustic televiewer logs have been analysed in the five wells in the shallow aquifer to acquire information on fracturing pattern and lithology (similar information was obtained from the BGS archived core logs for the Sellafield deep wells). Step pumping tests in West Cumbria ABH1, Rottington Trial and Bridge End Trial wells have been analysed using the Eden and Hazel (1973) step-test analysis methodology, which determines transmissivity from single-borehole tests in confined aquifers. Step test analysis has been preferred to analysis of the available constant flow rate tests in Bridge and Trial, Rottington Trial and West

Cumbria ABH 1, since the former takes into account well-loss correction (Eden and Hazel, 1973; Clark, 1977; Mathias et al., 2008; 2010; Houben, 2015). However, aquifer transmissivities have also been computed using the Theis (1935) methodology where data relating to recovery phase (or pressure build-up) associated with constant flow-rate tests are available, as is the case for the deep Sellafield borehole well tests (BH2 l, BH2 s, BH3 l, BH3 s; the letters l and s stand for the long and short interval tests conducted in these wells, see Table 5.4 for details).

Acoustic televiewer logs (Advanced Logic Technology QL40 mk5), calliper and conductivity and temperature fluid logs (pumped conditions sampling fluid each centimetre) have been realised in the shallow St Bees Sandstone aquifer by European Geophysical Services Limited (Shrewsbury, UK) in Rottington Trial borehole. Flow velocity was logged in Rottington Trial borehole while pumping water from ~15 m below the water table at 72 m^3/day, using an impeller flow-meter (Geovista mk2).

Flow-log analyses aimed to determine the hydraulic conductivity (k_i) of each identified hydraulic layer i, with thickness (Δz_i) from the computed partial transmissivity (T_i) using equation (1),

$$T_i = k_i \times \Delta z_i \tag{1}$$

A quantitative methodology has been used to analyse flow meter data in the Rottington Trial borehole to determine partial transmissivity (T_i) by combining overall well transmissivity values derived from the Eden and Hazel (1973) analysis with fluid velocity logs. Day-Lewis et al. (2011) provides a computer program for the latter model, called "Flow-Log Analysis of Single Holes (FLASH)". This program is based on the multi-layer Thiem (1906) equation (2), which describes confined radial flow in both ambient and stressed flow conditions,

$$Q_i = \frac{2\pi T_i(h_w - h_i)}{\ln(r_0/r_w)} \tag{2}$$

where Q_i is the volumetric flow into or out of the well from layer i; h_w and h_i are, respectively, the hydraulic head in the well (which has radius r_w) and in the far-field at r_0 (the radius of influence); T_i is the transmissivity of layer i. The FLASH program has an optimizing calibration method which minimize difference between data and model misfit. The model misfit is generated based on the differences (h_w-h_i) between the water level in the borehole (h_w) under pumped and ambient conditions and the far-field heads (h_i).

Drawdowns in the wells between pumped and ambient conditions are assumed to represent aquifer drawdowns; head losses between the well and the aquifer (skin effects, wells losses) are assumed to be small. Additionally, the FLASH program requires information concerning well construction (top and bottom elevations of open section, well diameter), depth of the water table and an estimate of the radius of influence of pumping (r_0=80 m, in the Rottington Trial borehole)[4].

Core logs, calliper, gamma-ray, neutron porosity, pumping tests, fluid conductivity and temperature logs (pumped conditions, sampling fluid every 0.15 m) in the deep confined St Bees Sandstone intercepted by Sellafield BH2 and 3 were provided by the British Geological Survey; these data were originally acquired by Schlumberger during the 1990s.

---

[4] Radius of influence for the entire pumped interval was found using the transient flow equation assuming a storativity value of 2×10^{-4} (Allen et al., 1997) and water that has been pumped for a period of 40 minutes. Radius of influence 80 m in Rottington Trial, although the FLASH program is strongly insensitive to r_0 since this parameter appears inside the logarithm of equation (2).

5.4.3 Upscaling hydraulic conductivity

Transmissivity values from short screen well tests (<25 m; BH2 s, BH3 s) from the deep St Bees Sandstone aquifer were compared with upscaled values derived from hydraulic conductivities from cored plugs from the same interval. The horizontal hydraulic conductivity from sandstone plugs was upscaled using the geometric mean of the plug values and the screen length to give screened interval transmissivity. Flow in this upscaling approach is assumed bed-parallel and sub-horizontal due to the shallow dip and layered nature of the aquifer (the dip of the beds is 17° and 8° for BH2 b and BH3 b, respectively). Geometric and harmonic means are typically used for upscaling of hydraulic conductivity in heterogeneous sandstone aquifers and hydrocarbon reservoirs (Chen et al., 2003; Jackson et al., 2003). We used the geometric mean in this work as it represents the sensitivity of bedding-parallel flow to layer permeability variation (Zheng et al., 2000).

5.4.4 Derivative analysis

The recovery phase from pumping tests in Bridge End Trial, Rottington Trial, West Cumbria ABH 1 and the deep Sellafield boreholes (BH2l, BH2s, BH3l and BH3s) wells have been studied calculating the first derivative with respect to time (ds/dt) using the ESI AquiferWin32 V.5 software package (first derivative computation followed Span and Wurster, 1993). This approach finds ds/dt through least-squares regression using specific values of abscissal length L (which represents the chosen derivation interval on the horizontal axis) and was chosen equal to 0.5 minutes here, to smooth noise. Derivative analysis of the recovery phase was preferred to the drawdown phase, since the former is not affected by variations in flow rates induced by the pump that typically introduce noise, which is then amplified in the numerical differentiation (Renard et al., 2009).

5.5 Results: plug-scale properties of fluvial deposits

5.5.1 Palaeoenvironmental significance of plugs

Twenty-two plugs from outcropping St Bees Sandstone Formation (Figure 5.1) have been tested for porosity, permeability and T_2 distribution. These same plugs have then been the object of SEM and petrographic microscope analysis aiming to define their micro-heterogeneities and mineralogical composition. The 22 plugs that have been tested cover a range of lithologies with different palaeoenvironmental significance. Where possible, plugs have been cored along directions both parallel and perpendicular to bedding (Table 5.1). Previous sedimentological analyses of the St Bees Sandstone Formation in the study area (Jones and Ambrose, 1994) link the tested plugs to architectural elements and lithofacies related to specific palaeoenvironments (e.g., floodplain, channel-fills). Twelve plugs coded 1 to 6 (including 6 cored horizontally and 6 cored vertically) have been grouped in a single sedimentary unit which has been named red-channel sandstone (Urs; Figure 5.2a-d). This sedimentary unit is red in colour and is characterized by medium grain size, medium to well sorted sandstone (Urs). These 12 plugs characterize both cross-bedded (planar and sigmoidal) and horizontally laminated sandstone representing the preserved deposits of sandy barforms deposited under lower and upper flow regime, respectively (Table 5.1). Plugs coded 7 and 8 are representative of white in-channel drapes (Uws) that overlie bedform deposits during episodes of low-flow stage. Additionally, this white-channel sandstone (Uws) shows mud-cracks which indicate periods of sub-aerial exposure and drying (Uws, Figure 5.2d, e). The occurrence of well-developed thin laminations and mud-cracks created a strong mechanical anisotropy and samples disintegrated during coring parallel to laminations. Eight plugs coded 9 to 12 (including 4 cored horizontally and 4 cored vertically) were tested from sheet-like sandstone interpreted to have been deposited by non-confined flood events in a floodplain environment (Ush, Figure 5.2c; Table 5.1). All 22 plugs analysed in this work have been compared with previous published porosity and plug-scale permeability

tests that have been realised on the St Bees Sandstone aquifer as part of the planning for the Sellafield nuclear waste repository (Nirex, 1992a, 1992c, 1993b, 1993c; Allen, 1997). This comparison with published literature allowed us to enlarge the database used for statistical analyses of porosity-permeability data to include that relating to floodplain mudstone (i.e. fluvial overbank) origin (Figure 5.2a, Um), as well as for interbedded fluvial channel and mudstone elements (Figure 5.2b, Umi). The mudstone deposits (Um, Umi) are related to non-confined flood events and were deposited from suspension when flow velocity progressively waned to zero (cf., Hampton and Horton, 2007; Ghazi and Mountney, 2011; Banham and Mountney, 2014).
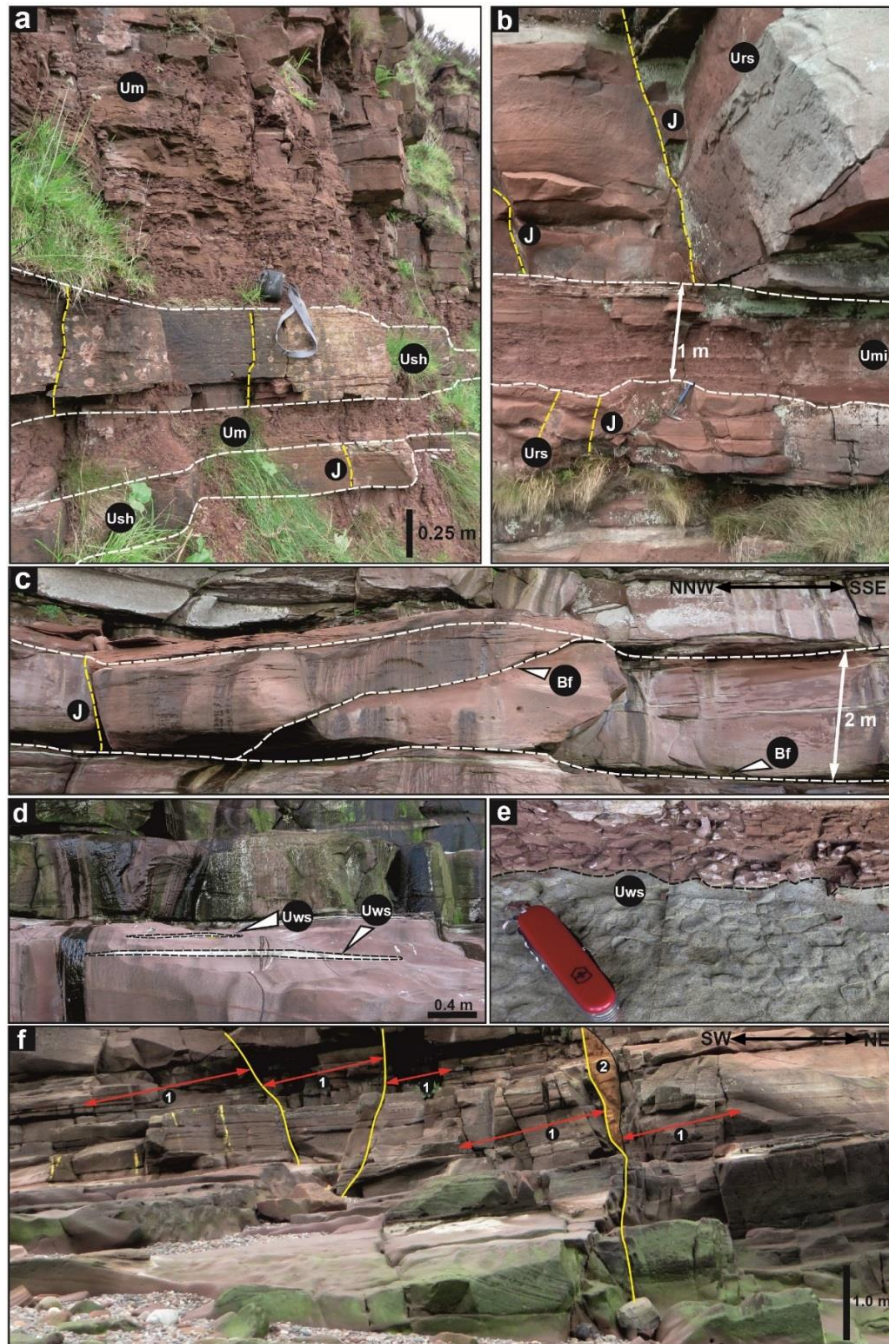
Figure 5.2: St Bees Sandstone Formation. (a) Lower North Head Member at Saltom Bay showing the basal alternation of sheet-like sandstone (Ush) and mudstone beds (Um) with vertical stratabound joints (J) occurring in the sandstone lithology, (b) Mudstone (Umi) interlayered in the red-channelized sandstone (Urs) showing vertical stratabound joints (J), (**c**) Outcrop expression of the amalgamated-channels of the South Head Member showing bedding-plane fractures (Bf) and vertical stratabound joints (J), (d) White-channel sandstone (Uws) layers which laterally extend ~ 2.5 meters, (**e**) Plan view of desiccation cracks in the white-channel sandstone (Uws), (f) Normal faults at South Head dominated by damage zones with open fractures (1) and non- continuous fault core (2).

5.5.2 SEM and Optical microscope analysis

SEM and optical microscope images (Figures 5.3 a-f, 5.4a-f) realised on three different sandstone units show how the sheet-like (Ush) and the white-channel (Uws) sandstones are characterized by a fine-grained sand, whereas the red-channel sandstone (Urs) is medium-grained sandstone. SEM and optical microscope (Figures 5.3, 5.4, 5.5a-c) analyses show how all the three analysed lithofacies (Urs, Ush, Uws) are characterized by quartzo-feldspathic sandstone (quartz 50-60%; feldspar 10-15%; other grains 25-40%). Quartz represents the main mineralogical component, followed by K-feldspar, plagioclase, biotite, muscovite and chlorite. Other minerals identified include hematite and titanite.

Energy-dispersive X-ray spectroscopy (EDX) analysis realized on red-channel (Urs) and sheet-like sandstone (Ush) and white-channel sandstone (Uws) reveal a systematic difference of cement composition between the two reddish sedimentary units (Urs, Ush) and the white sandstone (Uws). The cement (type-1) of the white-silty drape sandstone (Uws) is quarzo-feldspathic (96-100 wt%) and characterized by paucity or absence of hematite (0-2wt%) and calcite (0-2wt%). Although quartz and feldspars (80-95 wt%) also represent the main cement components in the sheet-like sandstone (Ush) and the red-channel sandstone (Urs), these units are typically characterized by a cement (type-2) with significant hematite component (5-20 wt%) and paucity or absence of calcite (0-1.5 wt%).

Optical microscope analyses show that samples of sheet-like (Ush) and white-channel (Uws) sandstones are characterized by a repetitive alternation of laminae of different grain and pore sizes which are 200 up to 500 μm thick (Figure 5.4c, d, f). Coarser grained laminations are characterized by larger pores (Figure 5.4c, d). Thin sections in the white-channel sandstone (Uws) show absence of pores with diameter > 150 μm since these pores are partially or completely filled by cement (Figure 5.3c, d). By contrast, relatively larger pores (>150 μm) are present in the sheet-like and red-channel sandstones and their dimension increases moving

from the sheet-like (Ush) to the red-channelized (Urs) sandstone (Figure 5.5b, c). Macro-pores show maximum diameter up 180 and 250 µm in sheet-sandstone and red-channel sandstone, respectively (Figures 5.4f; 5.5b-c). However, preferential orientation of platy minerals (biotite, muscovite, chlorite) parallel to bedding is systematically detectable at the microscopic scale in all the three sedimentary units (Figures 5.4c, e; 5.5a, e, f; Urs, Uws, Ush). This is because quartz grains of ellipsoid shape and mud-clasts are also oriented parallel to the bedding laminations in all the studied lithofacies.

Pores show a typical triangular shape in the white-channel sandstone (Uws). However, elliptical sections are the most common pore outline in the sheet-like sandstone (Ush) although this lithology also commonly shows triangular shape-type pores. The red-channel (Urs) sandstone is characterized by ellipsoid and coalescent pores of irregular shape. Thus, the shape of pores changes from triangular, to ellipsoid, to irregular with increasing pore dimension and connectivity (Figure 5.5a-c).
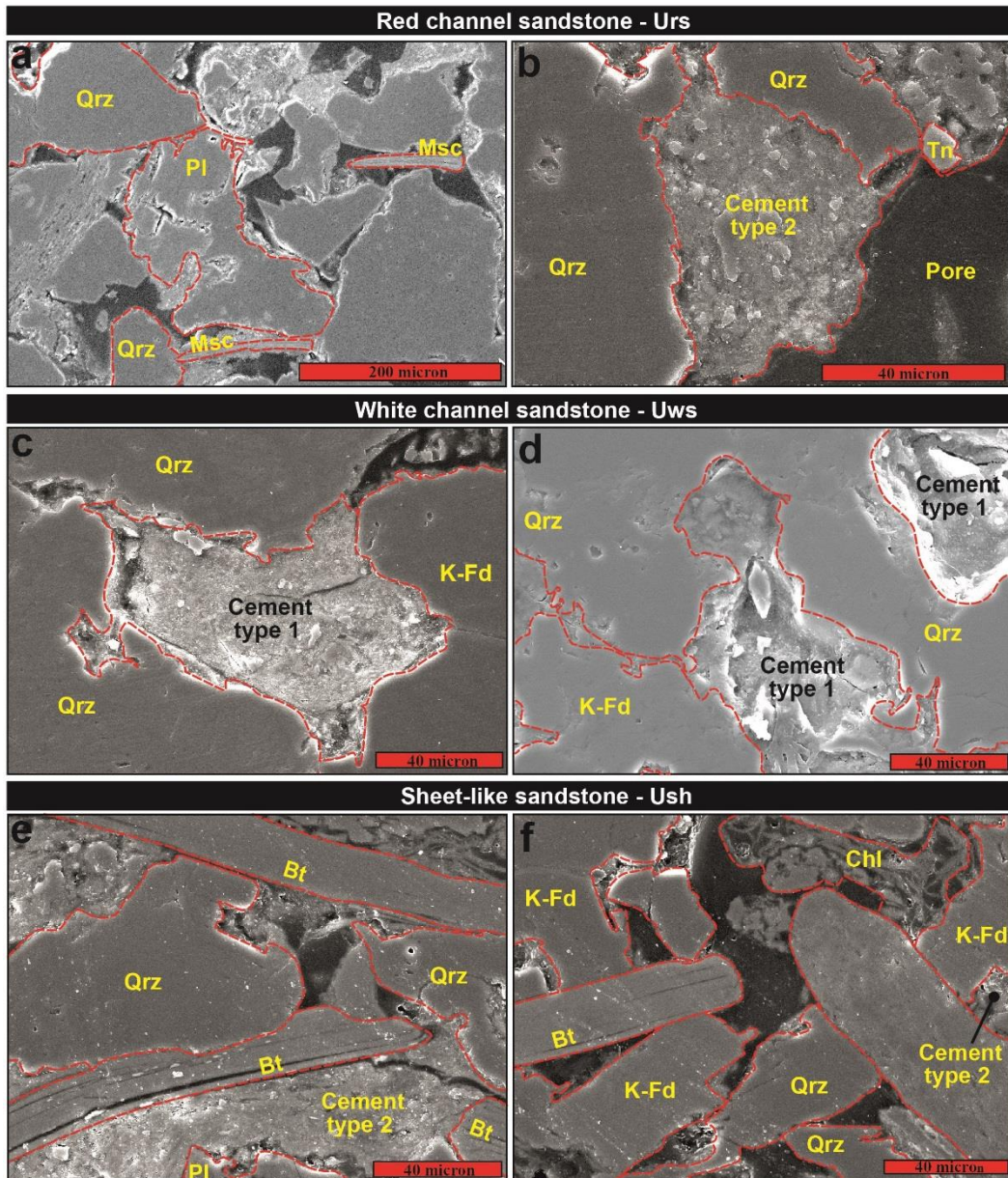
Figure 5.3: SEM images from the St Bees Sandstone Formation. (a) Quartz (Qrz), plagioclase (Pl) and muscovite (Msc) grains elongated parallel to the bedding in red-channel sandstone, (b) Quartz (Qrz) and titanite (Tn) grains and a large pore partially filled by cement-type 2 in red-channel sandstone, (c) Quartz (Qrz) and K-feldspar (K-Fd) and cement-type 1 which fills pores in white-channel sandstone, (d) Quartz (Qrz), K-feldspar (K-Fd) grains and cement-type 1 completely filling pores in white-channel sandstone, (e) Floodplain sheet-like sandstone: biotite (Bt) grains are elongated parallel to the sedimentary laminations, quartz (Qrz), plagioclase (Pl) and cement-type 2 were confirmed by EDX analysis, (f) Floodplain sheet-like sandstone: biotite (Bt) and chlorite (Chl) grains are elongated parallel to the sedimentary laminations, quartz (Qrz), K-feldspar (K-Fd) and cement-type 2 were also detected by EDX analysis.
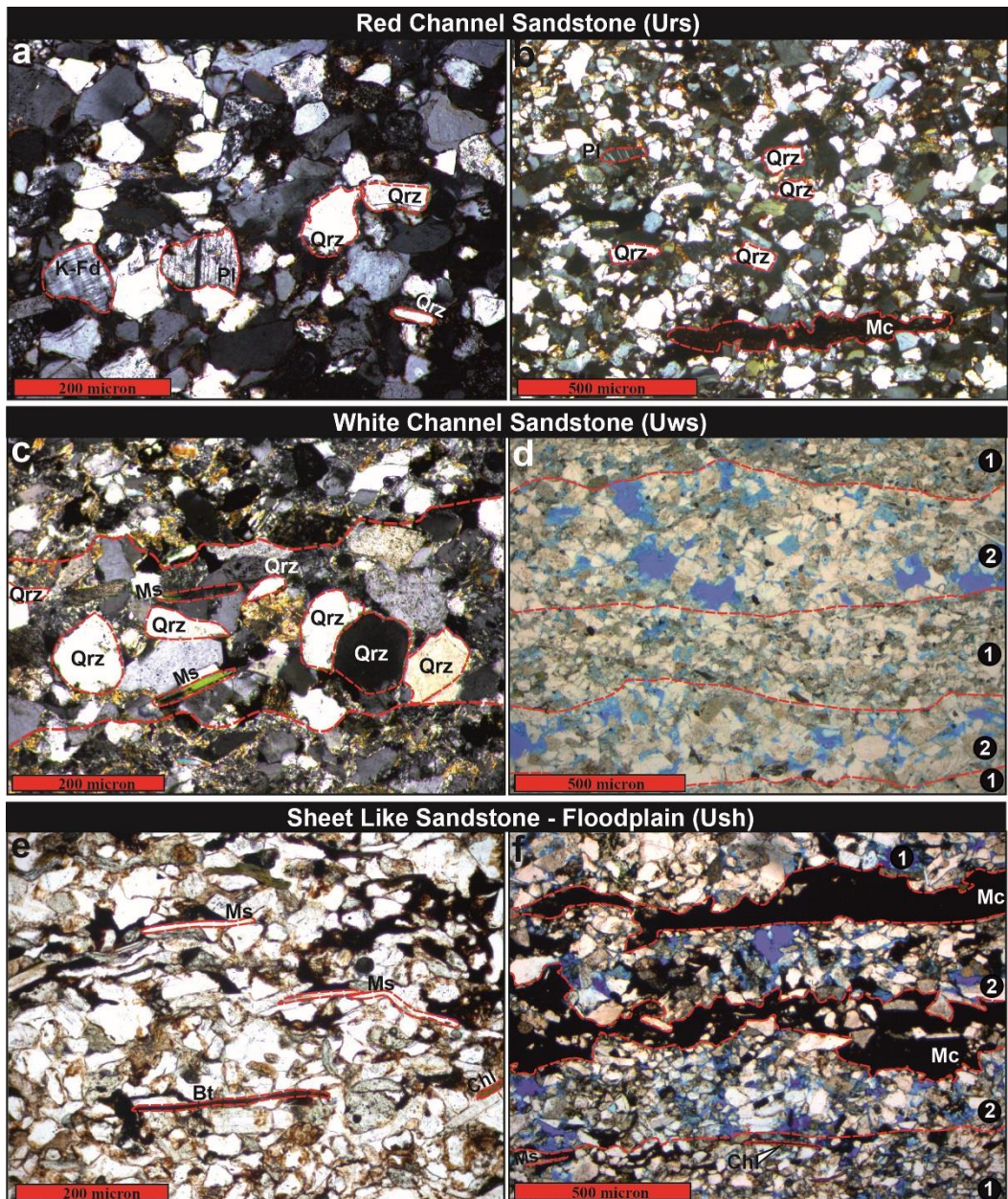
Figure 5.4: Petrographic optical microscope images from the St Bees Sandstone Formation (a, c, e, cross polarised light; b, d, f plane polarised light). (a) Quartz (Qrz), plagioclase (Pl) and K-feldspar (K-Fd) grains in a medium grained channel sandstone, (b) Quartz (Qrz) and plagioclase (Pl) ellipsoid grains and mud clasts (Mc) elongated parallel to the bedding in red-channel sandstone, (c) Coarse grained lamination with Quartz (Qrz) and muscovite (Ms) in white channel-sandstone, (d) White-channel sandstone with blue dye showing alternation of (1) fine-grained, low porosity laminae and (2) coarse grained laminae, (e) White-channel sandstone showing preferential orientation of muscovite, biotite and chlorite parallel to the bedding, (f) White-channel sandstone with blue dye showing mud-clasts elongated parallel to the bedding and alternation of (1) fine-grained, low porosity laminae and (2) coarse grained laminae.

5.5.3 Petrophysical analysis

Petrophysical measurements on 22 plugs from the St Bees Sandstone Formation included measurements of hydraulic conductivity, porosity and T_2 distribution. Total porosity of samples has been calculated both with the Archimedes (9.7-22.9%) and NMR (8.4-21.0%) methodologies (Table 5.1). NMR porosity yields values from equal to 18% lower than Archimedes measurements. Archimedes porosity provides more reliable values than NMR porosity for the St Bees Sandstone Formation due to presence of mineral species with high magnetic susceptibilities[5]. Archimedes porosity (Table 5.1) increases moving from the white-channel (9.7-11.3%) to the sheet-like sandstone (15.9-17.6%) up to the red-channel sandstone (19.1-22.9%). Wireline logs which were previously realised in the West Cumbrian St Bees Sandstone (see Chapter 4) confirm the contrast in porosity between the red-channel sandstone (Urs) that makes up the bulk of the rock and the thin white-silty drape sandstone (Uws) since lower neutron porosity values typically characterize the latter lithotype.

Hydraulic conductivity values measured on rock samples of the St Bees Sandstone Formation show values that range over five orders of magnitude (K_h=6.81×10^{-3}-3.65×10^{0} m/day; K_v=3.33×10^{-4}-3.70×10^{-1} m/day) and anisotropy values (K_h/K_v) that range from 1.5 to 30.0 (Table 5.1). Note, K_h values are not available for the white channel sandstones since samples disintegrated (samples 7h and 8h in Table 5.1). Optical microscope and SEM (Figures 5.3, 5.4) observations reveal how this anisotropy is related to (i) presence of finer-grained laminations characterized by small and low connectivity pores and (ii) preferential orientations of mud-clasts, platy (muscovite, biotite, chlorite) and ellipsoid mineral grains (quartz). The microscope optical images illustrate the origin of the relatively higher

---

[5] Presence of paramagnetic ions in iron-bearing minerals (e.g., hematite) represent an important factor influencing T_2 measurements. Paramagnetic ions increase the rate of relaxation of the hydrogen proton, consequently reducing T_2 values (Dodge et al., 1995). Additionally, chlorite, muscovite and biotite have large surface area and elevated magnetic susceptibilities, leading to large magnetic field gradients and low T_2 values (Morris et al., 1997; Hossain et al., 2011).

anisotropy values (K_h/K_v=12.0-30.0) for sheet-like sandstone compared to the red-channelized sandstone (K_h/K_v =1.5-8.5).

This contrast arises because the sheet-like sandstone facies (Ush) is characterized by laminations with different grain and pore sizes, whereas the red channelized sandstone facies (Urs) is not, and is therefore more isotropic. Notably, occurrence of well-developed laminations also occurs in the white silty sandstone which also appears strongly anisotropic at the petrographic microscope (Figure 5.4c-d). In fact, these laminations, together with desiccation cracks, form the strong mechanical anisotropy that prevented coring parallel to bedding.

T_2 distributions (Figure 5.5) for the white-channel (Uws), the sheet-like sandstone (Ush) and the red (Urs) channel sandstone are essentially unimodal, i.e. single intensity peaks at ~2, ~16 and ~100 ms, respectively. Also, the modal T_2 values show positive correlation with the plug-scale hydraulic conductivity (Figure 5.6), as reported in other studies of porous media (Bilardo et al., 1991; Hidajat et al, 2002; Lala and El-Sayed, 2015). The hydraulic conductivity ranges for the three sedimentary units are as follows: white-drape sandstone (K_v=3.33×10^{-4}-2.18×10^{-3} m/day); sheet-like sandstone (K_v=3.65×10^{-4}-7.30×10^{-3}; K_h=6.81×10^{-3}-0.22 m/day); red-channel sandstone (K_v=0.29-0.43; K_h=0.44-3.65 m/day). Results also show the same rank order of their peak T_2 values: ~2, ~16, and ~100 ms, respectively. Furthermore, optical images show how these petrophysical groups are characterized by evident different pore sizes which increase moving from white drape sandstone (Uws), to sheet-like sandstone (Ush), to the red-channelized sandstone (Figure 5.5a-c).

Permeability, pore-size and T_2 distribution in the St Bees Sandstone are therefore closely related which is a typical characteristic of siliciclastic rock types (Al-Mahrooqi et al., 2003, 2006; Lala and El-Sayed, 2015). Core plugs show positive correlation between T_2 values and hydraulic conductivity along both the horizontal and the vertical direction (Figure 5.6; Table 5.1). Notably, correlation between T_2 modal values and hydraulic conductivity is somewhat stronger along the horizontal direction (red

symbols in Figure 5.6), probably because the modal T_2 values are more markedly influenced by the larger pores, whereas the smaller pores control the minimum hydraulic conductivity (K_v).
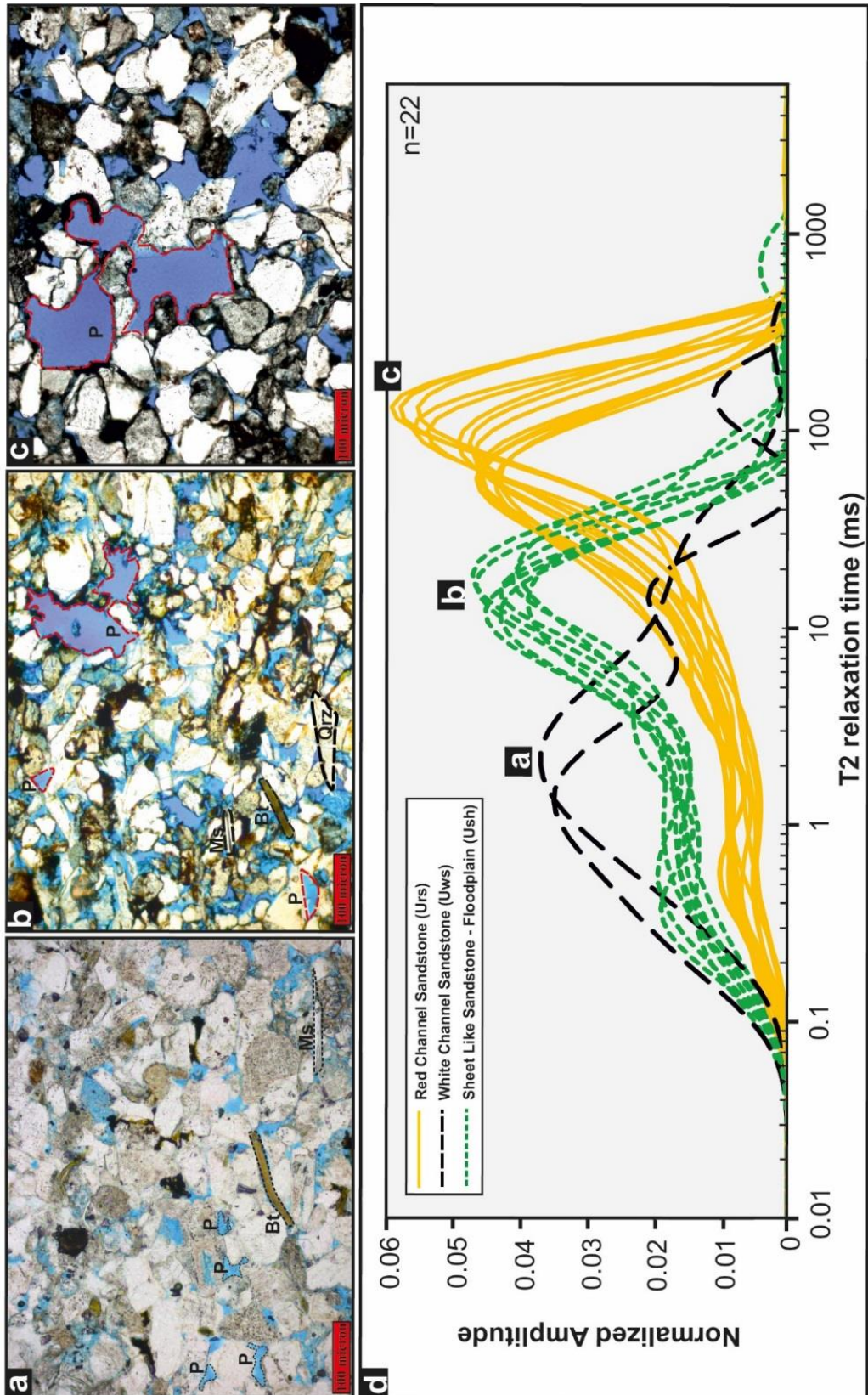
Figure 5.5: Pore size and NMR data from the St Bees Sandstone Formation. (a) White-channel, (b) sheet-like, (c) red-channel sandstone (plane polarized light), (d) T_2 distribution in the three sedimentary units shown.
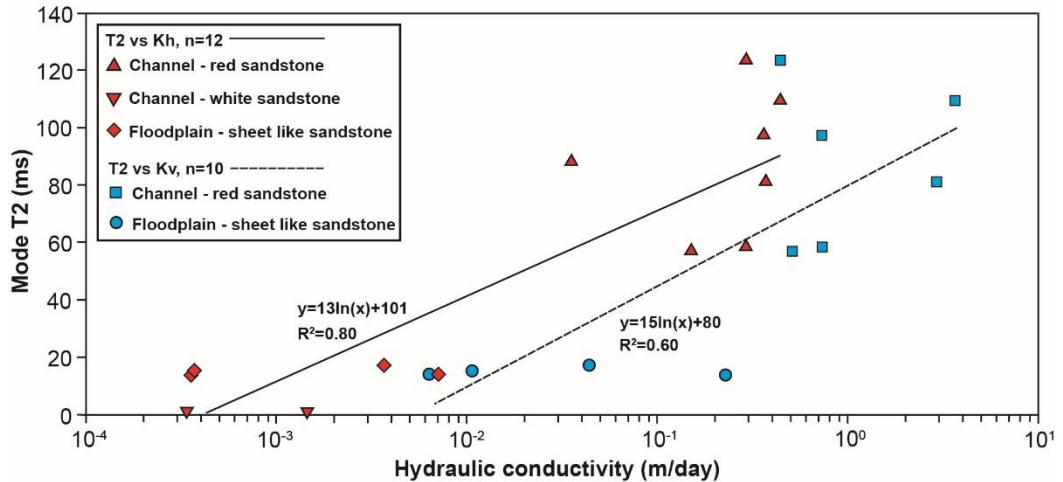
Figure 5.6: Hydraulic conductivity parallel (K_h – red symbols) and perpendicular (K_v- blue symbols) to bedding vs. modal NMR T_2.

5.5.4 Comparison with published literature

Plug-scale hydraulic conductivities measured in this work on outcrops of the St Bees Sandstone Formation in the Saltom Bay to South Head area are here compared with measurements from plugs cored from both shallow boreholes (Robertgate Bridge, Low Priory Scales) in the Egremont area, and deep cores obtained from the Sellafield data archive (see boxed area labelled 'proposed Sellafield repository in Figure 5.1 for locations). Plugs from outcrop were tested using simulated groundwater (67 µS/m). However, plugs from the previous investigations were tested using air; then the Klinkenberg correction was applied to allow comparison (Nirex, 1992a, 1992c, 1993b, 1993c). Porosity and hydraulic conductivity values from outcrop samples tested here and from the previous shallow and deep aquifer investigations are summarized in Figure 5.7 and Tables 5.1 and 5.2.

Table 5.1: Petrophysical values (porosity, permeability) of twenty two plugs from the St Bees Sandstone Formation outcrop.

Sample (plug code)	Sedimentary Lithofacies	Sedimentary unit	Archimede Porosity (%)	NMR Porosity (%)	K_h; K_v (m/day)	Anisotropy (K_h/K_v)
1 (1h; 1v)	Red-channel Sandstone (Urs)	Cross-bedded sandstone with sigmoidal foresets	22.9	21.0	0.73; 0.29	2.5
2 (2h; 2v)		Horizontally laminated sandstone	20.6	18.8	0.51; 0.15	3.5
3 (3h; 3v)		Planar cross-bedded sandstone	21.5	20.1	0.44; 0.29	1.5
4 (4h; 4v)		Horizontally laminated sandstone	21.7	20.7	3.65; 0.43	8.3
5 (5h; 5v)		Horizontally laminated sandstone	20.4	18.4	2.92; 0.37	8.0
6 (6h; 6v)		Planar cross-bedded sandstone	19.1	17.7	0.73; 0.36	2.0
7 (7v)	White-channel Sandstone (Uws)	White sandstone with mud cracks	9.7	8.4	N/A; 3.33×10^{-4}	N/A
8 (8v)		White sandstone with mud cracks	11.3	9.3	N/A; 2.18×10^{-3}	N/A
9 (9h; 9v)	Sheet-like Sandstone (Ush)	Horizontally laminated fine grained sandstone	15.9	13.1	0.22; 7.30×10^{-3}	30.0
10 (10h; 10v)		Horizontally laminated fine grained sandstone	17.6	15.1	4.38×10^{-2}; 3.65×10^{-3}	12.0
11 (11h; 11v)		Horizontally laminated fine grained sandstone	17.1	17.1	6.81×10^{-3}; 3.56×10^{-4}	19.2
12 (12h; 12v)		Horizontally laminated fine grained sandstone	17.3	17.3	1.06×10^{-2}; 3.65×10^{-4}	29.0

Table 5.2: Summary of porosity and plug-scale hydraulic conductivity parallel (K_h) and perpendicular (K_v) to the sedimentary laminations in the St Bees Sandstone aquifer from previous work (borehole core plugs).

Depth Interval (mBGL)	Population	Reference	Porosity range (%)	K_h (m/day)	K_v (m/day)
12 - 92	59	Allen et al., 1997	4.8 - 25.9	1.21-$9.14{\times}10^{-6}$	$0.26 - 4.16{\times}10^{-6}$
70 - 1070	161	Nirex, 1992a, 1992c, 1993b, 1993c	2.1 - 23.0	$0.77 - 4.16{\times}10^{-6}$	$0.71 - 2.49{\times}10^{-6}$

The porosity-permeability characteristics of four distinct sedimentary units are illustrated in Figure 5.7 a-c: red-channel sandstone (Urs), floodplain mudstone (Um), floodplain sandstone (Ush) and mudstone, and mudstone interlayered in channels (Um/Umi). Note that mudstone (Um), which characterizes the floodplain deposits, and mudstone that occurs interbedded with channel deposits (Umi) were not sampled from outcrop. There is broad agreement between matrix permeability values from shallow (up to 150 m) and relatively deep (Sellafield) investigations of the St Bees Sandstone aquifer (Figure 5.7c; Table 5.2). Plug-scale hydraulic conductivities were measured without simulation of overburden pressure; however this is probably unimportant since Daw et al. (1974) demonstrated, using multi-stage triaxial stress experiments, how intergranular plug-scale hydraulic conductivity is only slightly reduced (by 6%) in response to an increase in lithostatic pressure of 7 MPa, representing the overburden pressure at approximately 300 m below the ground surface for this lithology. However, some minor differences are evident: outcrop-derived plugs of channel-sandstone are slightly more porous and permeable than those from borehole cores (Figure 5.7c; Tables 5.1, 5.2); this may be partly an issue of representability, since all 22 measured plugs are sandstone lithotypes and mudstone has not been tested. Despite this, some difference may arise from increased dissolution of carbonate cement (calcite, dolomite) in the unsaturated zone sampled in outcrop. EDX analyses from outcropping samples collected from ~5 to 10

m beneath the Quaternary till cover show a paucity of carbonate cement (<2wt%) with respect to plugs from cores (from 15-100 m BGL) in which calcite and dolomite represent significant cement components (up to 50 wt%) of quartz and K-feldspar cement species (Waugh, 1978; Strong et al., 1994). Also, authors have previously remarked how the UK Sherwood Sandstone Group in the first 10 to 15 m below the Quaternary deposits (of glacial or alluvial origin) is commonly strongly weathered (McMillan et al., 2000; Hough et al., 2006).
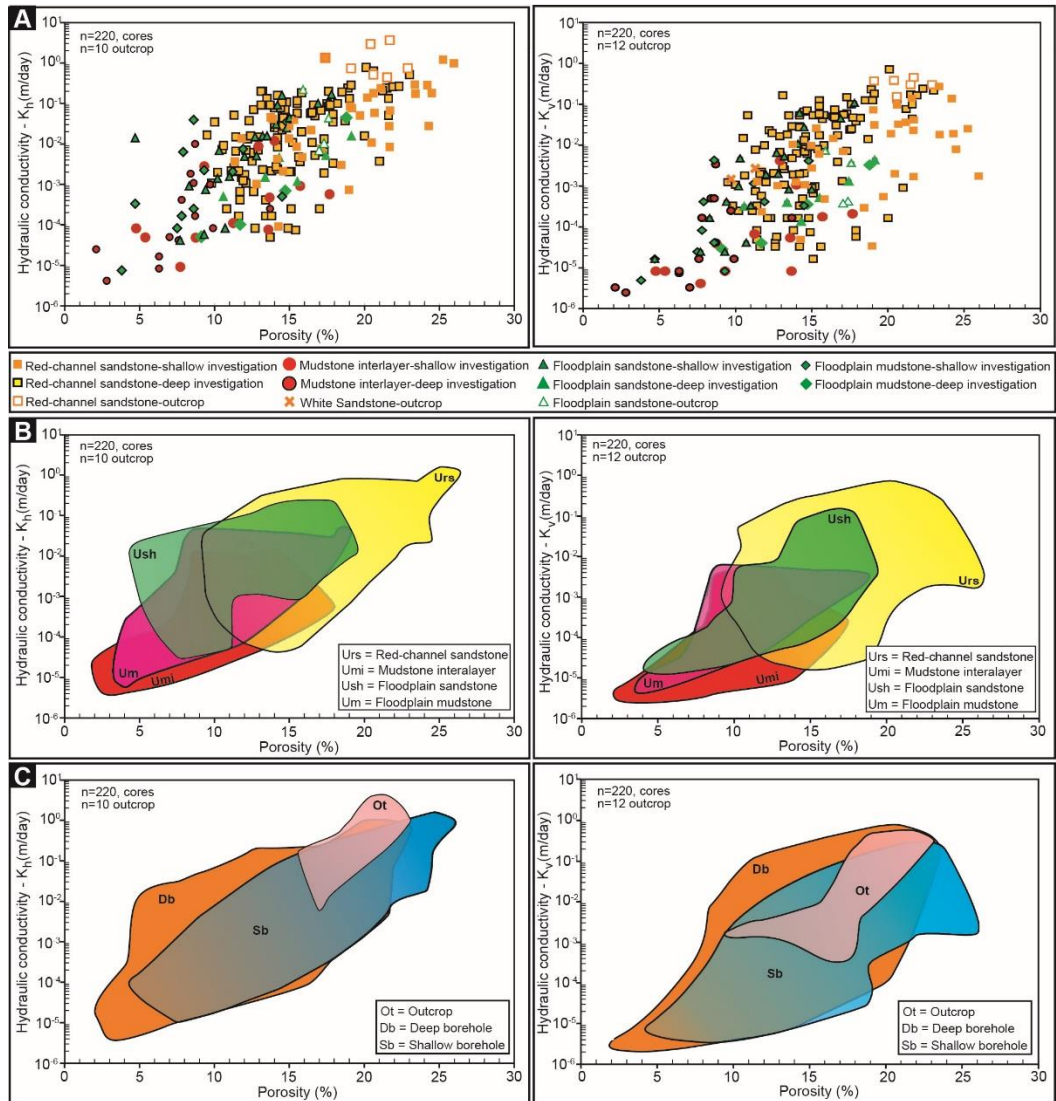
Figure 5.7: Porosity-permeability semi-log plots in the St Bees Sandstone Formation based on core plugs from outcrop (Table 5.1, this study) and boreholes (Tables 5.2-5.3, previous studies): left panels show K_h, right panels K_v. (a) data points distinguishing channel sandstone, mudstone interlayers (interbedded in channel sandstone), floodplain sandstone and floodplain mudstone, (b) Porosity-permeability fields defined by the different sedimentary units, (c) Porosity-permeability fields according to samples from outcrop, shallow and deep boreholes.

5.6 Results: field scale hydraulic properties of fluvial deposits

5.6.1 Shallow aquifer characterization

Single-borehole drawdown and recovery tests have been analysed in the St Bees-Egremont area in the Bridge End Trial (BET), Rottington Trial (RT) and West Cumbria ABH 1 (WCABH1) wells (Figure 5.8 a, Table 5.4), which provide hydraulic information on the shallow (10-120 m BGL) saturated part of the St Bees Sandstone aquifer. These three groundwater monitoring boreholes are characterized by similar lithostratigraphic features since all penetrate both the South and North Head members of the St Bees Sandstone Formation. Transmissivity values obtained (31 m^2/day for BET, 69 m^2/day for RT and 268 m^3/day for WCABH1, see Table 5.4) are typical for the St Bees Sandstone aquifer in West Cumbria at depths shallower than 150 m (see Allen et al. 1997). Indeed, all the transmissivity values that have been previously published (Allen et al., 1997) from the relatively shallow St Bees Sandstone aquifer (<150 m) range from ~10^1 to 10^3 m^2/day (K~10^{-1}-10^1 m/day). Fluid temperature, conductivity and flow velocity logs for Rottington Trial borehole (Figure 5.9, Table 5.5) were measured while pumping at 72 m^3/day from within the well casing. Fluid temperature and conductivity show sharp variation near the bottom of the borehole, representing in-flows. The main in-flow zones correspond with principal bedding fractures, identified in the acoustic log (Figure 5.9 and 5.10). Using the overall pumping test transmissivity (Table 5.4) as a constraint, the flow log was analysed using a method which allows calculation of hydraulic conductivity of individual layers selected by the user (Day-Lewis et al., 2011). Layer hydraulic conductivity values (Figure 5.9; Table 5.5) range up to 2.1 m/day. Additionally, all the conductive flow zones (with the exception of the layer L5 which is characterized by abundant calcite veins seen in the acoustic and optical log, which fill fractures; thereby preventing fracture flow) show hydraulic conductivity values (Table 5.5) which are between one (10^1) and two (10^2) orders of magnitude higher than plug-scale average (geometric mean) core values (Table 5.3) for the channel sandstone (Urs) facies, which represents the main lithology penetrated by the Rottington

Trial well (similar results have been obtained from flow-logging of other wells that penetrate the shallow aquifer as illustrated in Chapter 4). Thus, the comparison of the upscaled plug-matrix hydraulic conductivities with those derived from the pumping test and flow-log/acoustic log analysis indicates that bedding-parallel fractures, rather than the matrix, act as the main pathways for groundwater flow in the shallow St Bees Sandstone aquifer. Additionally, other elements indicate fractures as main flow drivers of water flow. The bottom of the RT well penetrates the North Head Member (Figure 5.9), which is typically more abundant in mudstone interlayers (Jones and Ambrose, 1994). Notably, the L2 flow zone located within the NHM is characterized by the most abundant occurrence of relatively impermeable mudstone beds (Figure 5.9, Table 5.5) but also the most permeable zone, suggesting that the matrix cannot represent the dominant flow pathway.

Table 5.3: Summary of geometric means (GM) of hydraulic conductivity parallel (K_h) and perpendicular (K_v) to the bedding and resulting permeability anisotropy (K_h/K_v) from cored plugs in the St Bees Sandstone aquifer (data from Nirex, 1992a, 1992c, 1993b, 1993c; Allen et al., 1997).

Petrophysical Groups	Population	K_h (m/day)	GM K_h (m/day)	K_v (m/day)	GM K_v (m/day)	GM K_h/K_v
Red Channel Sandstone (Urs)	150	4.99×10^{-5} - 1.21	1.57×10^{-2}	1.66×10^{-5} - 0.72	5.08×10^{-3}	3.1
Mudstone Interbedded with Channel Sandstone (Umi)	27	4.15×10^{-6} - 1.18×10^{-2}	2.14×10^{-4}	2.49×10^{-6} - 4.15×10^{-2}	5.50×10^{-5}	5.0
Sandstone Floodplain (Ush)	27	4.15×10^{-5} - 1.66×10^{-2}	5.01×10^{-3}	1.16×10^{-5} - 1.10×10^{-1}	1.21×10^{-3}	4.1
Mudstone Floodplain (Um)	16	7.50×10^{-6} - 4.44×10^{-2}	9.05×10^{-4}	4.49×10^{-6} - 4.32×10^{-3}	1.54×10^{-4}	5.9

The particularly high hydraulic conductivity (K = 2.1 m/day) of the L2 flow zone may be related to the strongly layered nature of this ~10 m stratigraphic interval which penetrate the upper part of the North Head Member of the St Bees Sandstone Formation. In fact, the L2 zone penetrates several bedding discontinuities (n = 6) localised in correspondence of the contact between sandstone and mudstone deposits. Also, the L2 zone penetrates the junction between a bedding fracture and a stratabound joint which further enhances flow in this highly conductive zone; fluid temperature, conductivity and flow velocity show rapid change at 105 m BGL (Figures 5.9, 5.10) in correspondence with this tectonic structure (a bedding plane fracture connected to a vertical joint, which may be similar, is shown in outcrop in Figure 5.2c).

These stratabound joints establish hydraulic communication between sub-horizontal bedding plane fractures, as suggested by other authors based

on numerical models of stratabound-fracture systems (Odling and Roden, 1997; Hitchmough et al., 2007).

Table 5.4: Hydraulic tests in the St Bees Sandstone including well construction details, flow rates, analysis methodology and derived transmissivity and hydraulic conductivity (K) values (for Sellafield BH2 and BH 3 tests, l and s refer to long and short interval tests, respectively). Field scale K was found from T and screen length, i.e. assuming homogeneity and sub-horizontal flow.

Field Site/Borehole Name	Flow rate, Q (m³day⁻¹)	Borehole Diameter (m)	Top Screen Depth (m)	Screen Length (m)	Transmissivity, T (m²/day)	Field Scale, K (m/day)	Methodology
SHALLOW ST BEES SANDSTONE AQUIFER (< 150 m BGL)							
Bridge End Trial	70, 240,464, 783, 1190, 1400	0.20	8	82	31	0.4	Eden and Hazel (1973)
Rottington Trial	1800	0.20	7	111	69	0.6	Theis (1935)
West Cumbria ABH 1	1100, 1500, 3000, 4000, 6000	0.38	10	38	268	7.0	Eden and Hazel (1973)
INTERMDIATE ST BEES SANDSTONE AQUIFER (> 150 - 400 m BGL)							
Sellafield Borehole 2 test l	94	0.16	154	356	0.70	2.0×10^{-3}	Theis (1935)
Sellafield Borehole 2 test s	29	0.16	200	23	0.53	2.3×10^{-2}	Theis (1935)
DEEP ST BEES SANDSTONE AQUIFER (> 400 - 1100 m BGL)							
Sellafield Borehole 3 test l	234	0.16	672	637	0.41	6.4×10^{-4}	Theis (1935)
Sellafield Borehole 3 test s	10	0.16	931	10	0.04	4.0×10^{-3}	Theis (1935)

Table 5.5: Parameters computed from the FLASH program for Rottington Trial well.

Code zone	Layer bottom depth (m ASL)	T_{factor}	T zone (m²/day)	Layer hydraulic conductivity, k_i (m/day)	Δh (m)
L8	11.6	0.15	10.4	0.7	-3.7
L7	2.65	0.25	17.3	1.9	-2.1
L6	-10.8	0.10	6.9	0.5	-0.1
L5	-25.3	0.01	0.7	<0.1	-1.5
L4	-32.5	0.11	7.6	1.1	1.5
L3	-51.3	0.03	1.7	0.1	-0.3
L2	-61.4	0.3	20.7	2.1	2.4
L1	-67.0	0.05	3.5	0.6	3.0
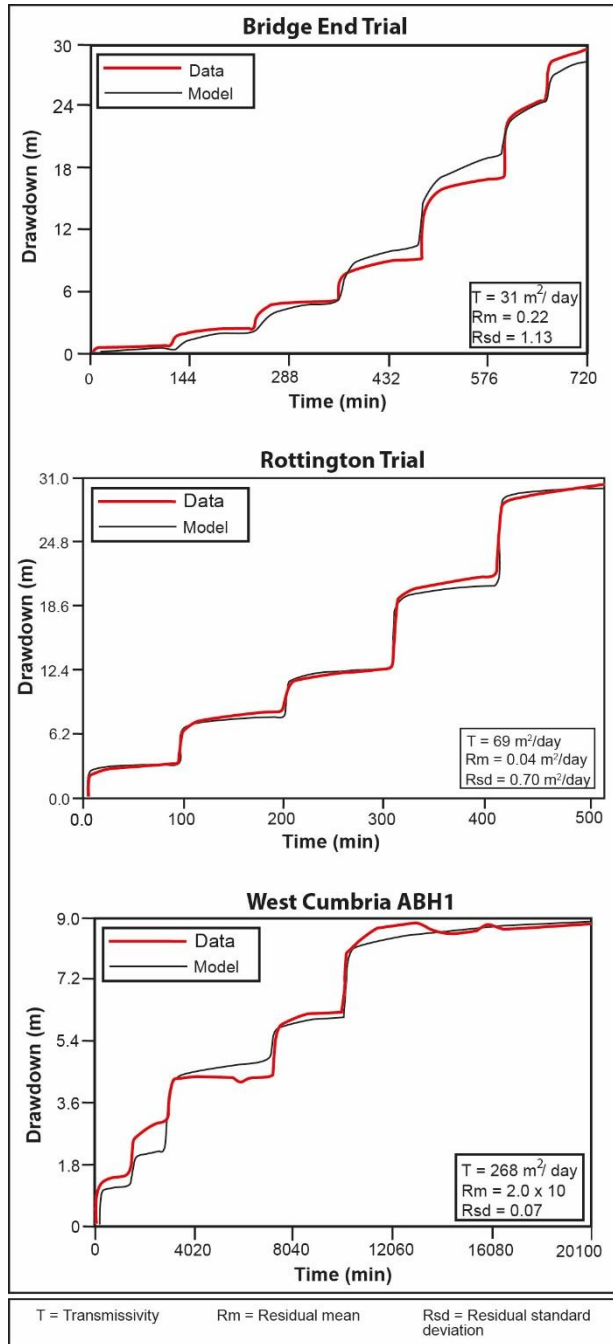
Figure 5.8: ESI AquiferWin32 solution of well test from the shallow St Bees Sandstone aquifer: observed and modelled step-test drawdown for Bridge End Trial, Rottington Trial and West Cumbria ABH1 boreholes (see Table 5.4 for flow rates).
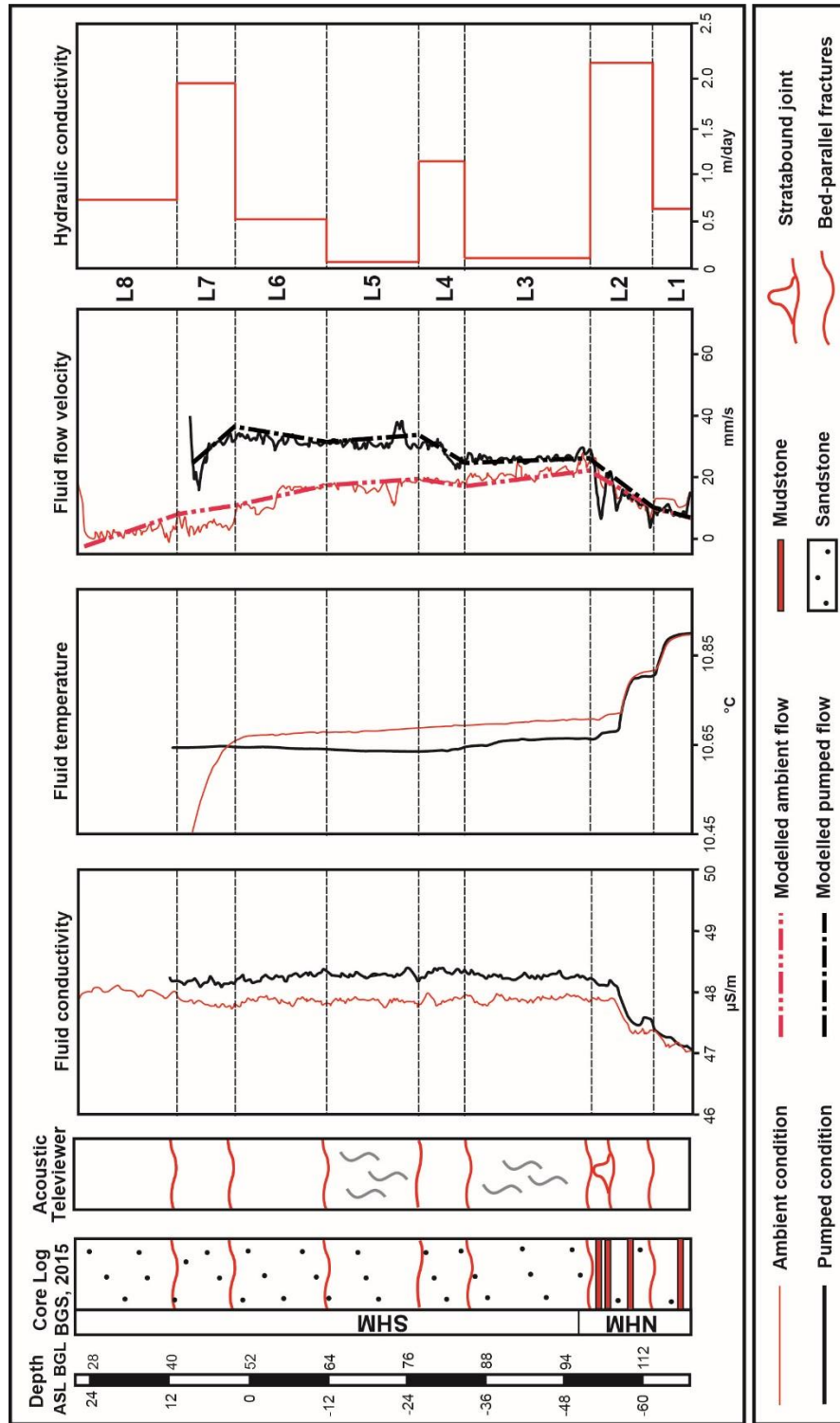
Figure 5.9: Rottington Trial well fluid log analysis. Fluid temperature, conductivity, fluid flow velocity all under pumped conditions and layer hydraulic conductivities computed with the FLASH program.
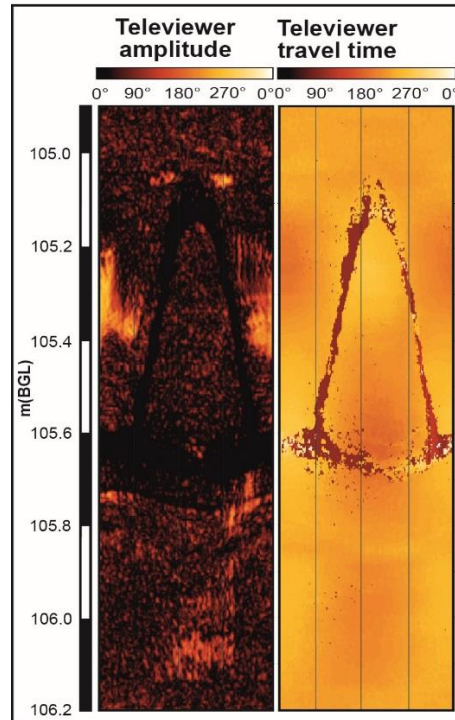
Figure 5.10: Amplitude and travel time acoustic logs in the shallow St Bees Sandstone aquifer showing intersection of bedding plane fractures (Bf) and vertical stratabound joints (J) in Rottington Trial well occurring at ~105.5 m BGL.

5.6.2 Intermediate and deep aquifer characterization

Pumping tests, fluid temperature and conductivity logs were obtained from the BGS archive for the two Sellafield deep boreholes (BH2 and BH3 wells). The St Bees Sandstone aquifer is intercepted between 150 and 420 m BGL in the Sellafield BH2 well and between 672 and 1100 m BGL in the BH3 well (Figure 5.1; Table 5.4). The fluvial St Bees Sandstone Formation is present in the BH2 and BH3 wells below the highly permeable aeolian deposits of the Calder Sandstone Formation (Allen et al., 1997). Thus, the aeolian deposits of the Calder Sandstone are not intercepted by the open screen of the BH2 and BH3 wells (Table 5.4). However, both the boreholes (BH2, BH3) intercept the entire St Bees Sandstone aquifer, including the North Head Member, which has relatively abundant mudstone beds, and is characterized by higher gamma-ray and lower neutron porosity values than the South Head Member (Figure 5.11). Hence, these two deep boreholes

allow investigation of the hydraulic properties of the St Bees Sandstone aquifer at relatively elevated depths up the geological boundary between the Sherwood Sandstone and underlying Permian deposits (Figure 5.1). The two long-screen well tests (BH2 I, BH3 I) tested > 300 m intervals that fully penetrate the St Bees Sandstone aquifer but that also penetrate underlying Permian deposits. The latter sedimentary deposits represent 27% and 28% of the screen lengths in the BH2 and BH3 long interval tests, respectively. However, short interval tests (<25 m) were also conducted at selected elevations within the South-Head Member, which is dominated by channelized architectural elements (Jones and Ambrose, 1994).

Analysis of the recovery phases of both long and short interval tests yield transmissivity ranging from 0.53 to 0.70 m^2/day (equivalent mean K of 2.0×10^{-3} and 2.3×10^{-2} m/day respectively) in Sellafield BH2 (intermediate depth aquifer). However, analysis of recovery data yield transmissivity ranging from 0.04 and 0.41 m^2/day (equivalent mean K of 4.0×10^{-3} and 6.4×10^{-4} m/day respectively) in Sellafield BH3 (deep aquifer). Based on the short interval tests that exclusively penetrate St Bees Sandstone, values of hydraulic conductivity are thus ~ 10^{-2} and 10^{-3} m/day for the intermediate (BH2) and deep (BH3) tests, respectively.
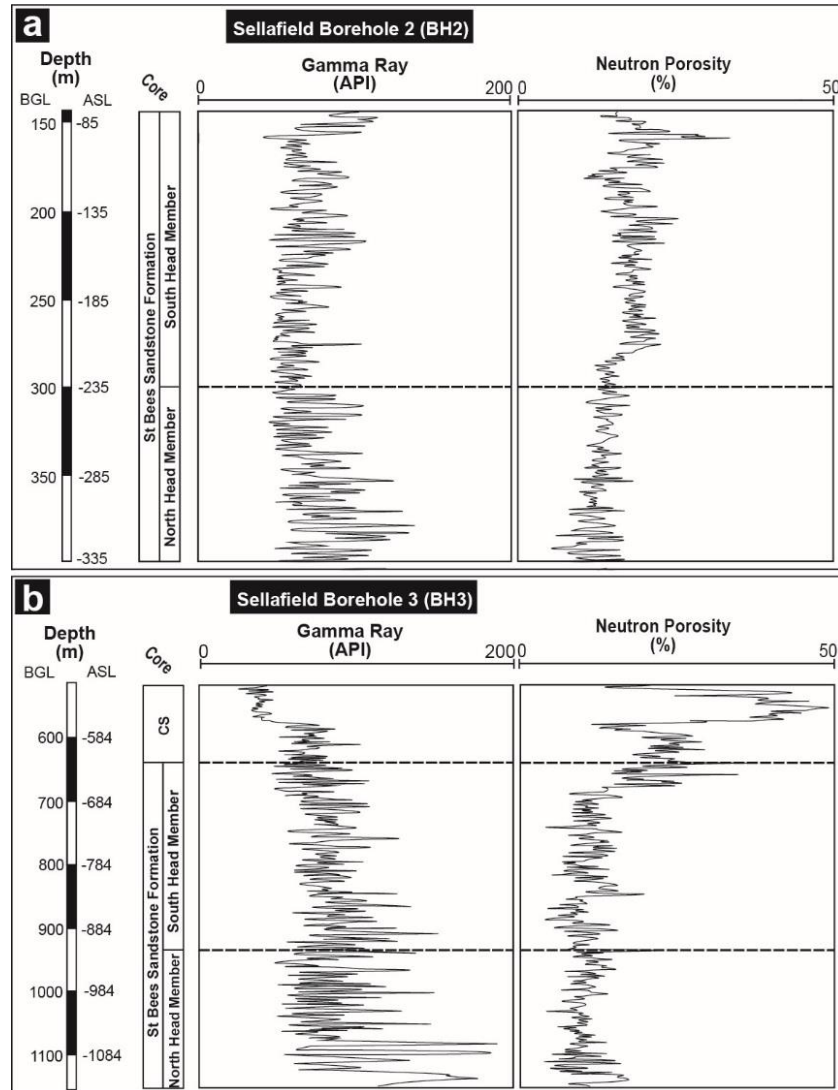
Figure 5.11: Gamma-ray and neutron porosity logs in Calder Sandstone Formation (CS) and in the North Head and South Head members of the St Bees Sandstone Formation. (a) Sellafield Borehole 2 (BH2), (b) Sellafield Borehole 3 (BH 3).

Sellafield BH2 and BH3 tests yield mean field-scale hydraulic conductivity values that are significantly lower (by a factor of ~10^2 to 10^3) with respect to the wells tested in the shallower aquifer in Bridge End Trial, Rottington Trial and West Cumbria ABH1 wells (Table 5.4). The fact that the hydraulic conductivity is much lower in the aquifer tested in Sellafield BH2 below ~150 m BGL may be because it is covered by the overlying (and more permeable) Calder Sandstone Formation at this location, and so has not been subjected to extensive meteoric water circulation. This is confirmed

by the fact that the lower part of the tested section in BH2 (below 315 m) shows fluid electrical conductivity well above freshwater values, Figure 5.12a. However, analysis of fluid logs from the deep aquifer here reveals a residual contribution of fractures to flow, as sharp changes in fluid temperature and conductivity logs occur in correspondence of fractures (Figure 5.12). The BH2 log also shows sharp changes in fluid temperature and conductivity at 327, 335 and 358 m BGL in correspondence of vertical joints bounded by bedding fractures. Sellafield BH3 temperature and conductivity logs show inflows associated with bedding plane fractures and normal faults (Figure 5.12).

The shallow St Bees Sandstone aquifer is characterized by low values of fluid conductivity (~50 mS/m; Figure 5.9) representative of freshwater, as seen in Rottington Trial and other wells in the part of the aquifer covered only by superficial deposits as also shown in Chapter 4. These waters represent recharge of fresh groundwater driven by topography, i.e. related to present day precipitation. Sellafield BH2 shows freshwater conductivity down to 315 m BGL but saline water ($>10^2$ mS/m) at about 350 m BGL (Figure 5.12a). However, freshwater circulation is likely to have been limited even in the shallower part of the formation penetrated here, owing to its down-dip location beneath the feather edge of the Calder Sandstone Formation (Figure 5.1b).

The field-scale hydraulic conductivity (K=2.3×10^{-2} m/day from ~200 m BGL, test BH2s see Table 5.4) indicates fracture alteration is not well developed here compared to that in the shallower aquifer (cavities have been detected in Chapter 4 by using optical televiewer logs at shallow depths). The Sellafield BH3 well (Figure 5.12b) is characterized by conductivity values of $>10^4$ mS/m, i.e. representative of particularly high salinity brines that characterize the deeper parts of the eastern Irish Sea Basin. In fact, at such depths groundwater is characterized by salt dissolution from the Permian evaporites and flow is minimal and driven by basin processes (Black and Brightman, 1996). Thus, the aquifer intercepted by BH3 has seen no freshwater circulation, which is

unsurprising considering its down-dip location (see Figure 5.1b). Fluid logs in BH3 at depths around 850 m BGL are characterized by less frequent slope changes with respect to those from BH2 at depths ranging up to 450 m BGL (Figure 5.12a, b). Significant changes in conductivity seems to occur only in correspondence of normal faults at ~850 and ~950 m BGL in BH3 well. Both tested intervals in BH2 and BH3 (Figure 5.12a, b) are characterized by a similar fracturing pattern (stratabound fracturing system). This suggests that, at increasing of lithostatic load, fractures progressively close (Jiang et al., 2009, 2010), which may explain the moderate permeability decrease between the intermediate and deep St Bees Sandstone aquifer (Table 5.4).
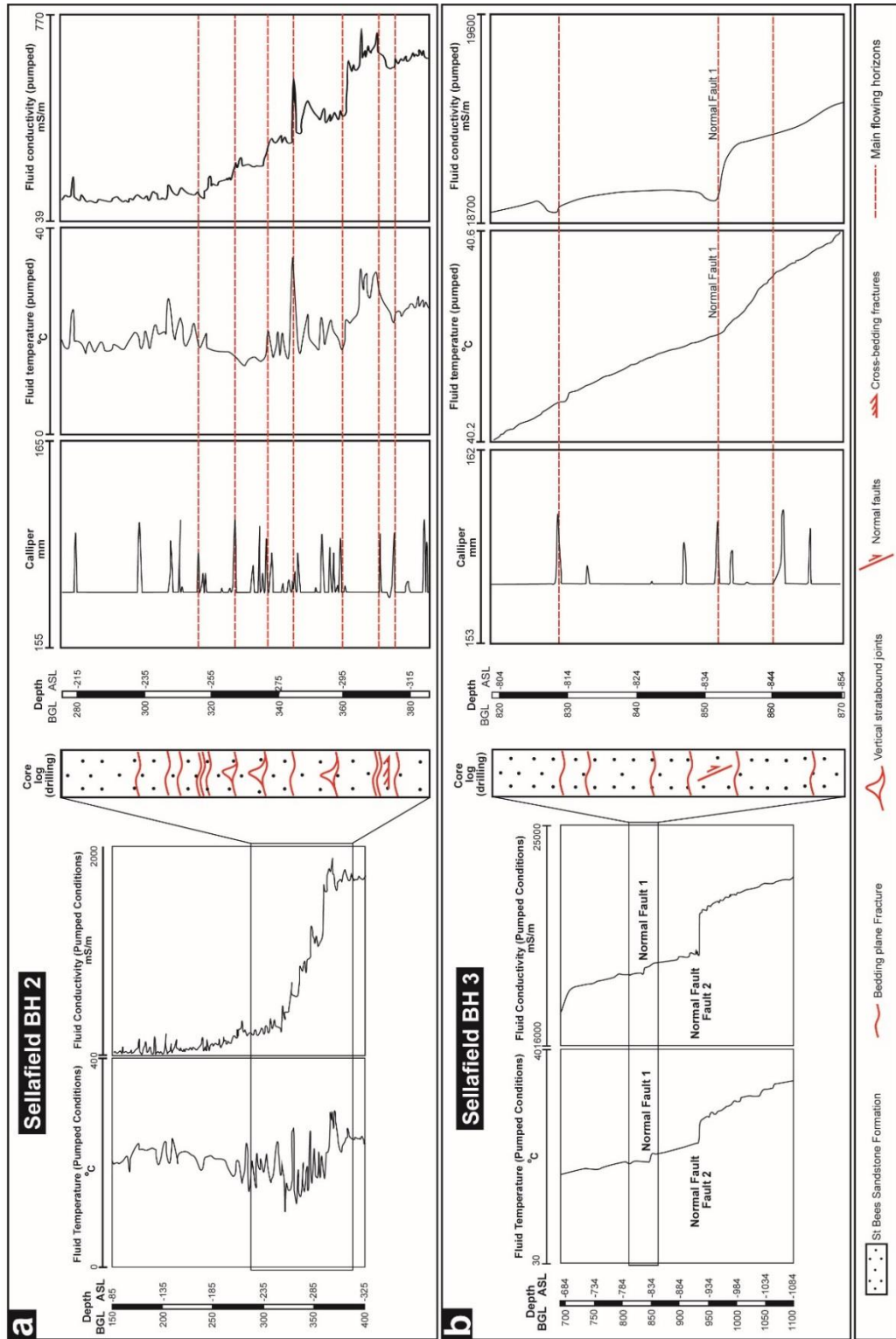
Figure 5.12: Fluid-logs from selected intervals in the intermediate and deep St Bees Sandstone aquifer respectively. (a) Fluid conductivity and temperature under pumped conditions for Sellafield BH 2, (b) Fluid conductivity and temperature under pumped conditions for Sellafield BH 3.

5.6.3 Plug upscaling for the deep and intermediate aquifer

Horizontal hydraulic conductivity (K_h) from plugs cored in correspondence with pumped intervals of the short interval length tests for Sellafield BH2 and BH3 were upscaled to give predicted transmissivity values based on the matrix flow component (Table 5.6). Results from the K_h geometric mean upscaling and measured well test transmissivities agree to within the same order of magnitude, although well test transmissivity is higher than upscaled transmissivity, most notably for the intermediate depth test (BH2s). This result is commensurate with analysis of fluid logs, which suggest large bedding fractures bounded by stratabound joints contribute to flow. Thus, the deep St Bees Sandstone aquifer (150 to 1100 m BGL) is likely to act as a dual permeability aquifer. The ratio ($T_{upscaled}/T_{well-test}$) between well test and upscaled transmissivity decreases from 2.8 to 1.3 at increasing depth (from BH2 a to BH3 b test intervals), respectively, consistent with progressive fracture closure at increasing depth producing increasingly matrix-dominated flow (Jiang et al., 2009; 2010).

Table 5.6: Comparison of upscaled transmissivity ($T_{upscaled}$) based on geometric means from cored plugs, versus well test transmissivity ($T_{well-test}$), for short interval tests in Sellafield BH2 s and BH3 s (intermediate and deep St Bees Sandstone aquifer respectively, see Table 5.4).

Test Name	Plug (n.)	Screen Length (m)	Screen Interval (mBGL)	K_h, Geometric Mean Plugs (m/day)	K_v, Harmonic Mean Plugs (m/day)	$T_{well-test}$ (m²/day)	$T_{upscaled}$ (m²/day)
BH2 s test	8	23	200-223	5.6×10^{-3}	4.7×10^{-4}	0.53	0.19
BH3 s test	4	10	931-941	2.7×10^{-3}	9.5×10^{-4}	0.04	0.03

5.6.4 Shallow vs. intermediate vs. deep aquifer well tests: derivative analysis

The response to water abstraction at constant flow rates in the shallow and deeper St Bees Sandstone aquifer has also been studied using the recovery first derivative with respect to time (ds/dt) following the Span and Wurster (1993) methodology. Recovery derivatives show strong sensitivity to flow regimes, providing information on aquifer heterogeneities and recharge variations (Zheng et al., 2000; Matter et al., 2006; Renard et al., 2009; Richard et al., 2014; Roques et al., 2014).

The recovery derivatives from the shallow St Bees Sandstone aquifer (Figure 5.13a) tested in Bridge End Trial, Rottington Trial and West Cumbria ABH1 wells show an initial rise (t <2 mins) which typically arises from wellbore storage effects in early-recovery time (Zheng et al., 2000; Corbett et al., 2012). Then, the recovery derivatives are irregular, showing a series of peaks and troughs. Derivatives of recovery phase from the intermediate (150-400 m BGL) and deep (400-1100 m BGL) St Bees Sandstone aquifer (Figure 5.13b, c), also show an initial rise due to well-bore storage effects (Bourdet et al., 1983, 1985; Ehilg-Economides, 1987; Corbett et al., 2012), peaking between 10 and 20 minutes, followed by steady falls which then flatten off, with absence of valleys or sharp slope changes. Notably, well-bore storage effects show longer durations at depths > 150 m BGL; these arise from the much lower aquifer transmissivities (Table 5.4).

The behaviour of the St Bees Sandstone aquifer at depth > 150 m BGL is generally consistent with a porous aquifer in which matrix represents an important component in conducting water flow to wells, with radial flow dominant towards the end of the test where the derivative flattens off (Ehilg-Economides, 1987; Zheng et al., 2000). In contrast, irregular derivative behaviour in the shallow aquifer may indicate the relative dominance of fracture flow, reflecting flow from matrix blocks to fractures, i.e. 'matrix pressure support' (Ehilg-Echonomides, 1988; Zheng et al., 2000; Van Tonder et al., 2001; Samani et al., 2006). However, this behaviour could

also simply be caused by temporal variations in recharge (e.g. from the streams feeding the aquifer which run off the impermeable rock the Lake District to the East), as previously observed at shallower depths in other aquifers (Samani et al., 2006; Odling et al., 2013).
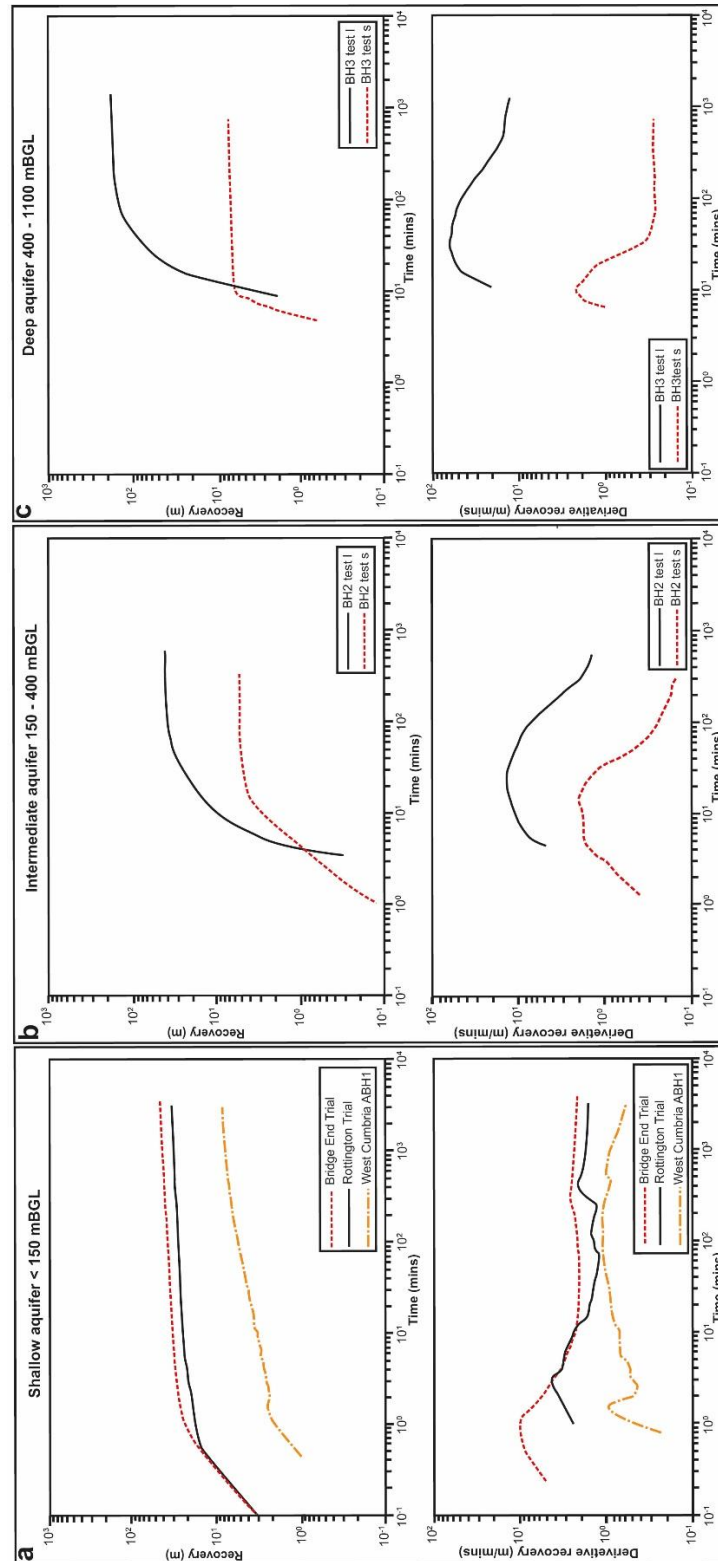
Figure 5.13: Hydraulic head and derivative for recovery phases of hydraulic tests. (a) Shallow St Bees Sandstone aquifer from Bridge End Trial, Rottington Trial and West Cumbria ABH1 wells, (b) Intermediate St Bees Sandstone aquifer (150-400 m BGL) from BH2, (c) Deep St Bees Sandstone aquifer (400-1100 mBGL) from BH3. (Note that l and s refer to long and short interval tests respectively, see Table 5.4 for details).

5.7 Discussion

5.7.1 Effect of sedimentary and diagenetic heterogeneity on matrix properties

The St Bees Sandstone Formation in the on-shore area of the eastern Irish Sea Basin represents a good example for the study of flow heterogeneities in lithified fluvial successions. Preservation of fine-grained deposits, such as white-silty drape, sheet-like sandstone and mudstone facies is favoured by the relatively high rate of subsidence of the eastern Irish Sea Basin at the time of sediment accumulation (Chapter 3). Hence, the characterization reported here has offered the opportunity to investigate the impact on fluid-flow of fine-grained layers, which represent potential flow barriers or baffles in fluvial aquifers (Alexander et al., 1987). Study of cement species of the reddish/yellowish lithotypes, which are represented by sheet-like sandstone (Ush), red-channel sandstone (Uws) versus the white-silty sandstone (Uws) suggests that the latter sedimentary unit represents a heterogeneity of diagenetic origin. In fact, the paucity of hematite cement (0-2 wt%) in the white-silty sandstone and its abundance in the sheet-like sandstone and red-channel sandstone (5-20 wt%) demonstrates how the white-silty sandstone (Uws) represents a locally reduced zone, examples of which typically extend laterally for up to 10 metres (Jones and Ambrose, 1994; Figure 5.2d) in a succession that is otherwise dominated by oxidizing conditions. Indeed, oxic conditions were dominant in the arid Triassic environments that were widespread across NW Europe at the time of deposition of the St Bees Sandstone Formation (Brookfield, 2008; McKie and Williams, 2009; McKie and Shannon, 2011). Such white-sandstone layers are common within fluvial red-bed deposits more widely; they are recognized in several regions across Europe, North Africa, South and North America (Waugh, 1973; Michalzik, 1991; Belittler et al., 2005; Bourquin et al., 2010; Costamagna, 2012). For example in the Triassic of the North German Basin they were interpreted as areas locally characterized by reducing conditions which were triggered by oxidation of organic material at early diagenetic stages (Weibel, 1998; Weibel and Friis, 2004). The low

porosity, permeability and small-pore size distribution (indicated by SEM, optical microscope and T_2 values) of the white-silty sandstone (Uws) may have protected these reducing areas from oxidizing fluids during later diagenetic stages.

Wireline-logs show lower neutron porosity and higher gamma-ray values in the basal unit of the St Bees Sandstone, the North Head Member (Figure 5.11), which is characterized by abundance of sheet-like sandstone and mudstone layers relating to the floodplain environment. Also, the plug-scale permeability of these sheet-like sandstone (Ush) and mudstone (Umi, Ush) layers is lower than those of the channelized facies (Figure 5.7, Table 5.3). The sheet-like sandstone (Ush) is less permeable than the red-channelized (Urs) facies due to its lower porosity coupled with an abundance of intergranular clay, which is indicated by the relatively high gamma-ray values in the North Head Member (Figure 5.11). Porosity and matrix permeability are, thus, related to the depositional palaeoenvironment.

5.7.2 Effect of burial history and exhumation

The burial history of the St Bees Sandstone aquifer around Sellafield was investigated by Chadwick et al (1994), who reconstructed palaeo-temperatures from apatite minerals from the BH3 borehole. Backstripping curves show how the St Bees Sandstone Formation was rapidly buried below 2 km in the early Triassic, and then up to 4 km depth during the Cretaceous (Chadwick et al., 1994). Since this period the formation has been exhumed reaching its current depth in the early Quaternary. Thus, the St Bees Sandstone aquifer was exposed to weathering and to the current flow conditions in its vadose and shallow saturated zones during the last 2.5 Myr. During the Quaternary, intense weathering developed up to ~10 m below the overlying glacial till; this was recognized in the St Bees Sandstone aquifer by McMillian et al. (2000) and Hough et al. (2006). Additionally, acidic conditions (pH=5) capable of dissolving calcite are common in the unsaturated zone of the UK Sherwood Sandstone aquifer

(Moss et al., 1992; Tellam and Barker, 1996). This work shows how samples collected ~5-10 m below the glacial till (see Figure 5.7c, outcrop samples) are characterized by porosity and permeability enhancement compared to samples from boreholes, i.e. removal of calcite, which represents an important component filling pores in the samples from the deeper, saturated aquifer (Strong et al., 1994, Waugh, 1978). Thus, ~2.5 Myr exposure to weathering created a very shallow matrix alteration zone of enhanced porosity and permeability up to ~10 m below the Quaternary till (schematically illustrated in Figure 5.14 a). Acoustic televiewer logs show that stratabound joints pervade the St Bees Sandstone aquifer; these probably arise due to the lithospheric uplift of NW Europe. Stratabound fractures typically characterize the outcropping Sherwood Sandstone Group across all the UK Triassic basins (Allen et al., 1998; Wealthall et al., 2001; Hitchmough et al., 2007). Additionally, core logs from the deep Sellafield boreholes (Nirex, 1996 a, b) indicate how such stratabound fractures exist up to ~1 km depth in the St Bees Sandstone aquifer. This is consistent with previous studies on unloading joints in NW Europe; for example, mining data indicate bed-bound joints at ~350 m BGL (Tratman, 1967). Also, numerical models suggest the transition between stratabound and non-stratabound joints typically occurs between 0.6 and 1.5 km (Gillespie et al., 2001). Optical logs in the shallow St Bees Sandstone aquifer (<150 m BGL) also show development of karst pathways in correspondence of intersections between bedding planes and stratabound fractures (see Chapter 4). Similarly, tracer tests undertaken by Barker et al. (1998) show karst-like flow velocities (140 m/day) in the Sherwood Sandstone aquifer of the Cheshire Basin. This suggests how ~2.5 Myr of exposure to the processes of enhancement fracture permeability typical of shallow aquifers may have played a key role on transmissivity distribution in this fractured fluvial aquifer, explaining its sharply decreased where tested at depths > 150 m below the ground surface (Chadwick et al., 1994; Allen et al., 1997; Warthington et al., 2016). Hence, we recognize a second groundwater alteration zone in the aquifer (see Figure 5.14), below the upper 10 m, that shows matrix porosity enhancement. This second alteration zone is characterized by development of karst-like features

related to flowing fractures which were detected up to 150 m BGL in this study (as illustrated schematically in Figure 5.14).

5.7.3 Matrix vs. fracture flow

Bedding parallel fractures have been recognized as principal flow pathways in other shallow sandstone aquifers (also at depths <150 m BGL) in several case studies across Europe and America (e.g., Morin et al., 1997; Runkel et al., 2006; Hitchmough et al., 2007; Leaf et al., 2012; Gellasch et al., 2013; Lo et al., 2014). However, this work shows how stratabound joints in shallow sandstone aquifers enhance flow, establishing connection between bedding plane fractures, as illustrated schematically in the conceptual model shown in Figure 5.14a. Indeed, fluid and acoustic televiewer logs indicate that inflow zones to wells at depths <150 m BGL in the St Bees Sandstone only occur associated with the junctions between bedding plane and bed-bound fractures (Figures 9, 10). The St Bees Sandstone aquifer characterised in this study is relatively permeable in its shallow part ($K\sim10^{-1}$-10^0 m/day) where it is covered only by permeable glacial deposits, and characterized by much lower field-scale hydraulic conductivity (by a factor of 10^2-10^3) where buried below the much more permeable Calder Sandstone Formation (below 150 m BGL). Data from the West Cumbria ABH1 well (Table 5.4) located ~3 km north locates this permeability transition at a maximum depth of 150 mGBL. However, this threshold is not constrained in the Egremont area further north, due to lack of deep wells (Figure 5.1). Similarly, a sharp permeability reduction has been detected using packer tests (in boreholes up to 400 m deep) in the Sherwood Sandstone sequence of the Cheshire Basin at 100 to 200 m BGL (Brassington and Walthall, 1985; Allen et al., 1997). In this study, borehole logging undertaken in the St Bees Sandstone aquifer provides evidence that the high permeability occurring at relatively shallow (~150 m BGL) depths arises from groundwater alteration in correspondence of fractures. Beyond this alteration zone, where the St Bees Sandstone is buried under increasing depths of the Calder and subsequently the Ormskirk Sandstone,

field-scale permeability decreases more gradually downdip to ~1 km BGL. This further reduction in field-scale permeability may arise from interplays between (i) fracture closure driven by lithostatic load (Jiang et al., 2009, 2010) and (ii) variation in matrix permeability due to salinity increase, i.e. moving from saline water to brine of the deep eastern Irish Sea Basin (Jiang et al., 1991; Black and Brightman, 1996). Plug-scale permeability tests (Daw et al., 1974; Nirex, 2001) suggest that the slight permeability reduction from the intermediate (150-400 m BGL) and deep (400-1100 m BGL) zones arises from fracture closure with depth. In fact, previous works show that only low permeability (sheet-like sandstone, mudstone) units (K<10^{-3} m/day) in this aquifer show sensitivity of K to salinity variation (Daw et al., 1974; Nirex, 2001). Reduction in field-scale permeability due to fracture closure with depth is likely, and is also supported by (i) reducing difference between plug- and field-scale permeability decreases (Table 5.6), and (ii) fluid temperature and conductivity logs, which show fewer irregularities at elevated depths (compare Figure 12a and b). This hypothesised change from fracture to matrix flow with increasing depth is illustrated schematically in Figure 5.14a.

In contrast to bedding parallel and stratabound joints, extensional faults show a similar hydraulic behaviour when intercepted by boreholes at range of depths as illustrated schematically in Figure 5.14a. Quantitative analyses of well-bore flow logs from the shallow St Bees Sandstone aquifer show that fault zones typically account for 50% of the overall transmissivity in boreholes cutting the fault-slip planes as shown in Chapter 4. Similarly, well tests undertaken by Streetley et al (2000) with packers in correspondence of extensional faults at intermediate (150-400 m BGL) depths in Sellafield BH2 show higher field-scale hydraulic conductivity (K of 0.38 m/day) compared to the un-faulted parts of the aquifer (K of 0.001 to 0.22 m/day). Fluid logs undertaken in this work show how normal faults in this high-mechanically resistant fluvial aquifer represent favourable flow pathways up to ~1 km depth (Figure 5.12b), typical of faults characterized by relatively highly connected open fractures in their damage zones (Figure 2f; Jiang et al., 1991; Caine et al., 1996; Ball et al., 2012; Bense et al.,

2013; Ran et al., 2014; Bauer et al., 2016). This structural style has been considered a typical characteristic of fluvial deposits since argillaceous matrix of the St Bees Sandstone Formation allows brittle failure at lower stresses with respect to deposits of aeolian origin (Knott, 1994). Note that the higher abundance of open fractures in these fault zones may also be related to the intense fault reactivation in this strongly lithified sandstone (Milodowski et al., 1998).

5.7.4 Anisotropy in the intermediate and deep St Bees Sandstone aquifer

Plug-scale anisotropy values from core plugs (Tables 5.1, 5.3) can be compared with those from field scale tests reported by Streetley et al. (2000), who analysed pumping tests at depths >150 m BGL in the St Bees Sandstone aquifer using Hantush (1961) methodology. Streetley et al. (2000) analysed two different tests penetrating the South Head and upper North Head members, respectively. The plug-scale anisotropy (K_h/K_v) for the channel-sandstone has a geometric mean of 3 (based on both plugs from outcrop obtained in this study and those from boreholes obtained in previous works, Tables 5.1, 5.3). This plug-scale average value matches the field-scale anisotropy which ranges from 2 to 6 according to Streetley et al. (2000). Explanation for this match between plug and field scale arises from the relative homogeneity of the South Head Member, for which 95% of the succession is characterized by fluvial channel elements (Jones and Ambrose, 1994) and for which red-mudstone units occur only rarely and exhibit lateral continuity of only up to 30 m (Jones and Ambrose, 1994; Nirex, 1997). Also, the diagenetic white-silty sandstones within the South Head Member are of restricted lateral extent (< 10 m) (see Chapter 3). Thus, the low lateral continuity of the low-permeability heterogeneities, coupled with their relatively low preservation in the sedimentary record, limit their influence on large-scale anisotropy. However, large-scale anisotropy (K_h/K_v=17-34, Streetly et al., 2000) is greater in more heterogeneous units such as the upper North Head Member (75%

sandstone; 25% mudstone); this is illustrated schematically in the lower part of Figure 5.14b, which represents a fluvial sequence in which the lower-permeability units are preserved. Notably, the field scale anisotropy in the upper North Head Member is greater than that from the geometric means of plug values from the constituent units: mudstone interbedded in amalgamated channel deposits ($K_h/K_v = 5$); sheet-like sandstone ($K_h/K_v = 4$); floodplain mudstone ($K_h/K_v = 6$); see Table 5.3. Additionally, field-scale anisotropy in the North Head Member exceeds those of individual plugs from channel deposits ($K_h/K_v = 2 - 8$) (Table 5.1). This contrast between field- and laboratory-scale anisotropy in the upper North Head Member reflects much higher lateral continuity (> 200 m) of low-permeability units such as mudstone interlayers typical of most fluvial successions (Nirex, 1997; Ielpi and Ghinassi, 2015), which impede vertical flow. The influence of mudstone units that partially impede flow at the field scale is also supported by the 20% transmissivity reduction moving from the South Head Member to the upper North Head Member of the St Bees Sandstone aquifer (Streetly et al., 2000). The presence of conductive low-angle-inclined (5°-20°) and bedding parallel fractures (Figure 2c), which are related to the mechanical reactivation of erosional bounding surfaces of the braided fluvial-system (Jones and Ambrose, 1994), might also enhance the large-scale anisotropy over that seen at plug-scale (as illustrated schematically in Figure 5.14b).

The absence of pumping tests using observation wells prevented field-scale anisotropy quantification in the shallow aquifer (< 150m BGL). However, other shallow fractured aquifers show anisotropy values ranging from 20 to 150 due to the effect of bedding plane fractures (Boulton, 1970; Neuman, 1975; Chen, 2000; Odling et al., 2013). Thus, it is likely that the shallow St Bees Sandstone aquifer (< 150 m BGL) is also strongly anisotropic due to the bedding parallel fractures which represent the main flowpaths, as observed in the fluid logs.
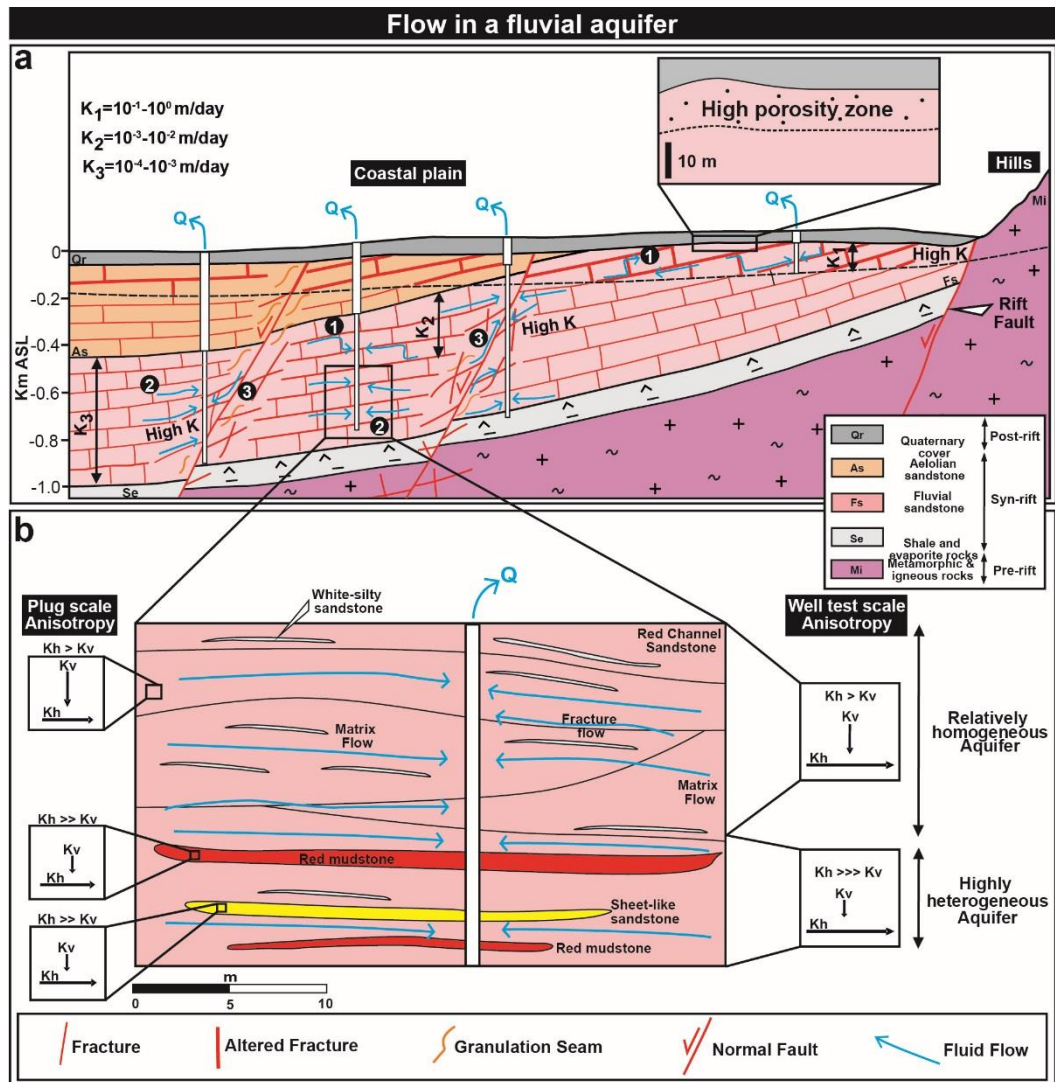
Figure 5.14: Conceptual models of fluid flow to wells under pumped conditions in fluvial aquifers in a rift-type basin and resulting plug vs. field scale anisotropy. (a) Nature of permeable pathways in a well-lithified fluvial aquifer showing flow to wells through the (1) stratabound fracturing system, (2) matrix and (3) fault structures, (b) Enlarged panel showing sedimentary structure and flow pattern at intermediate to high depths.

5.8 Conclusions

Study of the upscaling properties of the St Bees Sandstone Formation, which represents a cemented fluvial succession, demonstrates how such aquifers are influenced by a range of heterogeneities of sedimentary, tectonic and weathering-related origin. Plug-scale permeability and NMR (large T_2 values corresponding to coalescent pores) analyses indicate how

fluvial channel sandstone bodies, which dominate the St Bees Sandstone Formation, represent the most hydraulically conductive lithology. Mudstone and sheet-like sandstone facies of fluvial overbank origin and diagenetically produced white-silty sandstone facies represent low-permeability heterogeneities.

Weathering associated with over ~2.5 Myr of exposure has enhanced matrix porosity and permeability in the upper ~10 m of the vadose zone, immediately beneath the glacial till cover. Bedding-plane fractures, which are connected by uplift-induced stratabound joints, dominate the flow in the highly permeable ($K\sim10^{-1}$-10^0 m/day) shallow aquifer, tested here to a depth of 150 m BGL, which represents a zone of fracture alteration. Flow in this highly conductive zone arises from development of karst-like pathways associated with intersections of bedding-parallel and high-angle stratabound fractures, due to flow of meteoric water at these relatively shallow depths. Thus, contamination hazard to water wells is relatively high in lithified fluvial aquifers because of the potential for rapid transport of contaminants, such as wastewater from leaking sewers along such pathways.

Field-scale permeability was at least two orders of magnitude (10^2) lower beyond the zone of fracture alteration. A smaller permeability reduction is seen between the intermediate (150-400 m BGL) and deep (400-1100 m BGL) St Bees Sandstone aquifer (tested in Sellfield BH2 and 3 respectively, where it is present beneath the relatively permeable aeolian Calder Sandstone Formation). Notably, differences between plug and field-scale permeability, and frequency of well in-flows seen in temperature and conductivity logs, also decrease between intermediate and elevated depths. This most likely indicates how fracture closure leads to a progressively more important matrix contribution to flow with increasing depth. Thus, the most appropriate conceptual model to account for the behaviour of the deep St Bees Sandstone aquifer from 150 up to 1100 m BGL is a dual permeability aquifer, where flow to pumped wells is directly supported by both matrix and fractures. However, extensional faults show

consistent hydraulic behaviour up to ~1 km depth. More generally, normal faults in relatively mechanically resistant fluvial deposits represent flow pathways since their large damage zones are dominated by open fractures.

Plug-scale anisotropy (K_h/K_v ~3) of fluvial channel sandstone deposits matches field-measured values for the relatively homogeneous upper part of the sedimentary succession, where lateral continuity of low-permeability heterogeneities (sheet-like sandstone and mudstone) is low. However, field-scale anisotropy rises (to >30) in parts of the succession that preserve low-permeability layers in the sedimentary record; here the great lateral continuity of mudstone and sheet-like sandstone beds impedes vertical flow.

This work has quantitatively characterized a fluvial aquifer from the ground surface to 1100 m BGL. This represents an important depth interval in geoscience where, for example, fluvial deposits overlie nuclear waste repositories and where fluids are extracted from geothermal reservoirs.

Chapter 6

Discussion

The structural and sedimentary flow heterogeneities of the St Bees Sandstone aquifer have been quantitatively characterized from the plug up to the field scale in the eastern Irish Sea Basin of West Cumbria. In this Chapter, plug-, well-bore- and field-scale properties of this fluvial aquifer succession – acquired at a range of depths (up to ~1 km depth) – will be discussed and compared to the hydraulic properties of the UK Sherwood Sandstone Group more widely, and to other similar successions from around the world. This will allow establishment of generalised models for mixed fluvial and aeolian successions accumulated in rift-basins settings. Therefore, this study will provide a more complete understanding of the hydraulic properties of continental successions in rift settings, generally.

6.1 St Bees Sandstone aquifer

Many braided-fluvial successions are generally characterised by a relatively coarse-grained (sand) grain size, a relative paucity of mudstone, and the abundance of planar cross-bedded sets (Coleman, 1969; Bristow, 1988). In addition to these traits, the St Bees Sandstone is characterized by: (i) barform elements that are elongated in a downstream direction and which preserve avalanche deposits on their lee slopes, and (ii) a relative abundance of trough cross-bedded dune-scale deposits (Miall, 1977; Bridge, 1993, 2003). All of these sedimentological characteristics support the interpretation of the succession as representing a sandy braided river system. This interpretation has also been inferred for analogous and broadly time-equivalent successions across the UK Triassic basins for the majority of fluvial deposits of the Sherwood Sandstone Group (Smith, 1990; Steel and Thompson, 1993; Brookfield, 2004; McKie and Williams, 2009; Wakefield et al., 2015). Despite the general similarity with regards to the overall type of fluvial system, the St Bees Sandstone Formation of West

Cumbria has been selected for a hydraulic characterization of its sedimentary heterogeneities due to the well preserved nature of fine-grained layers (e.g., mudstone, white silty sandstone). The eastern Irish Sea Basin is characterized by the highest values of tectonic subsidence (210 m/Myr) and sediment preservation rates (119 m/Myr) in the UK Triassic realm (Evans et al., 1993; Chadwick et al., 1994; Nirex, 1997; Worden et al., 2016). This high subsidence rate favours preservation of fine-grained heterogeneities due to channel avulsion that do not fully rework them under such conditions (Colombera et al., 2013). Additionally, the St Bees Sandstone aquifer also represents an optimum laboratory for hydraulic characterization of tectonic structures. In fact, the layered nature of the St Bees Sandstone aquifer coupled with its relatively high mechanical resistance (UCS_{nat}=36 MPa) has allowed development of a pervasive stratabound fracturing network (Bell, 1992; Hawkins et al., 1992; Yates, 1992; Charalambous et al., 2012). Additionally, normal faults show damage zones that are dominated by open fractures with a relatively paucity of granulation seams (Knott, 1994). Thus, the St Bees Sandstone aquifer also represents an optimum laboratory to characterize the field-scale properties of a fractured sandstone succession, characterized by stratabound fractures and locally deformed by normal faults.

The St Bees Sandstone aquifer has been exploited since the 1980s for water, with abstraction at depths < 200 mBGL (Allen et al., 1997). Thus, an existing monitoring borehole network has been reutilised in this project, the aim being to characterize the field-scale properties at different distances from mapped fault traces. Well-test transmissivity values ($T \sim 10^1$-10^3 m^2/day) in the shallow St Bees Sandstone (<150 mBGL) aquifer are significantly higher than those implied for the matrix, determined using upscaling of plug values. In fact, the screen transmissivities which were obtained by the upscaling of K_h using geometric mean values, show T values $\sim 10^2$ lower than transmissivity from pumping tests ($T_{well\text{-}test}/T_{upscaled}$ = 35 - 913). This suggests that fractures act as dominant flow conduits during pumping tests. Thus, the hydro-geophysical characterization undertaken in this work at depths shallower than 150 mBGL did not permit

acquisition of information on the sedimentary flow heterogeneities. Flow logging undertaken at such depths show how major flow velocity anomalies in un-faulted wells occur in correspondence of the following: (i) clusters of minor bedding plane fractures; (ii) major bedding plane fractures showing conduits; and (iii) bedding plane fractures connected by stratabound joints. Such fractured horizons are typically bound by highly permeable flow zones showing hydraulic conductivities > 5 m/day. Optical and acoustic televiewer log analyses in un-faulted wells show development of karstic features (solution-enlarged fractures) which contribute to the creation of a highly permeable shallow aquifer (T = 31 - 913 m^2/day). Additionally, flow-log analysis and televiewer logs indicate how stratabound fractures establish connections between bedding plane fractures, thereby enhancing water flow, as previously inferred by numerical models (Odling and Royden, 1997; Hitchmough et al., 2007). Overall, the shallow St Bees Sandstone aquifer appears close to a dual porosity model, whereby flow is dominated by fractures, as demonstrated by upscaling and screen transmissivity. Despite this, water is additionally stored in pores due to the high porosity nature of the St Bees Sandstone aquifer (10-25% porosity of channel sandstone).

Around 50% of inflow into wells penetrating normal fault planes at shallow depths (<150 mBGL) is characterized by extension-related structures (major fault planes and open fractures in the damage zone). The other 50% of inflow into such wells derives from major bedding plane fractures, which represent further important flowing discontinuities. Despite this, the observed boreholes do not show a positive correlation between transmissivity and distance from fault trace. This likely arises from the nature of the aquifer, which in un-faulted areas is actually pervasively fractured, i.e. by stratabound and bedding plane fractures. Thus, targeting faults, at least at shallow depths (<~ 150 mBGL), does not improve water abstraction efficiency. Additionally, the presence of rivers running onto the St Bees Sandstone from the Lake District Massif (e.g. Rivers Ehin and Calder), results in focussed recharge; this represents a further factor that potentially develops transmissivity, as suggested for other relatively

shallow fractured aquifers (Domenico and Schwartz, 1988; Worthington et al., 2016). In fact, Thornhill Trial well (T_{screen} = 913 m^2/day) and West Cumbria ABH1 (T_{screen} = 267 m^2/day) which represent the most transmissive boreholes tested, are located at ~100 metres from the Ehin and Calder rivers which represents the principal streams on the Sellafield coastal plain (Heacothcote et al., 2000; McMillan et al., 2001).

Despite a lack of correlation between transmissivity and distance from fault traces, normal faults represent preferential flow pathways at shallow depths since they typically account for around 50% of the overall well-screen transmissivity in boreholes cutting the fault planes. The conduit behaviour of extensional faults intercepted by boreholes persists at increasing depth in the St Bees Sandstone aquifer. In fact, well tests undertaken by Streetley et al (2000) with packers in correspondence of extensional faults at intermediate (150-400 mBGL) depths show higher field-scale permeability ($T_{well-test}$ of 7.82 m^2/day) with respect to the un-faulted parts of the aquifer ($T_{well-test}$ of 0.46 to 4.49 m^2/day). Also, this work shows normal faults in this highly-mechanically resistant fluvial aquifer localize well inflows up to ~1 km depth, as expected for faults which are characterized by well-connected open fractures in their damage zones (Caine et al., 1996; Ball et al., 2012; Bense et al., 2013; Ran et al., 2014; Bauer et al., 2016). This structural style has been considered typical of fluvial deposits since the argillaceous matrix of the St Bees Sandstone Formation allows brittle failure at lower stresses compared to well-sorted sandstone-dominated aeolian dune deposits (Knott, 1994). However, higher abundance of open fractures in these fault zones may also be related to the intense fault reactivation which produced open fractures in this strongly lithified fluvial sandstone (Milodowski et al., 1998).

The hydraulic behaviour of the shallow (<150 mBGL) St Bees Sandstone aquifer contrasts those of the aquifer at intermediate (150 - 400 mBGL) and elevated (400 - 1100 mBGL) depths. In fact, the St Bees Sandstone aquifer is highly permeable in its shallow part ($T_{well-test}$ = 31 - 913 m^2/day), down to depths of at least 150 mBGL; tests from deeper parts of the St Bees

Sandstone Formation, where it occurs beneath the Calder Sandstone Formation, show much smaller transmissivity values. Similarly, a sharp permeability reduction has been detected at 100 to 200 mBGL in the Sherwood Sandstone aquifer of the Cheshire Basin (Allen et al., 1997, Brassington and Walthall, 1985). Our work provides evidence on how the high permeability in the shallow St Bees aquifer is related to development of karst-like conduits in correspondence with bedding-plane and stratabound joint fractures (optical televiewer log cavities and traces of calcite removal in correspondence of bedding and stratabound fractures) which has also been observed on other fluvial aquifers worldwide (Runkel et al., 2006; Swanson et al., 2006; Leaf et al., 2012). Thus, hazard for groundwater protection rises in highly mechanically resistant sandstone successions, such as the St Bees Sandstone Formation; transport of near-surface contaminants, such as wastewater from leaking sewers to public wells typically occur at higher flow rates along such fractures (Gellasch et al., 2013).

Below the shallow and highly permeable alteration zone of the St Bees Sandstone aquifer, fractures are increasingly closed with lithostatic stress due to increasing depth (Jiang et al., 2009, 2010). This is suggested by plug-scale permeability experiments showing strong K sensitivity to stress for fractured plugs of the St Bees Sandstone (Daw et al., 1974). Also, a fracture permeability reduction due to lithostatic load below the highly permeable zone is supported by field-scale experimental evidence. For example, the following observations are noteworthy: (i) field-scale permeability (after an abrupt decrease below the shallow alteration zone) continues to progressively decrease down to 1100 mBGL; (ii) the difference between upscaled plug and field-scale permeability also decreases with increasing depth; and (iii) fluid logs show more regular curves at high depth (i.e., 800 - 1100 mBGL). Thus, the matrix becomes progressively more important for flow with increasing depth, such that it dominates flow at ~1 km below the ground surface. Further evidence for dominance of matrix flow below 150 m BGL is provided by well-screen transmissivity values that match upscaled transmissivity values derived from plug-scale tests in the

intermediate ($T_{well-test}/T_{upscaled}$=2.8) and deep ($T_{well-test}/T_{upscaled}$=1.3) St Bees Sandstone aquifer.

The St Bees Sandstone aquifer at depths >150 mBGL also shows a 25% reduction in transmissivity moving from the relatively homogeneous South Head Member (sandstone = 95%; mudstone = 5%) to the more heterogeneous Upper North Head Member (sandstone = 75%; mudstone = 25%) (Streeley et al., 2000). The slightly lower transmissivity in the mudstone-rich lower part of the overall succession is likely to be related to flow through the low-permeability mudstone units. Likely, increasing occurrence of mudstone interlayers and their much higher lateral continuity (>200 m) reduces transmissivity, since the low-permeability mudstones represent partial barriers for the fluid flow. At the same time, laterally continuous mudstones impede vertical flow in the upper North Head Member, thereby accounting for its higher field-scale anisotropy. Field-scale anisotropy calculated by Streetley et al. (2000), reduces significantly from the upper North Head (K_h/K_v=17-34) to the South Head (K_h/K_v=2-6) members of the St Bees Sandstone Formation.

6.2 UK Sherwood Sandstone Group

The St Bees Sandstone Formation represents the basal part of the Sherwood Sandstone Group in West Cumbria, which is exclusively characterized by fluvial deposits (Jones and Ambrose. 1994; Ambrose et al., 2014). The geological, petrophyisical and hydraulic characterization undertaken as part of this research programme provides: (i) evidence for the tectonic control on preservation of fine-grained layers that effectively influence fluid flow; (ii) quantification of the impact of tectonic discontinuities on fluid flow in a lithified fluvial aquifer; and (iii) discernment of the respective role of matrix vs. fracture flow up to ~1 km below the subsurface. Coupling these findings with a critical review of the petro-hydraulic characteristics of the wider Sherwood Sandstone Group deposits allow for a new and improved understanding of the hydraulic properties of both

aeolian and fluvial deposits in Triassic rift settings of the UK, and in rift settings more generally.

6.2.1 Tectonics vs. physical properties

The fluvial Triassic Sandstone of Great Britain shows how basin tectonic subsidence rates (and thus accommodation generation rates) represent the primary control on physical properties that have not been subject to significant alteration and overprinting due to the Cenozoic uplift of NW Europe. Samples for the Sherwood Sandstone Group from regions subjected to relatively slow rates of subsidence and sediment accommodation generation rates, such as the Worcester Basin and the Eastern England Shelf, show UCS_{nat} values ranging from 0 up to 22 MPa (Thompson and Leach, 1985; Whithworth and Turner, 1989). By contrast, the Sherwood Sandstone Group in basins subject to the highest rates of subsidence, such as the Cheshire and eastern Irish Sea basins, show relatively higher UCS_{nat} values (UCS_{nat} = 17 - 36 MPa). Notably, the highest values of uniaxial compressive strength (36 MPa) correspond to the Sherwood Sandstone of the eastern Irish Sea Basin, which was the fastest subsiding Triassic basin in Great Britain (Hawkins et al., 1992; Yates, 1992; Evans et al, 1993; Chadwick et al., 1994; Worden et al., 2016). This demonstrates the control of tectonic subsidence (and resulting burial depth) on the matrix properties. In fact, this appears evident by comparing the half graben basin of the eastern Irish Sea with the shelf-edge basin of the eastern England Shelf. The fastest subsiding basin of the eastern Irish Sea Basin and the slowest subsiding eastern England Shelf are characterized by the lowest and highest porosity and matrix permeability values, respectively.

The relation between basin subsidence and the petro-mechanical properties of the Triassic continental deposits of Great Britain is more complicated with regards to field-scale permeability at relatively shallow depths (<~150 mBGL). In fact, transmissivity of the UK Triassic Sandstone

shows similar values ($T = \sim 10^1 - 10^2$ m^2/day) in Triassic basins of Great Britain due to interplays between groundwater alteration, fracture and matrix flow (Allen et al., 1997). However, tectonic subsidence plays a key role on the difference between plug and field scale permeability. High mechanical resistance favours development of open fractures such as stratabound joints and bedding plane fractures that dominate the flow in the fluvial red-beds of the eastern Irish Sea Basin. In fact, field-scale transmissivity, as shown in this work, is $\sim 10^2$ higher than transmissivity from upscaled plug permeability values in the eastern Irish Sea Basin of West Cumbria.

The ratio between upscaled plug and field scale transmissivity is ~ 4 in the Sherwood Sandstone aquifer in the Cheshire Basin; this value arises from a well-developed stratabound fracturing network (pervasive due to its relatively high mechanical resentence and permeable as demonstrated by packer tests) coupled with relatively high conductivity of the matrix (Brassington and Walthall, 1985; Hitchmough et al., 2007). However, the Triassic red-beds of Great Britain shows the lowest difference between upscaled plug and field scale transmissivities (<2.0) in the slowly subsiding of the eastern England Shelf and Worcester basins, which show the highest average values of porosity and plug-scale permeability (Allen et al., 1997). This is probably because low values of mechanical resistance (UCS_{nat}<20 MPa) do not permit development of fractures in the latter two sedimentary basins (Walsby et al., 1980; Whittaker and Turner, 1980; Yates, 1992).

6.2.2 Aeolian deposits, and their contrast with fluvial deposits

The distribution of aeolian facies in UK Triassic basins of Great Britain also suggests how interplays between tectonics and distance from the sediment source (Figure 6.1a) play an important role on preservation of high-porosity and high-permeability deposits of aeolian dune origin, and how such deposits influence reservoir quality (Jones and Ambrose, 1994; Allen et al., 1997; Ambrose et al., 2014; Olivarious et al., 2015; 2016). Mckie and

Williams (2009) pointed out a progressive northward increase in aeolian content from the Triassic of the Wessex Basin in southern England (Otter Sandstone Formation), to the Vale of Eden, eastern Irish Sea Basin and Carlisle basins in northern England (Figure 6.1; Purvis and Wright, 1991; Jones and Ambrose, 1994; Brookfield, 2004, 2008; Ambrose et al., 2014). This increase in aeolian facies can be interpreted through a transitional downstream reduction in the discharge of the braided fluvial system at increasing distance from the sediment source entering into the arid-climate basin network (Jones and Ambrose, 1994). At the same time, extensional tectonics likely plays a secondary role in determining the preservation of aeolian facies (Gawthorpe, Leeder, 2000; Mountney, 2012). In fact, aeolian deposits are absent throughout the entire eastern England Shelf Basin, which represents the slowest Triassic subsidence-rate basin in the UK (Smith and Francis, 1967; West and Truss, 2006; Wakefield et al., 2015). In contrast, preservation of aeolian facies (Figure 6.1a) occurs at similar distance from the main sediment source in the eastern Irish Sea Basin (Jones and Ambrose, 1994). Aeolian deposits are represented in all the other UK Triassic basins, which are bounded by normal faults, as well as in the Triassic deposits of the North Sea and Irish Sea in off-shore regions (Meadows et al., 1993a, b; McKie et al., 2005, 2010; Mckie and Williams, 2009; Olivarious et al., 2015, 2016). Thus, their absence in the shelf-edge basin of the eastern England Shelf might be related to slower rate of accommodation generation in this setting. High rates of tectonic subsidence in the eastern Irish Sea Basin assisted long-term preservation of aeolian deposits by placing them beneath the water table (Kocurek and Havholm, 1993; Howell and Mountney, 1997; Mountney, 2012; Rodríguez-López et al., 2014).
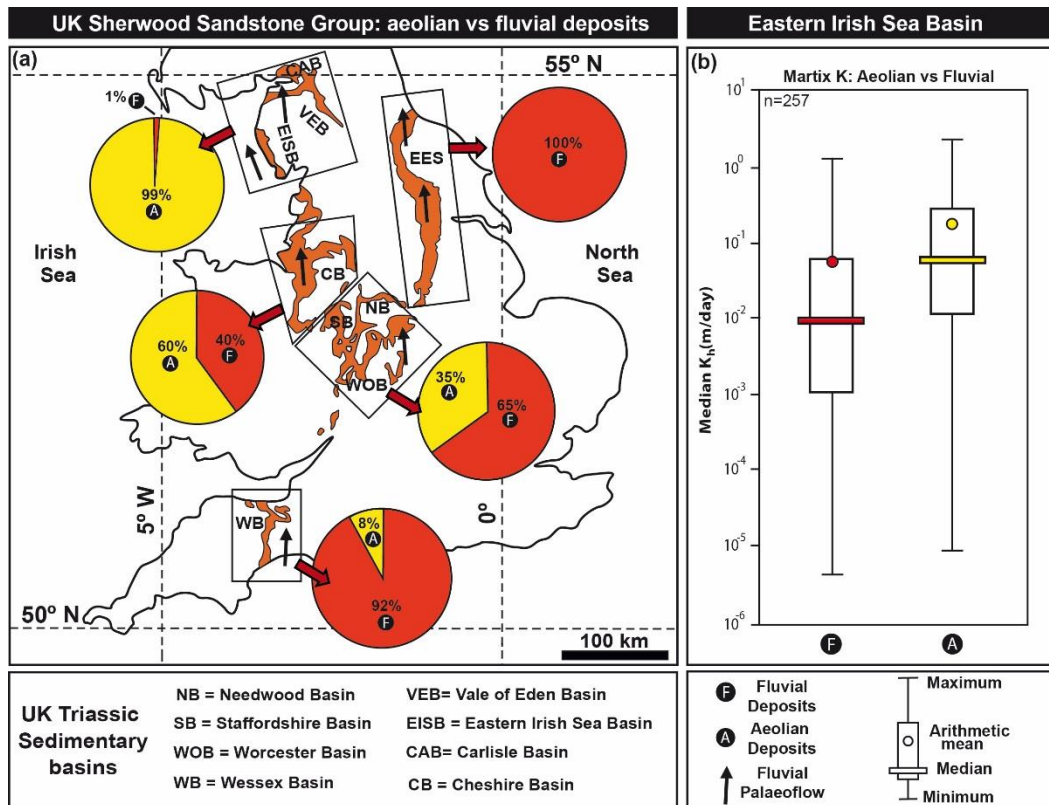
Figure 6.1: Aeolian and fluvial deposits in the UK Sherwood Sandstone Group. (a) Proportion of fluvial vs. aeolian facies in the Sherwood Sandstone Group post-Hardegsen unconformity (Purvis and Wright, 1991; Jones and Ambrose, 1994; Brookfield, 2004, 2008; Ambrose et al., 2014; Wakefield et al, 2015), (b) Aeolian vs. fluvial horizontal plug-scale hydraulic conductivity in the Sherwood Sandstone Group of the eastern Irish Sea Basin (Nirex, 1992a, 1992c, 1993b, 1993c; Allen et al., 1997)

The above discussion on preservation of aeolian facies in the Triassic rift system of the Sherwood Sandstone Group highlights how distance from the main sediment source (Armorican Massif) in a rift system affects reservoir quality. A general northward increase in typically highly permeable aeolian facies (see Fig. 6.1b) is most likely primarily due to a transitional downstream reduction in the discharge of the braided fluvial system at increasing distance from the sediment source (McKie and William, 2009; McKie and Shannon, 2011). At the same time, increasing distance from the Armorican Massif also influences the petro-hydraulic properties of the fluvial deposits. This is evident in the Eastern England Shelf which extends for ~ 200 km in latitude (Allen et al., 1997). Here, the

Sherwood Sandstone aquifer is characterized by a general northwards reduction in grain-size and porosity (Koukis, 1974; Allen et al., 1997; Pokar et al., 2006; McKie and Williams, 2009). Also, the proportion of highly permeable conglomerate and pebbly sandstone with respect to fine grained sandstone decrease at rising distance from the Variscan uplands (Figures 6.2, 6.3 lower part). Flow logs from the southern Eastern England Shelf show how these conglomerate and pebbly sandstone lithofacies dominate the flow at depths < 150 mBGL (Taylor et al., 2003). Thus, northwards reduction in such coarse-grained and permeable lithofacies well fit a corresponding northwards decrease in transmissivity (Figure 6.2 a-c).
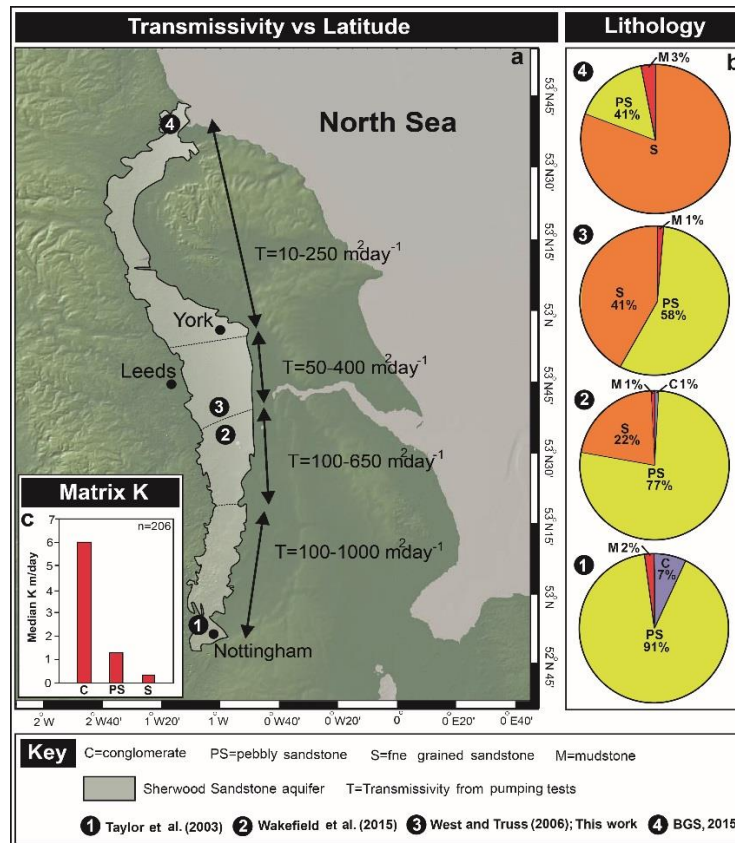
Figure 6.2: Sherwood Sandstone aquifer of the eastern England Shelf. (a) Northward reduction in transmissivity in the Sherwood Sandstone aquifer (from Allen et al., 1997), (b) Northward variation in the relative proportion in the principal lithofacies characterizing the aquifer (data from Taylor et al., 2003, West and Truss, 2006; BGS, 2015; Wakefield et al., 2015, this work); (c) Horizontal hydraulic conductivity in three different lithofacies (Lovelock, 1977).

Hence, increasing distance from the sediment source in continental deposits in rift systems improves hydrocarbon reservoir quality in mixed fluvial and aeolian successions because of an increase in the proportion of porous deposits of aeolian dune origin (see Figure 6.3, upper part and Figure 6.4 left side). At the same time, extensional tectonics favours preservation of aeolian facies in highly subsiding basins (>100 m/Myr) by rapidly placing them below the water table (Figure 6.3). By contrast, reservoir quality decreases at increasing distance from the uplands source of sediment in pure fluvial reservoirs, i.e. due to progressive reduction of coarse grained lithofacies, porosity and permeability (Figure 6.4).
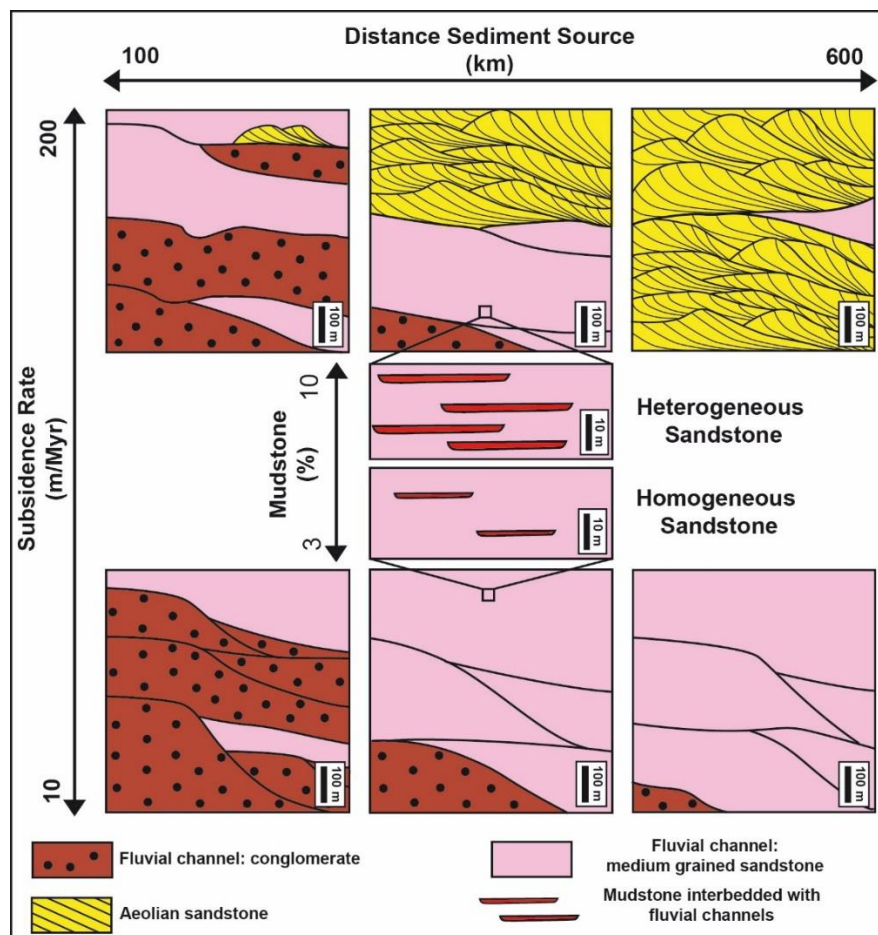
Figure 6.3: Fluvial and aeolian facies associations as a function of subsidence rate and distance from sediment source.
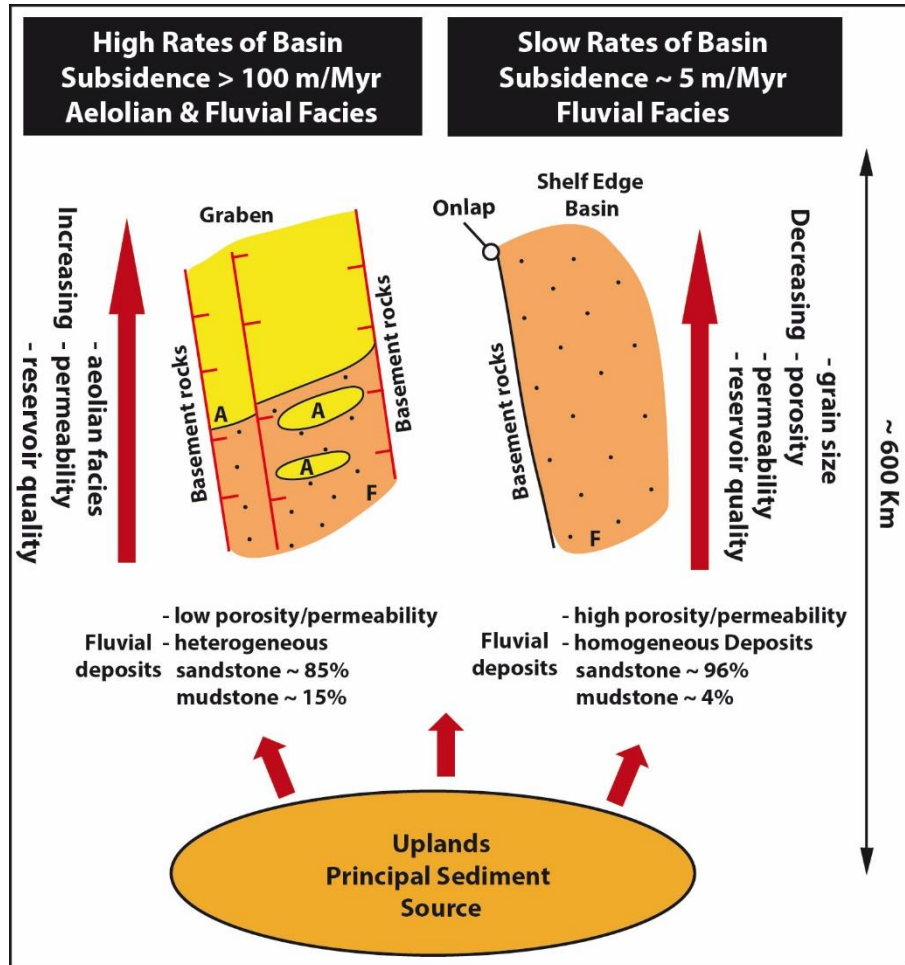
Figure 6.4: Conceptual maps of the petro-hydraulic properties of fluvial (F) and aeolian (A) deposits in rift settings.

6.2.3 Tectonic structures in the various sediment types

In the Sherwood Sandstone aquifer, principal tectonic structures are characterized by vertical joints, which terminate in correspondence of bedding plane fractures and normal faults (Ameen, 1995; Tellam and Barker, 2006; Hitchmough et al., 2007). Stratabound joints likely do not affect flow at reservoir depths (>1.0 Km): (i) such unloading structures do not persist at such depths (Gillespie et al., 2001); and (ii) dominance of matrix flow at ~1 km depth seen in this work. However, normal faults represent tectonic structures influencing oil recovery in different ways, depending on their structural style (Caine et al., 1996; Allen et al., 1997; Faulkner et al., 2009; Bense et al., 2013). In fact, normal faults in the

Triassic continental successions of Great Britain represent both barriers and preferential flow pathways for water (Tellam and Barker, 2006). Extensional faults deforming the aeolian Wilmslow and the Helsby Sandstone formations in the Cheshire Basin were recognized as flow-barriers based on (i) the geochemical evidence of limited water mixing between compartmentalized horsts and grabens (Mohamed and Worden, 2006), (ii) contouring of the water table depths, which follow the structural trends in the Cheshire Basin (Seymour et al. 2006), and sharp differences in hydraulic head depths in horst and graben structures (Mohamed and Worden, 2006; Tellam and Barker, 2006). Several authors recognized a particular development of granulation seams in the aeolian deposits of the Cheshire Basin, explaining the strong barrier behaviour of such normal faults (Beach et al., 1997; Tellam and Barker, 2006; Griffith et al., 2016).

However, extensional faults in the UK Sherwood Sandstone aquifer also reveal experimental evidence whereby such faults act as conduits for water flow parallel to the fault planes (Mohamed and Worden, 2006; Tellam and Barker, 2006; Bense et al., 2013). High artesian flows to wells (470 m^3/day) have been recognized in correspondence of an extensional fault in the fine- to medium-grained fluvial deposits of the Vale of Eden Basin. Additionally, springs are aligned in correspondence of some normal faults in the pebble beds of the Worcester Basin, such that water finds preferential pathways along the principal fault planes (Ingram, 1978; Fletcher, 1994). This Thesis shows how high values of field-scale permeability and localization of well in-flows occur up ~ 1 km depth in correspondence with fault damage zones in the St Bees Sandstone aquifer. This provides further evidence on how fault structures intercepted by boreholes represent preferential flow pathways parallel to the fault planes in fluvial deposits. This arises from the high mechanical resistance of the St Bees Sandstone Formation in West Cumbria (UCS_{nat} up to 36 MPa), which favours open fracture development (Hawkins et al., 1992; Yates, 1992; Gutmanis et al. 1998). Further reasons for the conduit behaviour of normal faults in the Triassic fluvial deposits of the eastern Irish Sea Basin lies in their mineralogical composition. The presence of argilliceous matrix in fluvial deposits creates a mechanical

anisotropy with respect to the quarzo-feldspatic grains, which favours brittle failure at relatively low yield stress (Knott, 1994; Strong et al., 1994). By contrast, aeolian deposits in the Sherwood Sandstone Group (as in other aeolian successions worldwide) show a quarzitic matrix which favours granulation seams in fault zones (Knott, 1994; Fossen et al., 2007; Deng and Aydin, 2012; Tueckmantel et al., 2012; Griffith et al., 2016). Hence, faults in aeolian deposits show strong barrier behaviour perpendicular to the fault plane. Additionally, such normal faults show no experimental evidence of flow conduit behaviour when intercepted by boreholes, based on a large amount of pumping tests on the Triassic aeolian sandstones of Great Britain (Allen et al., 1997). Thus, normal faults affecting aeolian deposits in oil reservoirs possibly reduce reservoir quality because plug-scale low-permeability zones reduce large-scale aquifer properties as demonstrated by the strong aquifer compartmentalization in the Triassic aeolian sandstone of the Cheshire Basin (Mohamed and Worden 2006; Griffith et al., 2016).

6.3 UK Sherwood Sandstone vs. analogous successions

The Sherwood Sandstone Group represents a siliciclastic sedimentary succession deposited in a continental rift that can be compared to other sandstone aquifers and reservoirs in similar palaeoenvironmental settings (Table 6.1). For example, the Permian Penrith Sandstone in NW England and the Cambrian Mount Simon aquifers in North America are similar to the Sherwood Sandstone aquifer in that they represent continental sedimentary successions characterized by the following attributes: (i) both carbonate and silicate cement (Hoholick et al., 1984; Strong et al., 1994); (ii) relatively high transmissivity due to fracture flow through bedding plane fractures at depths < 150 mBGL (Price et al., 1982; Gellasch et al., 2013).

Table 6.1: Geological and mechanical characteristics of selected fluvio-aeolian sandstone types shown in Figure 6.5.

Aquifer/Reservoir (Age)	Basin	Depositional Environment	Cement	UCS$_{nat}$ (MPa)
Aquifers				
St Bees Sandstone Formation (Triassic)	Eastern Irish Sea Basin	Fluvial (Macchi, 1991)	Silicate/ Carbonate (Strong et al., 1994)	17-36 (Thompson and Leach, 1985)
Wilmslow Sandstone Formation (Triassic)	Cheshire Basin	Aeolian/Fluvial (Thompson, 1969)	Silicate/ Carbonate (Naylor et al., 1989)	31 (West, 1979)
Undivided Sherwood Sandstone Group (Triassic)	Eastern England Shelf	Fluvial (Wackefield et al,, 2015)	Silicate/ Carbonate (Burley, 1984)	1-22 (Walsby et al., 1980)
Broomsgrove Sandstone Formation (Triassic)	Worcester Basin	Fluvial/Aeolian (McKie and Williams, 2009)	Silicate/ Carbonate (Burley, 1984)	0-16 (Whittaker and Turner, 1980)
Penrith Sandstone Formation (Permian)	Permian Basin	Aeolian (Waugh, 1970)	Silicate/ Carbonate (Waugh, 1970)	28-90 (Hawkins et al., 1992)
Mount Simon Formation (Cambrian)	Illinois Basin	Fluvial/Aeolian (Swanson et al., 2006)	Silcate/Carbonate (Hoholick et al., 1984)	24-52 (Dewers et al., 2014)
Hydrocarbon Reservoirs				
Skagerrak Formation (Triassic)	Viking Graben	Fluvial (McKie and Williams, 2009)	Silcate/Halite/Chlorite (Nguyen et al., 2013)	N/A
Mae Taeng Formation (Miocene)	Pattani Basin	Fluvial (Zheng et al., 2003)	Silcate/Kaolinite/Carbonate (Trevena and Clark, 1986)	N/A
Nugget Sandstone Formation	Fossil Basin	Aeolian (Linquist, 1988)	Silcate/Halite/Carbonate (James et al., 1986)	N/A

6.3.1 Synthesis of hydraulic behaviour of continental successions

A synthesis of information on the up-scaling properties of terrestrial siliciclastic sedimentary successions, from the near surface up to hydrocarbon reservoir depths, is shown in Figure 6.5. Field scale permeability (and transmissivity) decreases with depth (Figure 6.5a), as well as ratio of field and plug-scale permeability (Figure 6.5 b). The rate of

plug and field scale permeability is typically relatively high ($K_{field-scale}/K_{plug-scale}$>1.7) at shallow depths (<150 mGL) indicating important contribution of fracture flow at such depths. Despite this, difference is variable between the sedimentary successions analysed in Fig. 6.5. For example, the ratio between field- and plug-scale permeability is typically ~ 4 in the Mt Simon Sandstone aquifer in North America, the Penrith Sandstone in NW England and the UK Sherwood Sandstone Group in the Cheshire area (so these represent dual-permeability aquifers) but rises up to ~ 10^2 in essentially fracture flow aquifers such as the shallow St Bees Sandstone of the Eastern Irish Sea Basin. Hence, these shallow aquifers do not allow to extract information on the flow behaviour of sedimentary heterogeneities due to the dominance of fracture flow.

To address this issue, hydraulic data have been analysed in this work up to 1.1 km depth in the St Bees Sandstone which represents the fluvial part of the Sherwood Sandstone Group of the Eastern Irish Sea Basin. These data show how below the shallow alteration zone (<~150 mBGL) fractures progressively close. Hence, matrix dominates the flow and plug and field scale substantially coincide ($K_{well-test}/K_{plug-scale}$=1.3) at 1 km depth. Despite this, the findings of this investigation of a sandstone aquifer-type can be enlarged by comparing the Sherwood Sandstone Group to the hydraulic behaviour of hydrocarbon reservoirs at depth > 1 km BGL. Figures 6.5b shows how, at depths > 1 km BGL, flow is dominated by matrix and the ratio between plug- and field-scale permeability approximates to unity. In fact, in the three other examples of > 1 km depth that are included, field-scale permeability closely approximates intergranular permeability in siliciclastic continental deposits of the Mae Taeng Formation (~2.8 Km depth) in the Gulf of Thailand, of the Skagerrak Formation of the North Sea and of the Nugget Sandstone Formation in Wyoming (Bennet and Clark, 1985; Zheng et al., 2000; 2003). Thus, the St Bees Sandstone aquifer below its alteration zone represents (~150 mBGL) a valid hydraulic analogue of similar reservoir successions which progressively better approximate reservoir conditions at increasing depth (Figure 6.5b).
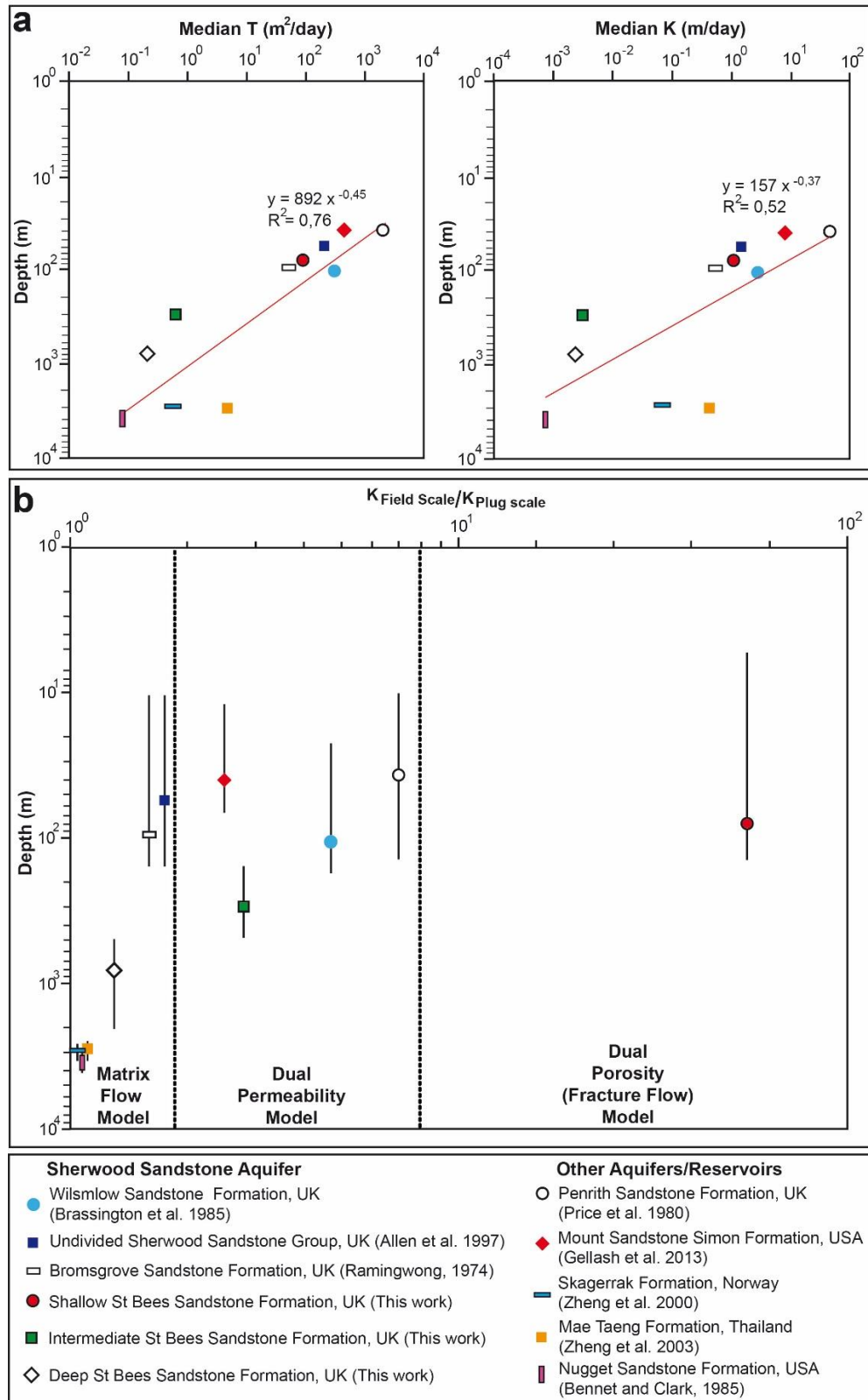
Figure 6.5: Aquifers and hydrocarbon reservoirs hosted in continental siliciclastic successions. (a) Decrease in median transmissivity and field-scale hydraulic conductivity at increasing depth, (b) Ratio between field and plug-scale hydraulic conductivity vs. depth (bars show screen length).

6.3.2 Nature of alteration and matrix versus fracture flow

Traces of alteration in correspondence of bedding plane and vertical joints have been detected, as for the St Bees Sandstone Formation in this work, using optical televiewer logs in both the Cambrian Mt Simon Sandstone aquifer of North America and the Permian Sandstone aquifer of NW England (Prince et al., 1980; Runkel et al., 2006). In the Cambrian Sandstone of North America the alteration was related, to dissolution of calcite in correspondence of fractures and the closest pores to discontinuities (Runkel et al., 2006; Swanson et al., 2006; Leaf et al., 2012). Additionally, isotope, major and trace element geochemistry show how calcite and dolomite cements dissolve to produce bicarbonate, magnesium and calcium ions in the UK Sherwood Sandstone Group (Cronin et al., 2005; Shand et al., 2007). Thus, dissolution of carbonate cement enlarging pores and fractures explain the high field scale permeability seen at shallow depth in Figure 6.5a.

However, carbonate dissolution processes do not fully explain the relative importance of fracture vs. matrix flow in shallow sandstone aquifers, which seems to be largely determined by the mechanical properties of the sandstone such as the UCS (Table 6.1). The Sherwood Sandstone aquifer of the eastern England Shelf and Worcester Basin, which are dominated by matrix flow, are mechanically weak (UCS_{nat} =0-22 MPa) and are not heavily fractured in outcropping faces and boreholes (West, 1979; Whithworth and Turner, 1989; Allen et al. 1997, 1998). Stratabound fractures are absent in the pebble beds units of the Worcester Basin and typically do not appear in the Triassic sandstone of the eastern England Shelf (Allen et al., 1998; Bouch et al., 2006). By contrast, fracture flow exceeds intergranular flow in the relatively highly mechanically resistant (UCS_{nat} = 17 - 90 MPa) continental successions of the Sherwood Sandstone Group in the Cheshire and eastern Irish Sea basins, in the UK Penrith and in the USA Mount Simon Sandstone aquifers (Price et al., 1980; Brassington et al., 1985; Swanson et al., 2006; Gellasch et al., 2013). Notably, the shallow St Bees Sandstone aquifer is characterized by

particularly elevated difference between field and plug scale transmissivity (~ 10^2), with respect to other mechanically resistant and fractured sandstone-types (Figure 6.5b).

The highly mechanically resistant sandstone aquifers (including St Bees Sandstone aquifer of the eastern Irish Sea Basin) show several common characteristics (Table 6.1). The St Bees Sandstone, the Wilsmlow and Penrith Sandstone aquifers of NW England and the USA Mount Simon aquifer are all characterized by silica-carbonate cement (Table 6.1). Additionally, these aquifers are currently exposed to weathering due to a wet climate, hence, show a similar potential in terms of carbonate dissolution by groundwater (Burley, 1984; Field et al., 1997; Hoholick et al., 1984; Naylor et al., 1989; Strong et al., 1994; Lawler et al., 2006). Furthermore, the St Bees Sandstone aquifer was exposed to wheathering for a similar time and is characterized by a similar stratabound fracturing network as the Wilsmlow and Penrith sandstone aquifers due to contemporaneous Cenozoic uplift in NW Europe (Evans et al., 1993; Chadwick et al., 1994; Chadwick, 1997; Allen et al., 1998; Carminati et al., 2009).

The case of the St Bees Sandstone aquifer of the St Bees-Egremont area remains somewhat unique with regards to its very high field-to-plug scale permeability ratio, see Figure 6.5b. This is because local conditions enhance alteration in correspondence of bedding and stratabound fractures. The St Bees Sandstone aquifer represents the only aquifer in this review that is located in a coastal setting, with tested boreholes which are located ~ 5 km west of the edge of the Lake District topographic high (Brassington et al., 1985; Black and Brightman, 1996; Gellasch et al., 2013). Thus, particularly rapid groundwater flow occurs, driven by topography towards the sea as indicated by hydraulic head measurements undertaken by the Westbay monitoring system in the Sellafield plain (Black and Brightman, 1996), enhancing carbonate dissolution.

6.3.3 Conceptual model of the hydraulic property variation with the depth in sandstone-porous media

This review on the hydraulic properties of sandstone aquifers of fluvial and aeolian origin depicts the conceptual model illustrated in Figure 6.6. Such sandstone-types are characterized by reduction of field-scale permeability due to decreasing of alteration and fracture closing processes at increasing depth. A key factor which controls the hydraulic properties of sandstone aquifers at relatively shallow depths (<~150 mBGL) is represented by the mechanical resistance. In fact, weak (UCS_{nat} < 20 MPa) sandstone-types (e.g., Bromgroove Sandstone Formation) which show a less developed fracturing network, even at shallow depths are characterized by dominance of matrix flow. However, fracture flow exceeds matrix flow in sandstone aquifers which are characterized by high mechanical resistance (e.g., St Bees Sandstone, Penrith and Mt Simon Sandstone formations) due to development of pervasive fracturing networks. This hydraulic scenario can be extreme, as for the St Bees Sandstone aquifer studied in this Thesis, when local conditions strongly enhance groundwater alteration in fractured aquifers (Figure 6.6). Steep morphologies occurring in the proximity of horsts typically trigger elevated groundwater flow and alteration (Black and Brightman, 1996). Alternatively, time of exposure to weathering > 500 Myr occurring in the African and Australian cratons develop karst-like features, up to a few meters (Wray, 1997; Worthington et al., 2016). Long exposure time thus potentially represents a further reason for large differences ($K_{well-test}/K_{plug-scale}$ ~ 10^2) between plug and field scale permeability in sandstone aquifers. Note that lack of hydraulic tests undertaken in remote areas such as the cratons mentioned do not allow direct comparison with the St Bees Sandstone aquifer.

After an abrupt decrease of the ratio in field to plug scale below the alteration zone; this ratio gradually decreases, as observed in the St Bees Sandstone aquifer of West Cumbria, up to approximate unity in deep (1-4 km) hydrocarbon reservoirs. Despite this, the majority of fractured sandstone aquifers (e.g., Penrith, Mt Simon and Wilmslow Sandstone

aquifers) do not display such an abrupt reduction of this ratio below the alteration zone, i.e. because lack of high groundwater flow does not allow high $K_{field\text{-}scale}/K_{plug\text{-}scale}$ at shallow depths (Figure 6.6).
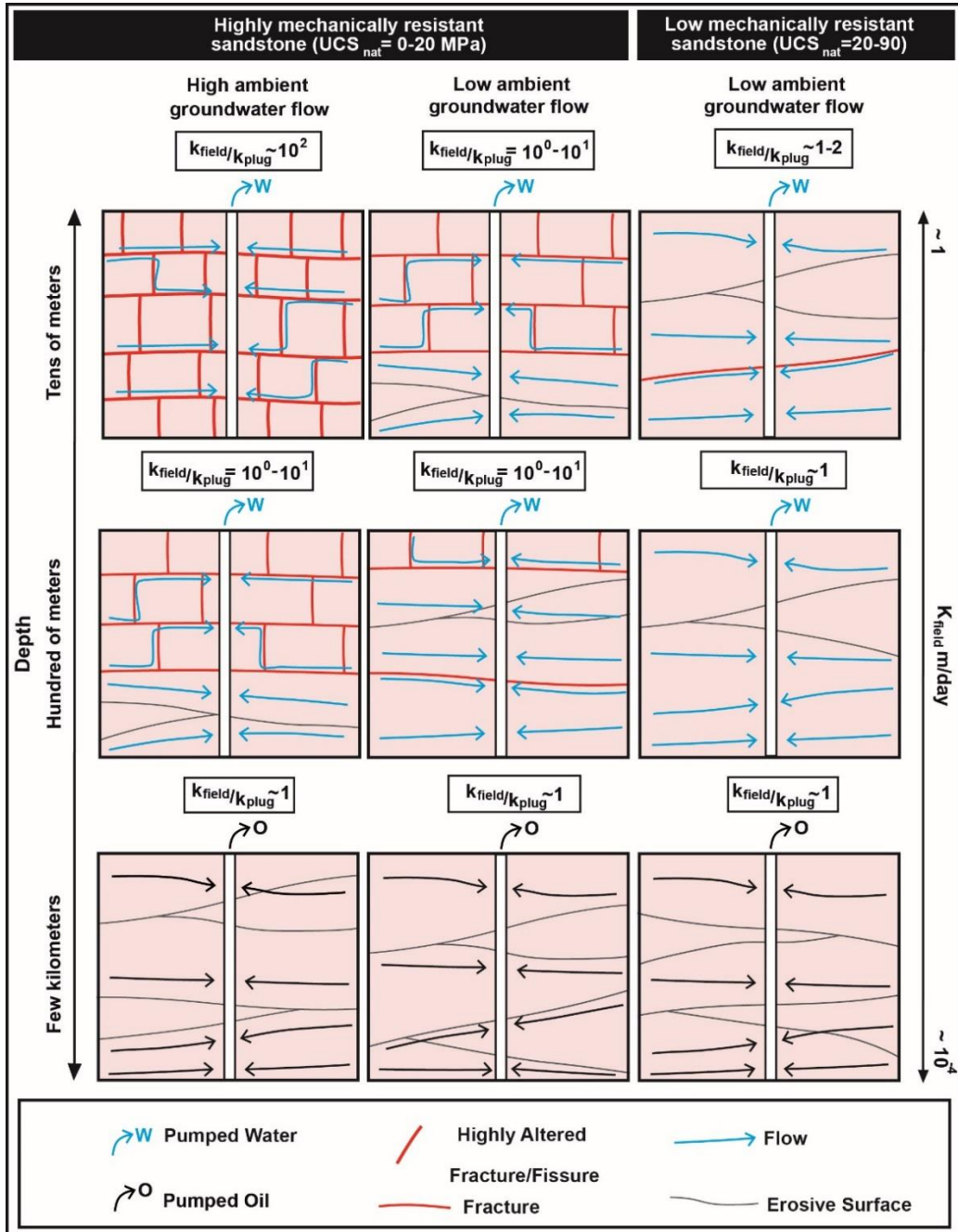
Figure 6.6: Conceptual model of the hydraulic behaviour of sandstone aquifers at increasing depths (un-faulted areas).

6.3.4 Role of tectonic structures such as faults

The Sherwood Sandstone Group is also characterized by other tectonic structures such as normal faults. These tectonic structures represent favourable flow pathways in the Triassic fluvial deposits of the eastern Irish Sea Basin when intercepted by boreholes up to ~ 1 km depth. The hydraulic behaviour of this sandstone aquifer at depths ~ 1 km closely reproduces those of deeper reservoirs, i.e. showing dominance of matrix flow (Figure 6.6). Thus, normal faults likely also represent favourable flow pathways in similar fluvial sandstone-types that represent producing reservoirs in the North Sea (McKie and Williams, 2009). However, normal faults in the aeolian deposits of the Sherwood Sandstone Group strongly compartmentalize the aquifer of the Cheshire Basin, i.e. via development of swarms of granulation seams (Figure 6.7a; Mohamed and Worden, 2006; Seymour et al., 2006; Griffith et al., 2016). Despite this, pumping tests in the aeolian Triassic sandstones of Great Britain are not obviously influenced by presence of faults, probably due to the wide variety of factors affecting field-scale permeability in their alteration zones (Allen et al., 1997). However, granulation seams effectively reduce permeability in well tests in the Jurassic aeolian reservoirs of the Nugget Formation in Wyoming, Idaho and Utah (Lewis, 1993; Olsson et al., 2004). Reduction in field-scale permeability (Figure 6.7b) in the latter aeolian reservoirs contrasts with the general hydraulic behaviour of faults in sedimentary basins which, despite the presence of a range of flow barriers (e.g., granulation seams, mineralized veins, normal drags and fault smears), typically represent favourable flow pathways where wells penetrate the main fault plane (Lewis, 1993; Caine et al., 1996; Olsson et al., 2004; Bense et al., 2013). This reduction in field-scale permeability in the aeolian reservoirs of the Nugget Sandstone Formation of Wyoming, Idaho and Utah associated with faults fits with the typically higher occurrence of granulation seams in such aeolian deposits compared to more typical continental fluvial successions (as illustrated in Figure 6.6, and by Knott, 1994).
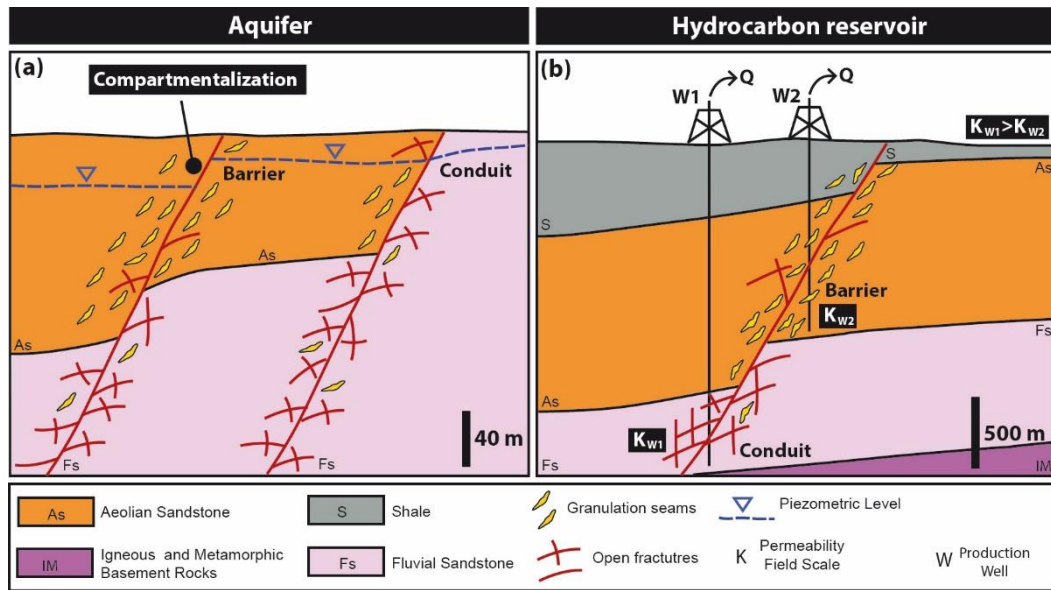
Figure 6.7: Conceptual model of hydraulic behaviour of normal faults in continental successions. (a) Normal faults in shallow aquifers, (b) Normal faults in on-shore reservoirs.

6.3.5 Effect of sedimentary facies

The effect of sedimentary facies on fluid flow is difficult to study in shallow sandstone aquifers due to the dominance of groundwater flow in correspondence with fractures. Studies from deeper fluvial successions accumulated in the NW Europe Triassic realm, show how mudstone and sheet-like sandstone (deposited by non-confined fluvial events) represent low-permeability heterogeneities that arose due to the presence of a relatively high abundance of clay minerals (Meadows and Beach, 1993 a; Henares et al., 2006; Olivarious et al., 2015). These mudstone and sheet-like sandstones reduce the field-scale permeability in zones where they represent > 10% of the succession, as typically occurs in rapidly subsiding basins (Figure 6.3). Deposits of aeolian dune origin are typically relatively permeable, due to their lower clay mineral content, thereby improving reservoir quality in mixed fluvial and aeolian successions (Newell, 2001; McKie and Williams, 2009). This is indicated by plug-scale analyses from the Triassic syn-rift successions of the West Cumbria as well as in the off-shore areas of the Irish Sea and the Norwigean and Danish North Sea (Fig.

6.1b; Olsen, 1987; Meadows and Beach, 1993 a; Nguyen et al., 2013, Olivarious et al., 2015).

6.4 Flow in continental sedimentary successions: concluding remarks

Aeolian and fluvial siliciclastic successions form thick successions (>1 km) in basins for which accommodation was generated in response to extensional, compressional and strike-slip tectonics as well as thermal subsidence. These deposits, such as the UK Sherwood Sandstone Group, cyclically occur over the geological time scale in rift settings due to break-up of supercontinents.

Extensional tectonics creates uplands representing the source of sediments for much of the fill of rift basins. This work shows how distance for the main sediment source and extensional tectonics play an opposite role on reservoir quality in mixed aeolian-fluvial and exclusively fluvial successions. Increasing distance from the main sediment source increases reservoir quality in mixed fluvial and aeolian reservoirs; content of highly porous and permeable deposits of aeolian dune origin rises due to reduction in the discharge of the fluvial system at increasing distance from the sediment source entering an arid basin. At the same time extensional tectonics favours preservation of aeolian facies in highly subsiding basins (> ~100 m/Myr) by rapidly placing them below the water table. By contrast, reservoir quality decreases in fluvial reservoirs due to reduction in grain size, porosity and permeability at rising distance from the principal sediment source. Additionally, high subsidence rates favour preservation of low permeability layers deposited by non-confined fluvial events which reduce permeability.

Normal faults represent flow heterogeneities of tectonic origin in rift settings. These tectonic structures typically represent favourable flow pathways, as for example in fluvial deposits, when intercepted by the production wells in sedimentary basins. However, normal faults in aeolian

deposits, which are characterized by development of granulation seams, are able to reduce field-scale permeability even in cases where they are intercepted by the producing well.

Both field-scale permeability and the ratio between field and upscaled plug-scale permeability decreases with depth in sediment sequences of fluvial and aeolian basins. Changes in this ratio arise from the much larger reduction in fracture permeability compared to matrix permeability, with increasing depth. This is due to fracture alteration (driven by calcite dissolution) being restricted to the zone of meteoric groundwater circulation in the upper hundred or so metres, and fracture closure by lithostatic pressure at greater depths. Difference between plug and field scale permeability is typically relatively high (~4) at shallow depths (<~150 mBGL) in relatively high mechanically resistant (UCS_{nat}>~20 Mpa) sandstone due to favourable fracture development. Despite this, difference in the ratio of field scale to plug scale permeability rises up to ~ 100, in the shallow St Bees Sandstone aquifer, in costal settings close to the bounding basin faults, probably due to particularly high groundwater flow related to the hilly topography due to the presence of a paleo-morpho-structural high (Lake District Massif) in the proximity of the boreholes.

The difference between plug- and field-scale permeability decreases in fractured sandstones at higher depths, approaching unity at ~ 1 km depth. Thus, at such depths, siliciclastic successions of continental origin are dominated by intergranular flow, hence representing optimum hydraulic analogues for successions hosting hydrocarbons at even higher depths (up ~ 4 km).

Chapter 7

Conclusions

7.1 Overview

The work reported in this thesis represents a multidisciplinary study of a fluvial aquifer of Triassic age in a rift setting. Results show how both sedimentary (mudstone, sheet-like and white fine-grained silty sandstone) and tectonic (stratabound joints, normal faults) heterogeneities effect fluid flow up to ~1 km depth. This multi-disciplinary project has involved a range of sedimentological, structural and hydro-geophysical analyses mainly focused on the Triassic St Bees Sandstone Formation of the eastern Irish Sea Basin. This formation is particularly well suited to such studies for the following reasons: (i) the succession preserves fine-grained mudstone units of fluvial overbank origin interbedded with coarser-grained sandstone units of fluvial channel origin (see Chapter 3); and (ii) the successions is characterised by development of pervasive open fractures up to several hundred meter depths (see Chapters 4 and 5). Well pumping tests and flow logs at both shallow and elevated depths have been analysed, the aim being to characterize the respective role of matrix vs. fracture flow (see Chapters 4 and 5). These analyses reveal how the St Bees Sandstone aquifer has a shallow fracture alteration zone persisting up to depths ranging from ~100 and ~200 mBGL, above which typical represents a dual porosity aquifer. Below this alteration zone, the fluvial St Bees Sandstone aquifer can be modelled as a dual permeability aquifer with matrix flow becoming dominant at ~1 km depth. At such depth (~1 km), highly mechanically resistant sandstone units are dominated by intergranular flow, hence representing optimum hydraulic analogues for hydrocarbon reservoirs at much higher depths (up ~ 5 km); see Chapter 6.

7.2 Summary of findings

The UK Sherwood Sandstone Group has been extensively investigated in the last few decades since it represents both the UK's second most important aquifer, and a strategic reservoir analogue for hydrocarbon reservoirs of the Irish Sea and North Sea.

The Sherwood Sandstone Group is generally characterized by both aeolian and fluvial deposits. In the fluvial parts, heterogeneities such as mudstones deposited by overbank flood events represent low permeability layers interbedded with highly permeable channels. However, open fractures and granulation seams represent tectonic heterogeneities acting as preferential flow pathways and barriers, respectively. Pumping tests in the UK Sherwood Sandstone aquifer have mostly been realised at shallow (~150 mBGL) depths and reveal relatively high transmissivity values of 10^1-10^3 m^2/day. However, average matrix permeability values and the ratio between plug- and field-scale ($K_{plug-scale}$/$K_{field-scale}$) hydraulic conductivity, show regional differences due to the different subsidence rates of Triassic basins of the UK.

7.2.1 Sedimentological work

The sedimentological work undertaken as part of this research demonstrates the influence of subsidence on preservation of fine-grained heterogeneities in fluvial sedimentary successions, which act as baffles for fluid flow in the St Bees Sandstone aquifer at depths > 150 mBGL. The fluvial depositional architecture of deposits of the Sherwood Sandstone Group of the eastern Irish Sea Basin (a half-graben) is compared with similar fluvial deposits of the eastern England Shelf (a shelf-edge basin).

The studied fluvial successions of both of these basins were affected by a similar set of allogenic factors, including climate, sediment source and sediment delivery style. However, a principal difference was the differential rates of accommodation generation at the time of sedimentation in

response to differing tectonic subsidence between basins. Dividing the pre-existing average thickness values by the age of the fluvial deposits of the eastern Irish Sea Basin and eastern England Shelf has allowed constraint on sedimentation rates using the preserved thickness: 119 m/Myr for the easternmost Irish Sea Basin. For the eastern England Shelf, values range from 18.0 to 19.4 m/Myr (given the uncertainty associated with the Hardegsen unconformity that if present typically cuts 150 m of stratigraphic sequence). Basins subject to a faster rate of subsidence (e.g., eastern Irish Sea Basin) tend to be characterized by greater preserved thickness and by the preserved expression of more complete fluvial depositional cycles representative of channel cutting, filling by fine-grained sandy barforms and abandonment as represented by silty drape bar-top deposits. Also, the faster rate of subsidence in the eastern Irish Sea Basin favoured preservation of mudstones deposited by overbank events interbedded with sandy channel deposits. By contrast, the fluvial Triassic deposits of the eastern England Shelf result in a more homogeneous sequence due to a paucity of fine-grained layers. In the eastern England Shelf, the vertical stacking of pebbly units and the general absence of fine-grained siltstone and mudstone units reflect the slow rate of accommodation generation. In this shelf-edge basin, successive fluvial cycles repeatedly reworked the uppermost parts of earlier fluvial deposits such that it is typically only the lowermost channel deposits (lags) that are preserved, whereas the finest uppermost parts of the cycles are reworked.

7.2.2 Fracture network characterization

Outcrop scanlines and optical televiewer logs have highlighted the presence of a pervasive stratabound fracture network characterizing the St Bees Sandstone aquifer of the eastern Irish Sea Basin in West Cumbria. This fracture network is characterized by two sets of orthogonal vertical joints that stop at their point of intersection with low-angle-inclined (bedding parallel) fractures. Normal faults, locally, complicate the fracturing pattern, since further open fractures cutting both stratabound joints and bedding

plane fractures occur in fault cores and damage zones. The key sedimentary heterogeneities which include thin, low-porosity layers characterized by mudstone and fine-grained sandstone were detected as low porosity layers by neutron porosity logs.

7.2.3 Importance of fractures for fluid flow

In the shallow St Bees Sandstone aquifer, marked temperature, conductivity and flow velocity variations in well-bore fluid logs are localized to bedding parallel fractures and faults, which represent the main borehole inflow and outflow points. Clear indications of the importance of fractures in contributing flow to wells in the shallow aquifer include (i) sharp changes in flow-log fluid velocity in association with principal fractures, and (ii) stratigraphic intervals up to 15 m thick showing no detectable inflows. Also, quantitative analysis of well-bore flow logs from the shallow (≤ ~150 m depth) St Bees Sandstone aquifer show that flow zones characterized by hydraulic conductivity higher than 5 m/day typically represent the 50% of the overall field-scale permeability, and are represented by the following structures: cataclasite sections where fault planes intersect the wells; single large bedding fractures; and clusters of minor bedding fractures. However, bedding fractures become the principal flow conduits to wells in the external part of fault damage zones or in non-faulted areas.

7.2.4 Effect of depth on fluid flow

The shallow St Bees Sandstone aquifer was compared with the relatively deep (150-1100 mBGL) part of the aquifer that was investigated by Streetly et al (2000) as part of the planning of the proposed Sellafield nuclear waste repository in the 1990s. This aquifer at such depths is characterized by transmissivity values which are two or three orders of magnitude lower than the St Bees Sandstone aquifer investigated in the field investigation conducted here at shallower depths (≤150 m). Such a difference may arise

because fractures are more open at relatively low vertical confining pressure (<5 MPa) in the shallower part of the aquifer. Additionally, tectonic fractures in the shallow aquifer show alteration, as indicated in optical televiewer logs. Further data, which include pumping tests, temperature and conductivity fluid logs up to ~1km depth, were analysed to further understand the cause of transmissivity reduction with depth. A match between upscaled plug and field-well test scale found at depth, suggesting that the matrix is a significant contributor to flow at depths of 150 to 1100 m. This does not seem to be the case in the shallower aquifer, because of the much larger permeability of the fracture network, which dominates over flow associated with the sedimentary matrix.

Field-scale permeability is at least two orders of magnitude (10^2) lower beyond the zone of fracture alteration. A smaller permeability reduction is seen between the intermediate (150-400 m BGL) and deep (400-1100 m BGL) St Bees Sandstone aquifer. Notably, differences between plug- and field-scale permeability, and frequency of well in-flows seen in fluid logs, also decrease between intermediate and elevated depths. This indicates how fracture closure leads to a progressively more important intergranular flow contribution with increasing depth. Thus, the most appropriate conceptual model for the behaviour of the deep St Bees Sandstone aquifer from 150 up to 1100 m BGL is a dual permeability aquifer, where flow to pumped wells is directly supported by both matrix and fractures. In contrast, normal faults show consistent hydraulic behaviour up to ~1 km depth. More generally, extensional faults in relatively mechanically resistant fluvial deposits represent flow pathways since their large damage zones are dominated by open fractures and likely represent favourable flow-pathways in analogous hydrocarbon reservoir successions.

7.2.5 Upscaling properties

The upscaling properties of the St Bees Sandstone Formation, which represents an example of cemented fluvial sandstone aquifer, were

analysed. Plug-scale permeability and NMR T_2 analyses indicate how fluvial channel sandstone bodies, which dominate the studied aquifer, represent the most hydraulically conductive lithology. However, mudstone and sheet-like sandstone facies of fluvial overbank origin and diagenetically produced white-silty sandstone facies represent low-permeability heterogeneities.

Plug-scale anisotropy (K_h/K_v ~3) of fluvial channel sandstone deposits fits field-measured values for the relatively homogeneous upper part of the sedimentary succession, where lateral continuity of low-permeability heterogeneities (sheet-like sandstone and mudstone) is low (<30 m). However, field-scale anisotropy rises (to > 34) in parts of the succession that preserve low-permeability layers in the sedimentary record; here the great lateral continuity (>200 m) of mudstone and sheet-like sandstone beds impedes vertical flow.

7.2.6 Comparison to the Sherwood Sandstone Group in other UK Triassic basins

The results of this work are compared with previous studies on the Sherwood Sandstone Group across the UK, mostly using the literature as an information source. This comparison shows how the shallow St Bees Sandstone aquifer approximates a dual porosity model. In fact, despite the porous nature of the aquifer flow is dominated by fractures as demonstrated by upscaling of screen transmissivity. This contrasts the behaviour of the Sherwood Sandstone in the other UK Triassic basins at relatively shallow depths, where flow is directly supported both by matrix and fractures. For example, field-scale permeability decreases northwards in the eastern England Shelf reflecting contemporaneous grain size and porosity reduction at increasing distance from the sediment sources which are represented by the Armorican and the London-Brabant massifs. In contrast, the effects of sedimentary facies on field scale permeability in highly mechanically resistant, fractured and low porosity aquifers is

detectable only at depths > ~150 m. In fact, above such depths, the St Bees Sandstone aquifer shows decreasing field-scale permeability and increasing anisotropy (K_h/K_v), with increasing preservation of mudstone and sheet-like sandstones.

In UK Triassic basins more widely (Wessex, Worcester, Needwood, Staffordshire, Cheshire, eastern Irish Sea Basin, Vale of Eden and Carlisle basins) which are characterized by both fluvial and aeolian sediments the latter deposits progressively become more abundant at increasing distance from the main sediment source. This arises from a transitional downstream reduction in the discharge of the braided fluvial system entering in arid basins. Thus, reservoir quality rises at increasing distance from the fluvial sediment source in mixed fluvial and aeolian successions, i.e. due to much higher porosity and plug-scale permeability of sediments of aeolian dune origin.

7.2.7 Comparison to other siliciclastic sequences

Field-scale permeability, and the ratio of field- to plug-scale permeability, decrease with depth as shown in hydraulic studies published on siliciclastic continental sequences worldwide. Changes in this ratio arise from the much larger reduction in fracture than matrix permeability with increasing depth. This is due to fracture alteration being restricted at depths < ~150mBGL, and also fracture closure by lithostatic pressure at greater depths. Difference between plug and field scale permeability ($K_{field-scale}/K_{plug-scale}$) is typically relatively high (> 4) at shallow depths (<~150 mGL) in relatively highly mechanically resistant (UCS_{nat}> 20 MPa) sandstone units due to fracture development. However, this ratio ($K_{field-scale}/K_{plug-scale}$) rises up to ~100, in settings with indirect recharge due to occurrence of particularly high groundwater flow. This was the case in the St Bees Sandstone aquifer investigated here, due to surface water input from the morphological high of the Lake District Massif. In this formation and others, the difference between plug- and field-scale permeability

decreased at greater depths, typically approaching unity at ~ 1 km depth or greater. Thus, at such depths siliciclastic successions of continental origin are dominated by intergranular flow, hence representing optimum hydraulic analogues for successions hosting hydrocarbons at higher depths (up ~ 1 - 4 km).

7.3 Future Work

The work presented in this Thesis has set the stage for further progress on understanding flow behaviour in heterogeneous and fractured sandstone aquifers, including investigating their hydraulic properties up to ~1 km depth (since the hydrogeological literature largely focuses on shallow depths). Also, this work has shown the potential of hydrogeological studies for improving understanding of hydrocarbon reservoirs. The research presented here would benefit from further extension, suggestions for which are listed below. This would yield the following additional and further outcomes: (i) advance the knowledge of sandstone aquifers at the plug and field scale; (ii) enlarge the research to the regional-scale (~30 km), to assess fracture connectivity at shallow depths in highly fractured sandstone lithologies.

7.3.1 Plug-scale properties of fluvial channel deposits

Channelised architectural elements typically represent the most conductive lithology in fluvial aquifers and reservoirs (Zhang et al., 2000; Henares et al., 2014). In the St Bees Sandstone Formation of West Cumbria, wire-line logs, NMR and plug-scale permeability tests have revealed how white-silty sandstone draping barforms during low flow stages represent low pore-size and relatively impermeable units within channelized elements. Despite this, additional plug-scale analyses may reveal further differences in the petrophyisical properties of channel-fill deposits that the limited number of plugs tested may hide. For example, horizontally laminated and cross-

bedded sandstone, which are respectively related to barforms deposited under upper and lower flow regime, are expected to show slight differences in terms of intergranular permeability and NMR T_2 distribution (Miall, 1977; Cheel and Middleton, 1986). Horizontally laminated sandstone (upper flow regime) is potentially less permeable, and characterized by a shorter modal T_2 picks with respect to cross-bedded sandstone (lower flow regime). Horizontally laminated sandstone in barforms deposited under upper flow-regime also appears finer grained and very well sorted in outcrop compared to those with cross-beds, in accordance to its hydro-dynamic depositional conditions. The fact that, in this study, permeability differences between these channelized fluvial bars deposited under upper and lower flow regime were not identified, is likely to be associated with the limited number of plugs which were tested in fluvial architectural elements.

7.3.2 Shallow aquifer anisotropy

Performing multi borehole pumping tests (i.e. with observation well measurements) in the shallow St Bees Sandstone aquifer will allow determination of the field-scale flow anisotropy at depths < 150 mBGL (i.e. following Hantush, 1961). This flow anisotropy is expected relatively high compared to that seen in the deep aquifer (K_h/K_v=2-34), due to the paramount importance of bedding fracture flow. Constraining the anisotropy value of the shallow St Bees Sandstone (<~150 mBGL) aquifer will allow an interesting comparison with other fractured aquifers at such depths, which show K_h/K_v values ranging from 20 up to 150 (Boulton, 1970; Neuman, 1975; Chen, 2000, Odling et al., 2013). This will potentially asses the possibility that sandstone aquifers may have a similar hydraulic behaviour with respect to the carbonate rocks due to karstification related to rapid groundwater flow occurring in coastal settings in the proximity of a morphological high.

7.3.3 Thickness of zone showing fracture alteration in lithified sandstone aquifers

Alteration in correspondence of fractures has been recognized at shallow depths in UK and USA sandstone aquifers (Price et al., 1982; Swanson et al., 2006). Packer testing in deep boreholes (230 up to 450 m) identifies this threshold in the Sherwood Sandstone Group in the Cheshire basin, although lack of optical and acoustic televiewer and wire-line logs do not allow a detailed characterization and interpretation. This work characterized the St Bees Sandstone aquifer up to ~1 km, at various depth intervals, but in different boreholes in slightly different settings. In fact, the deeper Sellafield boreholes were in areas overlain by the Calder Sandstone Formation, whereas the shallower wells were further north in the Egremont area, where the St Bees Sandstone is covered only by sandy glacial till deposits and hence subject to rapid meteoric water circulation. Pumping tests, flow velocity, wire-line and acoustic televiewer logs could be undertaken on wells with open screens penetrating the aquifer in the Egremont area up to ~350 m depth, i.e. where the shallower testing was conducted as part of this study. This would reduce ambiguity regarding the depth to which fracture alteration penetrates, in the area affected by rapid meteoric water circulation.

7.3.4 Permeability studies at regional scale

This work has investigated the hydraulic properties of a lithified sandstone aquifer from the plug up to the field-test scale using single borehole-tests. Thus, investigation scale ranged from the few centimeters of the plug up to several decametres of the pumping tests. Thus, regional value of hydraulic conductivity remains unknown as well as information on fracture connectivity at such scales (~10^3 m). In fact, enlarging the observation scale, permeability can sharply decrease where flow entirely enters the matrix, slightly decrease where the matrix represents short flow bridges connecting fractures, or increase where fracture connectivity rises with

increasing scale. Pulse tests allow determination of the regional-scale permeability; these involve a cyclic withdrawal of water from the pumping well followed by a shut in period, and by measurement of the resulting pressure pulse in an observation well. For example, pulse tests in carbonate karst aquifers of southern France allowed enlargement of the observation scale up to ~30 km, showing how permeability rises at the regional scale in such aquifers (Noushabadi et al., 2011). This experiment could be repeated using the pre-existing borehole network penetrating the Sherwood Sandstone Group at shallow (<150 mBGL) depths in West Cumbria, to assess the hydrauilc conductivity at the regional scale. Regional scale values from pulse tests may be appropriate for modelling of contaminant transport, e.g. using MODFLOW/MODPATH.

7.3.5 Flow modelling for characterization of reservoir analogues

Availability of a large amount of core logs in the BGS archives on the St Bees Sandstone Formation in the area of the proposed Sellafield repository at depths ranging from 150 up to 400 mBGL make this succession suitable for the construction of 3D geological models using the Petrel Software Package. The available data in the BGS archives distinguish the following petrophysical facies:

- Sheet-like sandstone (petro-facies 1) and mudstone (petro-facies 2) deposits of non-confined flow on the floodplain.
- Fluvial channel deposits (petro-facies 3) occurring either interbedded in the floodplain deposits or amalgamated, forming channel complexes.
- Mudstone (petro-facies 4) due to overbank events, occurring interbedded with fluvial channel deposits.
These groups of facies can be modelled in Petrel using the Object Model tools integrating background information with a relational database developed at the University of Leeds (Fluvial Architectural Knowledge Transfer System relational database, see Colombera et al., 2012a, b, 2013)

to constrain geometry of architectural elements, and hence petrophysical facies, integrating data from ancient and modern fluvial successions.

The availability of porosity and permeability plug data will allow construction of 3D facies, porosity and intergranular permeability models using the Petrel Software Package. Such 3D permeability models of the St Bees Sandstone Formation from upscaling of core plug data can represent an analogue model for similar successions which are dominated by matrix flow in deep reservoirs (> ~1 km depth). Despite this, the dual permeability nature of the St Bees Sandstone aquifer at intermediate depths (150-400 mBGL) requires the use of both fracture and matrix permeability modelling if the aim is to build a reliable 3D Petrel hydraulic model of the site surrounding for example, the previously proposed Sellafield repository, which was planned to be from 150 up to 400 mBGL.

References

Abesser, C. and Lewis M. 2015. A semi-quantitative technique for mapping potential aquifer productivity on the national scale: example of England and Wales (UK*). Hydrogeology Journal.* 23(8) pp.1677-1694.

Aitkenhead, N. 2002. British Geological Survey and Natural Environment Research Council. *British Regional Geology: The Pennines and adjacent areas.* Nottingham: British Geological Survey.

Akhurst, M.C., Chadwick, R.A., Holliday, D.W., McCormac, M., McMillan, A.A., Millward, D. and Young, B. 1997. *Geology of the west Cumbria district. Memoir of the British Geological Survey, Sheets 28, 37 and 47 (England and Wales).* Nottingham: British Geological Survey.

Akhurst, M.C., Barnes, R.P., Chadwick, R. A., Millward, D., Norton, M.G., Maddock, R. H., Kimbell, G.S. and Milodowski, A.E. 1998. Structural evolution of the Lake District Boundary Fault Zone in west Cumbria, UK. *Proceedings of the Yorkshire Geological Society*. 52, pp. 139-158.

Akin, S., 2001. Estimation of fracture relative permeabilities from unsteady state core floods. *Journal of Petroleum Science Engineering.* 30 (1), pp.1-14.

Alexander, M.C., Back, J.H. and Brightman, M.A. 1987. The role of low-permeability rocks in regional flow: In: Goff, J.C. and Williams, B.P.J. (Eds.), *Fluid flow in Sedimentary Basins and Aquifers.* Geological Society, London, Special Publications 34, pp.173-183.

Aldinucci, M., Gandin, A. and Sandrelli, F. 2008. The Mesozoic continental rifting in the Mediterranean area: insights from the Verrucano tectofacies of southern Tuscany (Northern Apennines, Italy). *International Journal of Earth Sciences*. 97(6), pp.1247-1269.

Allen D.J., Bloomfield J.P., Gibbs B.R. and Wagstaff S.J. 1998. Fracturing and the hydrogeology of the Permo-Triassic sandstones in England and Wales. *Technical Report WD/97/34*. Nottingham: British Geological Survey.

Allen, D.J., Brewerton, L.M., Coleby, B.R., Gibbs, M.A., Lewis, A.M., MacDonald, S.J., Wagstaff, A.T and Williams, L.J. 1997. The Physical Properties of Major Aquifers in England and Wales. *Technical Report WD/97/34, pp.157-287.* Nottingham: British Geological Survey.

Anketell, J.M., Cegla, J. and Dzulynsky, S. 1970. On the deformational structures in systems with reversed density gradients. *Annales de la Société Géologique Pologne.* 40, pp.3-30.

Allimendinger, R.W., Cardozo, N. and Fisher D., 2012. *Structural Geology Algorithms: Vectors and Tensors.* Cambridge: Cambridge University Press.

Al-Mahrooqi, S.H., Grattoni, C.A., Moss, A.K. and Jing, X.D. 2003. An investigation of the effect of wettability on NMR characteristics of sandstone rock and fluid systems. *Journal of Petroleum Science and Engineering.* 39(3), pp.389-398.

Al-Mahrooqi, S. H., Grattoni, C. A., Muggeridge, A. H., Zimmerman, R. W. and Jing, X. D. (2006). Pore-scale modelling of nmr relaxation for the characterization of wettability. *Journal of Petroleum Science and Engineering.* 52(1), pp.172-186.

Antonellini, M. Aydin, A.A. and Pollard D.D. 1994. Microstructure of deformation bands in porous sandstones at Arches National Park, Utah. *Journal of Structural Geology.* 16(7), pp.941-959.

Ambrose, K., Hough, E., Smith, N.J.P. and Warrington, G. 2014. Lithostratigraphy of the Sherwood Sandstone Group of England, Wales and south-west Scotland. *Research Report RR/14/01*. Nottingham: British Geological Survey.

Ameen, M.S. 1995. Fractography and fracture characterization in the Permo-Triassic sandstones and the Lower Palaeozoic Basement, West Cumbria, UK. In: Ameen, M.S. (Ed.), *Fractographic Studies-Fractography Applied to Fracture Analysis in Field Studies Aimed at Understanding Regional Tectonics.* Geological Society of London, Special Publications. 92, pp.97-147.

Appleton, P.R. 1993. Probabilistic safety assessment for the transport of radioactive waste to a UK repository at Sellafield. *International Journal of Radioactive Material Transaction*. 4(3-4), pp.205-211.

Ashworth, P.J., Sambrook Smith, G.H., Best, J.L., Bridge, J.S., Lane, A.N.D, Lunt, I.A., Reesink, A.O.J., Simpson, C.J. and Thomas, R.E. 2011. Evolution and sedimentology of a channel fill in the sandy braided South Saskatchewan River and its comparison to the deposits of an adjacent compound bar. *Sedimentology*. 58, pp.1860-1883.

Aslan, A., Austin, W.J. and Blum, M.D. 2006. Causes of river avulsion: insights from the late Holocene avulsion history of the Mississippi River, USA. *Journal of Sedimentary Research*. 76, pp.650-664

Audley-Charles, M.G. 1970. Triassic palaeogeography of the British Isles. *Quarterly Journal of the Geological Society of London*. 126, pp.49-89.

Avci, C.B. 1992. Flow occurrence between confined aquifers through improperly plugged boreholes. *Journal of Hydrology*. 139 (1-4), pp.97-114.

Baas JH, Hailwood EA, McCaffrey WD, Kay M and Jones R. 2007. Directional petrological characterisation of deep-marine sandstones using grain fabric and permeability anisotropy: methodologies, theory, application and suggestions for integration. *Earth-Science Reviews*. 82, pp.101-142.

Ball, L.B., Ge, S., Caine, J.S., Revil, A. and Jardani, A., 2010. Constraining fault-zone hydrogeology through integrated hydrological and geoelectrical analysis. *Hydrogeology Journal*. 18(5), pp.1057-1067.

Bachmann, G.H., Geluk, M.C., Warrington, G., Becker-Roman, A., Beutler, G., Hagdorn, H., Hounslow, M.W., Nitsch, E., Röhling, H.G., Simon, T. and Szulc, A. 2010. Triassic. In: Doornenbal, J.C. and Stevenson, A.G. (Eds.), *Petroleum Geological Atlas of the Southern Permian Basin Area*. Houten: EAGE Publications. pp.149-173.

Balsamo, F. and Storti F. 2010. Grain size and permeability evolution of soft-sediment extensional sub-seismic and seismic fault zones in high-

porosity sediments from the Crotone basin, southern Apennines, Italy. *Marine and Petroleum Geology*. 27(4) pp.822-837.

Banham, S.G. and Mountney N.P. 2014. Climatic versus halokinetic control on sedimentation in a dryland fluvial succession. *Sedimentology*. 61, pp.570-608.

Banham, S.G. and Mountney, N.P., 2013. Evolution of fluvial systems in salt-walled mini-basins: a review and new insights. *Sedimentary Geology*. 296, pp.142-166.

Barker, A.P., Newton, R.J., Bottrell, S.H. and Tellam, J.H. 1998. Processes affecting groundwater chemistry in a zone of saline intrusion into an urban sandstone aquifer. *Applied Geochemestry*. 13(6), pp.735-749.

Barnes, R.P., Ambrose, K., Holliday, D.W. and Jones, N.S. 1994. Lithostratigraphic subdivision of the Triassic Sherwood Sandstone Group in west Cumbria. *Proceedings of the Yorkshire Geological Society*. 50, pp.51-60.

Barrett, M. H., Kevin M.H., Stephen, P., Lerner D.N., Tellam J.H. and French, M.J. 1999. Marker species for identifying urban groundwater recharge sources: a review and case study in Nottingham, UK. *Water Resources*. 33(14), pp.3083-3097.

Bashar, K., Tellam, J.H. 2011. Sandstones of unexpectedly high diffusibility. *Journal of Contaminant Hydrology*. 122(1), pp.40-52.

Bath, A.H., Milodowski, A.E. and Strong, G.E., 1987. Fluid flow and diagenesis in the East Midlands Triassic sandstone aquifer. In: Dowing, S.A., Edmunds, W.M., Gale, I.N. (Eds.), *Fluid Flow in United Kingdom*. Geological Society of London, Special Publications 34, pp.127-140.

Bauer, S., Bayer-Raich, M., Holder, T., Kolesar, C., Müller nad D. and Ptak, T. 2004. Quantification of groundwater contamination in an urban area using integral pumping tests. *Journal of Contaminant Hydrology*. 75(3), pp.183-213.

Bauer, H., Schröckenfuchs, T.C. and Decker K. 2016. Hydrogeological properties of fault zones in a karstified carbonate aquifer (Northern Calcareous Alps, Austria). *Hydrogeology Journal*. 24(5) pp.1-24.

Beach, A., Brown, J.L., Webon, A., McCallum, J.E. and Brockbank P. and Knott S.D. 1999. In: Meadows, N.S., Trueblood, S.R., Hardman, M. and Cowan G. (Eds.), *Petroleum Geology of the Irish Sea and Adjacent Areas. Characteristics of fault zones in sandstones from NW Engalnd: application fault transmissibility*. Geological Society of London, Special Publications. 124(1), pp.315-324.

Beach, A., Welbon, A. I., Brockbank, P. J. and McCallum, J. E. 1999. Reservoir damage around faults: outcrop examples from the Suez rift. *Petroleum Geosciences*. 5(2), pp.109-116.

Bell, R.G. 1992. The durability of sandstone as building stone, especially in urban environments*. Environmental and Engineering Geoscience.* 29(1), pp.49-60.

Bennett, C.O. and Clark, T.J. 1985. Design and analysis of a nitrogen step-rate test, Anschutz Ranch east nitrogen injection project. In *SPE Annual Technical Conference and Exhibition*. Society of Petroleum Engineers.

Bense, V.F., Gleeson, T., Loveless, S.E., Bour, O. and Scibek, J. 2013. Fault zone hydrogeology. *Earth-Science Reviews*. 127, pp.171-192.

Berra, F. and Felletti, F. 2011. Syndepositional tectonics recorded by soft-sediment deformation and liquefaction structures (continental Lower Permian sediments, Southern Alps, Northern Italy): stratigraphic significance. *Sedimentary Geology*. 235, pp.249-263.

Bianchi, M., Liu, H.H. and Birkholzer J.T. 2015. Radionuclide transport behavior in a generic geological radioactive waste repository. *Groundwater*. 53(3), pp.440-451.

Berglund S., Kautsky U., Lindborg T. and Selroos J.O. 2009. Integration of hydrological and ecological modelling for the assessment of a nuclear waste repository. *Hydrogeology Journal*. 17, pp.95-113.

Berkowitz, B. 2002. Characterizing flow and transport in fractured geological media: A review. *Advances in Water Resources*. 25(8), pp.861-884.

Billi, A. 2005. Attributes and influence on fluid flow of fractures in foreland carbonates of southern Italy. *Journal of Structural Geology*. 27(9), pp.1630-1643.

Bilardo U, Borgia G.C., Bortolotti V., Fantazzini P. and Mesini E. 1991. Magnetic resonance lifetimes as a bridge between transport and structural properties of natural porous media. *Journal of Petroleum Science Engineering*. 5, pp.273-283.

Binley, A., Winship, P., West, L.J., Pokar, M. and Middleton, R. 2002. Seasonal variation of moisture content in unsaturated sandstone inferred from borehole radar and resistivity profiles. *Journal of Hydrology*. 267, pp.160-172.

Black, J.H. and Brightman, M.A. 1996. Conceptual model of the hydrogeology of Sellafield. *Quarterly Journal of Engineering Geology and Hydrogeology*. 29(1), pp.83-93.

Blanc, EJ.P., Blanc-Alétru, M.C. and Mojon., P.O. 1998. Soft-sediment deformation structures interpreted as seismites in the uppermost Aptian to lowermost Albian transgressive deposits of the Chihuahua basin (Mexico). *Geologische Rundschau*. 86, pp.875-883.

Bloomfield, J.P., Gooddy, D., Bright, M. and Williams, P. 2001. Pore-throat size distributions in Permo-Triassic sandstones from the United Kingdom and some implications for contaminant hydrogeology. *Hydrogeology Journal*. 9(3), pp.219-230.

Bloomfield, J.P., Moreau, M.F. and Newell, A.J. 2006. Characterization of permeability distribution in six lithofacies from the Helsby and Wilmslow

sandstone formations of the Cheshire Basin, UK. In: Barker, R.D., Tellam, J.H. (Eds.), *Fluid Flow and Solute Movement in Sandstones: The Onshore UK Permo-Triassic Red Bed Sequence.* Geological Society of London, Special Publications. 263, pp.83-101.

Bluck, B.J. 1971. Sedimentation in meandering River Endrick. *Scottish Journal of Geology.* 7, pp.93-138.

Bluck, B.J. 1979. Structure of coarse-grained braided-stream alluvium. *Transactions of the Royal Society of Edinburgh.* 70, pp.181-221.

Blundell, D.J. 2002. Cenozoic inversion and uplift of southern Britain. In: Doré, A.G., Cartwright, J.A., Stoker, M.S., Turner, J.P., White, N. (Eds.), Exhumation of the North Atlantic Margin; Timing, Mechanisms and Implications for Petroleum Exploration. *Geological Society of London, Special Publications.* 196, pp. 85-102.

Bond, G.C., Christie-Blick, N.K. and Delvin, W.J. 1985. An early Cambrian Rift Post-Rift Transition in the Cordiliera of Western North America. *Nature.* 315, pp.742-746.

Bosellini, A. 1989. Dynamics of Tethyan carbonate platforms. *Society Economic Paleontology and Mineralogy Special Publications.* 44, pp.3-13

Bottrell, S., Tellam, J.H., Bartlett, R., Hughes, A. 2008. Isotopic composition of sulfate as a tracer of natural and anthropogenic influences on groundwater geochemistry in an urban sandstone aquifer, Birmingham, UK. *Applied Geochemistry.* 23(8), pp.2382-2394.

Bouch, J.E., Hough, E., Kemp, S.J., McKervey, J.A., Williams, G.M. and Greswell, R.B. 2006. Sedimentary and diagenetic environments of the Wildmoor Sandstone Formation (UK): implications for groundwater and contaminant trans- port, and sand production. In: Barker, R.D. and Tellam, J.H. (Eds.). Fluid Flow and Solute Movement in Sandstones: The Onshore UK Permo-Triassic Red Bed Sequence. *Geological Society of London, Special Publications.* 263(1), pp.129-153

Boulton, N.S. 1970. Analysis of data from pumping tests in unconfined anisotropic aquifers. *Journal of Hydrology*. 10, pp.369-378.

Bourdet. D. 1983. Pressure behavior of layered reservoirs with crossflow. SPE California Regional Meeting. *Society of Petroleum Engineers*. doi:10.2118/13628-MS

Bourdet D 1985. Pressure behavior of layered reservoirs with crossflow. SPE California Regional Meeting. *Society Petroleum Engineers*. doi:10.2118/13628-MS

Bourquin, S., Peron, S. and Durnad, M. 2006. Lower Triassic sequence stratigraphy of the western part of the Germanic Basin (west of Black Forest); fluvial system evolution though time and space. *Sedimentary Geology*. 186, pp.187-211.

Bourquin, S., Guillocheau, F. and Peron, S. 2009. Braided rivers and arid alluvial plain (example from the Lower Triassic, western German Basin): recognition criteria and expression of stratigraphic cycles. *Sedimentology*. 56, pp.2235-2264.

Bourquin., S., Eschard. R., and Hamouche, B. 2010. High-resolution sequence stratigraphy of Upper Triassic succession (Carnian–Rhaetian) of the Zarzaitine outcrops (Algeria): A model of fluvio-lacustrine deposits. *Journal of African Earth Science*. 58, pp.365-386.

Bourquin, S., Bercovici, A., López-Gómez, J., Diez, J.B., Broutin, J., Ronchi, A., Durand, M., Arché, A., Linol, B. and Amour, F. 2011. The Permian–Triassic transition and the onset of Mesozoic sedimentation at the northwestern peri-Tethyan domain scale: palaeogeographic maps and geodynamic implications. *Palaeogeography, Palaeoclimatology, Palaeoecology*. 299(1), pp.265-280.

Bradbury, K.R., Borchardt, M.A., Gotkowitz, M., Spencer, S.K., Zhu, J. and Hunt, R.J. 2013. Source and transport of human enteric viruses in deep municipal water supply wells. *Environmental Science Technology*. 47(9), pp.4096-4103.

Brassington, FC. 1992. Measurements of head variations within observation boreholes and their implications for groundwater monitoring. *Water Environmental Journal.* 6(3), pp.91-100.

Brassington, F. C. and Walthall, S. 1985. Field techniques using borehole packers in hydrogeological investigations. *Quarterly Journal of Engineering Geology and Hydrogeology.* 18(2), pp.181-193.

Bray, R.J., Green, F. and Duddy, I.R. 1992. Thermal history reconstruction using apatite fission track analysis and vitrine reflectance: a case study from the UK East Midlands and Southern North Sea. In: Hardman. R.F.P. (Ed.), *Exploration Britain: Geological Insights for the Next Decade.* Geological Society of London, Special Publications. 67, pp.3-25.

Bricker, S.H., Barkwith, A.K.A.P., MacDonald, A.M., Hughes, A.G. and Smith, M. 2012. Effects of CO 2 injection on shallow groundwater resources: A hypothetical case study in the Sherwood Sandstone aquifer, UK. *International Journal of Greenhouse Gas Control.* 11, pp.337-348.

Bridge, J.S. and Leeder, M.R. 1979. A simulation model of alluvial stratigraphy. *Sedimentology.* 26, pp.617-644.

Bridge, J.S. 1985. Paleochannel Patterns Inferred From Alluvial Deposits: a Critical Evaluation Prospective. *Journal of Sedimentary Research.* 55, pp.579-589.

Bridge, J.S. 1993. The interaction between channel geometry, water flow, sediment transport and deposition in braided rivers. In: Best, J.L. and Bristow, C.S. (Eds.), *Braided Rivers.* Geological Society of London, Special Publications. 75, pp.13-71.

Bridge, J.S. 2003. *Rivers and Floodplains.* Oxford: Blackwell.

Bridge, J.S. 2006. Fluvial Facies models: Recent Developments. In: Posamentier, W. and Walker, R.G. (Eds.), *Facies Models Revisited.* SEPM Special Publication. 84, pp.85-170.

Bristow, C.S. 1988. Controls on the sedimentation of the Rough Rock Group (Namurian) from the Pennine Basin of northern England. In: Besly, B.M, Kelling, G. (Eds.), *Sedimentation in a synorogenic basin complex; the Upper Carboniferous of Northwest Europe*. Glasgow: Blackie, pp.114-131

British Geological Survey, 2015. *Onshore GeoIndex. Geological Map of Great Britain 1:650.000 scale*. Nottingham: British Geological Survey

Bristow, C.S 1988. Controls on the sedimentation of the Rough Rock Group (Namurian) from the Pennine Basin of northern England. In: Besley and B.M. and Kelling, G. (Eds.), *Sedimentation in a Synorogenic Basin Complex; the Upper Carboniferous of Northwest Europe*. Glasgow: Blackie, pp. 114-131.

Brodie, J. and White, N. 1994. Sedimentary basin inversion caused by igneous underplating: Northwest European continental shelf. *Geology*. 22(2), pp.147-150.

Bromley, M.H. 1991. Architectural features of the Kayenta Formation (Lower Jurassic), Colorado Plateau, USA: relationship to salt tectonics in the Paradox Basin. *Sedimentary Geology*. 73, pp.77-99.

Brookfield, M.E. 2004. The enigma of fine-grained alluvial basin fills: the Permo-Triassic (Cumbrian Coastal and Sherwood Sandstone Groups) of the Solway Basin, NW England and SW Scotland. *International Journal of Earth Sciences*. 93, pp.282-296.

Brookfield, M.E. 2008. Palaeoenvironments and palaeotectonics of the arid to hyperarid intracontinental latest Permian-late Triassic Solway basin (UK). *Sedimentary Geology*. 210, pp.27-47.

Burley, S.D. 1984. Patterns of diagenesis in the Sherwood Sandstone Group (Triassic), United Kingdom. *Clay Minerals*. 19, pp.403-440.

Bucher, K. and Stober, I. 2010. Fluids in the upper continental crust. *Geofluids*. 10(1-2), pp.241-253.

Butler, J.J. 1990. The role of pumping tests in site characterization: Some theoretical considerations. *Ground Water.* 28(3), pp.394-402.

Caine, J.S., Evans, J.P. and Forster, C.B. 1996. Fault zone architecture and permeability structure. *Geology.* 24(11), pp.1025-1028.

Campbell-Smith, W. 1963. Description of igneous rocks represented among pebbles from the Bunter Pebble Beds of the Midlands of England. *Bulletin of the Natural Hystory.* 2, pp.1-17.

Carminati, E., Cuffaro, M. and Doglioni, C. 2009. Cenozoic uplift of Europe. *Tectonics.* 28, TC4016, doi:10.1029/2009TC002472.

Carvalho, A.H. and Vesely F.F. 2017. Facies relationships recorded in a Late Paleozoic fluvio-deltaic system (Paraná Basin, Brazil): Insights into the timing and triggers of subaqueous sediment gravity flows. *Sedimentary Geology.* 352, 45-62

Cavinato, G.P., Carusi, C., Dall'Asta, M., Miccadei, E. and Piacentini, T. 2002. Sedimentary and tectonic evolution of Plio-Pleistocene alluvial and lacustrine deposits of Fucino Basin (central Italy). *Sedimentary Geology.* 148, pp.29-59.

Cassidy R., Comte J.C., Nitsche, W.C., Flynn R. and Ofterdinger U. 2014. Combining multi-scale geophysical techniques for robust hydro-structural characterisation in catchments underlain by hard rock in post-glacial regions. *Journal Hydrology.* 517, pp.715-731.

Chadwick, R.A., Kirby, G.A. and Baily H.E. 1994. The post-Triassic structural evolution of north-west England and adjacent parts of the East Irish Sea. *Proceedings of the Yorkshire Geological Society.* 50, pp.91-102.

Chadwick, R.A. and Evans, D.J., 1995. The timing and direction of Permo-Triassic extension in southern Britain. In: Boldy, S.A.R. (Ed.), *Permian and Triassic Rifting in Northwest Europe.* Geological Society of London, Special Publications. 91, pp.161-192.

Chadwick R.A. 1997. Fault analysis of the Cheshire Basin, NW England. In: Meadows N.S., Trueblood S.R., Hardman M. and Cowan G. (Eds.), *Petroleum Geology of the Irish Sea and Adjacent Areas*. Geological Society of London, Special Publications. 124, pp.297-313.

Charalambous, A.N., Packman, M. and Burnet, B.R. 2012. Sand pumping and well design in consolidated and semi-consolidated sandstone aquifers. *Quarterly Journal of Engineering Geology and Hydrogeology*. 45(2), pp.183-196.

Cheel, R.J. and Middleton, G.V. 1986. Horizontal laminae formed under upper flow regime plane bed conditions. *The Journal of Geology*. 94(4), pp.489-504.

Chen, X. 2000. Measurement of streambed hydraulic conductivity and its anisotropy. *Environmental Geology*. 39, pp.1317-1324.

Chen, Y., Durlofsky L.J., Gerritsen and Wen, X.H.M. 2003. A coupled local–global upscaling approach for simulating flow in highly heterogeneous formations. *Advance in Water Resources*. 26, pp.1041-1060.

Chisholm, J.I., Charsley, T.J. and Aitkenhead, N. 1988. *Geology of the country around Ashbourne and Cheadle*. London: HMSO.

Cilona, A., Aydin, A. and Johnson, N.M. 2015. Permeability of a fault zone crosscutting a sequence of sandstones and shales and its influence on hydraulic head distribution in the Chatsworth Formation, California, USA. *Hydrogeology Journal*, 23(2), pp.405-419.

Clark L. 1977. The analysis and planning of step drawdown tests. *Quarterly Journal of Engineering Geology and Hydrogeology*. 10, pp.125-143.

Clark, J.D. and Pickering, K.T., 1996. Architectural elements and growth patterns of submarine channels: application to hydrocarbon exploration. *AAPG Bulletin*. 80, pp.194-220

Clemmensen, L.B. 1985. Desert sand plain and Sabkha deposits from the Bunter Sandstone Formation (L. Triassic) at the northern margin of the German Basin. *Geologische Rundschau.* 74(3), pp.519-536.

Coleman, J.M. 1969. Brahmaputra River: channel processes and sedimentation. *Sedimentary Geology.* 3(2-3), pp.129-239.

Collinson, J.D., 1986. Alluvial Sediments. *Sedimentary environments and facies.* Oxford: Blackwell Scientific Publications.

Collinson, J.D., Mountney, N.P., Thompson, D.B. 2006. *Sedimentary Structures.* Harpenden: Terra Publishing.

Colombera, L., Felletti F., Mountney N.P. and McCaffrey W.D. 2012a. A database approach for constraining stochastic simulations of the sedimentary heterogeneity of fluvial reservoirs. *AAPG Bulletin.* 96, pp.2143-2166.

Colombera L., Mountney N.P. and McCaffrey W.D. 2012b. A relational database for the digitization of fluvial architecture: Concepts and example applications. *Petroleum Geoscience.* 18, pp.129-140.

Colombera, L., Mountney, N.P. and McCaffrey, W.D. 2013. A quantitative approach to fluvial facies models: methods and example results. *Sedimentology.* 60, pp.1526-1558.

Colombera, L., Mountney, N.P. and McCaffrey, W.D., 2015. A meta-study of relationships between fluvial channel-body stacking pattern and aggradation rate: implications for sequence stratigraphy. *Geology.* 43, pp.283-286.

Conrad, S.H., Glass, R.J. and Peplinski, W.J. 2002. Bench-scale visualization of DNAPL remediation processes in analog heterogeneous aquifers: surfactant floods and in situ oxidation using permanganate. *Journal of Contaminant Hydrology.* 58(1), pp.13-49.

Corbett P.W.M., Hamidreza H. and Hemant G. 2012. Layered fluvial reservoirs with internal fluid cross flow: a well-connected family of well test pressure transient responses. *Petroleum Geoscience*. 18, pp.219-229.

Costamagna L.G. 2012. Alluvial, aeolian and tidal deposits in the Lower to Middle Triassic "Buntsandstein" of NW Sardinia (Italy): a new interpretation of the Neo-Tethys transgression. *Zeitschrift der Deutschen Gesellschaft für Geowissenschaften*. 163, pp.165-183

Cox, F.C., 1987. Antitaxial crack-seal vein microstructures and their relationship to displacement paths. *Journal of Structural Geology*. 9, pp.779-787

Cowan, G. 1993. Identification and significance of aeolian deposits within the dominantly fluvial Sherwood Sandstone Group of the East Irish Sea Basin UK. In; North, C.P., Prosser, D.J. (Eds.). *Characterization of Fluvial and Aeolian Reservoirs*. Geological Society of London, Special Publications. 73, pp.231-245.

Coward, M.P., 1995. Structural and tectonic setting of the Permo-Triassic basins of northwest Europe. In: Boldy, S.A.R. (Eds.), *Permian and Triassic Rifting in Northewest Europe*. Geological Society of London, Special Publications. 91, pp.7-39.

Cronin, A.A., Barth, J.A.C., Elliot, T. and Kalin, R.M. 2005. Recharge velocity and geochemical evolution for the Permo-Triassic Sherwood sandstone, Northern Ireland. *Journal of Hydrology*. 315(1), pp.308-324.

Davison, C.C. and Kozak, E.T. 1988. Hydrogeological characteristics of major fracture zones in a granite batholith of the Canadian shield. In: Canadian/American Conference on Hydrogeology. *National Water Well Association*, pp.52–59.

Daw G.P., Howell F.T. and Woodhead G.A. 1974. The effect of applied stress upon the permeability of some Permian and Triassic sandstones of Northern England. *Internetional Journal of Rock Mechanics Mining Sciences, Geomechanics Abstracts*. 13, pp.537-542.

Day-Lewis, F.D., Johnson, C.D., Paillet, F.L. and Halford, K.J. 2011. A computer program for flow-log analysis of single holes (FLASH). *Ground Water* 49(6), pp.926-931.

Deng, S. and Aydin, A. 2012. Distribution of compaction bands in 3D in an aeolian sandstone: The role of cross-bed orientation. *Tectonophysics*. 574, pp.204-218.

Deramond, J., Souquet, P., Fondecave-Wallez, M.J. and Specht., M., 1993. Relationships between thrust tectonics and sequence stratigraphy surfaces in foredeeps: model and examples from the Pyrenees (Cretaceous-Eocene, France, Spain). In: Williams, G.D. (Eds.), *Tectonics and Seismic Sequence Stratigraphy*. Geological Society of London, Special Publications. 71, pp.193-219.

De Simone, L.A. 2008. Quality of water from domestic wells in principal aquifers of the United States. *US Geological Survey Science Investigation Report*. 2008-5227.

Dewers, T., Newell, P., Broome, S., Heath, J. and Bauer, S. 2014. Geomechanical behavior of Cambrian Mount Simon Sandstone reservoir lithofacies, Iowa Shelf, USA. *International Journal of Greenhouse Gas Control*. 21, pp.33-48.

Dodge W.S., Shafer J.L., Guzman-Garcia A.G. and Noble, D.A. 1995. In: *Core and Log NMR Measurements of an Iron-Rich, Glauconitic Sandstone Reservoir, 36th Annual Symposium of SPWLA, 26–29 June 1995, Paris.*

Doglioni, C., D'Agostino, N. and Mariotti, G. 1998. Normal faulting vs regional subsidence and sedimentation rate. *Marine and Petroleum Geology*. 15, pp.737-750.

Dewandel, B., Lachassagne, P., Zaidi, F.K. and Chandra S., 2011. A conceptual hydrodynamic model of a geological discontinuity in hard rock aquifers: Example of a quartz reef in granitic terrain in South India. *Journal of Hydrology*. 405(3), pp.474-487.

Domenico, P.A. and Schwartz, F.W., 1998. *Physical and chemical hydrogeology*. New York: Wiley.

Duperret, A., Vandycke, S., Mortimore, R.N. and Genter, A. 2012. How plate tectonics is recorded in chalk deposits along the eastern English Channel in Normandy (France) and Sussex (UK). *Tectonophysics*. 581, pp.163-181.

Eden, R.N. and Hazel, C.P. 1973. *Computer and graphical analysis of variable discharge pumping tests of wells*. Sydney: Civil Engineering Transactions, Institution of Engineers.

Edmunds, W.M. and Smedley, P.L. 2000. Residence time indicators in groundwater: the East Midlands Triassic sandstone aquifer. *Applied Geochemistry*. 15(6), pp.737-752.

Edwards, 1967. *Geology of the country around Ollerton*. Memoirs of the Geological Survey of Great Britain. H.M.S.O: London.

Edwards, R.A., Warrington, G., Scrivener, R.C., Jones, N.S., Haslam, H.W. and Ault L. 1997. The Exeter Group, south Devon, England: a contribution to the early post-Variscan stratigraphy of northwest Europe. *Geological Magazine*. 134(2), pp.177-197.

Ehlig-Economides, C. 1988. Use of the pressure derivative for diagnosing pressure-transient behavior. *Journal of Petroleum Technology*. 40(10), pp.1-280

Evans, D.J., Rees J.G. and Holloway, S. 1993. The Permian to Jurassic stratigraphy and structural evolution of the Cheshire Basin. *Journal of the Geological Society of London*. 150, pp.857-870.

Faulkner, J., Hu, B.X., Kish, S. and Hua, F. 2009. Laboratory analog and numerical study of groundwater flow and solute transport in a karst aquifer with conduit and matrix domains. *Journal of Contaminant Hydrology*. 110 (1), pp.34-44.

Faulkner, D. R., Jackson, C. A. L., Lunn, R. J., Schlische, R. W., Shipton, Z. K., Wibberley, C. A. J. and Withjack, M.O. 2010. A review of recent developments concerning the structure, mechanics and fluid flow properties of fault zones. *Journal of Structural Geology*. 32(11), pp.1557-1575.

Field, R., Pitt, R.E., Fan, C.Y., Heaney, J.P., Stinson, M.K., DeGuida, R.N., Perdek, J.M., Borst, M. and Hsu, K.F. 1997. *Urban wet-weather flows. Water Environment Research*, 69(4), pp.426-444.

Fienen MN, Kitanidis PK, Watson D and Jardine P. 2004. An application of inverse methods to vertical deconvolution of hydraulic conductivity in a heterogeneous aquifer at Oak Ridge National Laboratory. *Mathematical Geology*. 36, pp.101-126.

Fisher, M.J. and Mudge, D.C. 1998. Triassic. In: Glennie, K.W. (Ed.), *Petroleum Geology of the North Sea: Basic Concepts and Recent Advances*. Oxford: Blackwell Scientific Publications. pp.212-244.

Fisher, J.A., Nichols, G.J. and Waltham, D.A. 2008. Unconfined flow deposits in distal sectors of fluvial distributary systems: examples from the Miocene Luna and Huesca Systems, northern Spain. *Sedimentary Geology*. 195, pp.55-77.

Fitch, F.J., Miller, J.A. and Thompson, D.B. 1966. The palaeogeographic significance of isotopic age determinations on detrital micas from the Triassic of the Stockport-Macclesfield district, Cheshire, England. *Palaeogeography, Palaeoclimatology, Palaeoecology*. 2, pp.281-312.

Fossen, H., Schultz, R. A., Shipton, Z. K., and Mair, K. 2007. Deformation bands in sandstone: a review. *Journal of the Geological Society*. 164(4), pp.755-769.

Fowles, J. and Burley, S. 1994. Textural and permeability characteristics of faulted high porosity sandstones. *Marine and Petroleum Geology*. 11(5), pp.608-623

Fletcher, S W. 1994. *Report on the Pumping tests conducted at Nurton in 1985 and 1988.* Internal Report, Severn Trent National River Authority.

Galeazzi, S., Point, O., Haddadi, N., Mather, J. and Druesne, D. 2010. Regional geology and petroleum systems of the Illizi–Berkine area of the Algerian Saharan Platform: An overview. *Marine and Petroleum Geology.* 27(1), pp.143-178.

Gallois, R.W. 2004. The type section of the junction of the Otter Sandstone Formation and the Mercia Mudstone Group (mid Triassic) at Pennington Point, Sidmouth. *Geoscience in south-west England-Proceedings of the Ussher Society.* 11(1), pp.51-58.

Gaunt, G.D., Fletcher, T.P. and Wood, C.J. 1992. G*eology of the country around Kingston upon Hull and Brigg. Memoir for 1:50000 geological sheets 80 and 89.* London: H.M.S.O.

Gaunt, G.D. 1994. *Geology of the Country Around Goole, Doncaster and the Isle of Axholme: Memoir for One-Inch Sheets 79 and 88 (England and Wales).* London: H.M.S.O.

Gawthorpe, R.L. and Leeder, M.R. 2000. Tectono-sedimentary evolution of active extensional basins. *Basin Research.* 12, pp.195-218.

Gellasch, C.A., Bradbury, K.R., Hart, D.J. and Bahr, J.M. 2013. Characterization of fracture connectivity in a siliciclastic bedrock aquifer near a public supply well (Wisconsin, USA). *Hydrogeology Journal.* 21(2), pp.383-399.

Ghazi, S.and Mountney, N.P. 2009. Facies and architectural element analysis of a meandering fluvial succession: the Permian Warchha Sandstone, Salt Range, Pakistan. *Sedimentary Geology.* 221, pp.99-126.

Ghazi, S. and Mountney, N.P. 2011. Petrography and provenance of the Early Permian fluvial Warchha Sandstone, Salt Range, Pakistan. *Sedimentary Geology.* 233, pp.88-110.

Ghinassi, M. 2011. Chute channels in the Holocene high-sinuosity river deposits of the Firenze plain, Tuscany, Italy. *Sedimentology*. 58, pp.618-642.

Ghinassi, M., Libsekal, Y., Papini, M. and Rook L. 2009. Palaeoenvironments of the Buia Homo site: high-resolution facies analysis and non-marine sequence stratigraphy in the Alat formation (Pleistocene Dandiero Basin, Danakil depression, Eritrea). *Palaeogeography, Palaeoclimatology, Palaeoecology*. 280, pp.415-431.

Gibson, R.G. 1998. Physical character and fluid-flow properties of sandstone-derived fault zones. In: Coward, N.P. Daltaban, T.S. and Johnson, H. (Eds.), *Structural Geology in Reservoir Characterization*. Geological Society, London, Special Publications. 127(1), pp.83-97.

Gillespie, P.A., Walsh, J.J., Watterson, J., Bonson, C.G. and Manzocchi, T. 2001. Scaling relationships of joint and vein arrays from The Burren, Co. Clare, Ireland. *Journal of Structural Geology*. 23(2), pp.183-201.

Glennie, K.W. 1995. Permian and Triassic rifting in northwest Europe. In: Boldy, S.A.R. (Eds.), *Permian and Triassic Rifting in Northewest Europe*. Geological Society of London, Special Publications. 91, pp.1-5.

Gobo, K., Ghinassi, M., Nemec, W. and Sjursen, E. 2014. Development of an incised valley-fill at an evolving rift margin: Pleistocene eustasy and tectonics on the southern side of the Gulf of Corinth. *Sedimentology*. 61, pp.1086-1119.

Goldmith, P.J., Rich, B. and Standring, J. 1995. Triassic correlation and stratigraphy in the South Central Graben, UK, North Sea. In: Permian and Triassic Rifting in Northwestern Europe. Boldy S.A.R (Eds.), *Permian and Triassic Rifting in NW Europe*. Geological Society, London, Special Publications. 91, pp.123-143.

Gooddy, D.C., Bloomfield, J.P., Harrold, G. and Leharne, S.A. 2002. Towards a better understanding of tetrachloroethene entry pressure in the

matrix of Permo-Triassic sandstones. *Journal Contaminant Hydrology.* 59 (3), pp.247-265.

Grass, A.J. 1971. Structural features of turbulent flow over smooth and rough boundaries. *Journal of Fluid Mechanics.* 50(2), pp.233-255.

Green, P.F. 1989. Thermal and tectonic history of the East Midlands shelf (onshore UK) and surrounding regions assessed by apatite fission track analysis. *Journal of the Geological Society.* 146, pp.755-773.

Griffiths, J., Faulkener, D.R., Alexander, P.E. and Worden, R.H. 2016. Deformation band development as a function of intrinsic host-rock properties in Triassic Sherwood Sandstone. In: Armitage, P.J., Butcher, A.R., Churchill, J.M., Csoma, A.E., Hollis, C., Lander, R.H., Omma, J.E. and Worden, R.H. (Eds.), *Reservoir Quality of Clastic and Carbonate Rocks: Analysis, Modelling, Prediction.* Geological Society of London, Special Publications. 435. doi:10.1144/SP435.11

Gruber, W. and Sachsenhofer, R.F. 2001. Coal deposition in the Noric Depression (Eastern Alps): raised and low-lying mires in Miocene pull-apart basins. *International Journal of Coal Geology.* 48, pp.89-114.

Gutmanis, J.C., Lanyon, G.W., Wynn, T.J. and Watson, C.R. 1998. Fluid flow in faults: a study of fault hydrogeology in Triassic sandstone and Ordovician volcaniclastic rocks at Sellafield, north-west England. *Proceedings of the Yorkshire Geological Society.* 52(2), pp.159-175.

Hammond, P.A. 2016. The relationship between methane migration and shale-gas well operations near Dimock, Pennsylvania, USA. *Hydrogeology Journal.* 24(2), pp.503-519.

Hampton, B.A. and Horton, B.K. 2007. Sheet flow fluvial processes in a rapidly subsiding basin, Altiplano plateau, Bolivia. *Sedimentology.* 54, pp.1121-1147.

Hantush, M.S. 1961. Drawdown around a partially penetrating well. *Journal of Hydraulic Divisions.* 87, pp.83-98.

Hartmann, S., Odling, N.E. and West, L.J. 2007. A multi-directional tracer test in the fractured Chalk aquifer of E. Yorkshire, UK. *Journal of Contaminant Hydrology*. 94(3), pp.315-331.

Harms, J.C. and Fahnestock, R.K. 1960. Stratification, bed forms, and flow phenomena (with an example from the Rio Grande). In: Middleton, G.V. (Eds.), *Primary Sedimentary Structures and their Hydrodynamic Interpretation*. Society of Economic Paleontologists and Mineralogists, Special Publications. 12, pp.84-115.

Harris, P.T., Davies, P.J. and Marshall, J.F. 1990. Late Quaternary sedimentation on the Great Barrier Reef continental shelf and slope east of Townsville, Australia. *Marine Geology*. 94, pp.55-77.

Haszeldine, R.S. 1983. Fluvial bards reconstructed from a deep, straight channel, Upper Carboniferous coalfield of Northeast England. *Journal of Sedimentary Petrology*. 53, pp.1233-1247.

Hawkins, A.B. and McConnell, B.J. 1992. Sensitivity of sandstone strength and deformability to changes in moisture content. *Quarterly Journal of Engineering Geology and Hydrogeology*. 25(2), pp.115-130.

Heathcote, JA, Jones, MA and Herbert, AW 1996. Modelling groundwater flow in the Sellafield area. *Quarterly Journal Engineering Geology and Hydrogeology*. 29, pp.59-81.

Heinrichs, G. and Udluft, P. 1999. Natural arsenic in Triassic rocks: a source of drinking-water contamination in Bavaria, Germany. *Hydrogeology Journal*. 7(5), pp.468-476.

Hempton, M.R. and Dunne, L.A. 1984. Sedimentation in pull-apart basins: active examples in eastern Turkey. *The Journal of Geology*. 92, pp.513-530.

Henares, S., Caracciolo, L., Cultrone, G., Fernández, J. and Viseras, C. 2014. The role of diagenesis and depositional facies on pore system evolution in a Triassic outcrop analogue (SE Spain). *Marine and Petroleum Geology*. 51, pp.136-151.

Hidajat I., Singh M., Cooper J. and Mohanty K.K. 2002. Permeability of porous media from simulated NMR response. *Transport in Porous Media*. 48. pp.225-247.

Hillis, R. R., Holford, S P., Green, P.F., Doré, A.G., Gatliff, R. W., Stoker, M.S. and Williams, G.A. 2008. Cenozoic exhumation of the southern British Isles. *Geology*. 36(5), pp.371-374.

Hitchmough, A.M., Riley, M.S., Herbert, A.W. and Tellam, J.H. 2007. Estimating the hydraulic properties of the fracture network in a sandstone aquifer. *Journal of Contaminant Hydrology*. 93(1), pp.38-57.

Hoholick, J.D., Metarko, T. and Potter, P.E. 1984. Regional variations of porosity and cement: St. Peter and Mount Simon sandstones in Illinois Basin. *AAPG Bulletin*. 68(6), pp.753-764.

Holliday, H.D., Jones, N.S. and McMillan, A.A. 2008. Lithostratigraphical subdivision of the Sherwood Sandstone Group (Triassic) of the northeastern part of the Carlisle Basin, Cumbria and Dumfries and Galloway, UK. *Scottish Journal of Geology*. 44, pp.97-110.

Hossain Z., Grattoni C.A., Solymar, M. and Fabricius, I.L. 2011. Petrophysical properties of greensand as predicted from NMR measurements. *Petroleum Geoscience*. 17, pp.111-125.

Houben, G.J. 2015. Review: Hydraulics of water wells-head losses of individual components. *Hydrogeology Journal*. 23, pp.1659-1675.

Hough, E.P., Pearce, J.M., Kemp, S.J. and Williams, G.M. 2006. An investigation of some sediment-filled fractures within redbed sandstones of the UK. *Proceeding Yorkshire Geological Society*. 56, pp.41-53.

Howard, K.W.F. 1988. Beneficial aspects of sea–water intrusion. *Ground Water*. 25(4), pp.398-406.

Howell, J.A., Mountney, N.P., 1997. Climatic cyclicity and accommodation space in arid to semi-arid depositional systems: an example from the Rotliegend Group of the UK southern North Sea. In: Ziegler, K., Turner, P.

and Daines, S.R. (Eds.), *Petroleum geology of the southern North Sea: Future potential*. Geological Society of London, Special Publications. 123, pp. 63-86.

Hurst, A. 2000. Natural gamma-ray spectrometry in hydrocarbon-bearing sandstones from the Norwegian Continental Shelf. In: Hurst A., Lovell M.A., Morton A.C. (Eds.), *Geological Application of Wireline Logs*. Geological Society of London, Special Publications. 48(1), pp.211-222.

Huysmans M. and Dassargues, A. 2006. Stochastic analysis of the effect of spatial variability of diffusion parameters on radionuclide transport in a low permeability clay layer. *Hydrogeology Journal*. 14, pp.1094-1106

Ielpi, A. 2012. Anatomy of major coal successions: facies analysis and sequence architecture of a brown coal-bearing valley fill to lacustrine tract (Upper Valdarno Basin, Northern Appennines, Italy). *Sedimentary Geology*. 265, pp.163-181.

Ielpi, A. and Ghinassi, M. 2015. Planview style and palaeodrainage of Torridonian channel belts: Applecross Formation, Stoer Peninsula, Scotland. *Sedimentary Geology*. 325, pp.1-16.

Ingram, J A. 1978. *The Permo-Triassic Sandstone Aquifers of North Cumbria*. Hydrogeological Report, North West Water Authority.

Ixer, R.A., Turner, P. and Waugh, B. 1979. Authigenic iron and titanium oxides in Triassic red beds (St. Bees Sandstone), Cumbria, northern England. *Geological Journal*. 14(2), pp.179-192.

Jackson, M.D., Ann H.M., Shuji, Y., and Howard, D.J. 2003. Upscaling permeability measurements within complex heterolithic tidal sandstones. *Mathematical Geology*. 35(5), pp.499-520.

Jackson, J. and McKenzie, D. 1983. The geometrical evolution of normal fault systems. *Journal of Structural Geology*. 5(5), pp. 471-482.

James, W.C., Wilmar, G.C. and Davidson, B.G. 1986. Role of quartz type and grain size in silica diagenesis, Nugget Sandstone, south-central Wyoming. *Journal of Sedimentary Research.* 56(5).

Jiang, X.W., Wan, L., Wang, X.S., Liang, S.H. and Hu, B.X. 2009. Estimation of fracture normal stiffness using a transmissivity-depth correlation. *International Journal of Rock Mechanics and Mining Sciences.* 46(1), pp.51-58.

Jiang, X.W., Wang, XS. and Wan, L. 2010. Semi-empirical equations for the systematic decrease in permeability with depth in porous and fractured media. *Hydrogeology Journal.* 18(4), pp.839-850.

Jing, X.D. Archer, J.S. and Daltaban, T.S. 1992. Laboratory study of the electrical and hydraulic properties of rocks under simulated reservoir conditions. *Marine and Petroleum Geology.* 9, pp.115-127.

Jones, N.S. and Ambrose, K. 1994. Triassic sandy braidplain and aeolian sedimentation in the Sherwood Sandstone Group of the Sellafield area, west Cumbria. *Proceedings of the Yorkshire Geological Society.* 50, pp.61-76.

Jopling, A.V. and Walker, R.G. 1968. Morphology and origin of ripple-drift cross-lamination, with examples from the Pleistocene of Massachusetts. *Journal of Sedimentary Petrology.* 38, pp.971–984

Kana, A.A., West, L.J. and Clark, R.A. 2013. Fracture aperture and fill characterization in a limestone quarry using GPR thin-layer AVA analysis. *Near Surface Geophysics.* 11(3), pp.293-305.

Kattenhorn, S.A. and Pollard, D.D. 2001. Integrating 3-D seismic data, field analogs, and mechanical models in the analysis of segmented normal faults in the Wytch Farm oil field, southern England, United Kingdom. *AAPG Bulletin.* 85(7), pp.1183-1210.

Kerans, C. 1988. Karst-controlled reservoir heterogeneity in Ellenburger Group carbonates of west Texas. *AAPG Billetin.* 72(10), pp.1160-1183.

Knott, S.D. 1994. Fault zone thickness versus displacement in the Permo-Triassic sandstones of NW England. *Journal of the Geological Society*. 151(1), pp.17-25.

Knott, S.D., Beach, A., Brockbank, P.J., Brown, J.L., McCallum, J.E. and Welbon, A.I. 1996. Spatial and mechanical controls on normal fault populations. *Journal of Structural Geology*. 18(2), pp.359-372.

Kocurek, G. and Havholm, K.G. 1993. Eolian sequence stratigraphy-a conceptual framework. *Memoirs American Assocition of Petroleum Geologists*. pp.393-394.

Korneva, I., Tondi, E., Agosta, F., Rustichelli, A., Spina, V., Bitonte, R. and Di Cuia, R. 2014. Structural properties of fractured and faulted Cretaceous platform carbonates, Murge Plateau (southern Italy). *Marine and Petroleum Geology*. 57, pp.312-326.

Koukis, G. 1978. *Physical mechanical and chemical properties of the Triassic Sandstone aquifer of the Vale of York*. PhD thesis, University of Leeds.

Kumar, R., Ghosh, S.K. and Satish, J.S., 1999. Evolution of a Neogene fluvial system in a Himalayan foreland basin, India. In: Macfarlane, A., Sorkhabi, R.B., Quade, J. (Eds.), *Himalaya and Tibet Mountain Roots to Mountain Tops*. Geological Society of America, Special Papers. 328, pp. 239-256.

Lala A.M.S. and El-Sayed N.A.E.M. 2015. Calculating absolute permeability using nuclear magnetic resonance models. *Arabian Journal Geosciences*. 8, pp.7955-7960.

Lasdon, L.S. and Smith, S. 1992. Solving large sparse nonlinear programs using GRG. *ORSA Journal on Computing*. 4(1), pp.2-15.

Lawler, D.M., Petts, G.E., Foster, I.D. and Harper, S. 2006. Turbidity dynamics during spring storm events in an urban headwater river system: The Upper Tame, West Midlands, UK. *Science of the Total Environment*. 360(1), pp.109-126.

Lawrence, A., Stuart, M., Cheney, C., Jones, N. and Moss, R. 2006. Investigating the scale of structural controls on chlorinated hydrocarbon distributions in the fractured-porous unsaturated zone of a sandstone aquifer in the UK. *Hydrogeology Journal*. 14(8), pp.1470-1482.

Leaf, A.T., Hart, D.J. and Bahr, J.M. 2012. Active thermal tracer tests for improved hydrostratigraphic characterization. *Ground Water*. 50(5), pp.726-735.

Le Borgne, T., Bour, O., De Dreuzy, J.R., Davy, P. and Touchard, F. 2004. Equivalent mean flow models for fractured aquifers: Insights from a pumping tests scaling interpretation. *Water Resources Research*. 40(3), doi:10.1029/2003WR002436.

Le Borgne, T., Bour, O., Paillet, F.L., Caudal, J.P., 2006a. Assessment of preferential flow path connectivity and hydraulic properties at single-borehole and cross-borehole scales in a fractured aquifer. *Journal of Hydrology*. 328(1), pp.347-359.

Le Borgne, T., Paillet, F., Bour, O. and Caudal, J.P. 2006b. Cross-Borehole Flowmeter Tests for Transient Heads in Heterogeneous Aquifers. *Ground Water*. 44(3), pp.444-452.

Leeder, M.R. and Gawthorpe R.L. 1987. Sedimentary models for extensional tilt-block/half-graben basins. In: Coward, M.P., Dewey, J.F. and Hancock, P.L. (Eds.), *Continental Extensional Tectonics*. Geological Society of London, Special Publications. 28, pp.139-152.

Leeder, M.R., Mack, G.H. and Salyards, S.L. 1996. Axial-transverse fluvial interactions in half-graben: Plio-Pleistocene Palomas basin, southern Rio Grande rift, New Mexico, USA. *Basin Research*. 8, pp.225-241.

Lewin K, Young C.P., Bradshaw K., Fleet M. and Blakey N.C. 1994. *Landfill monitoring investigations at Burnstump Landfill, Sherwood Sandstone, Nottingham*. CWM 035/ 9, Final report for the Department of the Environment.

Lewis, H. and Couples, G.D. 1993. Production evidence for geological heterogeneities in the Anschutz Ranch East field, western USA. In: North, C.P. and Prosser, D.J. (Eds.), *Characterization of Fluvial and Aeolian Reservoirs*. Geological Society, London, Special Publications. 73(1), pp.321-338.

Lindquist, S.J 1988. Practical characterization of eolian reservoirs for development: Nugget Sandstone, Utah—Wyoming thrust belt. *Sedimentary Geology*. 56(1-4), pp.315-339.

Lo, H.C., Chen, P.J., Chou, P.Y. and Hsu, S.M. 2014. The combined use of heat-pulse flowmeter logging and packer testing for transmissive fracture recognition. *Journal of Applied Geophysics*. 105, pp.248-258.

Lovelock, P.E.R. 1977. *Aquifer properties of the Permo-Triassic sandstones of the United Kingdom*. Bulletin of the Geological Survey of Great Britain.

Macchi, L. 1991. *A field guide to the continental Permo-Triassic Rocks of Cumbria and northwest Cheshire*. Liverpool: Liverpool Geological Society.

Mader, D. Yardley, M.J. 1985. Migration, modification and merging in aeolian systems and the significance of the depositional mechanisms in Permian and Triassic dune sands of Europe and North America. Sedimentary Geology. 43(1-4), pp.85-218.

Manger, M., Turner, P., Ince, D., Pugh, J. and Wright, D. 1999. A new perspective on the zonation and correlation of barren strata: an integrated heavy mineral and palaeomagnetic study of the Sherwood Sandstone Group, East Irish Sea Basin and surrounding areas. *Journal of Petroleum Geology*. 22(3), pp.325-348.

Mariethoz, G., Renard, P. and Straubhaar, J. 2010. The Direct Sampling method to perform multiple‐point geostatistical simulations. *Water Resources Research*. 46 (11).

Marsalek, J. and Rochfort, Q.. 2004. Urban wet-weather flows: sources of fecal contamination impacting on recreational waters and threatening

drinking-water sources. *Journal of Toxicology and Environmental Health.* 67, pp.1765-1777.

Martin, C.D., and Christiansson R. 2009. Estimating the potential for spalling around a deep nuclear waste repository in crystalline rock. *Internetional Journal of Rock Mechanics and Mining Science.* 46, pp.219-228.

Martin, C.D., Davison, C.C. and Kozak, E.T. 1990. *Rock Joints.* Rotterdam: Balkeema

Mathias, S.A., Adrian P.B. and Hongbin, Z. 2008. Approximate solutions for Forchheimer flow to a well. Journal of Hydraulic Engineering. 134(9), pp.1318-1325.

Mathias, SA and Lindsay CT 2010. Step-drawdown tests and the Forchheimer equation. *Water Resources Research.* 46(7), doi:10.1029/2009WR008635.

Mattax, C.C. and Kyte, J.R. 1962. Imbibition oil recovery from fractured, water-drive reservoir. *Society of Petroleum Engineers Journal.* 2(2), pp.177-184.

Matter J.M., Goldberg D.S., Morin R.H. and Stute M. 2006. Contact zone permeability at intrusion boundaries: new results from hydraulic testing and geophysical logging in the Newark Rift Basin, New York, USA. *Hydrogeology Journal.* 14, pp.689-699.

McKie, T. and Audretsch, P. 2005. Depositional and structural controls on Triassic reservoir performance in the Heron Cluster, ETAP, Central North Sea. In: *The Geological Society, Petroleum Geology Conference series.* London: The Geological Society, pp. 285-297.

McKie, T. and Williams, B. 2009. Triassic palaeogeography and fluvial dispersal across the northwest European Basins. *Geological Journal.* 44, pp.711-741.

McKie, T., Jolley, S.J. and Kristensen, M.B. 2010. Stratigraphic and structural compartmentalization of dryland fluvial reservoirs: Triassic Heron Cluster, Central North Sea. Jolley, S.G., Fisher Q.J., Ainsworth R.B., Vrolijk, P.J. and Delisle, S. (Eds.), *Reservoir Compartmentalization*. Geological Society of London, Special Publications. 347(1), pp.165-198.

McKie, T. and Shannon, P.M. 2011. Comment on "The Permian-Triassic transition and the onset of Mesozoic sedimentation at the northwestern peri-Tethyan domain scale: palaeogeographic maps and geodynamic implications". *Palaeogeography, Palaeoclimatology, Palaeoecology*. 311, pp.136-143.

McKinley, J.M., Richard, H.W., Ruffell, A.H. 2001. Contact Diagenesis: The Effect of an Intrusion on Reservoir Quality in the Triassic Sherwood Sandstone Group, Northern Ireland. *Journal of Sedimentary Research*. Section A: Sedimentary Petrology and Processes. 71, pp.484-495.

McLaughlin, R.J. and Nilsen, T.H. 1982. Neogene non‐marine sedimentation and tectonics in small pull‐apart basins of the San Andreas fault system, Sonoma County, California. *Sedimentology*. 29(6), pp.865-876.

McMillan, A.A., Heathcote, J.A., Klinck, B.A., Shepley, M.G., Jackson, C.P. and Degnan, P.J. 2000. Hydrogeological characterization of the onshore Quaternary sediments at Sellafield using the concept of domains. *Quarterly Journal of Engineering Geology and Hydrogeology*. 33(4), pp.301-323.

Meadows, N.S. and Beach, A., 1993a. Structural and climatic controls on facies distribution in a mixed fluvial and aeolian reservoir: the Triassic Sherwood Sandstone in the Irish Sea. In: North, C.P. and Prosser, D.J. (Eds.), *Characterization of Fluvial and Aeolian Reservoirs*. Geological Society of London, Special Publications. 73, pp.247-264.

Meadows, N.S. and Beach, A., 1993b. Controls on reservoir quality in the Triassic Sherwood Sandstone of the Irish Sea. In: Parker, J.R. (Eds.),

Petroleum Geology of North-west Europe. Proceedings of the 4th Conference, Geological Society of London. 4, pp. 823-833.

Megawati M, Madland MV and Hiorth A. 2012. Probing pore characteristics of deformed chalk by NMR relaxation. *Journal Petroleum Science Engineering.* 100, pp.123-130.

Merritt J.W. and Auton C.A. 2000. An outline of the lithostratigraphy and depositional history of Quaternary deposits in the Sellafield district, west Cumbria. *Proceeding Yorkshire Geological Society.* 53, pp.129-154.

Miall, A.D. 1977. A review of the braided-river depositional environment. *Earth-Science Reviews.* 13(1), pp.1-62.

Miall, A.D. 2006. The geology of fluvial deposits. *Sedimentary Facies, Basin Analysis and Petroleum Geology.* Berlin: Springer.

Michalzik, D. 1991. Facies sequence of Triassic-Jurassic red beds in the Sierra Madre Oriental (NE Mexico) and its relation to the early opening of the Gulf of Mexico. *Sedimentary Geology.* 71, pp.243-259.

Michie, U. 1996. The geological framework of the Sellafield area and its relationship to hydrogeology. *Quarterly Journal Engineering Geology and Hydrogeology.* 29(1), pp.13-27.

Milodowski, A.E., Gillespie, M.R., Naden, J., Fortey, N.J., Shepherd, T.J., Pearce, J. M. and Metcalfe, R. 1998. The petrology and paragenesis of fracture mineralization in the Sellafield area, west Cumbria. *Proceedings of the Yorkshire Geological Society.* 52, pp.215-241.

Min, K.B., Jing L. and Stephansson O. 2004. Determining the equivalent permeability tensor for fractured rock masses using a stochastic REV approach: method and application to the field data from Sellafield, UK. *Hydrogeology Journal.* 12, pp.497-51.

Mobile, M., Widdowson, M., Stewart, L., Nyman, J., Deeb, R., Kavanaugh, M., Mercer, J. and Gallagher, D. 2016. In-situ determination of field-scale

NAPL mass transfer coefficients: Performance, simulation and analysis. *Journal of Contaminant Hydrology*. 187, pp.31-46.

Mohamed, E.A. and Worden, R.H. 2006. Groundwater compartmentalisation: a water table height and geochemical analysis of the structural controls on the subdivision of a major aquifer, the Sherwood Sandstone, Merseyside, UK. *Hydrology and Earth System Sciences Discussions.* 10(1), pp.49-64.

Mohindra, R. and Bagati, T.N. 1996. Seismically induced soft-sediment deformation structures (seismites) around Sumdo in the lower Spiti valley (Tethys Himalaya). *Sedimentary Geology*. 101, pp.69-83.

Molz, F.J., Morin, R.H., Hess, A.E., Melville, J.G. and Guven, O. 1989. The impeller meter for measuring aquifer permeability variations: Evaluation and comparison with other tests. *Water Resources Research*. 25(7), pp.1677-1683.

Moore, C.C. 1902. The study of the volume composition of rocks, and its importance to the geologist. *Proceeding Liverpool Geological Society*. 9, pp.129-162.

Morend, D., Pugin, A. and Gorin, G.E. 2002. High-resolution seismic imaging of outcrop-scale channels and an incised-valley system within the fluvial-dominated Lower Freshwater Molasse (Aquitanian, western Swiss Molasse Basin). *Sedimentary Geology*. 149, pp.245-264.

Moretti, M. 2000. Soft-sediment deformation structures interpreted as seismites in middle-late Pleistocene aeolian deposits (Apulian foreland, southern Italy). *Sedimentary Geology*. 135, pp.167-179.

Moretti, M., Soria J.M. and Alfaro P. 2001. Asymmetrical Soft-sediment Deformation Structures Triggered by Rapid Sedimentation in Turbiditic Deposits (Late Miocene, Guadix Basin, Southern Spain). *Facies*. 44, pp.283-294.

Morin, R.H., Carleton, G.B. and Poirier, S., 1997. Fractured-aquifer hydrogeology from geophysical logs, the Passaic Formation, New Jersey. *Ground Water*. 35(2), pp.328-338.

Morriss C, Rossini D, Straley C, Tutunjian P and Vinegar H (1997). Core analysis by low-field NMR. *Log Analyst*. 38, pp.84-94

Morton, G.H. 1870. Anniversary Address by the President. *Proceeding Liverpool Geological Society*. S20, pp.1-29.

Morton, A., Hounslow, M.W. and Frei, D. 2013. Heavy-mineral, mineral-chemical and zircon-age constraints on the provenance of Triassic sandstones from the Devon coast, southern Britain. *Geologos*. 19, pp.67-85.

Moss, PD and Edmunds, WM (1992) Processes controlling acid attenuation in the unsaturated zone of a Triassic sandstone aquifer (UK), in the absence of carbonate minerals. *Applied Geochemistry*. 7, pp.573-583.

Mountney, N.P. 2012. A stratigraphic model to account for complexity in aeolian dune and interdune successions. *Sedimentology*. 59, pp.964-989.

Mountney, N.P. and Thompson, D.B., 2002. Stratigraphic evolution and preservation of aeolian dune and damp/wet interdune strata: an example from the Triassic Helsby Sandstone Formation, Cheshire Basin, UK. *Sedimentology*. 49, pp.805-833.

Naylor, H., Turner, P., Vaughan, D.J., Boyce, A.J. and Fallick, A.E. 1989. Genetic studies of red bed mineralization in the Triassic of the Cheshire Basin, northwest England. *Journal of the Geological Society*. 146(4), pp.685-699.

Neuman, S.P. 1975. Analysis of pumping test data from anisotropic unconfined aquifers considering delayed gravity response. *Water Resources Research*. 11, pp.329-342.

Neuman, S.P. and Di Federico, V. 2003. Multifaceted nature of hydrogeologic scaling and its interpretation. *Reviews of Geophysics.* 41(3). doi: 10.1029/2003RG000130.

Newell, A.J. 2001. Bounding surfaces in a mixed aeolian–fluvial system (Rotliegend, Wessex Basin, SW UK). *Marine and Petroleum Geology.* 18(3), pp.339-347.

Newell, A.J., Tverdokhlebov, V.P. and Benton, M.J. 1999. Interplay of tectonics and climate on a transverse fluvial system, Upper Permian, Southern Uralian Foreland Basin, Russia. *Sedimentary Geology.* 127, pp.11-29.

Newton, R.C. and Manning, C.E. 2002. Experimental determination of calcite solubility in H2O-NaCl solutions at deep crust/upper mantle pressures and temperatures: Implications for metasomatic processes in shear zones. *American Mineralogist.* 87(10), pp.1401-1409.

Nirex 1992a. Liquid Permeability - Gas Permeability Correlation for Permo-Trias Samples from Sellafield Boreholes Nos 2 3 5 and 7. *Nirex Ltd Report 226.* Nottingham: British Geological Survey.

Nirex 1992b. The Geology and Hydrogeology of Sellafield. *Nirex Ltd Report 263.* Nottingham: British Geological Survey.

Nirex 1992c. Permeability and Porosity results for samples from the Permo-Trias Carboniferous and Borrowdale Volcanic Group of Sellafield Borehole 10. *Nirex Ltd Report 226.* Nottingham: British Geological Survey.

Nirex 1993a. The Geology and Hydrogeology of the Sellafield Area: Interim Assessment. *Nirex Ltd Report 524.* Nottingham: British Geological Survey.

Nirex 1993b. Permeability and Porosity Results for samples from The Permo-Trias and Borrowdale Volcanic Group of Sellafield Borehole RCF3 and the Permo-Trias of Sellafield Borehole RCM2. *Nirex Ltd Report 806.* Nottingham: British Geological Survey.

Nirex 1993c. Permeability and porosity results for samples from the Permo-Triassic and Carboniferous of Sellafield Boreholes 13A 13B 14A RCF1 and RCF2. *Nirex Ltd Report 818*. Nottingham: British Geological Survey.

Nirex 1996a. Geological Core Logs 500 mbRT to 1000 mbRT. *Nirex Ltd Report 107*. Nottingham: British Geological Survey.

Nirex 1996b. Geological Core Logs 500 mbRT to 1000 mbRT. *Nirex Ltd Report 108*. Nottingham: British Geological Survey.

Nirex 1997. Sellafield Geological and Hydrogeological Investigations. Sedimentology and sedimentary architecture of the St Bees Sandstone Formation in West Cumbria. *Nirex Ltd Report SA/97/023*. Nottingham: British Geological Survey

Nirex 2001. Laboratory measurements of the mass transfer properties of samples from the Permo-Triassic strata from Cumbria. *Nirex Ltd Report, NSS/R278*. Nottingham: British Geological Survey.

Noushabadi, M.R., Jourde, J.H. and Massonnat, G. 2011. Influence of the observation scale on permeability estimation at local and regional scales through well tests in a fractured and karstic aquifer (Lez aquifer, Southern France). *Journal of Hydrology*. 403(3), pp.321-336.

Nguyen B.T., Jones S.J., Goulty N.R., Middleton, A.J., Grant N., Ferguson A. and Bowen L. 2013. The role of fluid pressure and diagenetic cements for porosity preservation in Triassic fluvial reservoirs of the Central Graben, North Sea. *AAPG Bulletin*. 97, pp.1273-1302

O'Brien, P.E. and Wells, A.T. 1986. A small, alluvial crevasse splay. *Journal of Sedimentary Petrology*. 56, pp.876-879.

Odling, N.E. and Roden J.E. 1997. Contaminant transport in fractured rocks with significant matrix permeability, using natural fracture geometries. *Journal of Contaminant Hydrology*. 27(3), pp.263-283.

Odling, N.E., West, L.J., Hartmann, S. and Kilpatrick, A. 2013. Fractional flow in fractured chalk; a flow and tracer test revisited. *Journal of Contaminant Hydrology*. 147, pp.96-111.

Olivarius, M., Weibel, R., Hjuler, M.L., Kristensen, L., Mathiesen, A., Nielsen, L.H. and Kjøller, C. 2015. Diagenetic effects on porosity–permeability relationships in red beds of the Lower Triassic Bunter Sandstone Formation in the North German Basin. *Sedimentary Geology*. 321, pp.139-153.

Olivarius, M. and Nielsen, L.H. 2016. Triassic paleogeography of the greater eastern Norwegian-Danish Basin: Constraints from provenance analysis of the Skagerrak Formation. *Marine and Petroleum Geology*. 69, pp.168-182.

Olsen, H. 1987. Ancient ephemeral stream deposits: a local terminal fan model from the Bunter Sandstone Formation (L. Triassic) in the Tønder-3, -4 and -5 wells, Denmark. In: Frostick, L. and Reid, I. (Eds.), *Desert Sediments: Ancient and Modern*. Geological Society Special Publications. 263, pp. 69– 86.

Olsson, W.A., Lorenz, J.C. and Cooper, S.P. 2004. A mechanical model for multiply-oriented conjugate deformation bands. *Journal of Structural Geology*. 26(2), pp.325-338.

Oostrom, M., Hofstee, C., Walker, R.C., J.H. and Dane, J.H. 1999. Movement and remediation of trichloroethylene in a saturated heterogeneous porous medium: 1. Spill behavior and initial dissolution. *Journal of Contaminant Hydrology*. 37(1), pp.159-178.

Owen, G. and Moretti, M., 2011. Identifying triggers for liquefaction-induced soft-sediment deformation in sands. *Sedimentary Geology*. 235, pp.141-147.

Owen, G., Moretti, M. and Alfaro, P. 2011. Recognising triggers for soft-sediment deformation: current understanding and future directions. *Sedimentary Geology*. 235, pp.133-140.

Owen, G. and Santos, M.G.M. 2014. Soft-sediment deformation in a pre-vegetation river system: the Neoproterozoic Torridonian of NW Scotland. *Proceedings of the Geologists' Association*. 125, pp.511-523.

Owens, P.M., Walling, D.E and Leeks, G.J.L., 1999. Deposition and storage of fine-grained sediment within the main channel system of the River Tweed, Scotland. *Earth Surface Processes and Landforms*. 24, pp.1061-1076.

Paillet, F.L. 1998. Flow modeling and permeability estimation using borehole flow logs in heterogeneous fractured formations. *Water Resources Research*. 34(5), pp.997-1010

Paillet, F.L. 2000. A field technique for estimating aquifer parameters using flow log data. *Ground Water*. 38 (4), pp.510-521.

Paillet, F.L. 2004. Borehole flowmeter applications in irregular and large-diameter boreholes. *Journal of Applied Geophysics*. 55(1), pp.39-59.

Parker, A.H., L. West, J.L., Odling, N.E. and Bown, T.R. 2010. A forward modeling approach for interpreting impeller flow logs. *Ground Water*. 48 (1), pp.79-91.

Pittman, E.D. 1981. Effect of fault-related granulation on porosity and permeability of quartz sandstones, Simpson Group (Ordovician), Oklahoma. *AAPG Bulletin*. 65(11), pp.2381-2387.

Plant, J.A., Jones., D.G. and Haslam, H.W. 1999. *The Cheshire Basin: Basin evolution, fluid movement and mineral resources in a Permo-Triassic rift setting*. Nottingham: British Geological Survey Memoir.

Platt, N.H. and Keller, B. 1992. Distal alluvial deposits in a foreland basin setting-the Lower Freshwater Miocene), Switzerland: sedimentology, architecture and palaeosols. *Sedimentology*. 39, pp.545-565.

Pokar, M., West, L.J. and Odling, N.E. 2006. Petrophysical characterization of the Sherwood Sandstone from East Yorkshire, UK. In: Barker, R.D. and Tellam, J.H. (Eds.), *Fluid Flow and Solute Movement in Sandstones: The*

Offshore UK Permo-Triassic Red Bed Sequence. Geological Society of London, Special Publications. 263, pp. 103-118.

Powell, J.H., Cooper, A.H. and Benfield, A.C. 1992. Geology of the country around Thirsk. Memoir for 1:50000 geological sheet 52 (England and Wales). London: H.M.S.O.

Powell, K.L., Taylor, R.G., Cronin, A.A., Barrett, M.H., Pedley, S., Sellwood, J., Trowsdale, S.A. and Lerner, D.N. 2003. Microbial contamination of two urban sandstone aquifers in the UK. *Water Resources*. 37(2), pp.339-352.

Price, M., Morris, B. and Robertson, A. 1982. A study of intergranular and fissure permeability in Chalk and Permian aquifers, using double-packer injection testing. *Journal of Hydrology*. 54(4), pp.401-423.

Purvis, K. and Wright, V.P. 1991. Calcretes related to phreatophytic vegetation from the Middle Triassic Otter Sandstone of south west England. *Sedimentology*. 38(3), pp.539-551.

Qin, R., Wu, Y., Xu, Z., Xie, D. and Zhang C. 2013. Numerical modeling of contaminant transport in a stratified heterogeneous aquifer with dipping anisotropy. *Hydrogeology Journal*. 21(6), pp.1235-1246.

Ramingwong, T. 1974. Hydrogeology of the Keuper sandstone in the Droitwich syncline area-Worcestershire. *PhD thesis, University of Birmingham*.

Ran, G., Eyal, S., Yoseph, Y., Amir, S. and Noam, W. 2014. The permeability of fault zones: a case study of the Dead Sea rift (Middle East). *Hydrogeology Journal*. 22(2), pp.425-440.

Reesink, A.J.H. and Bridge, J.S. 2009. Influence of bedform superimposition and flow unsteadiness on the formation of cross strata in dunes and unit bars. *Sedimentary Geology*. 222, pp.274-300.

Reks, IJ, Gray, DR 1982. Pencil structure and strain in weakly deformed mudstone and siltstone. *Journal of Structural Geology*. 4(2), pp.161-176.

Renard, P., Glenz, D. and Mejias, M, 2009. Understanding diagnostic plots for well-test interpretation. *Hydrogeology Journal*. 17(3), pp.589-600.

Rider, M.H., 2000. Gamma-ray log shape used as a facies indicator: critical analysis of an oversimplified methodology. In: Hurst A., Lovell M.A. and Morton A.C. (Eds), *Geological Application of Wireline Logs. Geological Society of London*, Special Publications. 48(1), pp.27-37.

Rivett, M.O., Lerner, D.N., Lloyd, J.W. and Clark, L. 1990. Organic contamination of the Birmingham aquifer, UK. *Journal of Hydrology*. 113, (1), pp.307-323.

Rivett, M.O., Wealthall, G.P., Dearden, R.A. and McAlary, T.A. 2011. Review of unsaturated-zone transport and attenuation of volatile organic compound (VOC) plumes leached from shallow source zones. *Journal of Contaminant Hydrology*. 123(3), pp.130-156.

Rivett, M.O., Turner, R.J., Glibbery, P. and Cuthbert, M.O. 2012. The legacy of chlorinated solvents in the Birmingham aquifer, UK: Observations spanning three decades and the challenge of future urban groundwater development. *Journal of Contaminant Hydrology*. 140, pp.107-123.

Rodríguez-López, J.P., Clemmensen, L., Lancaster, N., Mountney, N.P. and Veiga, G. 2014. Archean to Recent aeolian sand systems and their preserved successions: current understanding and future prospects. *Sedimentology*. 61, pp.1487-1534.

Roques, C., Bour, O., Aquilina, L., Dewandel, B., Leray, S., Schroetter, J.M., Longuevergne, L., Le Borgne, T., Hochreutener, R., Labasque, T. and Lavenant, N. 2014. Hydrological behavior of a deep sub-vertical fault in crystalline basement and relationships with surrounding reservoirs. *Journal of Hydrology*. 509, pp.42-54.

Rossi, C., Kälin, O., Arribas, J. and Tortosa, A., 2002. Diagenesis, provenance and reservoir quality of Triassic TAGI sandstones from Ourhoud field, Berkine (Ghadames) Basin, Algeria. *Marine and Petroleum Geology*. 19(2), pp.117-142.

Rowe, J. and Burley, S.D. 1997. Faulting and porosity modification in the Sherwood Sandstone at Alderley Edge, northeastern Cheshire: an exhumed example of fault-related diagenesis. In: Meadows, N.S., Trueblood, S.R., Hardman, M. and Cowan G. (Eds.), *Petroleum Geology of the Irish Sea and Adjacent Areas*. Geological Society of London, Special Publications. 124(1), pp.325-352.

Rubin, D.M. and Carter, C.L. 2006. *Bedforms and cross-bedding in animation*. Tulsa (Oklahoma): SEPM.

Ruffell, A. and Shelton, R. 1999. The control of sedimentary facies by climate during phases of crustal extension: examples from the Triassic of onshore and offshore England and Northern Ireland. *Journal of the Geological Society*. 156, pp.779-789.

Runkel, A.C., Tipping, R.G., Alexander, E.C. and Alexander, S.C. 2006. Hydrostratigraphic characterization of intergranular and secondary porosity in part of the Cambrian sandstone aquifer system of the cratonic interior of North America: Improving predictability of hydrogeologic properties. *Sedimentary Geology*. 184, pp.281-304.

Rustichelli, A., Agosta, F., Tondi, E. and Spina, V., 2013. Spacing and distribution of bed-perpendicular joints throughout layered, shallow-marine carbonates (Granada Basin, southern Spain). *Tectonophysics*. 582, pp.188-204.

Rustichelli, A., Di Celma, C., Tondi, E. and Bianucci, G. 2016. Deformation within the Pisco basin sedimentary record (southern Peru): Stratabound orthogonal vein sets and their impact on fault development. *Journal of South America Earth Science*. 65, pp.79-100.

Rutqvist, J. and Tsang, C.F. 2003. Analysis of thermal–hydrologic–mechanical behavior near an emplacement drift at Yucca Mountain. *Journal of Contaminant Hydrology*. 62, pp.637-652.7

Sadooni F.N. and Alsharhan A.S. 2004. Stratigraphy, lithofacies distribution, and petroleum potential of the Triassic strata of the northern Arabian plate. *AAPG Bulletin*. 88, pp.515-538

Samani, N., Pasandi, M. and Barry D.A. 2006. Characterizing a heterogeneous aquifer by derivative analysis of pumping and recovery test data. *Geological Society of Iran Journal*. 1, pp.29-41

Santos, M.G.M., Almeida, R.P., Mountney, N.P. and Fragoso-Cesar, A.R.S., 2012. Seismites as a tool in the palaeoenvironmental reconstruction of fluvial deposits: the Cambrian Guarda Velha Formation, southern Brazil. *Sedimentary Geology*. 277, pp.52-60.

Santos, M.G.M., Almeida, R.P., Godinho, L.P.S., Marconato, A. and Mountney, N.P. 2014. Distinct styles of fluvial deposition in a Cambrian rift basin. *Sedimentology*. 61, pp.881-914.

Shand, P., Edmunds, W.M., Lawrence, A.R., Smedley, P.L. and Burke, S. 2007. The natural (baseline) quality of groundwater in England and Wales. *Report RR/07/06.* Nottingham: British Geological Survey.

Schmid, S., Worden, R.H. and Fisher, Q.J. 2004. Diagenesis and reservoir quality of the Sherwood Sandstone (Triassic), Corrib Field, Slyne Basin, west of Ireland. *Marine and Petroleum Geology*. 21, pp.299-315.

Schmid, S., Worden, R.H. and Fisher, Q.J. 2006. Sedimentary facies and the context of dolocrete in the Lower Triassic Sherwood Sandstone group: Corrib Field west of Ireland. *Sedimentary Geology*. 187, pp.205-227.

Schnaiberg, J., Riera, J., Turner, M.G. and Voss, P.R. 2002. Explaining human settlement patterns in a recreational lake district: Vilas County, Wisconsin, USA. *Environmental Management*. 30(1), pp.24-34.

Selley, R.C. 1978. Porosity gradients in North Sea oil-bearing sandstones. *Journal of the Geological Society*. 135, pp.119-132.

Sethi, R., 2011. A dual-well step drawdown method for the estimation of linear and non-linear flow parameters and wellbore skin factor in confined aquifer systems. *Journal of Hydrology*. 400(1), pp.187-194.

Seymour, K.J., Ingram, J.A. and Gebbett, S.J. 2006. Structural controls on groundwater flow in the Permo-Triassic sandstones of NW England. In: Barker, R.D. and Tellam, J.H. (Eds.), *Fluid Flow and Solute Movement in Sandstones: The Onshore UK Permo-Triassic Red Bed Sequence. Geological Society of London, Special Publications*. Geological Society of London, Special Publications. 263(1), pp.169-185.

Sibson, R.H., Robert, H and Poulsen, K.H. 1988. High-angle reverse faults, fluid-pressure cycling, and mesothermal gold-quartz deposits. *Geology.* 16, pp.551-555.

Sibson, R.H. 1996. Structural permeability of fluid-driven fault-fracture meshes. *Journal of Structural Geology*. 18, pp.1031-1042.

Smedley, P.L. and Edmunds, W.B. 2002. Redox Patterns and Trace-Element Behavior in the East Midlands Triassic Sandstone Aquifer, UK. *Ground Water*. 40, pp.44-58.

Smith, D.B. and Francis, E.A. 1967. Geology of the country between Durham and West Hartlepool, Geological Survey of Great Britain Memoirs. H.M.S.O: London..

Smith, B., 1924. On the West Cumberland Brockram and its associated rocks. *Geological Magazine*. 61(7), pp.289-308.

Smith, S.A. 1990. The sedimentology and accretionary styles of an ancient gravel-bed stream: the Budleigh Salterton Pebble Beds (Lower Triassic), southwest England. *Sedimentary Geology*. 67(3-4), pp.199-219.

Smith, R.M.H., 1993. Vertebrate taphonomy of Late Permian floodplain deposits in the southwestern Karoo Basin of South Africa. *Palaios*. 8, pp.45-67.

Smith, D.B. and Francis E.A. 1967. *Geology of the country between Durham and West Hartlepool. Geological Survey of Great Britain Memoirs*. London: H.M.S.O.

Spane F.A. and Wurstner S.K. 1993. DERIV: A computer program for calculating pressure derivatives for use in hydraulic test analysis. *Ground Water*. 31, pp.814-822.

Stanistreet, I.G. and Stollhofen, H., 2002. Hoanib River flood deposits of Namib Desert interdunesas analogues for thin permeability barrier mudstone layers in aeolianite reservoirs. *Sedimentology*. 49, pp.719-736.

Steele, A. and Lerner, D.N. 2001. Predictive modelling of NAPL injection tests in variable aperture spatially correlated fractures. *Journal of Contaminant Hydrology*. pp.49(3) 287-310.

Steel, R.J. and Thompson, D.B. 1983. Structures and textures in Triassic braided stream conglomerates ('Bunter' Pebble Beds) in the Sherwood Sandstone Group, North Staffordshire, England. *Sedimentology*. 30, pp.341-367.

Stephens, M. 1994. Architectural element analysis within the Kayenta Formation (Lower Jurassic) using ground-probing radar and sedimentological profiling, south-western Colorado. *Sedimentary Geology*. 90, pp.179-211.

Štolfová, K. and Shannon, P.K. 2009. Permo-Triassic development from Ireland to Norway; basin architecture and regional controls. *Geological Journal*. 44, pp.652-676

Stouthamer, E., Berendsen, H.J.A., 2001. Avulsion frequency, avulsion duration, and interavulsion period of Holocene channel belts in the Rhine-Meuse delta, the Netherlands. *Journal of Sedimentary Research*. 71, pp.589-598.

Streetly, M., Chakrabarty, C. and McLeod, R. 2000. Interpretation of pumping tests in the Sherwood Sandstone Group, Sellafield, Cumbria, UK.

Quarterly Journal of Engineering Geology and Hydrogeology. 33(4), pp.281-299.

Strong, G.E., Milodowski, A.E., Pearce, J.M., Kemp, S.J., Prior, S.V. and Morton, A.C. 1994. The petrology and diagenesis of Permo-Triassic rocks of the Sellafield area, Cumbria. *Proceedings of the Yorkshire Geological and Polytechnic Society.* 50, pp.77-89.

Swanson, S.K., Bahr, J.M., Bradbury, K.R. and Anderson, K.M. 2006. Evidence for preferential flow through sandstone aquifers in Southern Wisconsin. *Sedimentary Geology.* 184(3), pp.331-342.

Sutton J.S. 1996. Hydrogeological testing in the Sellafield area. *Quarterly Journal of Engineering Geology Hydrogeology.* 29, pp.29-38.

Tellam, J.H. 2004. 19th century studies of the hydrogeology of the Permo-Triassic Sandstones of the northern Cheshire Basin, England. In: Mather, J. (Ed.), *200 Years of British Hydrogeology.* Geological Society of London, Special Publications. 225, pp.89-105.

Tellam, J.H. and Barker, R.D. 2006. Towards prediction of satured-zone pollutant movement in groundwaters in fractured permeable-matrux aquifers: the case of the UK Permo-Triassic sandstones. In: Barker, R.D. and Tellam, J.H. (Eds.), *Fluid Flow and Solute Movement in Sandstones: The Onshore UK Permo-Triassic Red Bed Sequence.* Geological Society of London, Special Publications. 263, pp.1-48.

Terzaghi, R.D. 1965. Sources of errors in joint surveys. *Geotechnique.* 15 (3), pp.287-304

Theis, C.V., 1935. The relation between the lowering of the piezometric surface and the rate and duration of discharge of a well using groundwater storage. *Transactions American Geophysics Union.* 16 (2), pp.519-524.

Thiem, G., 1906. Hydrologische Methoden. Leipzig: Gebhardt.

Thompson, R.P. and Leach, B.A. 1985. *Strain-stiffness relationship for weak sandstone rock. In: Proceedings of the 11th International Conference*

on Soil Mechanics and Foundation Engineering, San Francisco. pp.673~576.

Thompson, D.B. 1969. Dome-shaped aeolian dunes in the frodsham member of the so-called "keuper" sandstone formation (scythian-anisian: triassic) at Frodsham, Cheshire (England). *Sedimentary Geology.* 3(4), pp.263-289.

Thompson, D.B. 1970a. Sedimentation of the Triassic (Scythian) red pebbly sandstones in the Cheshire Basin and its margins. *Geological Journal.* 7, pp.183-216.

Thompson, D.B. 1970b. The stratigraphy of the so-called Keuper Sandstone Formation (Scythian-?Anisian) in the Permo-Triassic Cheshire Basin. *Quarterly Journal of the Geological Society.* 126, pp.151-181.

Thompson, J., Meadows, N.S., 1997. Clastic sabkhas and diachroneity at the top of the Sherwood Sandstone Group: East Irish Sea Basin. In: Meadows, N.S. and Hardman, M. (Eds.), Petroleum Geology of the Irish Sea and Adjacent Areas. *Geological Society of London, Special Publications.* 124, pp.237-251.

Toccalino, P.L., Norman, JE and Hitt, K.J. 2010. Quality of source water from public-supply wells in United States, 1993-2007. *United States Geological Survey, Science Invesitigation Report. 2010-5024*

Torabi, A. and Fossen, H. 2009. Spatial variation of microstructure and petrophysical properties along deformation bands in reservoir sandstones. *AAPG Bulletin.* 93(7), pp.919-938.

Tratman, E.K. 1967. The caves of Northwest Clare, Ireland; The University of Bristol Spelaeological Society. Newton Abbot (UK): David and Charles.

Trevena, A.S. and Clark, R.A. 1986. Diagenesis of sandstone reservoirs of Pattani Basin, Gulf of Thailand. *AAPG Bulletin.* 70(3), pp.299-308.

Tsang, C.F., Hufschmied, P. and Hale, F.V. 1990. Determination of fracture inflow parameters with a borehole fluid conductivity logging method. *Water Resources Research*. 26(4), pp.561-576.

Tsang, C.F., Barnichon, J.D., Birkholzer, J., Li, X.L., Liu, H.H. and Sillen, X. 2012. Coupled thermo-hydro-mechanical processes in the near field of a high-level radioactive waste repository in clay formations. *International Journal of Rock Mechanics and Mining Sciences*. 49, pp.31-44.

Tueckmantel, C., Fisher, Q.J., Knipe, R.J., Lickorish, H. and Khalil, S.M. 2010. Fault seal prediction of seismic-scale normal faults in porous sandstone: a case study from the eastern Gulf of Suez rift, Egypt. *Marine and Petroleum Geology*. 27(2), pp.334-350.

Tueckmantel, C., Fisher, Q.J., Grattoni, C.A. and Aplin, A.C. 2012. Single- and two-phase fluid flow properties of cataclastic fault rocks in porous sandstone. *Marine and Petroleum Geology*. 29, pp.129-142.

Tunbridge, I.P. 1984. Facies model for a sandy ephemeral stream and clay playa complex; the Middle Devonian Trentishoe Formation of North Devon, UK. *Sedimentology*. 31, pp.697-715.

Turner, P. 1981. Relationship between magnetic components and diagenetic features in reddened Triassic alluvium (St Bees Sandstone, Cumbria, UK). *Geophysical Journal International*. 67(2), pp.395-413.

Truesdell A.H. and White D.E. 1973. Production of superheated steam from vapor-dominated geothermal reservoirs. *Geothermics*. 2, pp.154-173.

Tyrrell, S., Haughton, P.D.W., Souders, A.K., Daly, J.S. and Shannon, P.M. 2012. Large-scale, linked drainage systems in the NW European Triassic: insights from the Pb isotopic composition of detrital K-feldspar. *Journal of the Geological Society*. 169,pp.279-295.

Üner, S., Yeşilova, C. and Türker, Y. 2012. The Traces of Earthquake (Seismites): Examples from Lake Van Deposits (Turkey). In: D'Amico, S. (Ed.), *Earthquake Research and Analysis-Seismology, Seismotectonic and Earthquake Geology*. Rijeka (Croatia): InTech Publishers, pp. 21-32.

Van Tonder, G.J., Botha, J.F., Chiang, W.H., Kunstmann, H. and Xu, Y. 2001. Estimation of the sustainable yields of boreholes in fractured rock formations. *Journal of Hydrology*. 241(1), pp.70-90.

Ventra, D. and Nichols, G.J. 2014. Autogenic dynamics of alluvial fans in endorheic basins: outcrop examples and stratigraphic significance. *Sedimentology*. 61, pp.767-791.

Voss, C.I. and Andersson, J. 1993. Regional flow in the Baltic Shield during Holocene coastal regression. *Ground Water*. 31, pp.989-1006.

Walker, T.R. 1967. Formation of red beds in modern and ancient deserts. *Geological Society of American Bulletin*. 78, pp.353-368.

Walsby, J.C., Lowe, G.J. and Forster, A. 1993. The "caves" of the city of Nottingham, their geology, history, extent and implications for engineers and paners. In: Cripps, J.C. and C.F. (Eds.). *The Engineering Geology of Weak Rock*. Rotterdam: Balkema, pp.479-487.

Wakefield, O.J., Hough, E. and Peatfield, A.W. 2015. Architectural analysis of a Triassic fluvial system: the Sherwood Sandstone of the East Midlands Shelf, UK. *Sedimentary Geology*, 327, pp.1-13.

Waugh, B. 1978. Authigenic K-feldspar in British Permo-Triassic sandstones. *Journal of the Geological Society*. 135, pp.51-56.

Waugh, B., 1970. Petrology, provenance and silica diagenesis of the Penrith Sandstone (Lower Permian) of northwest England. *Journal of Sedimentary Research*. 40(4).

Waugh B. 1973. The distribution and formation of Permo-Triassic red beds. *Petroleum Geologists Memoirs*. 2, pp.678-693

Warrington, G., Audley-Charles, M.G., Elliott, R.E., Evans, W.B., Ivimey-Cook, H.C., Kent, P.E., Robinson, P.L., Shotton, F.W. and Taylor, F.M. 1980. *A correlation of the Triassic rocks in the British Isles, special Report of the Geological Society of London*. Oxford: Blackwell Scientific.

Warrington, G. and Ivimey-Cook, C., 1992. Triassic. In: Cope, J.C.W., Ingham, J.K. and Rawson, P.F. (Eds.), *Atlas of Palaeogeography and Lithofacies*. Geological Society of London Memoirs. 13, pp.97-106.

Wakefield, O.J.W., Hough, E. and Peatfield, A.W. 2015. Architectural analysis of a Triassic fluvial system; the Sherwood Sandstone of the East Midlands Shelf, UK. *Sedimentary Geology*. 327, pp.1-13.

Wealthall, G.P., Steele, A., Bloomfield, J.P., Moss, R.H. and Lerner, D.N., 2001. Sediment filled fractures in the Permo-Triassic sandstones of the Cheshire Basin: observations and implications for pollutant transport. *Journal of Contaminant Hydrology*. 50(1), pp.41-51.

Wees, V.J.D., Stephenson, R.A., Zeigler, P.A., Bayer, U., McCann, T., Dadlez, R., Gaupp, R., Narkiewicz, M., Bitzer, F. and Scheck, M. 2000. On the origin of the Southern Permian Basin, Central Europe. *Marine and Petroleum Geology*. 17, pp.43-59.

Weibel,R. 1998. Diagenesis in oxidising and locally reducing conditions - an example from the Triassic Skagerrak formation, Denmark. *Sedimentary Geology.* 121, pp.259-276.

Weibel, R. and Friis, H. 2004. Opaque minerals as keys for distinguishing oxidising and reducing diagenetic conditions in the Lower Triassic Bunter Sandstone, North German Basin. *Sedimentary Geology*. 169, pp.129-149

Welch, M.J., Souque, C., Davies, R.K. and Knipe, R.J. 2015. Using mechanical models to investigate the controls on fracture geometry and distribution in chalk. In: Agar. S.M. and Geiger, S. (Eds.), *Fundamental Controls of Fluid Flow in Carbonates: Current Workflows to Emerging Technologies*. Geological Society of London, Special Publications. 406(1), pp.281-309.

Weissmann, G.S., Hartley, A.J., Nichols, G.J., Scuderi, L.A., Olson, M., Buehler, H. and Banteah, R. 2010. Fluvial form in modern continental sedimentary basins: distributive fluvial systems. *Geology*. 38, pp.39-42.

West, G. 1979. *Strength properties of Bunter Sandstone*. Tunnels and Tunnelling, 27-29 September.

West, L.J. and Truss, S.W. 2006. Borehole time domain reflectometry in layered sandstone: Impact of measurement technique on vadose zone process identification. *Journal of Hydrology*. 319, pp.143-162.

Whithworth, L.J. and Turner, A.J. 1989. Rock socket piles in the Sherwood Sandstone of Central Birmingham. In: *Proceedings of the Conference on Piling and Deep Foundations*. London: Institution of Civil Engineers. pp.327-334.

Whittaker, A. 1985. *Atlas of onshore sedimentary basins in England and Wales: post-Carboniferous tectonics and stratigraphy*. Blackie: Glasgow.

Wills, L.J. 1956. *Concealed Coalfields*. London: Blackie.

Williams, J.H. and Johnson, C.D. 2004. Acoustic and optical borehole-wall imaging for fractured-rock aquifer studies. *Journal of Applied Geophysics*. 55(1), pp.151-159.

Willis, B., 1993a. Ancient river systems in the Himalayan foredeep, Chinji Village area, northern Pakistan. *Sedimentary Geology*. 88, pp.1-76.

Willis, B. 1993b. Evolution of Miocene fluvial systems in the Himalayan foredeep through a two kilometer-thick succession in northern Pakistan. *Sedimentary Geology*. 88, pp.77-121.

Wills, L.J. 1970. The Triassic Succession in the central Midlands in its regional setting. *Quarterly Journal of Engineering Geology and Hydrogeology*. 126, pp.225-283.

Willis, B. 2000. Tectonic control of nested sequence architecture in the Sego Sandstone, Neslen Formation and Upper Castlegate Sandstone (Upper Cretaceous), Sevier Foreland Basin, Utah, USA. *Sedimentary Geology*. 136, pp.277-317.

Wilson, J.T. 1963. Continental Drift. *Scientific American*. 208(4), pp.86-103.

Worden, R.H. and Burley, S.D. 2003. Sandstone diagenesis: the evolution of sand to stone. Sandstone Diagenesis: Recent and Ancient. 4, pp.3-44.

Worden, R.H. and Benshatwan, M.S., Potts, G.J. and Elgarmadi, S.M. 2016. Basin-scale fluid movement patterns revealed by veins: Wessex Basin, UK. *Geofluids*. 16(1), pp.149-174.

Worthington S.R.H., Gareth J. and Alexander E.C. 2016. Enhancement of bedrock permeability by weathering. *Earth-Science Reviews*. 160, pp.188-202.

Wray, R.A.L. 1997. A global review of solutional weathering forms on quartz sandstones. *Earth-Science Reviews*, 42(3), pp.137-160.

Wu, J., Boucher, A. and Zhang, T. 2008. A SGeMS code for pattern simulation of continuous and categorical variables: FILTERSIM. *Computers and Geosciences*, 34(12), pp.1863-1876.

Yates, P.G.J. 1992. The material strength of sandstones of the Sherwood Sandstone Group of north Staffordshire with reference to microfabric. *Quarterly Journal of Engineering Geology and Hydrogeology*. 25(2), pp.107-113.

Yang, Y. and Aplin, A.C., 2007. Permeability and petrophysical properties of 30 natural samples. *Journal of Geophysical Research: Solid Earth*. 112 (B03), doi: 10.1029/2005JB004243.

Zhang, H. and Hiscock, K.M. 2010. Modelling the impact of forest cover on groundwater resources: A case study of the Sherwood Sandstone aquifer in the East Midlands, UK. *Journal of Hydrology*. 392(3), pp.136-149.

Zhao, W.Z., Wang, Z.C., Wang, H.J. and Wang, Z.Y. 2008. Principal characteristics and forming conditions for medium-low abundance large scale oil/gas fields in China. *Petroleum Exploration and Development*. 35(6), pp.641-650.

Zhang, H. and Hiscock, K.M. 2011. Modelling the effect of forest cover in mitigating nitrate contamination of groundwater: A case study of the

Sherwood Sandstone aquifer in the East Midlands, UK. *Journal of Hydrology.* 399(3), pp.212-225.

Zheng, S.Y., Corbett, P.W.M. and Emery, A. 2003. Geological interpretation of well test analysis: A case study from a fluvial reservoir in the Gulf of Thailand. *Journal of Petroleum Geology.* (1), pp.49-64.

Zheng, S. Y., Corbett, P. W., Ryseth, A. and Stewart, G. 2000. Uncertainty in well test and core permeability analysis: a case study in fluvial channel reservoirs, northern North Sea, Norway. *AAPG Bulletin.* 84(12), pp.1929-1954.

Zoback, M.D. and Byerlee, J.D. 1975. Permeability and effective stress: geologic notes. *AAPG Bulletin.* 59(1), pp.154-158.

Zhu, C. and Burden D.S. 2001. Mineralogical compositions of aquifer matrix as necessary initial conditions in reactive contaminant transport models. *Journal of Contaminant Hydrology.* 51(3), pp.145-161.

Ziegler, P.A. 1982. Triassic rifts and facies patterns in Western and Central Europe. *Geologische Rundschau.* 71, pp.747-772.

Ziegler, P.A. 1987. Late Cretaceous and Cenozoic intra-plate compressional deformations in the Alpine foreland—a geodynamic model. *Tectonophysics.* 137(1-4), pp.389-420.

Ziegler, P.A. and Dèzes, P. 2006. Crustal evolution of Western and Central Europe. In: Gee, D.G. (Ed.), *European Lithosphere Dynamics.* Geological Society of London, Memoirs. 32, pp.43-56.

Appendix A: well test analysis

ESI AquiferWin32 solution (Eden and Hazel, 1973), modelled and observed step-test drawdown for the Bridge End Trial, Blak Ling, Ellergill Bridge, Pallaflat Reservoir and Thornihill Trial boreholes (data Chapter 4).
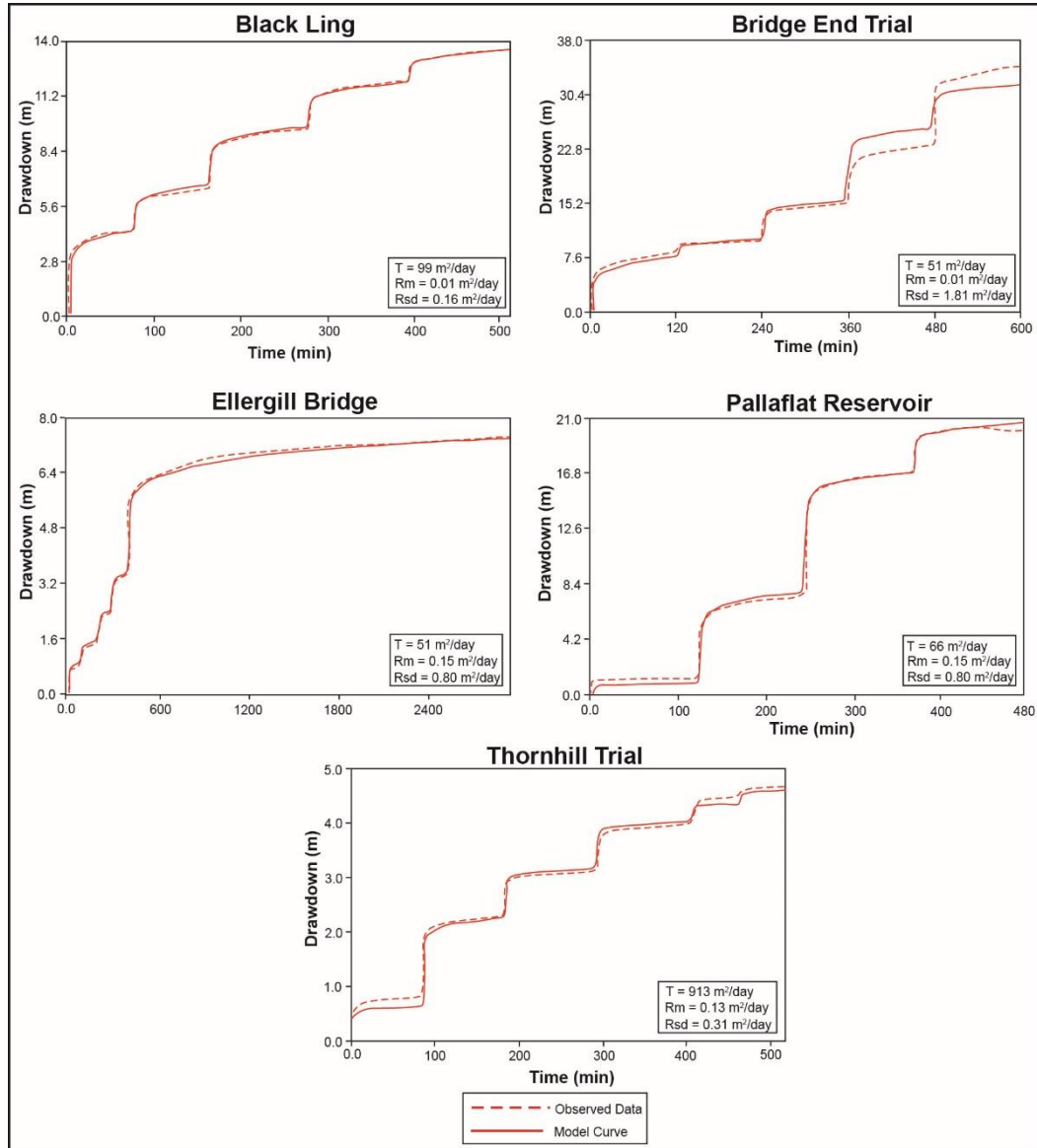
ESI AquiferWin32 solution (Theis, 1935) for the recovery of constant flow rate tests for the Bridge End Trial, Black Ling, Ellergill Bridge, Pallaflat Reservoir and Thornihill Trial boreholes (data Chapter 4).
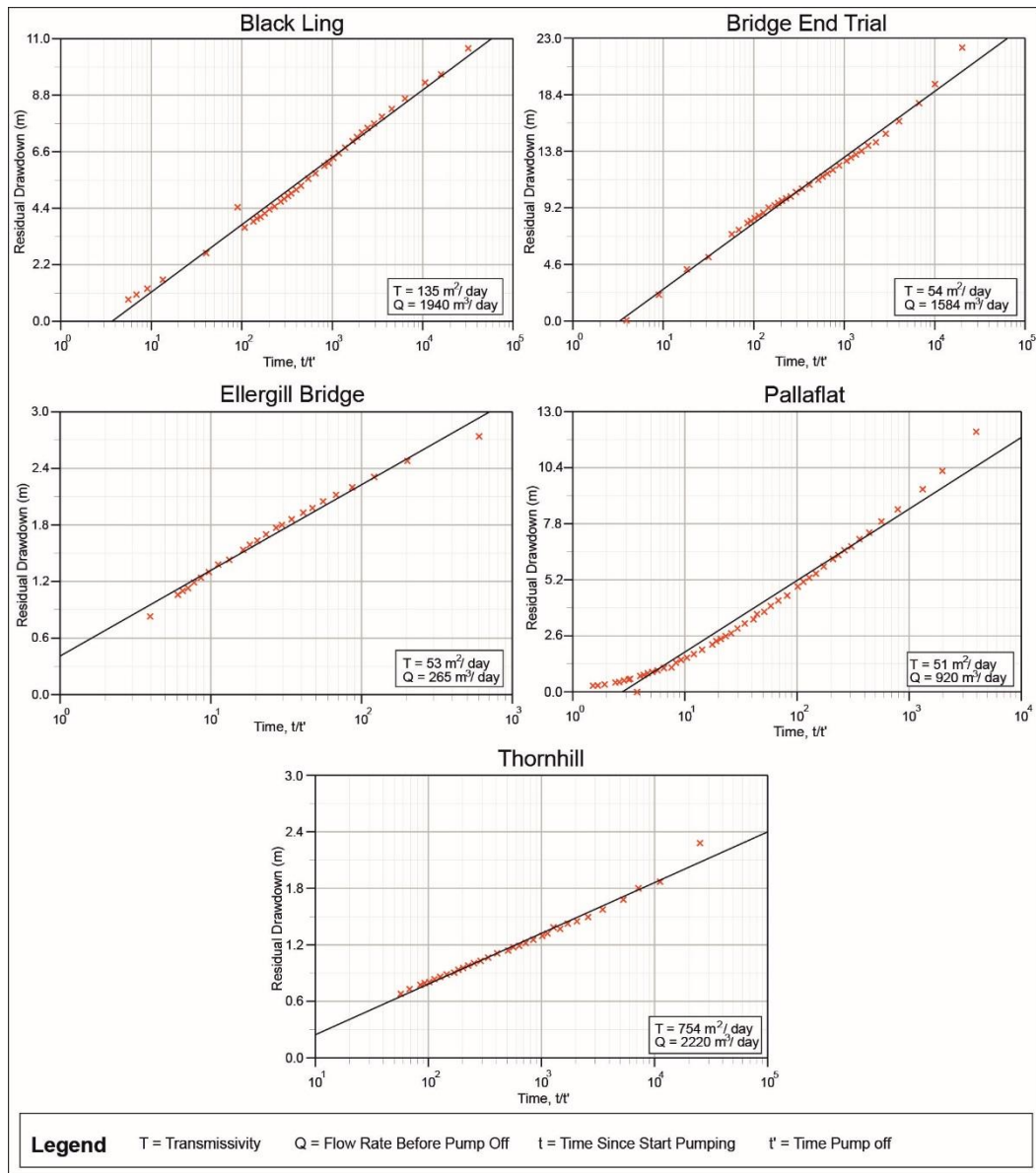
ESI AquiferWin32 solution (Theis, 1935) for the recovery of step tests for the Bridge End Trial, Black Ling, Ellergill Bridge, Rottington Trial and Thornihill Trial boreholes (data Chapter 4).
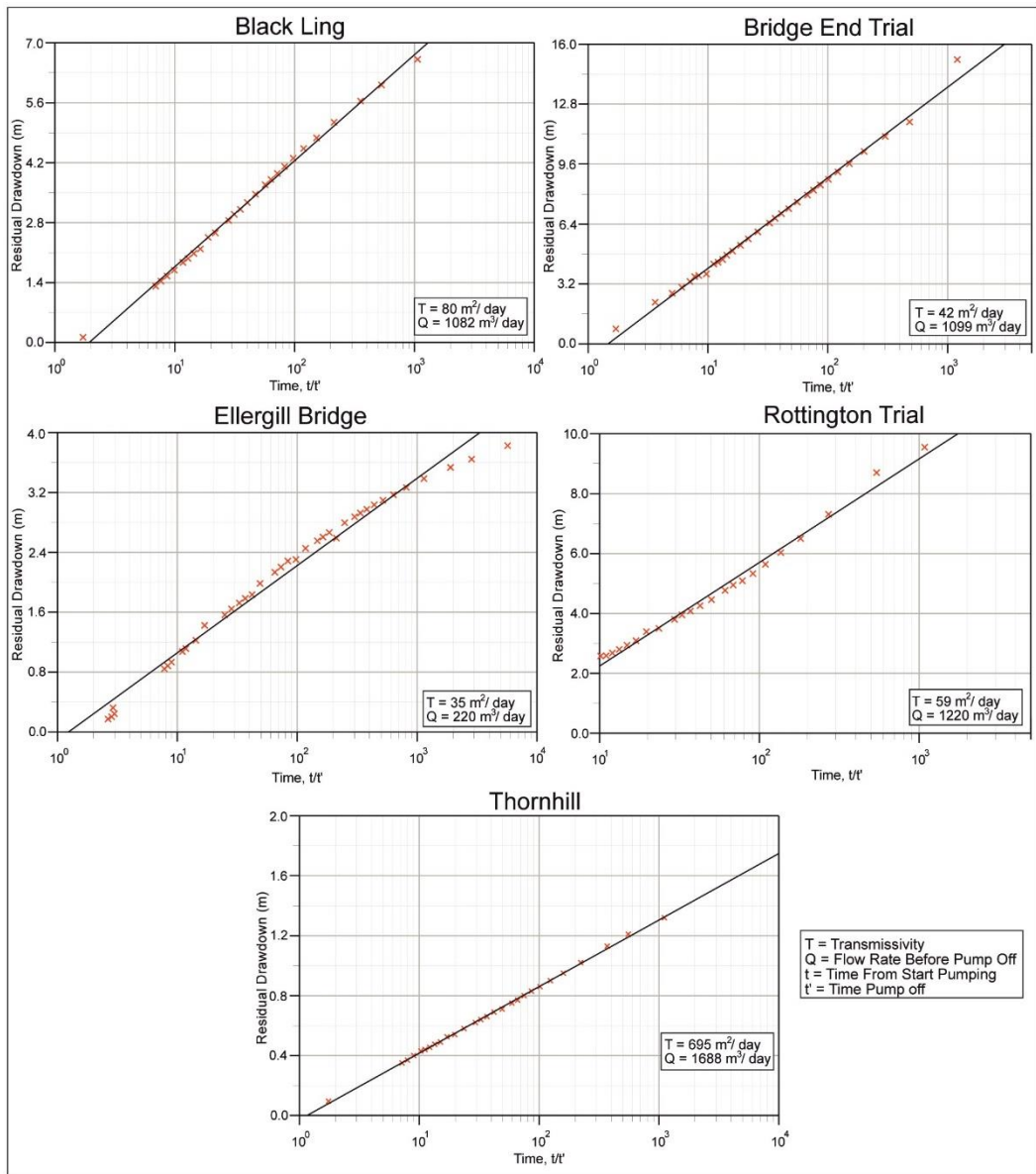
ESI AquiferWin32 solution of well tests (data Chapter 5). (a) Intermediate (150-450 mGL) St Bees Sandstone aquifer in Sellafield BH2 borehole: recovery (Theis, 1935) of constant flow rate tests, (b) Deep (450-1100 mBGL) St Bees Sandstone aquifer in Sellafield BH3 borehole: recovery of constant flow rate tests (Theis, 1935).
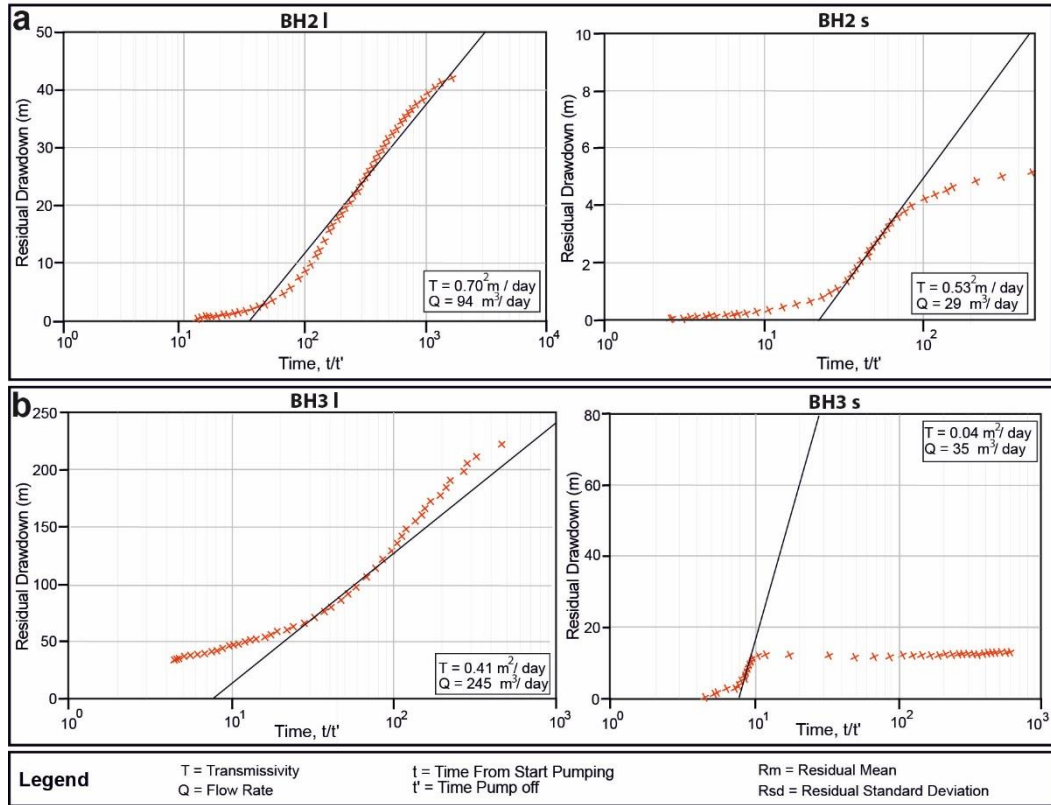
Appendix B: plug-scale permeability tests

Constant flow rate permeamiter tests of 22 plugs measured with saline water (pH = 7.7; Salinity = 670 µS/cm) from the outcropping St Bees Sandstone aquifer in the St Bees area (data Chapter 5).

Q = Flow Rate   ΔP = Pressure Difference   L = Length Plug   A = Area Plug Circle   k = Permeability   K = Hydrailic conductivity

Q = Flow Rate   ΔP = Pressure Difference   L = Length Plug   A = Area Plug Circle   k = Permeability   K = Hydrailic conductivity

10h

$y = 6 \times 10^{13} - 5 \times 10^{8}$
$R^2 = 0.99$

A=1.06x10^{-3} m^2
L=3.3 x10^{-2} m

K= 4.38x10^{-2} m/day

10v

$y = 5 \times 10^{14} - 4 \times 10^{7}$
$R^2 = 0.99$

A=1.06x10^{-3} m^2
L=4.2x10^{-2} m

K= 3.65x10^{-3} m/day

11h

$y = 9.4 \times 10^{14} - 4 \times 10^{7}$
$R^2 = 0.99$

A=1.10x10^{-3} m^2
L=5.4x10^{-2} m

K= 6.81x10^{-3} m/day

11v

$y = 4.9 \times 10^{14} - 9 \times 10^{8}$
$R^2 = 0.96$

ΔP/L (Pa/m)

A=1.10x10^{-3} m^2
L=5.2x10^{-2} m

K= 3.56x10^{-4} m/day

12h

$y = 1.5 \times 10^{13} - 1 \times 10^{6}$
$R^2 = 0.99$

A=1.10x10^{-3} m^2
L=5.6x10^{-2} m

K=1.06x10^{-2} m/day

12v

$y = 5.0 \times 10^{15} + 9 \times 10^{8}$
$R^2 = 0.97$

A=1.10x10^{-3} m^2
L=5.2x10^{-2} m

K=3.65x10^{-4} m/day

Q = Flow Rate   ΔP = Pressure Difference   L = Length Plug   A = Area Plug Circle   k = Permeability   K = Hydraulic conductivity

Appendix C: Physical properties and units

Symbol	Quality	Units
h	Hydraulic head	m
z	Thickness	m
r_0	Borehole radius	m
r_w	Radius of influence	m
A	Area	m^2
V	Volume	m^3
v	velocity	mm/s
P	Pressure	KPa
T_2	MNR relaxation time	ms
K	Hydraulic conductiviy	m/day
Q	Flow rate	m^3/day
T	Transmissivity	m^2/day
φ	Total/matrix porosity	-
Rsd	Residual standard deviation	-
Rm	Residual mean	-